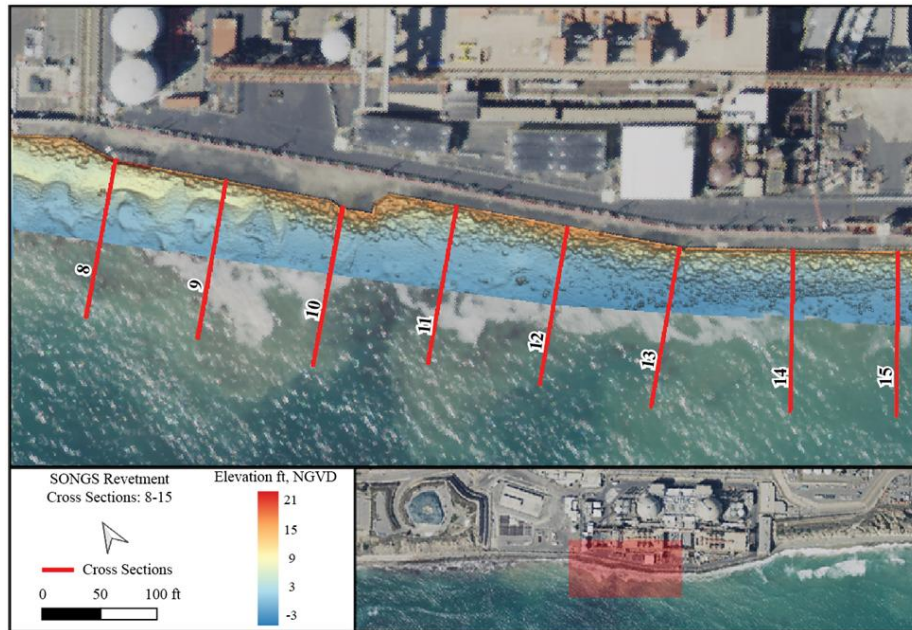


**SAN ONOFRE NUCLEAR GENERATING STATION (SONGS)
MEAN SEA LEVEL RISE IMPACT ASSESSMENT**

**2022 Technical Report
Provision 14 in Lease No. PRC 6785.1**



by

Hany Elwany, Ph.D.
Reinhard E. Flick, Ph.D.
Tim Norall, MS.

for

Southern California Edison
2244 Walnut Grove Avenue
Rosemead, CA 91770

Coastal Environments, Inc.
2166 Avenida de la Playa, Suite E
La Jolla, CA 92037

CE Reference No. 23-07
30 March 2023

TABLE OF CONTENTS

EXECUTIVE SUMMARY	vii
1.0 INTRODUCTION.....	1
2.0 MEAN SEA LEVEL RISE IMPACT ASSESSMENT	3
2.1 SONGS SEA LEVEL INFORMATION	3
2.2 MEAN SEA LEVEL RISE GUIDANCE	5
2.2.1 California OPC (2018) MSLR Projections	5
2.2.2 IPCC (2021) MSLR Projections	7
2.2.3 NOAA Global and Regional MSLR Scenarios	10
2.3 SONGS SEA LEVEL EXTREMES	11
3.0 SONGS REVETMENT	21
3.1 DESCRIPTION OF THE SONGS REVETMENT	21
3.1.1 Revetment and Walkway Maintenance 2018-2019	21
3.2 SITE VISIT	22
3.2.1 Rock Measurements.....	22
3.2.2 Revetment Laser Scanner Survey	22
3.3 RIPRAP ROCK UNIT WEIGHT	23
3.4 DESIGN WATER LEVEL	23
3.5 DESIGN WAVE ESTIMATION.....	24
3.6 SONGS REVETMENT STABILITY ESTIMATION	25
3.7 ASSESSMENT OF SAN ONOFRE BEACH.....	25
3.8 EVALUATION CRITERIA	27
3.9 REVETMENT STABILITY FROM FEBRUARY 2020 TO FEBRUARY 2023.....	27
3.10 MAINTENANCE AND ADAPTIVE CAPACITY	28
4.0 RUN-UP AND OVERTOPPING ANALYSIS	62
4.1 RANDOM WAVE METHOD	62
4.2 OVERTOPPING	63
4.3 RESULTS.....	64
4.4 PROBABILITY ANALYSIS.....	64
4.5 DISCUSSION	65
5.0 CONCLUSIONS	72
6.0 REFERENCES.....	74

LIST OF APPENDICES

Appendix A.	Digital Elevation Models (DEM) from 2023 & 2020 Revetment Surveys	A-1
Appendix B.	Cross Section Elevations of SONGS Revetment.....	B-1
Appendix C.	Aerial Photographs North and South SONGS, 2003-2020.....	C-1
Appendix D.	Photographs from 2023 & 2020 Surveys.....	D-1
Appendix E.	2022 Beach Profile Surveys at San Onofre.....	E-1
Appendix F.	2022 Groundwater Levels at San Onofre Nuclear Generating Station.....	F-1

LIST OF TABLES

Table 2-1.	OPC (2018) MSLR projections, La Jolla.....	13
Table 2-2.	IPCC (2021) mid-range MSLR projections, Los Angeles.....	13
Table 2-3.	IPCC (2021) low-high range MSLR projections, Los Angeles.....	13
Table 2-4.	NOAA (2022) scenarios related to IPCC (2021) scenarios	14
Table 2-5.	NOAA (2022) median MSLR projections/extrapolations, Los Angeles	15
Table 2-6.	NOAA (2022) and IPCC (2021) median MSLR projections 2030 and 2050.....	15
Table 2-7.	Highest maximum observed total water levels, La Jolla	16
Table 2-8.	NOAA La Jolla extreme water level statistics	16
Table 3-1.	Riprap and walkway wall heights and revetment slope (β)	44
Table 3-2.	Length, width, height, and estimated weight of the measured rocks	46
Table 3-3.	Mean and standard deviation for rocks parameters	47
Table 3-4.	Design wave characteristics at San Onofre.....	51
Table 3-5.	Largest 20 waves at San Onofre ranked in descending order (1976-1994).....	52
Table 3-6.	Rock weights (W50) for 2020 and 2050.....	53
Table 3-7.	Mean beach widths (ft) at San Onofre, 1990-1993 vs 2017-2022.....	56
Table 4-1.	Run-up and overtopping summary for Medium-High Risk Aversion	67
Table 4-2.	Run-up and overtopping summary for Extreme Risk Aversion (H++)	68

LIST OF FIGURES

Figure 2-1.	Annual and monthly average water level relative to NAVD88 at La Jolla, 1925-2022, and annual global MSL reconstruction.....	17
Figure 2-2.	La Jolla average MSL data, 1925-2022, annual, monthly. Same for 2000-2022. Both with OPC (2018) La Jolla MSLR projections, 2000-2050	18
Figure 2-3.	La Jolla average MSL data, 1925-2022, annual, monthly, with IPCC (2021) LA MSLR projections, 2004.5-2050.....	19
Figure 2-4.	Monthly maximum sea level at La Jolla relative to NAVD88 datum, 1925-2022. Maximum observed 7.62 ft height on 25 November 2015 during 2015-16 El Niño	20
Figure 3-1.	Photograph taken on 20 August 2018, showing the SONGS revetment	30
Figure 3-2.	The revetment at its southern end	31
Figure 3-3.	Top photograph taken on 20 March 2018, before placement of riprap. Bottom photograph taken on 17 December 2019, after placement of riprap within gaps and depredated areas of the revetment	32
Figure 3-4.	Top photograph taken on 15 October 2019, showing the sheet pile seawall before repairing the south end of the walkway. Bottom photograph taken on 17 December 2019, showing the sheet pile seawall after repairing the south end of the walkway	33
Figure 3-5.	Measurements of the long axis of the rock (length)	34
Figure 3-6.	Histograms of rock length, width, and height.....	35
Figure 3-7.	Cumulative distributions of rock length, width, and height.....	36
Figure 3-8.	Trimble SX10 scanning total station.....	37
Figure 3-9.	Location of 21 transects along the revetment, spaced 100 ft apart.....	38

Figure 3-10.	Elevation models of SONGS revetment from Laser Scanner for Transects 1 to 6	39
Figure 3-11.	Elevation models of SONGS revetment from Laser Scanner for Transects 6 to 12	40
Figure 3-12.	Elevation models of SONGS revetment from Laser Scanner for Transects 12 to 18	41
Figure 3-13.	Elevation model of SONGS revetment from laser scanner for Transects 18 to 21	42
Figure 3-14.	Typical revetment cross sections showing slope “ β ” at the indicated section	43
Figure 3-15.	Elevation of the top of revetment for the 21 transects	45
Figure 3-16.	Weight distribution of SONGS revetment rocks	48
Figure 3-17.	Design wave heights for various return periods at San Onofre	49
Figure 3-18.	Measured spectrum density for various storms	50
Figure 3-19.	Historical beach width adjacent to Unit 1, 1928-2000	54
Figure 3-20.	Beach width measured between 1991 through 1993 and between 2016 through 2020	55
Figure 3-21.	Erosion rates for contours at 5, 15, 25, 30, and 50 ft	57
Figure 3-22.	Wave height and wave period from 01 January 2020 to 17 February 2022	58
Figure 3-23.	Wave height and wave period from 01 December 2022 to 17 March 2023	59
Figure 3-24.	North portion of the revetment covered by beach sand in 2020 and a small amount of cobbles exposed in 2022	60
Figure 3-25.	Groundwater elevations for 2022 and for the OPC projections in 2050	61
Figure 4-1.	Wave run-up on a slope	66
Figure 4-2.	Exposed area in the walkway wall	69
Figure 4-3.	Probability of 10-, 25-, 50-, and 100-year waves return period to occur in the next 100 years	70
Figure 4-4.	Joint Probability distribution between significant wave height and tide level	71
Figure A-1.	Location of 21 transects along the revetment, spaced 100 ft apart	A-2
Figure A-2.	DEM comparison between 2020 and 2023, showing Transect 1	A-3
Figure A-3.	DEM comparison between 2020 and 2023, showing Transect 2	A-4
Figure A-4.	DEM comparison between 2020 and 2023, showing Transect 3	A-5
Figure A-5.	DEM comparison between 2020 and 2023, showing Transect 4	A-6
Figure A-6.	DEM comparison between 2020 and 2023, showing Transect 5	A-7
Figure A-7.	DEM comparison between 2020 and 2023, showing Transect 6	A-8
Figure A-8.	DEM comparison between 2020 and 2023, showing Transect 7	A-9
Figure A-9.	DEM comparison between 2020 and 2023, showing Transect 8	A-10
Figure A-10.	DEM comparison between 2020 and 2023, showing Transect 9	A-11
Figure A-11.	DEM comparison between 2020 and 2023, showing Transect 10	A-12
Figure A-12.	DEM comparison between 2020 and 2023, showing Transect 11	A-13
Figure A-13.	DEM comparison between 2020 and 2023, showing Transect 12	A-14
Figure A-14.	DEM comparison between 2020 and 2023, showing Transect 13	A-15
Figure A-15.	DEM comparison between 2020 and 2023, showing Transect 14	A-16
Figure A-16.	DEM comparison between 2020 and 2023, showing Transect 15	A-17

Figure A-17.	DEM comparison between 2020 and 2023, showing Transect 16.....	A-18
Figure A-18.	DEM comparison between 2020 and 2023, showing Transect 17.....	A-19
Figure A-19.	DEM comparison between 2020 and 2023, showing Transect 18.....	A-20
Figure A-20.	DEM comparison between 2020 and 2023, showing Transect 19.....	A-21
Figure A-21.	DEM comparison between 2020 and 2023, showing Transect 20.....	A-22
Figure A-22.	DEM comparison between 2020 and 2023, showing Transect 21.....	A-23
Figure B-1.	Cross sections of SONGS revetment along ranges 1-3	B-2
Figure B-2.	Cross sections of SONGS revetment along ranges 4-6	B-3
Figure B-3.	Cross sections of SONGS revetment along ranges 7-9	B-4
Figure B-4.	Cross sections of SONGS revetment along ranges 10-12	B-5
Figure B-5.	Cross sections of SONGS revetment along ranges 13-15	B-6
Figure B-6.	Cross sections of SONGS revetment along ranges 16-18	B-7
Figure B-7.	Cross sections of SONGS revetment along ranges 19-21	B-8

LIST OF PHOTOGRAPHS

Photo C-1.	Photograph showing revetment covered by sand and fronted by a wide beach at the northern end of SONGS (10 March 2003).....	C-2
Photo C-2.	Photograph showing waves from north swell attacking SONGS revetment at the southern end of SONGS (10 March 2003).....	C-2
Photo C-3.	Photograph showing waves attacking the revetment and the presence of a sand beach at the northern end of SONGS (26 November 2003).....	C-3
Photo C-4.	Photograph showing waves attacking SONGS revetment at the southern end of SONGS (26 November 2003).....	C-3
Photo C-5.	Photograph showing revetment covered by sand and fronted by a wide beach at the northern end of SONGS (02 August 2006)	C-4
Photo C-6.	Photograph showing waves from north swell attacking SONGS revetment at the southern end of SONGS (02 August 2006).....	C-4
Photo C-7.	Photograph showing revetment covered by sand and fronted by a wide beach at the northern end of SONGS (31 January 2006).....	C-5
Photo C-8.	Photograph showing waves from north swell attacking SONGS revetment and refracting towards south at the southern end of SONGS (31 January 2006)	C-5
Photo C-9.	Photograph showing revetment covered by sand and fronted by a wide beach at the northern end of SONGS (31 January 2008).....	C-6
Photo C-10.	Photograph showing waves attacking SONGS revetment at the southern end of SONGS (31 January 2008)	C-6
Photo C-11.	Photograph showing revetment covered by sand and fronted by a wide beach at the northern end of SONGS (12 November 2013)	C-7
Photo C-12.	Photograph showing waves attacking SONGS revetment and refracting towards south at the southern end of SONGS (12 November 2013).....	C-7
Photo C-13.	Photograph showing revetment exposed and fronted by a wide beach at the northern end of SONGS (27 April 2014).....	C-8
Photo C-14.	Photograph showing waves attacking SONGS revetment and refracting towards south at the southern end of SONGS (27 April 2014)	C-8

Photo C-15.	Photograph showing revetment exposed and fronted by a sand beach at the northern end of SONGS (19 February 2018).....	C-9
Photo C-16.	Photograph showing waves from north swell attacking SONGS revetment and refracting towards south at the southern end of SONGS (19 February 2018).....	C-9
Photo C-17.	Photograph showing revetment exposed and fronted by a wide beach at the northern end of SONGS (24 August 2018).....	C-10
Photo C-18.	Photograph showing waves from north swell attacking SONGS revetment and refracting towards south at the southern end of SONGS (24 August 2018)	C-10
Photo C-19.	Photograph showing revetment exposed and fronted by a wide beach at the northern end of SONGS (15 October 2020)	C-11
Photo C-20.	Photograph showing waves attacking SONGS revetment and refracting towards south at the southern end of SONGS (15 October 2020).....	C-11
Photo D-1.	Photograph for Transect 1 taken on 16 February 2023 and 05 March 2020	D-2
Photo D-2.	Photograph for Transect 2 taken on 16 February 2023 and 05 March 2020	D-3
Photo D-3.	Photograph for Transect 3 taken on 16 February 2023 and 05 March 2020	D-4
Photo D-4.	Photograph for Transect 4 taken on 16 February 2023 and 05 March 2020	D-5
Photo D-5.	Photograph for Transect 5 taken on 16 February 2023 and 05 March 2020	D-6
Photo D-6.	Photograph for Transect 6 taken on 16 February 2023 and 05 March 2020	D-7
Photo D-7.	Photograph for Transect 7 taken on 16 February 2023 and 05 March 2020	D-8
Photo D-8.	Photograph for Transect 8 taken on 16 February 2023 and 05 March 2020	D-9
Photo D-9.	Photograph for Transect 9 taken on 16 February 2023 and 05 March 2020	D-10
Photo D-10.	Photograph for Transect 10 taken on 16 February 2023 and 05 March 2020	D-11
Photo D-11.	Photograph for Transect 11 taken on 16 February 2023 and 05 March 2020	D-12
Photo D-12.	Photograph for Transect 12 taken on 16 February 2023 and 05 March 2020	D-13
Photo D-13.	Photograph for Transect 13 taken on 16 February 2023 and 05 March 2020	D-14
Photo D-14.	Photograph for Transect 14 taken on 16 February 2023 and 05 March 2020	D-15
Photo D-15.	Photograph for Transect 15 taken on 16 February 2023 and 05 March 2020	D-16
Photo D-16.	Photograph for Transect 16 taken on 16 February 2023 and 05 March 2020	D-17
Photo D-17.	Photograph for Transect 17 taken on 16 February 2023 and 05 March 2020	D-18
Photo D-18.	Photograph for Transect 18 taken on 16 February 2023 and 05 March 2020	D-19
Photo D-19.	Photograph for Transect 19 taken on 16 February 2023 and 05 March 2020	D-20
Photo D-20.	Photograph for Transect 20 taken on 16 February 2023 and 05 March 2020	D-21

Photo D-21.	Photograph for Transect 21 taken on 16 February 2023 and 05 March 2020	D-22
Photo D-22.	Photograph showing the start of southern riprap at end of walkway taken on 16 February 2023 and 05 March 2020	D-23
Photo D-23.	Photograph showing the middle of southern riprap at end of walkway taken on 16 February 2023 and 05 March 2020	D-24
Photo D-24.	Photograph showing the end of southern riprap at end of walkway taken on 16 February 2023 and 05 March 2020	D-25

EXECUTIVE SUMMARY

This report is being written to comply with California State Lands Commission Special Provision 14 for standards addressing sea level rise that may be required or adopted by local, state, or federal agencies related to the Lease Premises. The report presents the current information about sea level rise projections from the state and federal agency guidelines; assessments for San Onofre Beach and the San Onofre Nuclear Generating Station (SONGS) revetment walkway and seawall; and the impacts of Mean Sea Level Rise (MSLR) on SONGS, including the premises located east of the seawall, such as the Independent Spent Fuel Storage Installation (ISFSI) and its Security Building, and the adaptive capacity of the Lease Premises and facilities therein. This report presents:

- a. MSLR and beach profile assessments; site photographs taken in 2023 of shoreline structures such as riprap, walkways, and seawalls; and descriptions of repair and maintenance operations of shoreline structures. The sea level rise vulnerability information considered the Medium-High Risk Aversion (0.5% probability) projection scenarios from the most recent state guidance (issued by the Ocean Protection Council [OPC] every five years), as well as the extreme H++ projection scenario, and a new technical study by the National Oceanic and Atmospheric Administration (NOAA, 2022) in combination with the annual and 20-year events, as well as extreme high tide heights (“King Tides”). Pertinent information may be sourced from Southern California Edison (SCE), or any other research conducted within the region that is relevant to conditions at the Lease Provision 14(a).
- b. Quarterly groundwater elevation data collected from onsite monitoring wells relevant to conditions at Lease Provision 14(b).

Chapter 1 presents the overall structure of this report and provides a summary of the key information presented in this study with emphasis on the main points outlined in Special Provision 14.

Projections of future MSLR are evolving continuously as the understanding of key climate change processes improves (Chapter 2). In Sections 2.2.1 and 2.2.2, we summarize the currently existing guidelines applicable MSLR guidance, unchanged since OPC (2018), and the newly issued Intergovernmental Panel on Climate Change (IPCC 2021, 2022) findings. In Section 2.2.3, we present sea level rise projection from the NOAA (2022) technical study; these results were lower than OPC (2018) medium- high and H++ scenarios and within the range of IPCC (2021, 2022) projections for global sea level rise projections. The NOAA (2022) is the key technical input for the Fifth National Climate Assessment NCA5 to be published in 2024-2025. A summary Maximum high-water level applicable to SONGS is discussed in Section 2.3. Overall, the new IPCC (2021, 2022) projections are lower than existing guidance.

The beach prevents toe scouring, which can undermine the revetment and cause rock units to settle. When the beach is narrow or water level unusually high, or both, waves breaking on the revetment can cause dislocation of individual rocks, which contributes to revetment instability. Section 3.7 gives a summary of San Onofre Beach assessments based on SCE’s beach

monitoring program at San Onofre Beach from 1964 to the present, with gaps, presented in Appendix E. These data will be valuable as sea level rise accelerates in the future. Elwany *et al.* (2017, 2022) have addressed the impacts of sea level rise on San Onofre Beach and the cliffs.

The assessment of the SONGS revetment is reviewed in Chapter 3. Revetment maintenance carried out in 2018 and 2019 is summarized in Section 3.1.1. In Section 3.2 and Appendices A, B, C, and D, we gauge the current revetment condition and describe the characteristics of the riprap, namely rock, and dimension and weight distributions, based on a site inspection carried out on 19-20 January 2023 and 16 February 2023. We evaluate the revetment stability based upon these observations and standard coastal engineering criteria (Sections 3.8 to 3.10).

This study finds that the revetment, in its present condition, is likely to tolerate wave forces with acceptable rock movement that will not affect the integrity of the revetment as a whole. The study found that, as designed and with minimum regular maintenance, the revetment will withstand wave forces over the next 30 years (Section 3.10). The revetment, retaining wall, and walkway also provide additional protection to the SONGS seawall. Appendix C presents historical aerial photographs of the revetment for the period from 2003 to 2020. Photographs were taken during the site visits. Selected photographs of the beach taken on 16 February 2023, after the revetment laser scanner survey on 19 January 2023, are presented in Appendix D.

Section 3.10 addresses the maintenance and adaptive capacity of the Lease Premises. The major threats to revetment stability in the future include wave storms, or clusters of wave storms, such as those that occurred from 1981 to 1983. In this respect, the revetment's adaptive capacity to MSLR is high, in the sense that its current stable condition, along with occasional maintenance, will allow it to continue functioning as intended.

Impacts of groundwater on the ISFSI based on quarterly measurements of the groundwater from 9 coastal wells out of 16 total wells are presented in Appendix F. The OPC (2018) medium-high (0.5%) and H++ SLR scenarios for groundwater elevation for 2050 are 4.74 and 5.54 feet (ft) National Geodetic Vertical Datum (NGVD) (Appendix F, Section 3) and are 1.62 and 0.82 ft lower than the bottom of the ISFSI support foundation, respectively. The ISFSI support foundation is 3 ft thick.

The analysis of vulnerability of the revetment to wave run-up and overtopping of the revetment is presented in Chapter 4. This study considers the Medium-High Risk Aversion projection (0.5%) and extreme H++ projection scenarios from the most recent state guidance issued by the OPC (2018) in combination with the annual, 2-, 5-, 10-, 25-, 50-, and 100-year wave return period wave and high water events, which include storm surges and King Tides. Our conclusions are stated in Chapter 4.

SAN ONOFRE NUCLEAR GENERATING STATION (SONGS) MEAN SEA LEVEL RISE IMPACT ASSESSMENT

Technical Report Provision 14 in Lease No. PRC 6785.1

1.0 INTRODUCTION

This report has been compiled per Lease Provision 14 in the California State Lands Commission Lease No. PRC 6785.1 for the use, maintenance, and decommissioning of existing offshore improvements associated with the San Onofre Nuclear Generating Station (SONGS). Lease Provision 14 requires, as part of compliance with applicable provisions or standards addressing sea level rise that may be required or adopted by local, state, or federal agencies related to and affecting the lease premises, that the Lessee provide an annual summary, including information related to sea level rise vulnerability, structural integrity, and adaptation capacity of the Lease Premises and the facilities therein.

The information in this report includes sea level rise discussion and beach profile assessments, annual site photographs of shoreline facilities (i.e., riprap, pedestrian walkway, and seawall), and description of repair and maintenance operations for shoreline facilities. Sea level rise vulnerability information considers the Medium-High Risk Aversion (0.5% probability) projection scenarios from the most recent state guidance (issued by the Ocean Protection Council [OPC] every five years), as well as the extreme H++ projection scenario, in combination with the annual, 20-year, and 100-year storm events, as well as with extreme high tide heights (“King Tides”). The information in this report also includes the sea level rise projection from the National Oceanic and Atmospheric Administration (NOAA; 2022) technical study. Pertinent information may be sourced from Southern California Edison (SCE), and likewise quarterly groundwater elevation data collected from onsite monitoring wells, or any other research conducted within the region that is relevant to conditions at the Lease Provision 14(b).

In Chapter 2 of this report, we summarize the present knowledge of Mean Sea Level Rise (MSLR) using state and federal agency guidelines. These guidelines are evolving constantly in response to the rapid pace of data acquisition and scientific understanding of MSLR, especially concerning the long-term consequences of accelerating ice sheet melt in Greenland and Antarctica. We presented agency guidance current as of 2018 and the associated MSLR projections in order to determine impacts on the SONGS shoreline and cliffs, and the likelihood of wave overtopping of the seawall in Elwany *et al.*, 2016 and 2017. The latest MSLR projections from the Intergovernmental Panel on Climate Change (IPCC), Sixth Assessment reports (AR6, IPCC 2021, 2022), and results from NOAA (2022) technical report are also discussed. This study is the basis for the Fifth National Climate Assessment NCAS.

The SONGS revetment provides protection to the SONGS seawall and is essential to maintaining the walkway that enables safe lateral access for beach users. The revetment shelters the walkway from most wave run-up and overtopping, thus preventing or reducing negative impacts to lateral beach access due to flooding and other hazards of high water levels and waves.

The presence of the revetment and walkway fronting the seawall eliminates wave impacts on the seawall.

The assessment of the SONGS revetment is reviewed in Chapter 3. In Chapter 3, we also determine the current revetment and walkway exposure and vulnerability to waves and high water level events by gauging their present condition. We describe the characteristics of the riprap, namely rock, and dimension and weight distributions, based on a site inspection in January 2022. We evaluate its stability based upon these observations and standard coastal engineering criteria. The importance of the sand beach fronting the revetment is discussed in Section 3.7, along with the recent characteristics of the beach nearby SONGS and observed short- and long-term erosion and accretion patterns based on the ongoing beach profile surveys carried out in 2017-2022 (Appendix F). Additionally, in Section 3.10, we discuss the adaptive capacity of the Lease Premises and structures and present an adaptive management plan to maintain the facilities, such as the revetment, walkway, and seawall, Independent Spent Fuel Storage Installation (ISFSI), and its Security Building in good condition during the lease agreement.

MSLR will likely increase both the wave forces on the rocks (due to greater water depth and wave height fronting the revetment), and sand scour undermining that could lower and destabilize the revetment (due to beach retreat). This study considers the Medium-High Risk Aversion projection (0.5%) scenarios from the most recent state guidance issued by the OPC (2018), as well as the extreme H++ projection scenario, in combination with the annual 2-, 5-, 10-, 25-, 50-, and 100-year return period wave and high water events, which include King Tides. The vulnerability of the revetment to wave run-up and the overtopping analysis of the revetment are presented in Chapter 4.

Our study finds that the revetment, in its present condition, is likely to tolerate wave forces with acceptable rock movement that will not affect the integrity of the revetment as a whole. The study found that, as designed and with minimum regular maintenance, the revetment will withstand wave forces over the next 30 years.

The walkway behind the revetment at elevation 14 feet (ft NGVD) is relatively low and likely will be overtopped under large wave conditions, especially if these occur during extreme high water levels. However, the impact of wave run-up and overtopping on the walkway itself or on public access is limited and temporary, since the beach will not be accessible during such conditions, and floodwater has adequate drainage from the site and off the public walkway. Our major conclusions are stated in Chapter 5.

Chapter 6 provides a reference list, followed by six Appendices (A-F). Appendices A, B, C, and D provide information regarding the 19 January 2023 survey carried out at the SONGS revetment, including the location of the transects, the profiles analyzed along the riprap, and the photographs taken during the survey. Appendix E presents our assessment of the San Onofre Beach and the results of the beach profile surveys carried out at San Onofre Beach from 2017 through 2022. Appendix F is written in compliance with Provision 14(b); this Chapter discusses the groundwater elevations measured quarterly in 2022 and the MSLR impacts on the ISFSI up to 2050. The 2022 quarterly groundwater elevation monitoring program was carried out by SCE.

2.0 MEAN SEA LEVEL RISE IMPACT ASSESSMENT

This chapter presents future MSLR and extreme high-water levels in order to determine facility flooding and structural integrity risks. In this chapter, we summarize the latest MSLR projections developed by the California OPC (2018) and adopted by the California Coastal Commission (CCC 2015, updated 2018) as official stage guidance for coastal development. The latest MSLR projections from the Intergovernmental Panel on Climate Change (IPCC), Sixth Assessment reports (AR6, IPCC 2021, 2022) and technical study prepared by NOAA (2022) entitled “Global and Regional Sea Level Rise Scenarios for the United States (U.S.)” which is the key technical input for the Fifth National Climate Assessment (NCA5), are also discussed.

Sea level in this context refers to past measured and future projected mean and extreme (high) water levels, both globally and regionally. Coastal water levels in the San Diego area, including San Onofre, are well represented by data from the La Jolla tide gauge (NOAA Station 941-0230) located at the end of the UC San Diego/Scripps Institution of Oceanography (SIO) pier. SONGS area tide and other water level fluctuations are also well represented by data from the Los Angeles (LA) tide gauge (NOAA Station 941-0660) located in Los Angeles Harbor, although the overall historical MSL upward trend is lower at LA than La Jolla.

Figure 2-1 shows the annual and monthly average water levels measured at the La Jolla tide gauge from 1925 to 2022 (black line/symbols, and grey dots, respectively), compared with the global trend (red line) reconstructed by Church and White (2011) from 1880-2009, and extended to 2021 using NASA data (Beckley *et al.*, 2010). Note that the trend of 0.67 ft/century at La Jolla is about 30% greater than the overall global trend of 0.51 ft/century. The acceleration of MSLR about 1970 is also evident, as recognized in the AR6 reports (IPCC 2021, 2022), further considered below.

As expected, regional month-to-month, year-to-year, and decadal water level fluctuations are much larger than corresponding variations in global sea level. This is mainly due to seasonal fluctuations mainly driven by weather changes for the monthly data, as well as El Niño and large-scale oscillations in North Pacific Ocean circulation (e.g., Bromirski *et al.*, 2011, 2012; Flick, 1998, 2016) for monthly, year-to-year, and decadal variability that varies from region to region. Note for example that 2016-2022 annual levels at La Jolla show a small and likely short-term downward trend associated with large-scale cooling in the North Pacific.

2.1 SONGS SEA LEVEL INFORMATION

Over multi-decades timescales, the primary reasons of changes in sea level are the thermal expansion due to the heating of the addition of water mass associated with ice-mass loss from ice sheets and glaciers. On shorter term changes in sea level rise are driven by the El-Niño Southern Oscillation. Sea level rates can deviate significantly from one regional location to another and are not uniform across the globe, since it regionally responds to several key factors important at regional and local scales, such as subsidence or uplift, that can change the height of sea level relative to land (Kopp *et al.*, 2014).

Elwany, *et al.* (2016) “*Coastal Analysis for End-State Planning of San Onofre Nuclear Generating Station, Phase 1*” presented a detailed description of the regional tide patterns; reconstructed and observed mean sea levels, including long-term sea level rise since the last global deglaciation 20,000 years ago, and modern changes from before the industrial revolution (about 1700), through 2015; conditions that cause extreme high coastal water levels, including El Niño and storm surges; and MSLR projections being used by state and federal agencies at the time. The report presented a table summarizing all MSLR projections available at the time. The projections included the first CCC guidance document (2015), NRC (2012) that contained projections through 2100 for Washington, Oregon, and California, and those from the IPCC Fourth Assessment Report (AR4, IPCC 2013).

Elwany, *et al.* (2017) “*Coastal Processes Analysis at San Onofre Nuclear Generating Station, Phase 2*” refined and expanded the MSLR projections in Elwany *et al.* (2016) by including work sponsored by the State of California (Cayan *et al.*, 2016) that produced probability estimates associated with each scenario. This work eventually led to the OPC (2018) guidance adopted state-wide, and especially by the CCC (2015, updated 2018). Elwany *et al.* (2017) also considered the influence of extreme water elevations combined with large waves and the quantified the run-up for these conditions, particularly as it affected potential SONGS sea wall overtopping.

Elwany, *et al.* (2020) “*San Onofre Nuclear Generating Station (SONGS) Mean Sea Level Rise Impact Assessment, Summary Report*” introduced new California state agency documents that provide updated MSLR policy, plans, or other information potentially affecting SONGS activities. State agency advances include four reports that essentially laid out the guidance provisions still in effect as of this writing in early 2022. These reports were: Griggs *et al.* (2017) from the California Ocean Protection Council and Ocean Science Trust; Bedsworth *et al.* (2018) titled, “*California’s Fourth Climate Change Assessment, Statewide Summary Report*” from the California Governor’s Office of Planning and Research, Scripps Institution of Oceanography, California Energy Commission, and California Public Utilities Commission; OPC (2018) with update sea level rise guidance; and CCC (2015, updated 2018), which adopted the OPC (2018) framework as its official policy.

Elwany, *et al.* (2021) “*San Onofre Nuclear Generating Station (SONGS), SONGS Mean Sea Level Rise Impact Assessment, Technical Report, Provision 14 in Lease No. PRC 6785.1*” gave a discussion of MSLR vulnerability of the revetment fronting SONGS and an update of the sea level information presented in Elwany *et al.* (2020). This included a summary of existing State of California guidance; 2020 mean sea level (MSL) data and the relation of measurements and projections of future MSLR since 2000; 2020 monthly peak total water level data; a review of published scientific literature potentially influencing future MSLR projections, and therefore state guidance; and an update of 2020 California state agency developments with respect to MSLR that may impact SONGS activities. New California state agency documents included CCC (2020a), CCC (2020b), OPC (2020), and CNRA-CEPA (2020).

2.2 MEAN SEA LEVEL RISE GUIDANCE

Current CCC MSLR guidance (CCC 2015, updated 2018) for coastal development is based on findings from OPC. OPC (2018) developed a set of probability-of-occurrence future MSLR scenarios through 2150, relative to 2000. This study considers the extreme H++ projection scenario from this guidance, and in combination with the 1-, 2-, 10-, and 100-year return period high-water events, which include so-called “King Tides” through 2050. We compare the OPC (2018) guideline scenarios with newly published future MSLR trajectories (also made to 2150), from the latest IPCC reports (AR6, IPCC 2021, 2022). In summary, the IPCC projections are lower than those from OPC.

OPC (2018) contains MSLR projections specific to numerous California coastal areas, including La Jolla. This was part of a statewide effort to improve upon projections from IPCC AR5 (IPCC 2013, 2014) in three respects: First, to produce a low-probability but large-impact extreme high scenario (i.e., H++) that AR5 was missing due to lack of consensus on future rates of Greenland and Antarctic ice contributions; Second, to assign likelihood probabilities for an array of future MSLR scenarios based on the IPCC AR5 “Representative Concentration Pathway” (RCP) future global socio-economic ranges considered; And finally, to make available regional projections for different parts of the California coast.

MSLR projections are continuously evolving in response to rapid data acquisition and improved scientific understanding of key climate change processes (e.g., IPCC 2021, 2022 for a full discussion). Of special concern are the possible ongoing and future ranges and rates of glacial ice loss in Greenland and Antarctica (e.g., DeConto and Pollard, 2016). Future MSLR is highly uncertain, especially after about 2050, for several reasons. The largest unknown is what mitigation strategies humans will employ to decrease the rates and amounts of greenhouse gas (GHG) emitted and ultimately resident in the atmosphere. Second, the climate sensitivity, or amount and rate of warming for a given increase in GHGs is not precisely known. In particular, polar ice response to existing and future warming is not yet reliably predictable.

2.2.1 California OPC (2018) MSLR Projections

With one caveat concerning a potential increase in the maximum State of California MSLR guidance target value from 2.8-3.5 ft by 2050 (please see Elwany *et al.*, 2021 for details), the currently existing guidance, so far unchanged, is summarized herein. OPC (2018) and CCC (2015, updated 2018) MSLR projections for La Jolla from 2000-2050 are listed in Table 2-1. These projections have probability ranges associated with them that originated from IPCC AR5 (2013) by calculating probabilities of each RCP scenario, as mentioned above. Each RCP has a numerical designation condensing a host of projected socio-economic factors into a final average global radiation imbalance in Watts/m² by 2100. The full range is RCP2.6 to RCP8.5, respectively from “Low” to “High.” Thus, for example, “RCP4.2” represents a “Moderate” total GHG trajectory that results in a net radiative Earth heating imbalance 4.2 Watts/m² by 2100. The probability estimates use the framework of Kopp *et al.* (2014).

From 2000-2050, only the “High” MSLR set of trajectories are considered in OPC (2018). This is based on two factors: First, there are no ambitious global GHG emissions reduction plans presently apparent, and second, even if emissions immediately dropped to net-zero, warming and MSLR would continue for at least many more decades owing to ocean warming and ice-melt inertia. In effect, both High and Low trajectories produce near-identical projections between 2000 and 2050, and only begin to differ after mid-century.

Table 2-1 shows five columns (Columns 2-6) headed with percentage probability numbers, and one (Column 7) indicated as H++. Column 2 titled “50%” indicates the median projected MSLR each year (Column 1) relative to 2000. That means, for example, there is a 50:50, or “even” chance that MSLR will be less than or greater than 0.9 ft by 2050, that is from 2.5-3.4 ft NAVD88¹ relative to 2000. Columns 3-4 titled “Lo > 67% < Hi” bracket the 2/3 probability that MSLR will fall outside these numbers. In other words, it is 2/3 likely that MSLR will be above the 67% Lo trajectory (Column 3) and 2/3 likely that it will be below the 67% Hi projection (Column 4). Equivalently, it is 1/3 likely that MSL will reach between 3.2-3.7 ft by 2050, and 1/3 likely each that it will remain either below 3.2 ft, or rise above 3.7 ft. Columns 5 and 6, respectively, provide the MSLR path that has a 5%, or “1 in 20,” and a 0.5% or “1 in 200” chance of being exceeded. This means there is only a 1 in 200 chance that MSL will reach or exceed 4.5 ft by 2050. The H++ scenario (Column 7) is included in OPC (2018) to account for the for now still remote possibility that “...rapid ice sheet loss on Antarctica could drive rates of sea level rise in California above 50 mm/year (2 inches/year) by the end of the century, leading to potential sea level rise exceeding 10 feet. This rate of sea level rise would be about 30-40 times faster than the sea level rise experienced over the last century.” This suggests there is an unquantifiable, but small, probability that MSL will reach 5.3 ft or higher by 2050 Table 2-1, Column 7).

Figure 2-2 (upper and lower) illustrate the OPC (2018) trajectories described above along with the actual average annual and monthly MSL data measured at the La Jolla tide gauge also shown in Figure 2-1. The projections in Figure 2-2 were adjusted so their average over the 19-year epoch 1991-2009 (centered on year 2000) was 2.5 ft NAVD88¹ to be 2.5 ft NAVD88 to match the corresponding average value of the observations over the same epoch.² Figure 2-2 (upper) shows the entire measured water level record from 1925-2022, along with the projections from 2000-2050. Figure 2-2 (lower) is the same information but focused from 2000-2050 to facilitate comparison between data and projections. This shows that all annual average except 2015 so far fall close to or below the 50-50 trajectory (blue broken line). This could be interpreted to mean that the OPC (2018) projections since 2000 overestimate actual MSLR. However, as Figure 2-1 indicates, the natural inter-annual variability range is about 0.5 ft, while the seasonal and other variations in monthly means ranges about 1.2 ft, which is larger than the current difference between the highest and lowest scenarios (~0.4 ft). Which trajectory MSLR is

¹ NAVD88 – North American Vertical Datum of 1988 – A fixed geodetic reference for elevations determined by geodetic leveling of the United States, Canada, and Mexico. NAVD88 is currently the official national reference used by engineers and surveyors and supported by NOAA-National Geodetic Service. Geodetic reference elevations do not change with MSL, as opposed to tidal datums, which do.

² For details concerning datum adjustments for these purposes please see Flick *et al.* (2013).

actually on should become more apparent approaching mid-century (2035-2050), when projected values increase significantly and their range broadens to 1-2 ft

2.2.2 IPCC (2021) MSLR Projections

Following the IPCC (2013, 2014) AR5 reports, and in accord with its approximately seven-year cycle, the IPCC has prepared the Sixth Assessment Report (AR6, IPCC 2022) released in September 2022. Three specialized working groups have contributed to this undertaking, including Working Group I (WGI), which published its findings concerning the “*Physical Science Basis*” in IPCC (2021). The topics assessed by WGI cover: atmospheric GHGs and aerosols; air, land, and ocean temperature changes; climate sensitivity; extreme weather; and hydrological, glacier, ice sheet, ocean, sea level, carbon cycle, and biogeochemical processes. WGI combined modern observations, paleoclimate data, and extensive, international, inter-comparison data-adaptive modeling to build a more robust picture of Earth’s climate and its rapid changes.

Not surprisingly, the primary conclusion of the WGI (IPCC 2021) report is²:

A.1 It is unequivocal that human influence has warmed the atmosphere, ocean and land. Widespread and rapid changes in the atmosphere, ocean, cryosphere and biosphere have occurred.

Specific to sea level rise, key findings include:³

A.1.7 Global mean sea level increased by 0.20 m between 1901 and 2018. The average rate of sea level rise was 1.3 mm yr⁻¹ between 1901 and 1971, increasing to 1.9 mm yr⁻¹ between 1971 and 2006, and further increasing to 3.7 mm yr⁻¹ between 2006 and 2018. Human influence was very likely the main driver of these increases since at least 1971.

A.2.4 Global mean sea level has risen faster since 1900 than over any preceding century in at least the last 3,000 years. The global ocean has warmed faster over the past century than since the end of the last deglacial transition (around 11,000 years ago).

B.5 Many changes due to past and future greenhouse gas emissions are irreversible for centuries to millennia, especially changes in the ocean, ice sheets and global sea level.

B.5.4 Sea level is committed to rise for centuries to millennia due to continuing deep ocean warming and ice-sheet melt and will remain elevated for thousands of years. Over the next 2,000 years, global mean sea level will rise by about 2-3 m if warming is limited to 1.5°C, 2-6 m if limited to 2°C and 19-22 m with 5°C of warming, and it will continue to rise over subsequent millennia (low

³ Some conclusions edited or shortened for clarity and brevity. Original report heading numbers retained.

confidence). Projections of multi-millennial global mean sea level rise are consistent with reconstructed levels during past warm climate periods: likely 5-10 m higher than today around 125,000 years ago, when global temperatures were very likely 0.5°C-1.5°C higher than 1850-1900; and very likely 5-25 m higher roughly 3 million years ago, when global temperatures were 2.5°C-4°C higher.

A vital part of the massive 3,949-page WGI “*The Physical Science Basis*” document (IPCC 2021) is the development of new MSLR projections, both for the global mean trajectory, and for regional trajectories at hundreds of coastal and island locations around the world. Projection data are publicly available, through a creative commons international license, from the National Aeronautics and Space Administration (NASA)⁴ (Fox-Kemper *et al.*, 2021, Garner *et al.*, 2021). Inexplicably, only projections from San Diego Bay Quarantine Station and LA are available nearest San Onofre, while La Jolla is absent. While the LA tide regime closely matches that at La Jolla, the overall historical upward MSLR trend at LA (1 mm/yr) is half that at La Jolla (2 mm/yr), over the period of 1925-2020. However, the trends are much more similar from 1975-2021, with 1.6 mm/yr at LA and 1.8 mm/yr at La Jolla. In addition, IPCC (2021) projection trends at other southern California locations and Ensenada, Mexico available on the NASA website suggest that these are at least similar or nearly identical to LA. It is therefore assumed that projections at La Jolla, if they had been made, would be the same as those at LA, so these are utilized in this report.

IPCC uses two conditional descriptors, “*likelihood*,” and “*confidence*” to characterize their conclusions and projections, including, MSLR. “*Likelihood*” gauges the probability spread that a projection will fall in a specified numerical range. Likelihood is quantifiable, and spans high to low (probability) from, “*virtually certain*” (99-100%); “*very likely*” (90-100%); “*likely*” (66-100%); “*about as likely as not*” (33-66%); “*unlikely*” (0-33%); “*very unlikely*” (0-10%); to “*exceptionally unlikely*” (0-1%). “*Confidence*,” on the other hand, is not quantitative or statistical, but a more subjective assessment of how reliable a particular result may be. Confidence levels range from “*very low*,” “*low*,” “*medium*,” “*high*,” to “*very high*.” These terms are based on IPCC “*author teams’ judgments about the validity of findings as determined through evaluation of evidence and agreement*” (Mastrandrea *et al.*, 2010).

Like OPC (2018), the IPCC (2021) MSLR projections are based on an intricate analysis of a wide range of possible future Earth warming scenarios and the processes that contribute to MSLR. These include ocean warming and resulting expansion, addition of water from land-based ice melt, changes in freshwater runoff due to global groundwater pumping and dam construction, changes in ocean circulation that affect the dynamical water height at coasts, and land movement such as uplift from glacial unweighting, among others.

AR6 (IPCC 2021) produced future MSLR projections that could be made with at least “*medium confidence*,” or somewhere near the middle of the confidence range. The projections

⁴ <https://sealevel.nasa.gov/ipcc-ar6-sea-level-projection-tool>

were based on five possible future climate evolutions termed “*Shared Socioeconomic Pathway*” (SSP) scenarios that are analogous to, but broader than, the “Representative Concentration Pathway” (RCP) trajectories used in AR5 (IPCC 2013). The MSLR projections are assessed based on the combination of uncertainty in temperature change associated with emissions scenarios, and uncertainty in the relationships between global temperature and processes responsible for projected MSLR. In this context, “*likely*” means a probability of occurrence at least 66%. Each scenario has a low, median, and high MSLR amount associated with it for 2030, 2050, and additional years through 2150 relative to 2004-2005 (adjusted to 2000).

The five IPCC (2021) scenarios are described as follows and involving “*very likely*” (i.e., at least 90% probable) global temperature increases by 2100 above the 1850-1900 median:

- **SSP1-1.9** – Low emissions scenario with net-zero CO₂ by mid-century (~2050). Temperature warming projected as 1.0°-1.8°C by 2100, after a slight overshoot.
- **SSP1-2.6** – Low to moderate pathway with net zero emissions in second half of century (2050-2100). Warming 1.3°-2.4°C.
- **SSP2-4.5** – Moderate scenario in line with upper end of aggregate “Nationally Determined Contribution” emission by 2030. Warming 2.1-3.5°C.
- **SSP3-7.0** – Medium to high “reference” scenario with no additional climate policy (i.e., “business as usual”), resulting in particularly high non-CO₂ emissions, including high aerosols. Warming 2.8°-4.6°C.
- **SSP5-8.5** – High “reference” scenario with no additional climate policy. Emission levels from fossil fueled SSP5 socioeconomic development pathway. Warming 3.3-5.7°C.

A sixth “*low confidence*” but high potential impact scenario projection (“**SSP5-8.5Lo**” herein, where “Lo” stands for “Low Confidence”) added for the first time by IPCC in AR6 indicates the possible, but as yet unlikely, effects of deeply uncertain ice sheet processes supported by limited evidence and little current agreement among experts. The projection uses Greenland and Antarctic findings from a “Structured Expert Judgement” study by Bamber *et al.* (2019), and results from Antarctic marine ice cliff instability simulations by DeConto *et al.* (2021). This scenario is roughly comparable to the OPC (2018) H++ trajectory, albeit with a considerably lower upper range of MSLR.

The IPCC (2021) projections use the 20-yr period 1995-2014 (center years 2004-2005) as their base with MSLR reckoned from there. This is slightly different from the OPC projections, which used a 19-yr base of 1991-2009 (center year 2000). However, the adjustment for the LA MSLR projections to make their start year 2000 is small, about 0.014 ft, which has been applied in what follows.

This report concerns projected MSLR through 2050. The relevant IPCC (2021) values are summarized in Tables 2-2 and 2-3 and plotted in Figure 2-3. Table 2-2 shows the median MSLR value for each SSP scenario for 2000, 2030, and 2050 in ft NAVD88. Table 2-3 shows the range low to high for each scenario. Comparison with the OPC (2018) scenarios (Table 2-1, Column 7)

shows that the IPCC (2021) SP5-8.5Lo values in 2030 and 2050 (Column 7) are 0.7 ft and 1.9 ft lower, respectively, than the OPC (2018) H++ numbers. Furthermore, Tables 2-2 and 2-3 (Columns 7) suggest that the range from 2000-2050 of the SSP5-8.5Lo scenario is fairly small, with the median value rising 0.8 ft (2.5-3.3 ft), and a low to high range change of 0.6-1.4 ft (2.5-3.1 ft and 2.5-3.9 ft, respectively). Except for the H++ and SSP5-8.5Lo scenarios, the (respective) OPC (2018) and IPCC (2021) trajectories in Tables 2-1 to 2-3 are not directly comparable, since the IPCC SSP scenarios do not have associated probabilities of occurrence, only that they are “*very likely*.” However, the overall results suggest that all IPCC scenarios produce mostly lower, or at most equal, projected MSLR by 2050 than all OPC trajectories, including H++.

Figure 2-3 illustrates the narrow range of likely MSLR from IPCC (2021) between now and 2050. The high, median, and low SSP5-8.5Lo MSLR scenarios are shown with solid red lines. The spread between high and low in 2050 is 0.8 ft (i.e., 3.1-3.9 ft, Column 7). The remaining SSP scenario median value trajectories (broken lines) are labelled only with their numerical value range, and “Conf” indicating “*medium confidence*,” and “Mid” meaning “*median*” values (Table 2-2), as opposed to the “low” to “high” range (Table 2-3). All median values of the lowest five SSP trajectories (Table 2-2, Columns 2-6) fall between the median and low SSP5-8.5Lo projections. Finally, it is apparent that the IPCC (2021) projections more closely fit the data from 2000-2021 compared to the OPC (2018) scenarios.

2.2.3 NOAA Global and Regional MSLR Scenarios

The report considers two sources of uncertainty which are: 1) increase emissions will cause ice-mass loss and ocean expansions causing local ocean dynamic changes; 2) increasing the amount of greenhouse gases in the atmosphere leading to climate change and its effects on temperature and sea level rise. These uncertainties are combined to generate five sea level scenarios (low, intermediate-low, intermediate, intermediate-high, and High) The sea level scenarios are related to but distinct from the emissions pathway scenarios IPCC AR6 (Table 2-4).

With increasing tidal gauges number and the surface elevation records over decades the impact of natural sea level variability on estimated rates and accelerations is not significant. Tidal gauges provide data exceeding 100 years in some locations and satellite altimeter record is nearing 30 years. These data with appropriate consideration of uncertainty can be informative in the near term (2000-2050).

Over near term (2000-2050) natural variabilities in tidal data due to El Niño-Southern Oscillation, Pacific Decadal Oscillation and North Atlantic Oscillation were removed through regression analysis (Calafat *et al.*, 2012; Hamlington *et al.*, 2021). Estimates of sea level rise and acceleration were estimated from extrapolating of historical tidal time series and each term is assessed in order to account for the influence of remaining natural variability.

After 2050 the assessments and comparison made using the observations-base extrapolations of future sea level rise become less informative. In addition, these estimates will

be associated with large projected ranges, and they may not be reflective of shifts or process that may occur in the future. Emissions and climate changes are main sources of uncertainties for sea level projections after 2050.

Computation made for the trajectories of the five scenarios from low to high were updated based on global warming levels (see Table 2-4) rather than the emissions scenarios and establishes connection to global temperature monitoring efforts. This approach is based on method used on IPCC AR6 (Fox-Kemper *et al.*, 2021; Garner *et al.*, 2021). The results of sea level projections / extrapolation (2000-2050), at Los Angeles from NOAA (2022) is presented in Table 2-5 for intermediate low, intermediate, intermediate High, and High scenarios from 2020 to 2100 relative to 2000. Columns 2 to 4 indicates the median projected MSLR each year relative to 2000. That means, there is a 50:50 chance that MSLR per year will be less than or greater than presented numbers. Currently the NOAA 2022 report does not give scenario occurring after 2100.

Comparison by year between NOAA (2022) median MSLR values and IPCC (2021) mid and low-high MSLR projections are presented in Table 2-6 for years 2030 and 2050.

2.3 SONGS SEA LEVEL EXTREMES

It is important to recognize that water elevation at or around MSL generally does not cause flooding, erosion, or infrastructure damage. Damages almost always occur during times of extreme high water levels that, on the California coast, are driven mainly by coincidence of peak high tides and large storm waves. Elevated water levels due to El Niño-Southern Oscillation, Pacific Decadal Oscillation, North Atlantic Oscillation, and other large-scale oceanographic phenomenon also raise maximum water levels for months to several years. Of course, a continued and likely accelerated MSLR will continuously worsen these effects causing them to become more severe and last longer.

Observed maximum monthly water levels (in ft NAVD88) published by NOAA for the La Jolla tide gauge are plotted in Figure 2-4, which is updated from Elwany *et al.* (2020). It is apparent that monthly maxima are increasing as sea level rises, which is expected to continue in the future. Table 2-7 lists the six highest maximum monthly water levels observed at La Jolla relative to NAVD88 and NGVD.⁵ The legacy NGVD was useful since it regionally lay close to MSL in the past. While NGVD is no longer supported by NGS or routinely employed by surveyors and engineers, it is still beneficial because of its extensive and long use for coastal measurements and studies, including many at SONGS. NGVD lies 0.43 ft below current MSL (as defined by the 1983-2001 epoch), and 2.11 ft below NAVD88.).

The all-time maximum reading occurred on 25 November 2015 during the 2015-16 El Niño warming event, which also produced the highest-ever annual average level observed at

⁵ NGVD – National Geodetic Vertical Datum - A fixed geodetic reference for elevations determined by leveling in the United States and Canada. Also known as “NGVD29” or “MSL29.” This is a legacy datum no longer supported by NOAA-National Geodetic Survey.

La Jolla. Note that the four highest events exceeding the previous record elevation of 1983 occurred in only 18 years, from 1997-2015.

NOAA-NOS also provides statistics of extreme sea levels based on the observations discussed. Their current estimates of return periods or the probability of exceeding a given value in any year are summarized in Table 2-8 relative to NAVD88 and NGVD. Note the relatively small spread of less than 1 ft between the 1% (100-yr) and 99% (1-yr) extreme high water level events. This illustrates the dominant influence of the astronomical tide on extreme water levels along the California coast. The highest tide is about 7 ft above NAVD88, less than about 0.5 ft below the 100-yr return event. It also illustrates the exceedingly rare coincidence of peak high tides with extraordinary storm surges or other water level enhancing processes, such as El Niño, which can raise MSL up to about 1.5 ft over time scales of days to a year.⁶

⁶ See Flick (2016) for details exemplified by the 2015-16 El Niño winter.

Table 2-1. OPC (2018) MSLR projections, La Jolla (ft NAVD88).

1	2	3	4	5	6	7
Year	50%	Lo > 67% < Hi		5%	0.5%	H++
2000	2.5	2.5	2.5	2.5	2.5	2.5
2030	3.0	2.9	3.1	3.2	3.4	3.6
2040	3.2	3.0	3.4	3.5	3.8	4.3
2050	3.4	3.2	3.7	3.9	4.5	5.3

Table 2-2. IPCC (2021) mid-range MSLR projections, Los Angeles (ft NAVD88).

1	2	3	4	5	6	7
Year⁷	SSP1-1.9	SSP1-2.6	SSP2-4.5	SSP3-7.0	SSP5-8.5	SSP5-8.5⁸
2000	2.5	2.5	2.5	2.5	2.5	2.5
2030	2.8	2.9	2.9	2.9	2.9	2.9
2050	3.1	3.2	3.2	3.2	3.3	3.3

Table 2-3. IPCC (2021) low-high range MSLR projections, Los Angeles (ft NAVD88).

1	2	3	4	5	6	7
Year⁸	SSP1-1.9	SSP1-2.6	SSP2-4.5	SSP3-7.0	SSP5-8.5	SSP5-8.5⁹
2000	2.5	2.5	2.5	2.5	2.5	2.5
2030	2.7-3.0	2.7-3.0	2.7-3.0	2.7-3.0	2.8-3.0	2.8-3.1
2050	2.9-3.4	3.0-3.5	3.0-3.5	3.0-3.5	3.1-3.6	3.1-3.9

⁷ IPCC (2021) 2004-2005 base year projections adjusted to base year 2000 (see text).

⁸ SSP5-8.5 “low confidence” projection conceptually equivalent to OPC (2018) H++ scenario (see text).

Table 2-4. NOAA (2022) scenarios related to IPCC (2021) scenarios.

NOAA (2022)		IPCC (2021)	
Scenario	Air Temperature C°	Scenario	Air Temperature C°
Low	1.5	SSPI-2.6	1.3-2.4
Intermediate-Low	2.0	SSP1-2-6-SSPI 4.5	2.1-3.5
Intermediate-High	3.0	SSP1 4.5-SSP3 7.0	2.8-4.6
High	4.0	SSP1-7.0	2.8-4.6
Very High	5.0	SSP1-8.5	3.3-5.7

Table 2-5. NOAA (2022) median MSLR projections/extrapolations, Los Angeles (ft NAVD 88).

Year	Low	Intermediate Low	Intermediate High	High
2020	2.66	2.7	2.7	2.7
2030	2.78	2.83	2.88	2.93
2040	2.89	2.96	3.06	3.16
2050	2.99	3.16	3.35	3.7
2060	3.12	3.39	3.88	4.3
2070	3.25	3.68	4.53	5.22
2080	3.42	2.657	5.29	6.34
2090	4.3	4.67	6.08	7.52
2100	3.75	5.32	6.99	8.77

Table 2-6. NOAA (2022) and IPCC (2021) median MSLR projections 2030 and 2050 (ft, NAVD).

Year	Technical Report	Low	Intermediate Low	Intermediate High	High
2030	NOAA ^a	2.78	2.83	2.88	2.93
	IPCC ^b	2.7-3.0	2.7-3.0	2.7-3.0	2.8-3.0
2050	NOAA	2.99	3.16	3.35	3.7
	IPCC	2.9-3.4	3.0-3.5	3.0-3.5	3.1-3.6

^a.From Table 2-5

^b From IPCC (2021) Low-High Range MSLR Projections.

Table 2-7. Highest maximum observed total water levels, La Jolla (ft).

Year Month	NAVD88	NGVD
2015 Nov	7.62	5.51
2005 Jan	7.47	5.36
1997 Nov	7.46	5.35
2012 Dec	7.42	5.31
1983 Aug	7.36	5.25
1983 Jan	7.26	5.15

Table 2-8. NOAA La Jolla extreme water level statistics (ft).

Percent/Yr	Return (Yrs)	NAVD88	NGVD
1%	100	7.43	5.32
10%	10	7.20	5.09
50%	2	6.94	4.82
99%	1	6.51	4.40

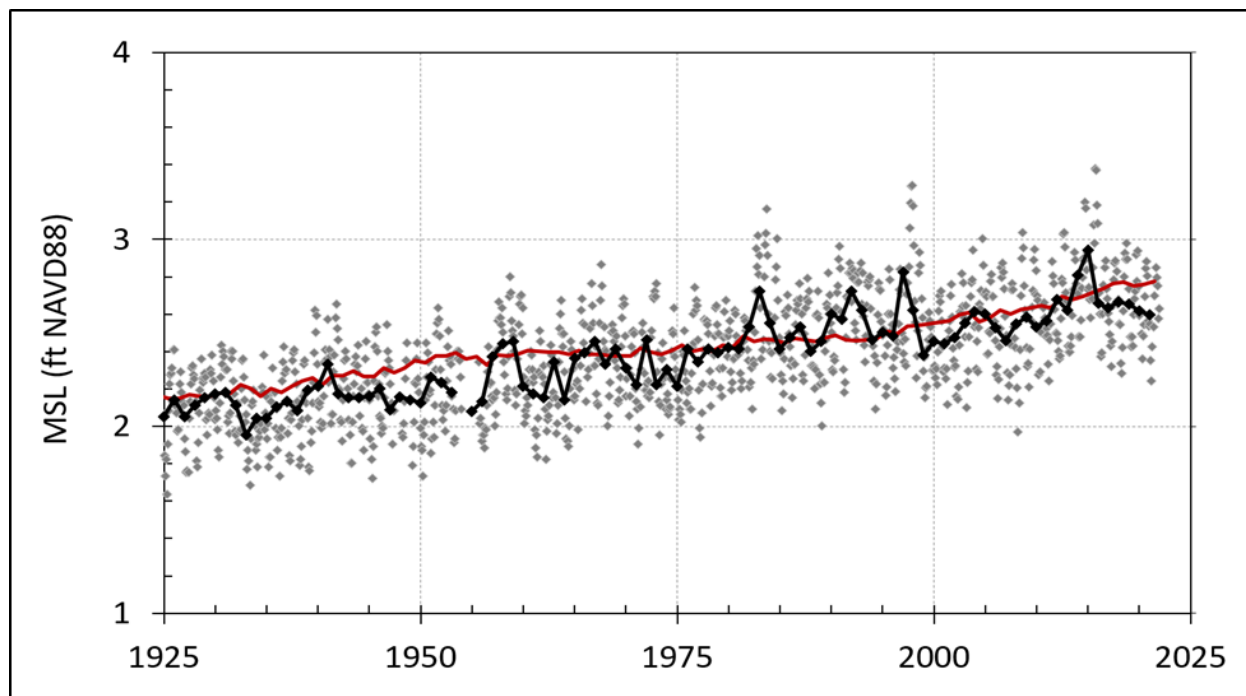


Figure 2-1. Annual and monthly average water level relative to NAVD88 at La Jolla, 1925-2022 (black line/symbols, grey symbols, respectively), and annual global MSL reconstruction (red line).

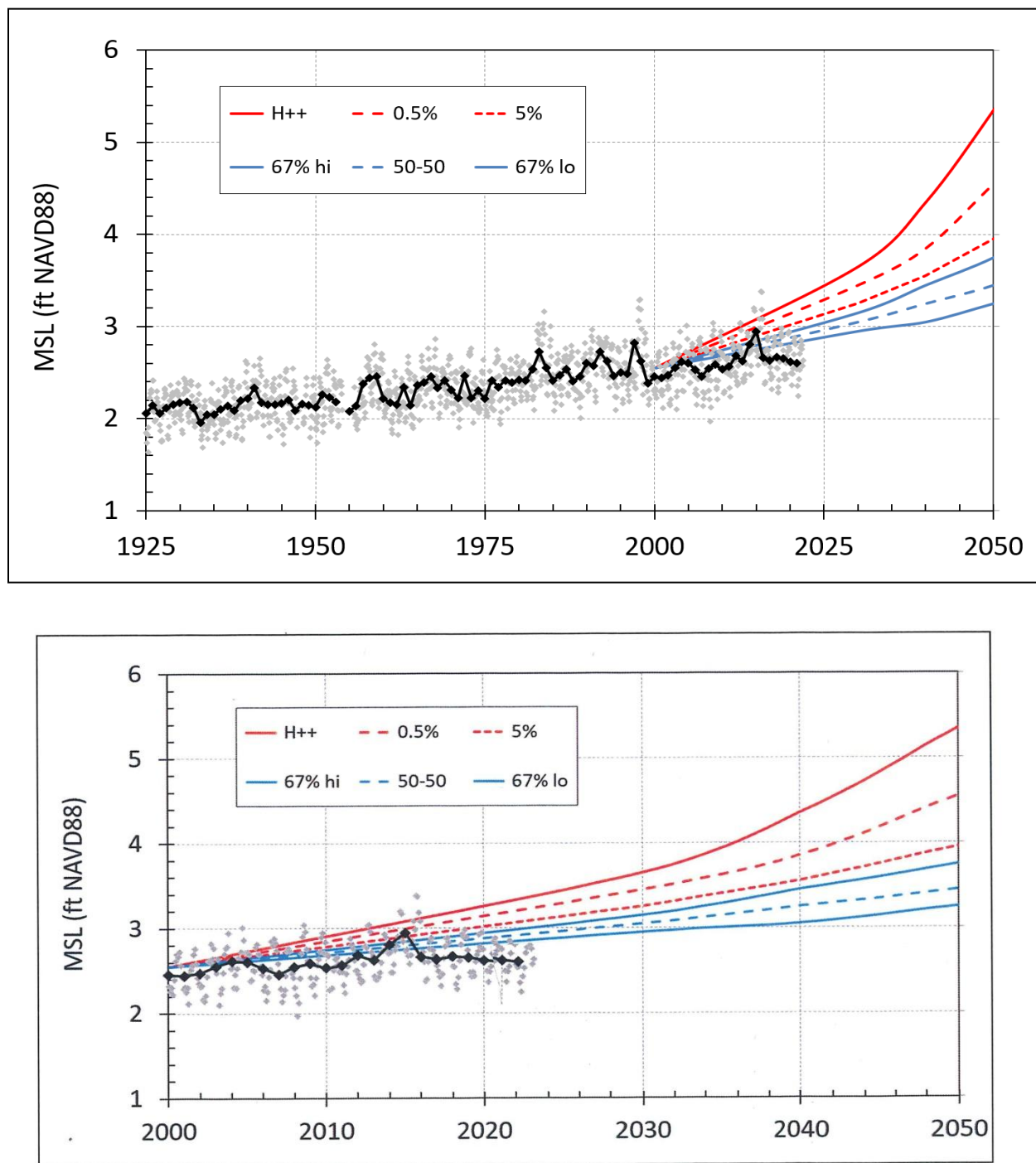


Figure 2-2. La Jolla average MSL data, 1925-2022, annual (black), monthly (grey) (upper). Same for 2000-2022 (lower). Both with OPC (2018) La Jolla MSLR projections, 2000-2050 (see legend and text).

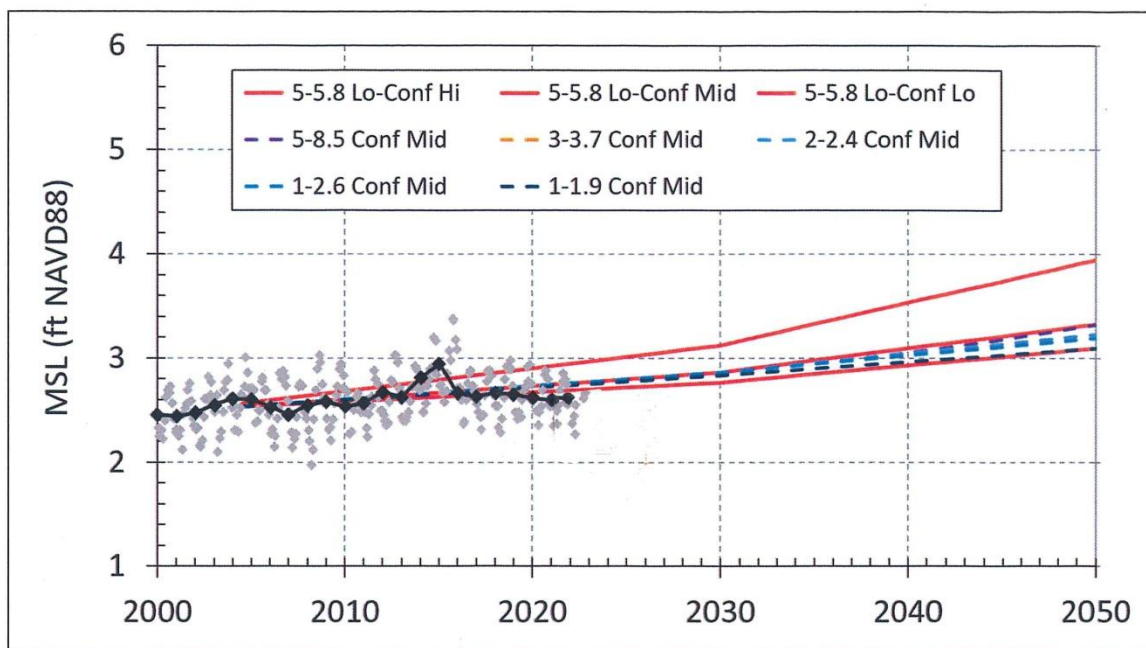


Figure 2-3. La Jolla average MSL data, 1925-2022, annual (black), monthly (grey), with IPCC (2021) LA MSLR projections, 2004.5-2050 (see legend and text).

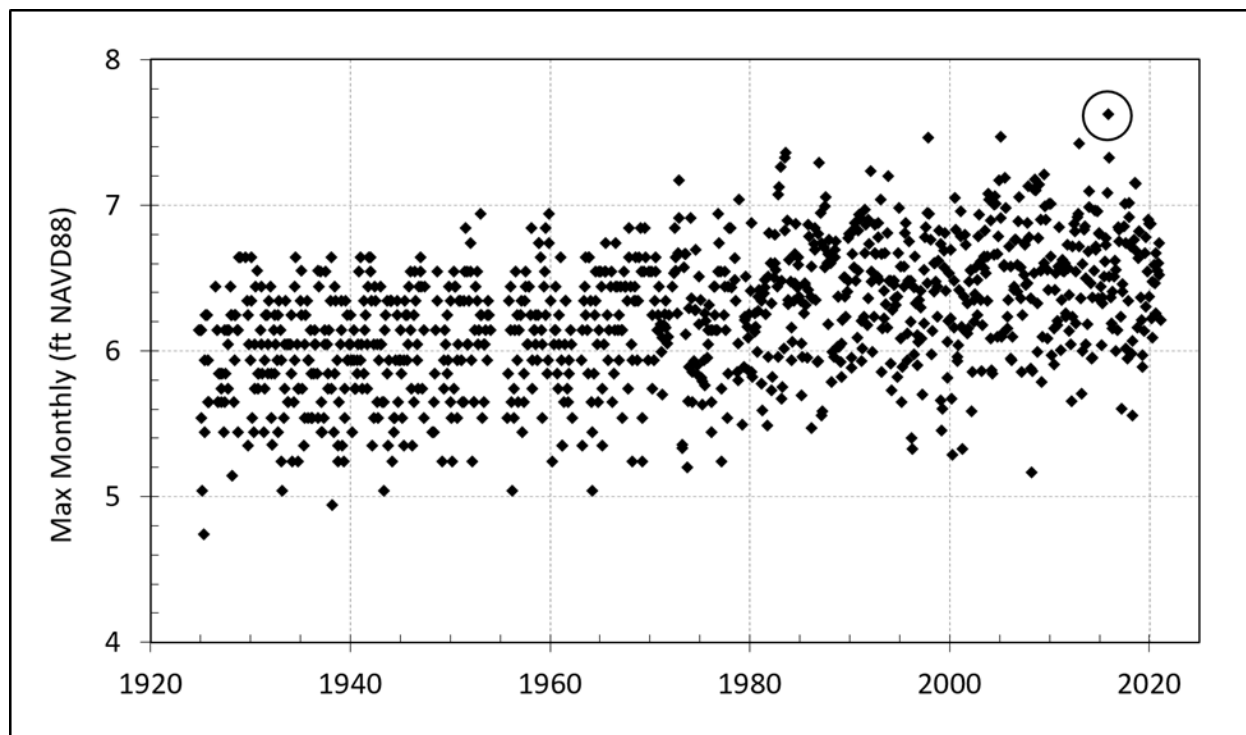


Figure 2-4. Monthly maximum sea level at La Jolla relative to NAVD88 datum, 1925-2022 (black symbols). Maximum observed 7.62 ft height (circled) on 25 November 2015 during 2015-16 El Niño.

3.0 SONGS REVETMENT

3.1 DESCRIPTION OF THE SONGS REVETMENT

The SONGS revetment provides partial front-line protection for the SONGS seawall; it is essential to maintaining the walkway that enables safe lateral access for beach users. The revetment shelters the walkway from most wave run-up and overtopping, thus preventing or reducing negative impact to lateral beach access due to flooding and other hazards from high water levels and waves.

Figure 3-1 is an aerial photograph showing the revetment, which extends along the entire length of SONGS on the beach fronting the walkway. Figure 3-2 is a close-up of the revetment at its southern end. The revetment is about 2,200 ft long, extending from the north end of Unit 1 to the south end of Units 2 and 3. The revetment is constructed of multiple layers of placed riprap consisting of quarry rock “rubble.” A well-known desirable characteristic of placed rubble structures is their ability to adjust and resettle under wave attack. The advantage of using rock riprap is that it is highly durable and readily available in southern California. Furthermore, due to their rough surface, rock revetments produce less wave run-up and overtopping as opposed to smoothed-faced structures.

3.1.1 Revetment and Walkway Maintenance 2018-2019

The repairs of the SONGS revetment (fronting Units 2 and 3) were done in two phases. Phase 1 started on 7 May 2018 and ended on 10 October 2018, and Phase 2 started on 15 October 2019 and finished on 16 December 2019. No substantial repairs were carried out in 2020, 2021 and 2022.

During Phase 1, SCE: (1) placed imported riprap along 500 linear ft at the southern portion of the public access walkway (Figure 3-3); and (2) elevated the access ramp of the southern public walkway using imported cobbles and sand.

The elevating of the south public access ramp was needed to compensate for the sand lost due to wave action, which resulted in an approximately 10 ft lowering of the beach at the south end of the walkway and scouring of the revetment riprap that protects the sheet pile seawall. Consequently, the riprap has been undermined and without the improvements, eventually the revetment would no longer be effective.

During Phase 2, SCE: (1) placed an additional 150 linear ft of imported riprap north of the previously placed riprap, for a total of 650 linear ft of revetment repair; and (2) added 70 ft of riprap in front of the sheet pile seawall closure section at the south end of the public walkway and reinstalled the Vehicle Barrier System at the south end of the public walkway. Figure 3-4 shows the south end of the walkway before and after the repair.

3.2 SITE VISIT

On 19 and 20 January, and 16 February 2023, an inspection of the revetment was made for this study. During these visits, we took photos fronting the revetment; these photos are presented in Appendix D. A laser scan survey was also carried out in order to construct a digital elevation model (DEM) of the revetment and discussed in Section 3.2.2.

3.2.1 Rock Measurements

The size of individual rocks is expressed by the dimensions of their three axes. The long axis, ‘a,’ is the maximum length of the stone (Figure 3-5); the intermediate axis, ‘b,’ is the maximum width perpendicular to the long axis; and the short axis, ‘c,’ is the height of the stone perpendicular to the plane of the a-axis and b-axis. The size of an individual rock is usually expressed as its b-axis dimension, or alternatively by its calculated or actual weight. Rock weight estimates, which are needed to evaluate riprap stability, are discussed in Section 3.3 below. Histograms of the lengths, widths, and heights of the 80 sample rocks measured at SONGS are presented in Figure 3-6, and their cumulative distributions in percentage are shown in Figure 3-7.

3.2.2 Revetment Laser Scanner Survey

A laser scanner survey was carried out using a Trimble SX10 scanning total station (Figure 3-8) for the purpose of creating a DEM (Digital Elevation Model) to visualize the spatial characteristics of the revetment. Control points were established to aid in subsequent station setups. The revetment was scanned from the beach and the scanner location was determined from the control points. The system scanned in a vertical direction and slowly rotated horizontally to cover the areas of the revetment at a high resolution. A total of 14 scans were carried out to capture the entire SONGS revetment.

Tide was a limiting factor in obtaining complete coverage from the beach at the southern portion of the revetment. Therefore, some scans were carried out from the top of the revetment near the walkway to fill data gaps.

The survey on 19, 20 January acquired over 50 million data points, assembled in a “point cloud.” The data set was pre-processed using “Global Mapper” software, which enables the outlier points, and those points likely reflected from the walkway wall, to be removed. The pre-processed data were then graphically presented to show the revetment and adjacent beach. The DEM results at each of these transect are presented in Appendix A.

An advantage of creating a DEM is that the model can be “sampled” to show cross sections and contour maps that would otherwise be difficult or impossible to derive in a reliable way. Twenty-one cross section transects were generated from the DEM at locations shown in Figure 3-9. Results of the revetment laser scanner survey are shown in Figures 3-10 through 3-13 for the 21 transects. Between transects 6 and 7 few of the rocks were either scoured down or moved due to the large waves in early January 2023 (Figures A-6, A-7 and 3-15). For clarity, Appendix A shows the DEM comparison between 2023 and 2020 for each transect.

Representative cross sections are shown in Figure 3-14; all 21 transect cross sections are presented in Appendix B. Table 3-1 provides riprap height, walkway wall height, and the revetment slope β for each transect.

The DEM was also used to determine the height of the revetment along its upper edge adjacent to the walkway retaining wall (Figure 3-15). The height of this upper edge varies from about 8 ft to 12 ft (NGVD), a few feet lower than the upper edge of the retaining wall, which lies at about 14 ft.

3.3 RIPRAP ROCK UNIT WEIGHT

Riprap rock unit weights and their variations are essential to estimating the stability of a revetment. Individual rock weight is proportional to volume and specific weight (or density) of the stone. The estimation of weight is complicated by the fact that each rock unit is not a simple geometric form, such as a sphere or rectangular shape, like a brick.

Individual rock weight, $W(x)$, was estimated from Equation 3-1, which assumes each rock (x) is equivalent to a sphere with diameter $D(x) = b(x)$, the maximum width perpendicular to the long axis, as described in Section 3.2 above. Dimension ‘b’ is often referred to as rock “diameter.” Then:

$$W_x = \frac{\pi \gamma_s D(x)^3}{6} \quad (3-1)$$

Where:

γ_s = Specific weight of revetment rock.

Table 3-2 gives the dimensions and weights of each randomly sampled rock in 2020. The mean and standard deviations for the length, width, and weight of the rocks are presented in Table 3-3. Percent distribution of rock weights and the cumulative distribution of estimated rock weights are shown in Figure 3-16.

A key design parameter for any revetment is the median rock weight, designated W_{50} . Half of the rocks are heavier, and the other half are lighter than W_{50} . We estimated W_{50} in two different ways using standard coastal engineering practice (U.S. Army Corps of Engineers [USACE] 1994a, b). These gave nearly identical results.

First, we determined the individual rock weight estimates from each rock diameter, $D(x)$, as described above in equation 3-1. The result was $W_{50} = 600$ kg. Second, we calculated the median diameter of the 80 sampled rocks, D_{50} . The result was $D_{50} = 2.5$ ft. We then used this number in place of $D(x)$ in Equation 3-1, which resulted in $W_{50} = 580$ kg.

3.4 DESIGN WATER LEVEL

Water surface elevation is dependent on tides, storm surge, and MSLR in response to climate change. These factors are discussed in Section 2.1.3, and the values of current extreme

water levels are given in Table 2-3. Table 2-3 gives the NOAA estimates for the extreme water level for various return estimates. The 100-year return period for surface water elevation at La Jolla is 5.32 ft, NGVD (7.43 ft NAVD88) while the maximum observed water surface elevation of 5.5 ft occurred on 25 November 2015 during the 2015-16 El Niño warming event (Table 2-7 and Figure 2-4).

These estimations include astronomical tide, storm surge, and sea level fluctuations due to normal seasonal heating and cooling, as well as El Niño condition enhancements. They do not include wave setup caused by breaking waves, since tide gauges are located offshore of the surf zone, and their water level sampling system filters out relatively high-frequency fluctuations such as wave surges. The design water level used for this study is the extreme thus far observed: 5.5 ft (1.7 m) NGVD, or 7.6 ft (2.3 m) NAVD88 (rounded to one significant figure).

3.5 DESIGN WAVE ESTIMATION

Wave run-up can be the dominant contribution to high water levels on beaches, depending on the state of the tide, and the height, direction, and period of the waves, especially during storms. The wave record for San Onofre, estimated from measurements at SONGS and a comparison with the Oceanside wave array data between 1978 through 1994, were used to calculate wave height return periods for San Onofre (see Section 5.2 in Elwany *et al.*, 2016).

The Seasonal Maxima Distribution Model (SMDM), developed by L. E. Borgmann and published in USACOE (1988), was selected as the appropriate analysis method to estimate the design wave height at a range of return periods. Monthly wave maxima were extracted from the wave data and split into seasonal sets. The seasonal maximum wave-height distribution functions were calculated for each season and then multiplied together to produce the annual maximum distribution. This distribution function was used to estimate extreme wave-height return periods.

The design wave analysis shown in Figure 3-17 was used to identify the significant wave heights associated with 5-, 10-, 25-, 50-, and 100-year wave events at San Onofre. Wave spectra matching those wave heights were selectively extracted from the record. The wave spectra from these storms (Figure 3-18) were extracted from the Coastal Data Information Program (CDIP) database (<https://cdip.ucsd.edu/>) and used to estimate the peak period associated with wave-height return period. A typical wave storm on this southern California coast has a wave height of about 6.9 ft (2.1 m). Extreme-values for the 5-, 10-, 25-, 50-, and 100-year return period wave heights at San Onofre are given in Table 3-4.

The largest storm on record between 1980 and 2016 occurred on 18 January 1988. The deepwater wave height was 16 ft (4.9 m) with a period of 17 sec (as measured at the Oceanside buoy). The corresponding wave height at San Onofre was about 12.5 ft (3.8 m) approaching the shore from the west. Table 3-5 represents the highest significant wave heights at San Onofre in descending order estimated from the Oceanside measured wave data for summer, winter, and all data.

3.6 SONGS REVETMENT STABILITY ESTIMATION

As outlined above, the median rock weight W_{50} is a key parameter in assessing the stability of a revetment. Hudson's formula (Ahrens, 1981a,b; USACOE 1984, 1994a,b; BCMELP, 2000) is the standard practice method used to estimate W_{50} necessary for revetment stability:

$$W_{50} = \frac{\gamma_r H^3}{K_D \frac{\gamma_r}{\gamma_w} - 1 \cot \alpha} \quad (3-2)$$

Where:

W_{50} = required median armor unit weight,
 γ_r = specific weight of the rock unit, Kg/m^3 ,
 H = wave height at the toe of the revetment,
 K_D = stability coefficient,
 γ_w = specific weight of water at the site, and
 α = revetment slope angle from horizontal.

K_D values vary primarily with the shape of the rocks, surface roughness, sharpness of edges, and degree of interlocking. Typically, $K_D = 2.1$. Wave height H at the structure is estimated by shoaling the design waves to the breaking point (H_b). If H_b is less than the wave height at the toe, H_{toe} , of the revetment, we use H_b ; otherwise, H_{toe} is used.

The height of the wave at the toe of the revetment is depth limited. The extreme water depth at the toe of the SONGS revetment (D_s) is $5.5 \text{ ft} + 2.29 = 7.79 \text{ ft}$, MLLW, where 5.5 ft, NGVD is extreme water level (Section 3.4) and 2.29 is the difference in elevation between datums NGVD and MLLW.

The water depth at the toe of the structure (D_s) varies as the sea level rises. In 2050, the water depth at the toe of the structure is projected to be 9.79 ft, MLLW (OPC, 2018, Medium-High Scenario) and 10.59 ft, MLLW (OPC, 2018 H++ Scenario). A calculation of the wave height (H) was made from the equation $H = 0.56 \times D_s$ (Thornton and Guza, 1982 and 1983).

Equation 3-2 is used to compute the W_{50} for stable revetment. Table 3-6 gives the values of W_{50} for the MSLR projections (medium-high and H++ in 2020 and 2050).

3.7 ASSESSMENT OF SAN ONOFRE BEACH

The condition of the beach fronting SONGS is significant since it prevents or buffers wave attack of the revetment and retaining wall, which in turn protect the walkway required for lateral beach access. The stability of the SONGS revetment depends on the condition of the beach. Presence of a healthy beach causes waves to break farther seaward of the revetment, thus reducing wave run-up, splashing, and overtopping. The beach also prevents toe scouring that can undermine the revetment and cause rock units to settle. When the beach is narrow, or water level

unusually high, or both, waves breaking on the revetment can cause dislocation of individual rocks, which contributes to revetment instability.

Recent beach conditions are defined by the 2017 through 2022 quarterly profile measurements (Appendix E), which characterize the beach configuration in autumn, winter, spring, and summer seasons. Comparison with earlier beach profiles dating back as early as 1964 show long-term erosion or accretion tendencies. The main factors controlling erosion or accretion are waves and sand supply. Other contributing factors are the nearshore and offshore bathymetry of the region, particularly any wide, flat shelf areas, and the presence of reefs, all of which limit wave height. Structures, particularly the SONGS temporary laydown pads used for Units 1, 2, and 3 constructions, also influence beach width and stability. In the future, MSLR will cause beaches worldwide to migrate landward and upward. Depending on the state of the backshore, especially its erodibility, beaches may or may not continue to exist. The study documents the complex changes of beach conditions at SONGS and puts these into their Southern California context.

Two surveys each year include the offshore portion of the beach at SONGS. The results of each survey have been presented in reports by Coastal Environments (CE, 2017, 2018, 2019, 2020, 2021, and 2022). Longer-term beach change patterns are characterized by comparing beach widths from these recent surveys to comparable measurements from 1985-1993 sponsored by SCE. The earliest directly comparable data were taken in May 1985, just after the sand release of the SONGS Units 2 and 3 laydown pad (Flick and Wanetick, 1989), and from 1990-1993 (Elwany *et al.*, 1994), 2000 (CE, 2000), 2016 (Elwany *et al.*, 2016), and 2017-2021 (CE, 2022).

In Sections 2 and 3 of Appendix E, we present an overview of the data and how it was collected. In Section 4, we then discuss the characteristics of SONGS beach profiles and how these relate to typical Southern California beaches. Beach width changes and shoreline trends are discussed in Sections 5 and 6. In Section 7, we utilized the available historical information to better understand beach width fluctuations over a long time scale and shoreline changes at San Onofre. Our conclusions are detailed in Section 8.

For convenience, Figures 3-19 and 3-20, and Table 3-7 are reproduced from Appendix E in this section to show the long-term changes of beach width.

The beach profile surveys and photography programs sponsored by SCE since 1964 have provided valuable information and understanding of the response at San Onofre to beach filling and the construction of stabilizing structures (Flick and Wanetick, 1989; Flick *et al.*, 2010). This insight will be valuable as MSLR accelerates in the future. Elwany *et al.* (2017) addressed the impacts of MSLR on San Onofre Beach.

The cliffs' erosion rate was estimated using the DEM data obtained through airborne LIDAR data from 1998 through 2016. The data were available for download from the NOAA website (<https://coast.noaa.gov/dataviewer/#/lidar/search/>). The the DEM data were resampled to a 1x1 m grid size which was the cell size of the 1999 DEM. Using Geographic Information System (GIS), we extracted at 5, 15, 25, 30, and 50 ft, NGVD contour lines. We used a tool

developed by USGS for the Digital Shoreline Analyses System (DSAS) to determine the rate and the net horizontal movement of the contour lines.

Figure 3-21 shows the erosion rate from 1998 to 2016 at SONGS, which indicates that most of the erosion occurs at the 5 ft contour at a rate that varies from -9.8 to -6.6 ft/yr (-3 to -2 m/yr) north and south of SONGS, and 1.6 ft to -1.6 ft (0.5 to -05 m) in front of SONGS and its proximity. The 15 ft, 25 ft, 30 ft, and 50 ft show a low erosion rate that varies from 1.6 ft to -1.6 ft (0.5 to -05 m) since 1998. The net movement of the 5 ft contour from 1998 through 2016 was about -130 ft (39 m), other contours present movement that varied from -16 to -3 ft (-5 to -1 m).

3.8 EVALUATION CRITERIA

A “stable” rock revetment must perform satisfactorily in the sense that it functions as designed even though individual rocks may move such that portions or the entire revetment settles or changes slope. Such changes are expected in rock revetments, and as previously noted, and are accounted for in the original design. In short, a revetment is functioning properly if it provides protection as designed and is considered stable if no damage exceeds ordinary maintenance needs. At a minimum, the design must withstand conditions that have a 50% probability of being exceeded during the revetment’s economic life.

Revetment failure can be caused by: (1) large dislocation of individual rocks such that they become sufficiently separated to no longer function as a unit to dampen wave attack; or (2) extreme settlement where the height is no longer sufficient to prevent excessive overtopping. In addition, failure of the project during probable maximum conditions should not result in loss of life or unreasonable cost.

3.9 REVETMENT STABILITY FROM FEBRUARY 2020 TO FEBRUARY 2023

Wave data (wave height, period, and direction) from wave buoy number 46224, located offshore of the City of Oceanside in 238 m water depth, were used to roughly represent the wave heights and periods in front of the SONGS revetment. These computed wave heights and periods are shown in Figures 3-22 and 3-23. The waves from January 2020 up to date were generally calm except for the periods from 07 November to 09 November 2020, from 25 January 2021 to 21 February 2021 (Elwany *et al.*, 2021, 2022), 14-16 December 2022 and January to early March 2023. These wave events offered a good opportunity to examine the stability of the revetment. The major wave events between January 2020 and today are described below:

1. The period from January through February 2021 was characterized by a series of large wave storms having an average wave height of about 2 m (6.6 ft) with maximum wave height of 4.34 m (14.2 ft) observed between 25 January through 26 January 2021 as shown in Figure 3-22. The wave period during the wave storms varied between 8 to 12 secs.

2. The period from 10 December and 16 December 2021 was characterized by average wave height of 2.8 m (9.24 ft), maximum wave height of 3.38 m (11.1 ft), and a short wave period of 7 secs.
3. The period from January 2023 to early March 2023 have noticeable large set of waves storms started on 06 January 2023 and lasted for few weeks followed by large sets of waves in mid and at the end of February and early March.

Examining the DEM (Appendix A) and the photographs taken during the site visits, it is noticeable that no significant changes or damages occurred on the revetment from 2020 through 2022. The photographs taken during the 25 and 31 January and 01 February 2022 site visits (Appendix D) were important to this study; they complement the laser scanner survey and show the beach conditions at each of the 21 ranges after the 2021-2022 winter wave storms. The laser scanner survey clearly described the rock shape (sizes) while the photographs highlighted the sand and cobble areas on the beach. Aerial photographs of the revetment for the period from 2003 to 2020 are presented in Appendix C. Close up photos of the revetment at and after 2020 are present in Appendix D (Elwany *et al.* 2020, 2021, and 2022).

3.10 MAINTENANCE AND ADAPTIVE CAPACITY

As described in Section 3.9, the SONGS revetment is currently in good condition and can likely provide wave protection to the retaining wall and walkway through at least 2050. The major threats to revetment stability in the future include wave storms, or clusters of wave storms, such as those that occurred from 1981 to 1983. As described above, revetment damages depend on the height of waves and the duration of wave attack. Large waves can cause dramatic narrowing and lowering of the beach fronting the revetment, leading to rock settlement and displacement, wave run-up, and overtopping.

Section 3.9 of this study showed that the revetment was capable of withstanding both a single large wave event of 2-4 days and a series of large wave storms. It should be pointed out that the revetment is expected to occasionally sustain future damages larger than were observed during January and February 2021, December 2021, and January and February 2023 and, therefore, the revetment will require occasional maintenance in the future. It is not expected to collapse or fail in a way that would prevent its function if properly maintained. Such damages are expected in rock revetments, as previously noted, and accounted for in the original design such that no damage exceeds ordinary maintenance needs. In this respect, the revetment's adaptive capacity to MSLR is high in the sense that it is currently in a stable condition and has already been tested by the January-February 2021 and January-February 2023 waves. Occasional maintenance will allow it to continue functioning as intended.

For these reasons, it is important to monitor the cross sections of the revetment at various locations by surveys and photographs (Sections 3.2.1 and 3.2.2), especially before and after large wave storms. It is also important to monitor the beach fronting the revetment and at the north and south of it as described in Section 3.7 and Appendix E.

The revetment, retaining wall, and walkway also provide additional protection to the main SONGS seawall. It is crucial that the seawall remain in place at least until the deconstruction efforts of Units 2 and 3 are completed. The seawall also provides critical protection for the ISFSI and its security building.

Impacts of groundwater on the ISFSI based on quarterly measurements of the groundwater from 9 coastal wells out of 16 total wells are presented in Appendix F. The OPC (2018) 0.5% (medium-high) and H++ SLR scenarios for groundwater elevation for 2050 are 4.35 ft and 5.15 ft, NGVD, and are 1.62 ft and 0.80 ft lower respectively than the bottom of the ISFSI support foundation, which is 3 ft thick (Figure 3-25).

Continued maintenance of the SONGS revetment is necessary (Section 3.1.1), as is maintaining the main SONGS seawall. These both substantially decrease exposure and risk to SONGS from future MSLR and, therefore, increase the resilience and adaptive capacity of all SONGS facilities and the Lease Premises in compliance with the SCE lease agreement.



Figure 3-1. Photograph taken on 20 August 2018, showing the SONGS revetment. Notice the north part of the revetment is covered by beach sand.



Figure 3-2. The revetment at its southern end.



Figure 3-3. Top photograph taken on 20 March 2018, before placement of riprap. Bottom photograph taken on 17 December 2019, after placement of riprap within gaps and depredated areas of the revetment. Direction of the photograph taken towards the south.

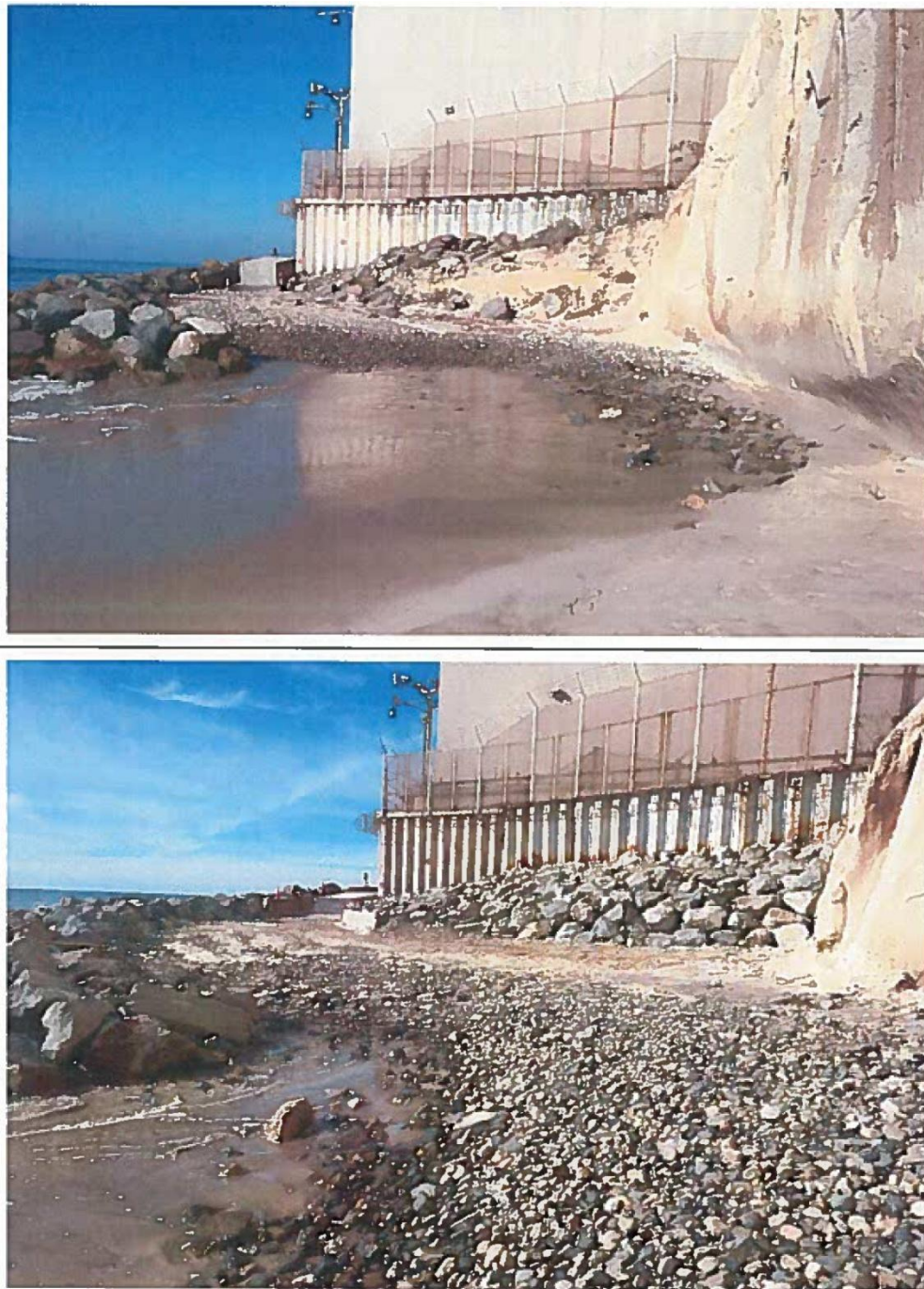


Figure 3-4. Top photograph taken on 15 October 2019, showing the sheet pile seawall before repairing the south end of the walkway. Bottom photograph taken on 17 December 2019, showing the sheet pile seawall after repairing the south end of the walkway.



Figure 3-5. Measurements of the long axis of the rock (length).

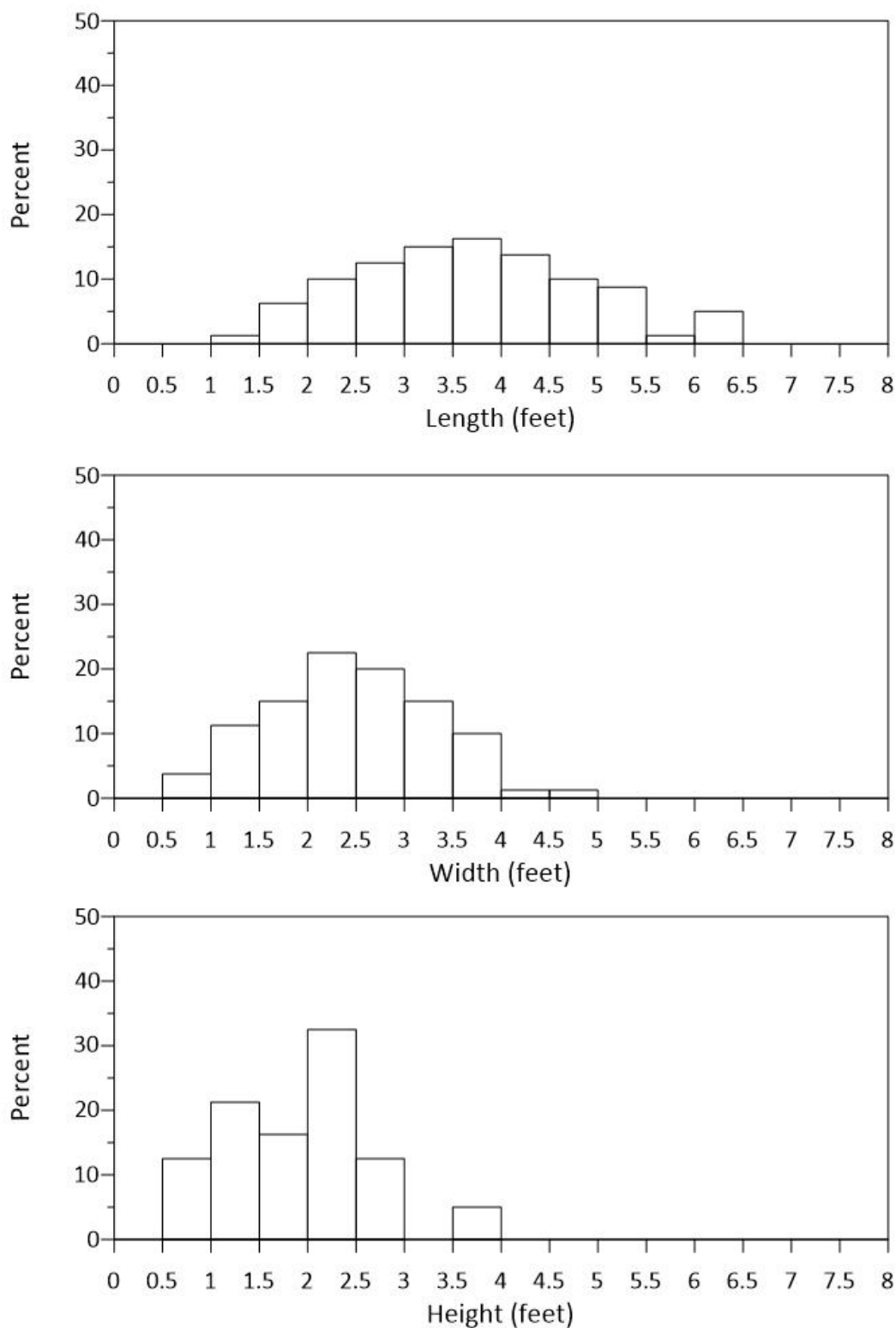


Figure 3-6. Histograms of rock length, width, and height.

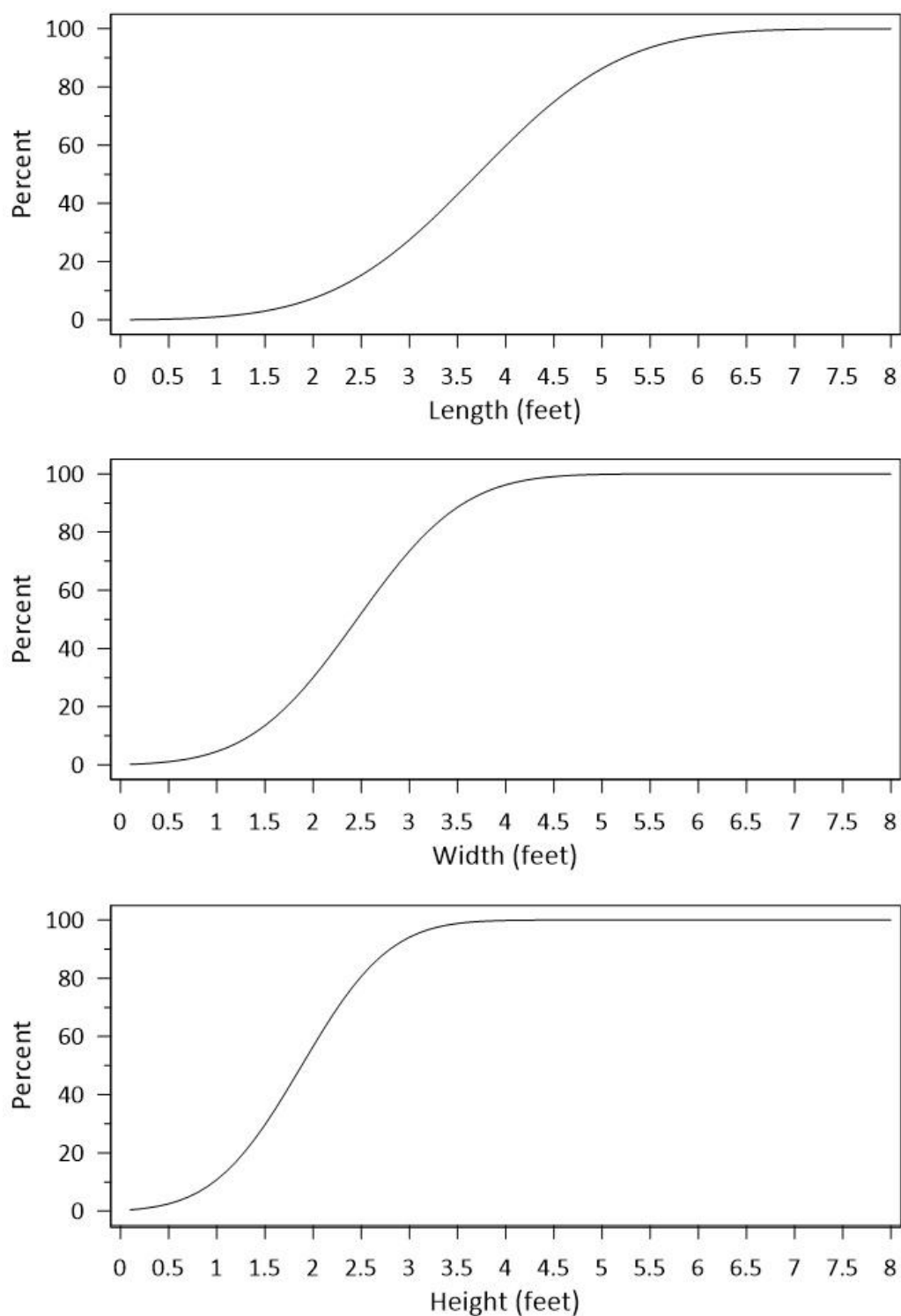


Figure 3-7. Cumulative distributions of rock length, width, and height.



Figure 3-8. Trimble SX10 scanning total station.

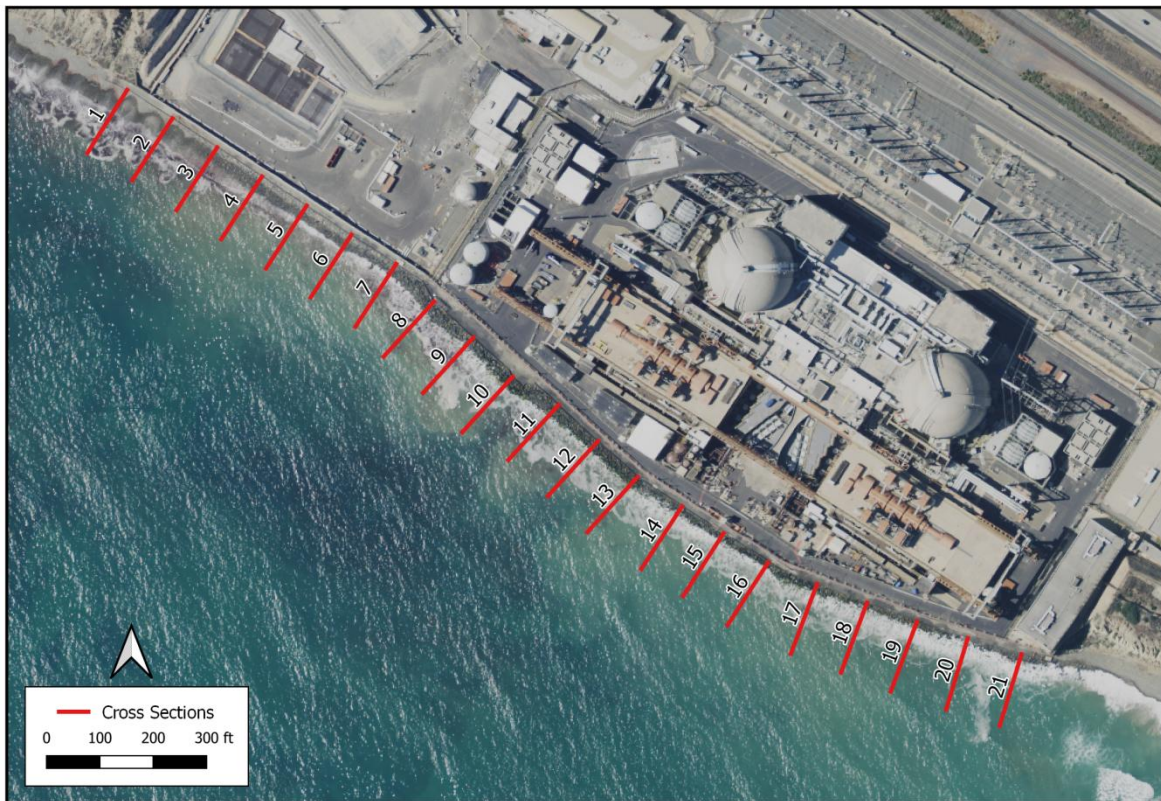


Figure 3-9. Location of 21 transects along the revetment, spaced 100 ft apart.

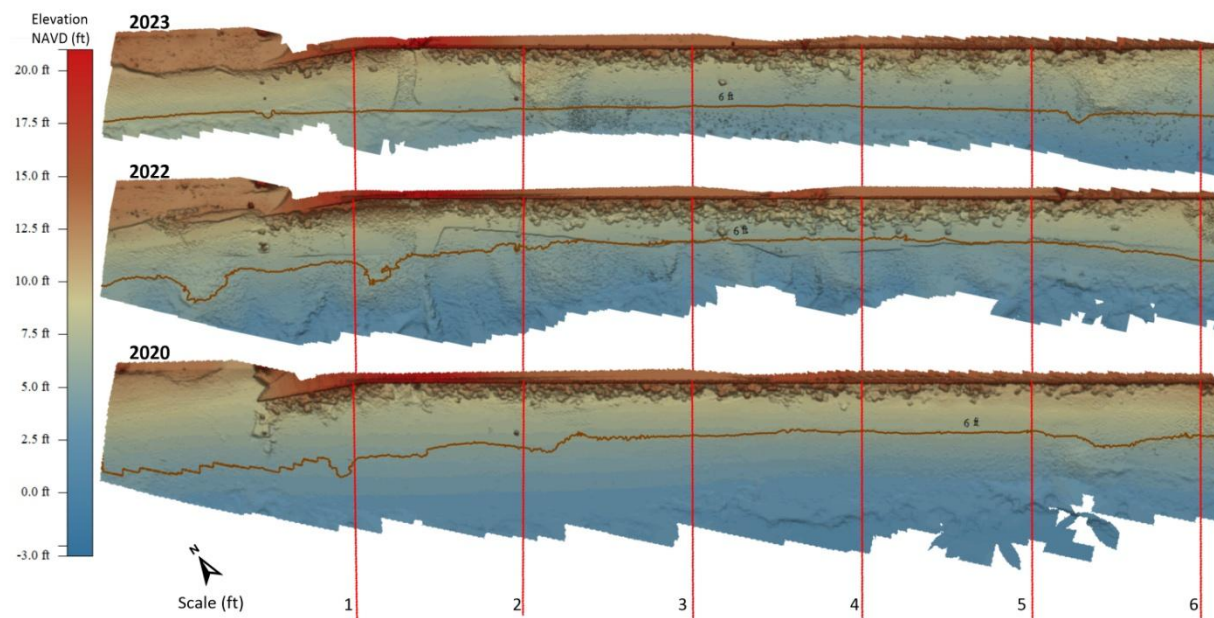


Figure 3-10. Elevation model of SONGS revetment from laser scanner for Transects 1 to 6 for years 2023 (top), 2022 (middle), and 2020 (bottom).

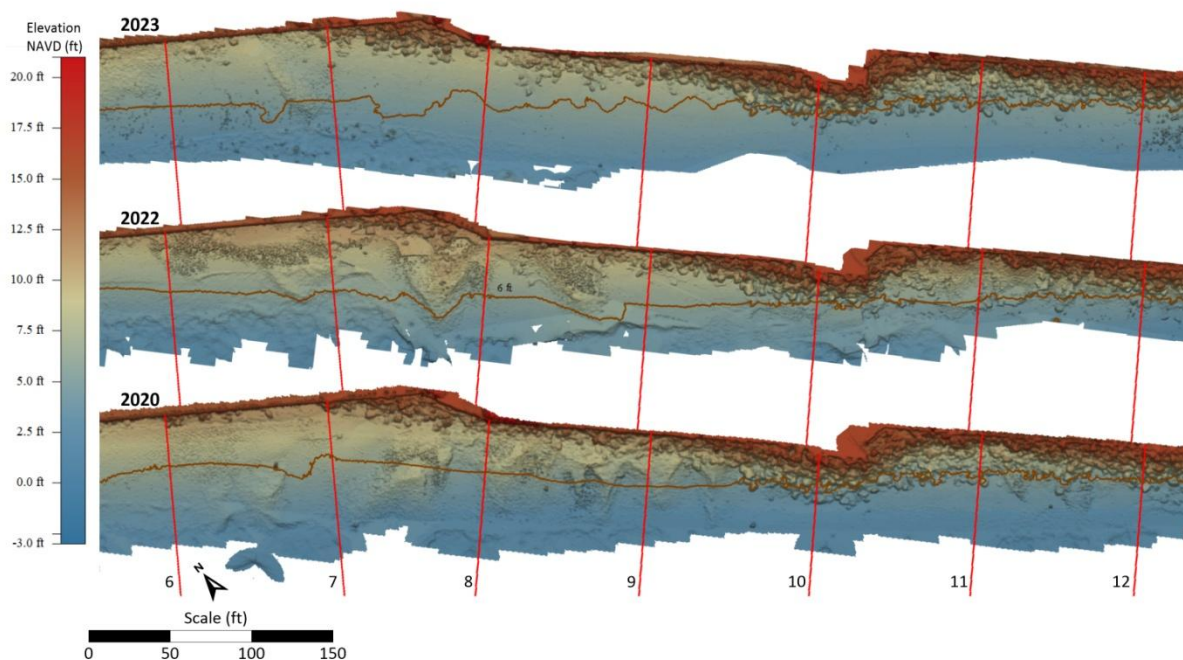


Figure 3-11. Elevation model of SONGS revetment from laser scanner for Transects 6 to 12 for years 2023 (top), 2022 (middle) and 2020 (bottom). The contour line in red-brownish color at 6 ft, NGVD indicates whether the beach is eroding or acceding as comparing the beach condition from one year to another.

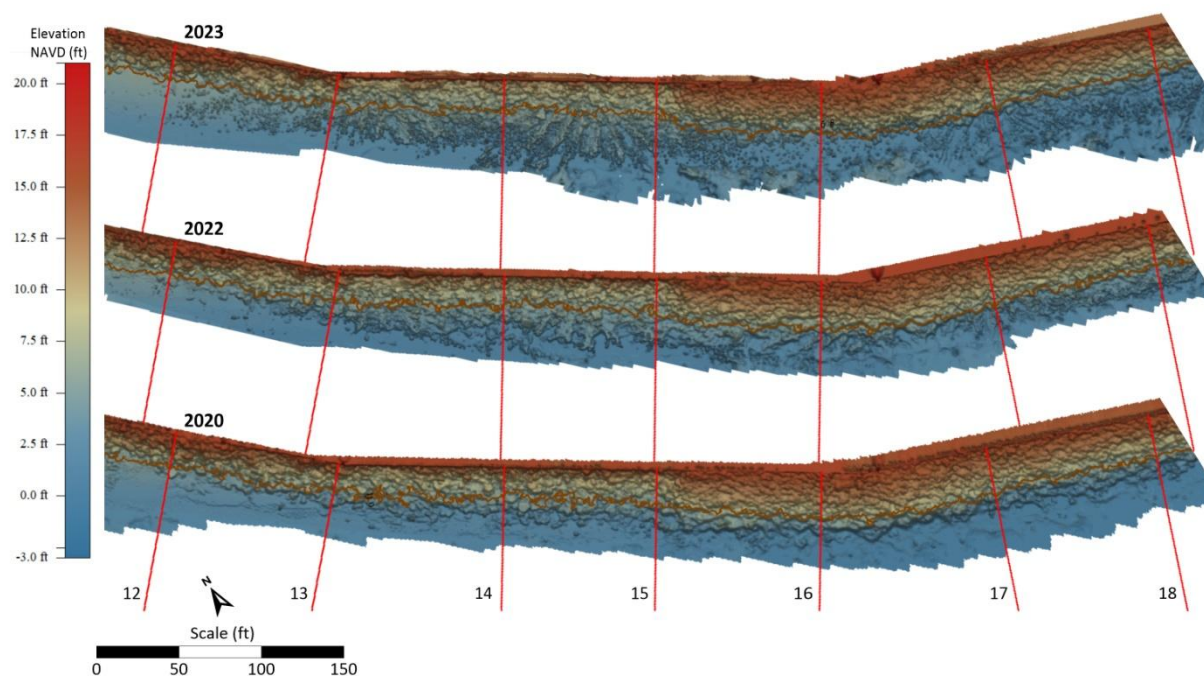


Figure 3-12. Elevation model of SONGS revetment from laser scanner for Transects 12 to 18 for years 2023 (top), 2022 (middle) and 2020 (bottom). The contour line in red-brownish color at 6 ft, NGVD indicates whether the beach is eroding or acceding as comparing the beach condition from one year to another.

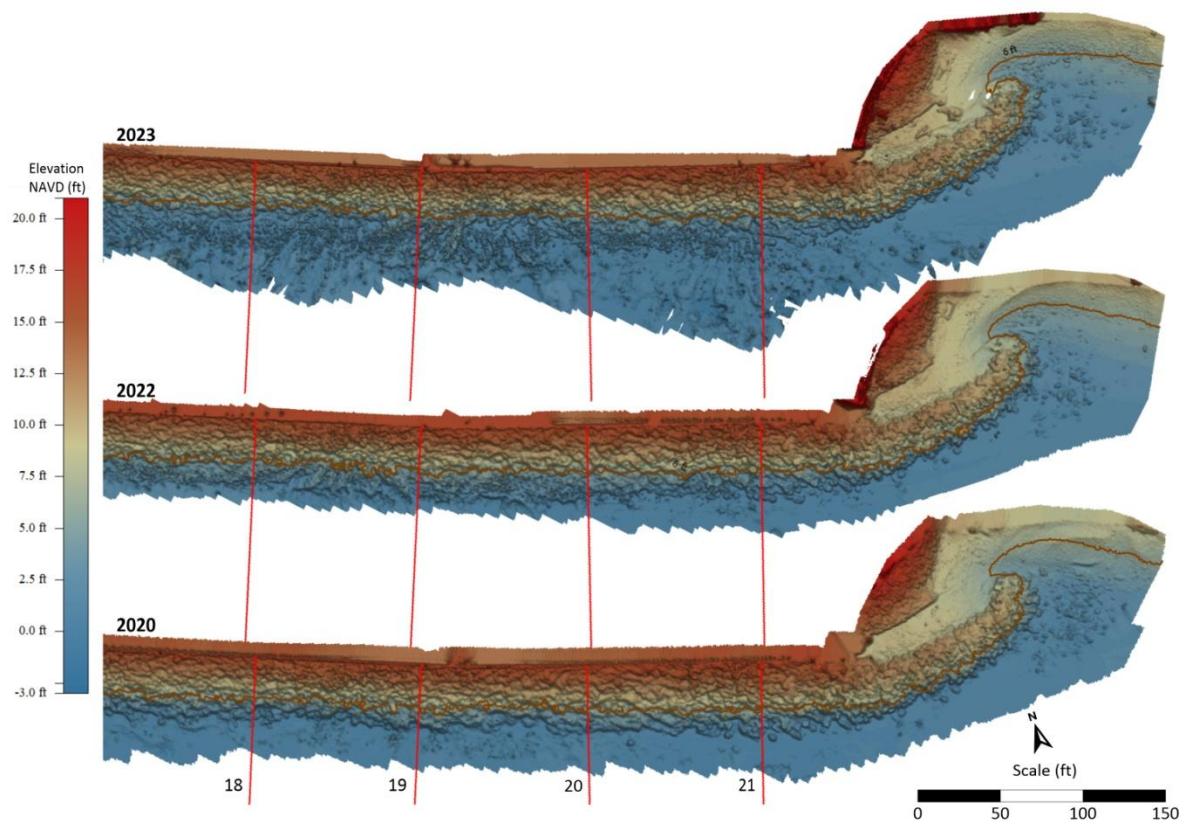


Figure 3-13. Elevation model of SONGS revetment from laser scanner for Transects 18 to 21 for years 2023 (top), 2022 (middle) and 2020 (bottom). The contour line in red-brownish color at 6 ft, NGVD indicates whether the beach is eroding or acceding as comparing the beach condition from one year to another.

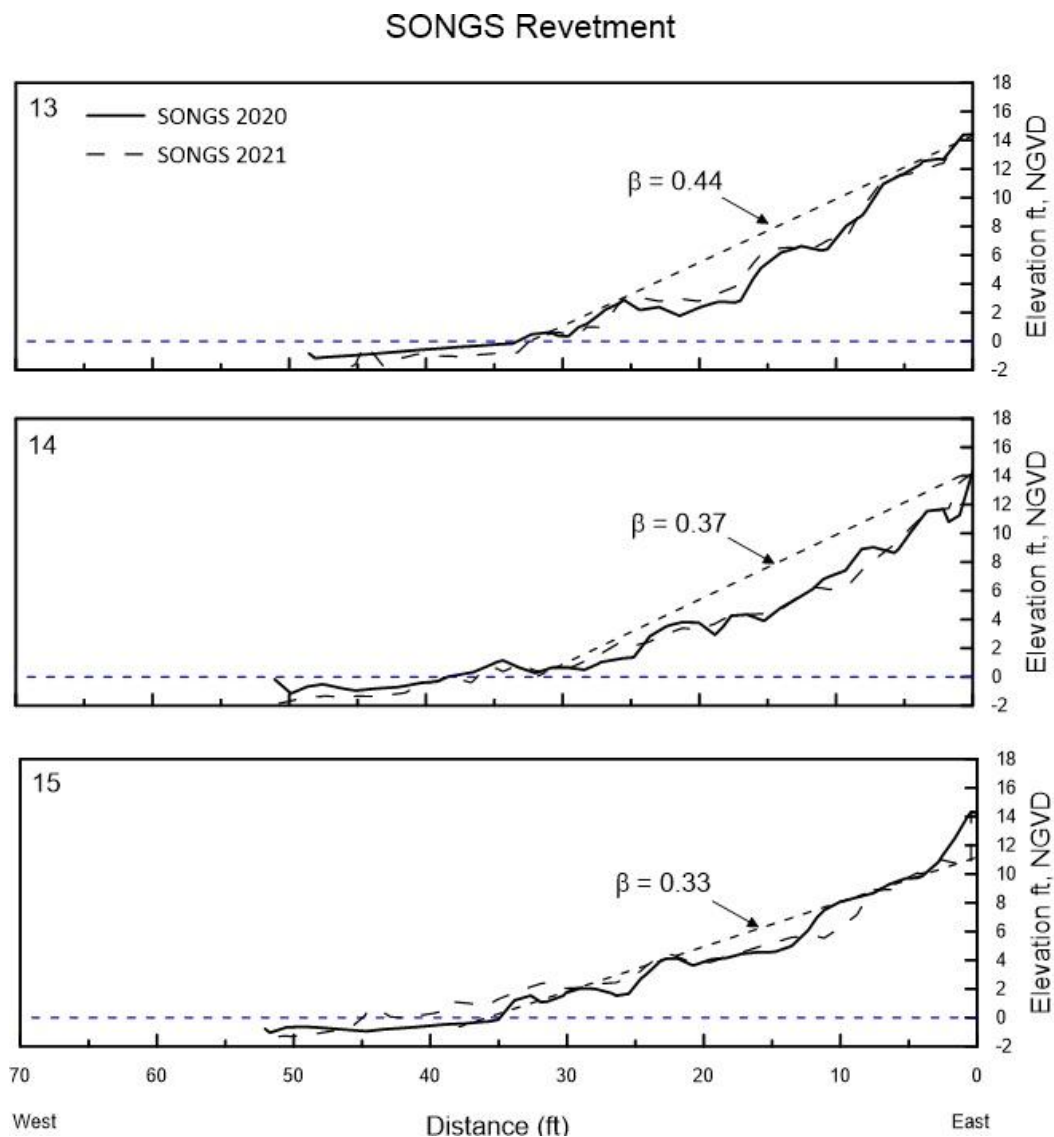


Figure 3-14. Typical revetment cross sections showing slope “ β ” at the indicated section.

Table 3-1. Riprap and walkway wall heights and revetment slope (β).

Transect #	Riprap Height ft, NGVD29	Wall Height ft, NGVD29	Slope (β)
1	12.89	16.79	0.90
2	12.27	14.27	0.66
3	12.15	14.27	1.52
4	9.22	14.32	1.13
5	9.44	14.27	0.35
6	10.13	14.2	0.43
7	12.48	14.34	0.67
8	9.55	14.39	0.20
9	10.59	14.29	0.38
10	15.12	14.39	0.46
11	13.69	14.34	0.40
12	13.63	14.39	0.54
13	12.37	14.39	0.44
14	12.34	14.37	0.37
15	10.34	14.34	0.33
16	14.24	14.21	0.42
17	12.98	14.27	0.38
18	13.58	14.22	0.39
19	14	14.31	0.40
20	13.49	14.32	0.37
21	14.4	14.32	0.35

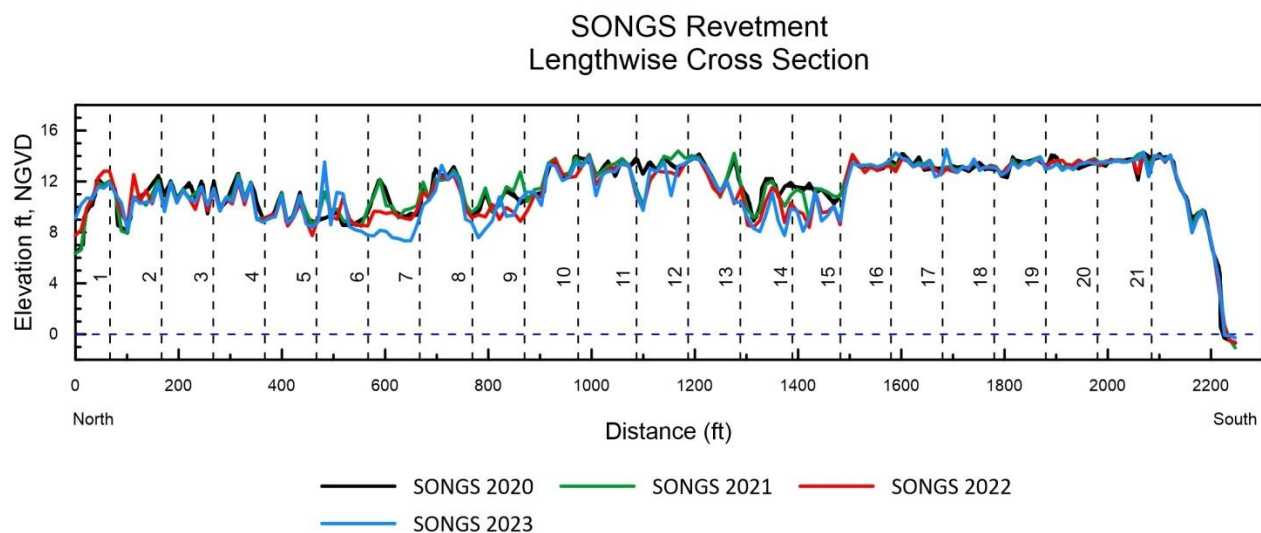


Figure 3-15. Elevation of the top of revetment for the 21 transects.

Table 3-2. Length, width, height, and estimated weight of the measured rocks.

Rock	Length (ft)	Width (ft)	Height (ft)	Weight (kg)
1	2.6	2.1	2	369
2	3.3	2.4	2.7	551
3	3.3	2.9	2.1	973
4	2	1.8	1.4	233
5	4.8	3.9	1.8	2,366
6	3.5	1.7	1.2	196
7	3.2	2.6	2.5	701
8	2.8	1.6	1	163
9	3.2	2.4	1.7	551
10	1.9	1	1	40
11	3.5	1.9	2	274
12	2	1.5	0.9	135
13	2.6	2.3	1.1	485
14	4.3	3.5	2.5	1,710
15	3.8	2.6	1.3	701
16	2.3	1.7	1	196
17	5.2	3	1.4	1,077
18	4.3	3.9	1.2	2,366
19	5.3	3.6	3	1,861
20	4.4	3.2	2.1	1,307
21	4.3	3.5	2.7	1,710
22	4.7	3	2.6	1,077
23	2.6	1.4	1.5	109
24	4.8	3.2	1.8	1,307
25	5.2	2.9	2.3	973
26	3.7	2.5	2.5	623
27	3.4	1.9	1.6	274
28	4.6	2.2	2.1	425
29	4	3.4	2.1	1,568
30	3.4	1.9	1.3	274
31	3.8	2.7	2.1	785
32	4.6	3.9	0.9	2,366
33	4.3	3.2	2.3	1,307
34	4.9	2.4	2.3	551
35	3.5	2.7	2.2	785
36	2.8	2.8	1.5	876
37	3	2.2	1.6	425
38	3.6	1.8	0.9	233
39	4.5	3.8	3.7	2,189
40	3.8	2.2	2	425
41	4.9	4.6	2.4	3,883
42	2.9	2.7	2.4	785

Rock	Length (ft)	Width (ft)	Height (ft)	Weight (kg)
43	3.6	2.1	2.1	369
44	4	2.4	2.6	551
45	4.3	2.7	3.6	785
46	3.8	2.2	3.6	425
47	4.1	3.3	2.1	1,433
48	3.6	2.5	1.5	623
49	3.9	2.4	1.2	551
50	6.3	3.4	2.3	1,568
51	5.1	2.9	2.2	973
52	2.2	1.5	1.1	135
53	2	1.2	0.9	69
54	2.3	1.6	1.6	163
55	4.4	2.7	2.1	785
56	3.3	2.6	1.2	701
57	2.4	2.1	1.1	369
58	2.5	2.1	2.1	369
59	5.5	3.7	2.7	2,020
60	3.4	1.9	2.2	274
61	4.2	1.7	1.9	196
62	2.9	1.4	2.1	109
63	5.4	4.2	2.8	2,955
64	2.9	1.9	2.3	274
65	5	3.2	1.6	1,307
66	5.8	3.3	2	1,433
67	6.1	3.4	3.7	1,568
68	6.4	4	2.8	2,553
69	4.2	3.7	2.9	2,020
70	6.3	3.2	2.2	1,307
71	3	1.1	2.2	53
72	3.4	2.2	1.3	425
73	2.2	1.1	1.3	53
74	1.3	1.1	0.6	53
75	1.6	1	0.8	40
76	3.8	2.7	2.7	785
77	5.4	2.4	2.1	551
78	2.3	1.2	0.7	69
79	2.1	0.7	1.4	14
80	3.8	2.9	2	973

Table 3-3. Mean and standard deviation for rocks parameters.

Rock Parameters	Length (ft)	Width (ft)	Height (ft)	Calculated weight (kg)
Mean	3.8	2.5	1.9	849
Minimum	1.3	0.7	0.6	14
Maximum	6.4	4.6	3.7	3,882
Std Dev	1.2	0.9	0.7	779

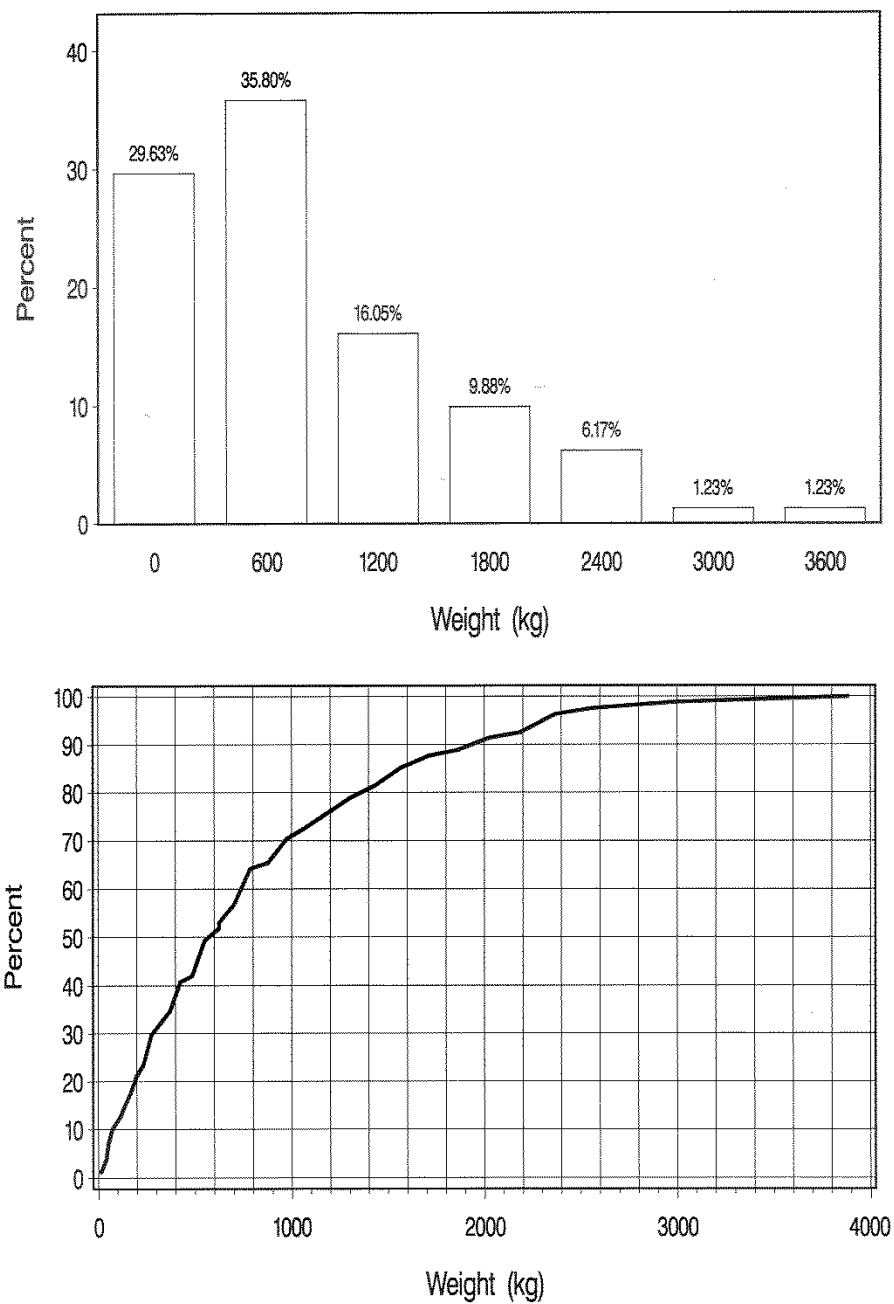


Figure 3-16. Weight distribution of SONGS revetment rocks.

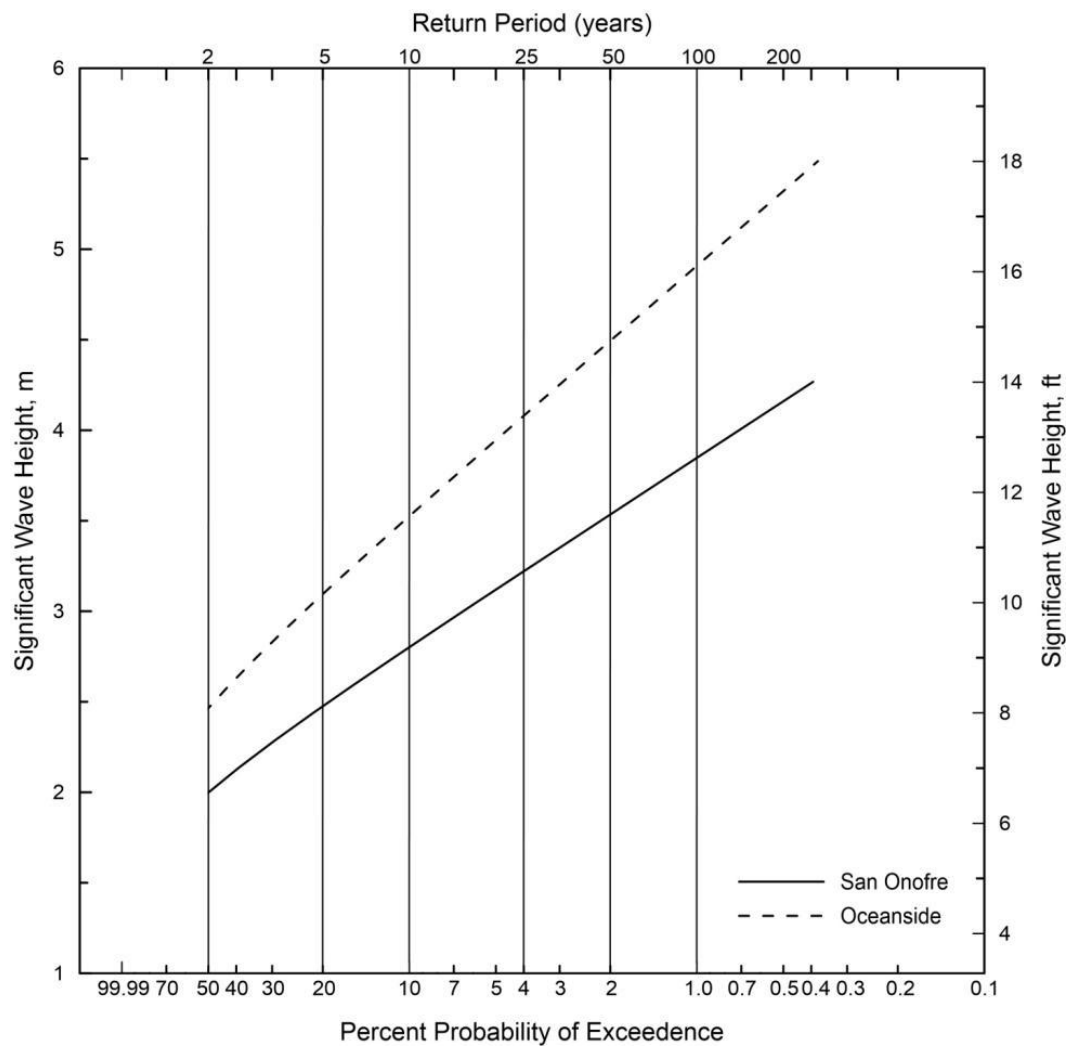


Figure 3-17. Design wave heights for various return periods at San Onofre.

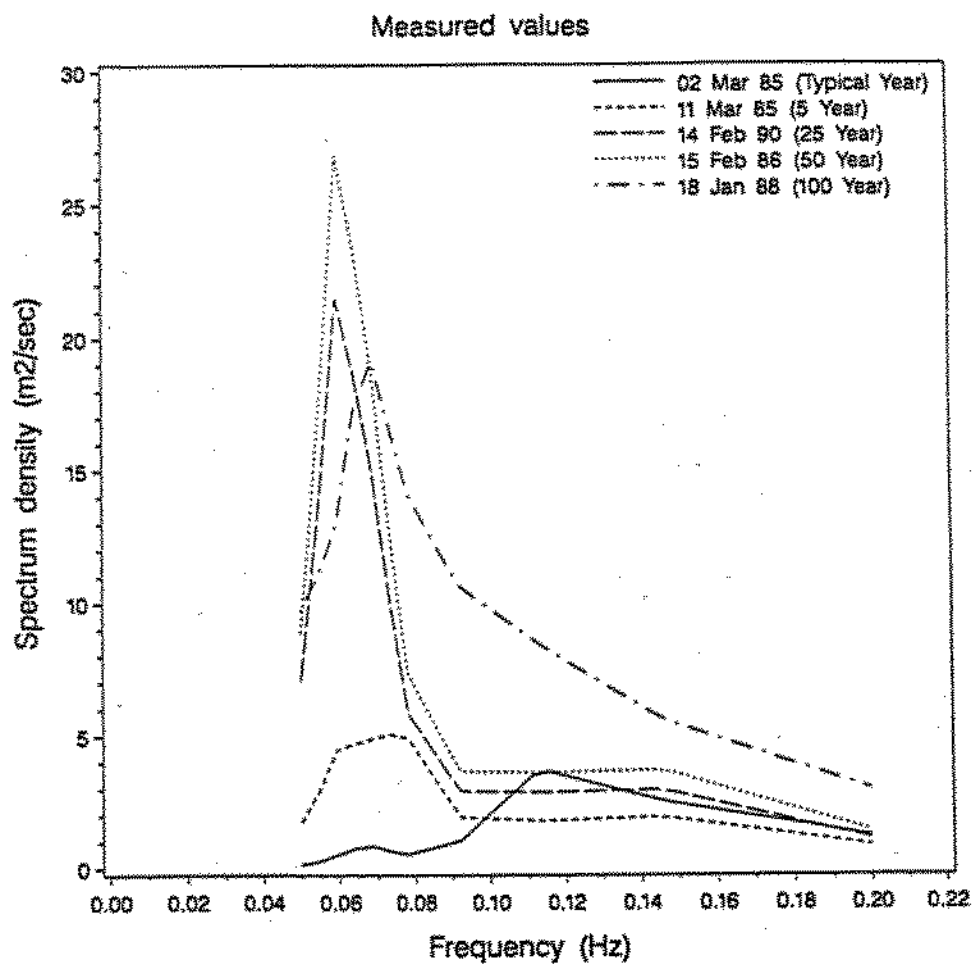


Figure 3-18. Measured spectrum density for various storms.

Table 3-4. Design wave characteristics at San Onofre.

Storm Return Period (yr)	Significant Wave Height, Hs (m)	Peak Period, Tp (sec)
2	2.0	9
5	2.4	12
10	2.8	12
25	3.2	17
50	3.5	17
100	3.8	16

Table 3-5. Largest 20 waves at San Onofre ranked in descending order (1976-1994).

Rank	Winter		Summer		All	
	Hs (m)	Tp (secs)	Hs (m)	Tp (secs)	Hs (m)	Tp (secs)
1	3.85	14.22	2.01	8.00	3.85	14.22
2	3.28	12.80	1.76	8.53	3.28	12.80
3	2.88	14.22	1.73	7.11	2.88	14.22
4	2.88	8.53	1.70	8.53	2.88	8.53
5	2.52	12.80	1.64	16.00	2.52	12.80
6	2.41	8.53	1.64	8.26	2.41	8.53
7	2.36	8.53	1.60	7.53	2.36	8.53
8	2.31	7.53	1.59	7.11	2.31	7.53
9	2.26	6.74	1.52	8.53	2.26	6.74
10	2.25	12.80	1.50	7.53	2.25	12.80
11	2.25	12.80	1.47	8.00	2.25	12.80
12	2.12	12.80	1.47	9.48	2.12	12.80
13	2.06	7.53	1.44	14.22	2.06	7.53
14	2.06	14.22	1.44	7.53	2.06	14.22
15	2.06	12.80	1.42	7.53	2.06	12.80
16	2.05	14.22	1.42	7.53	2.05	14.22
17	2.04	7.53	1.42	16.00	2.04	7.53
18	2.03	9.14	1.41	6.74	2.03	9.14
19	2.03	7.53	1.41	9.85	2.03	7.53
20	2.03	14.22	1.41	16.00	2.03	14.22

Table 3-6. Rock weights (W50) for 2020 and 2050.

Year	Water Depth Ds (ft)	H (ft)	H (m)	W50 (kg)
2020	7.79	4.4	1.33	276
2050 (P .05%)	9.79	5.5	1.67	548
2050 (H++)	10.59	5.9	1.8	685

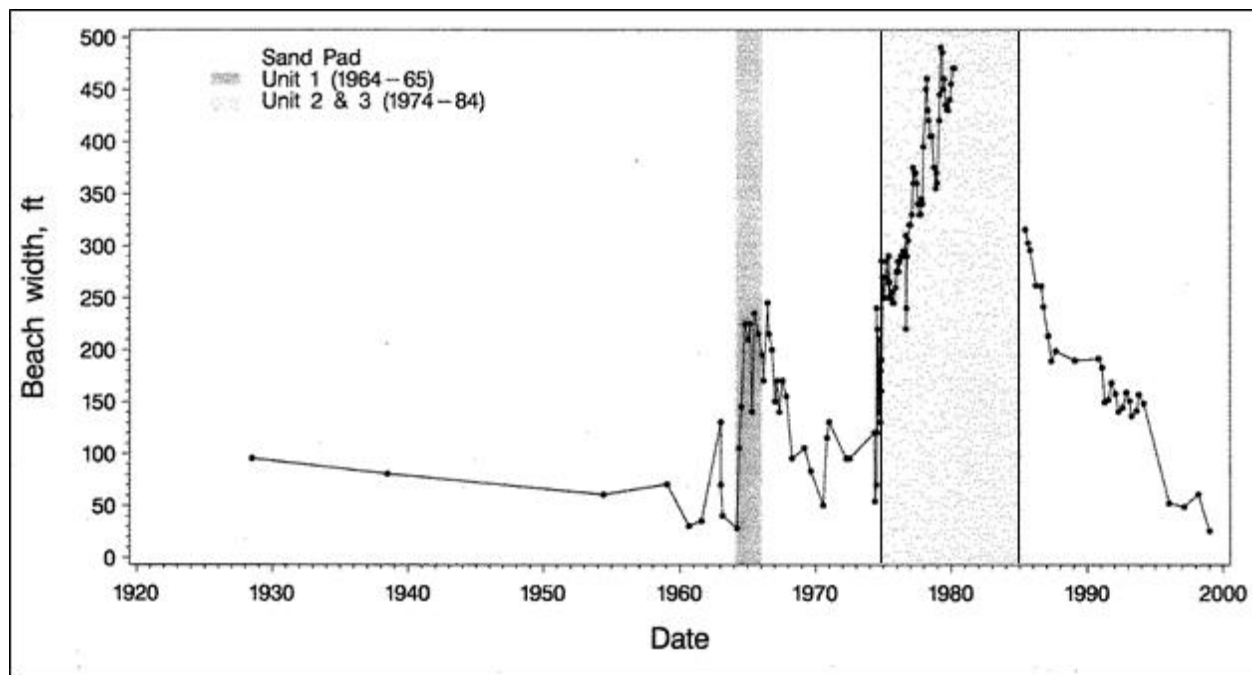


Figure 3-19. Historical beach width adjacent to Unit 1, 1928-2000. Vertical columns show periods when laydown pads were present. From Appendix E.

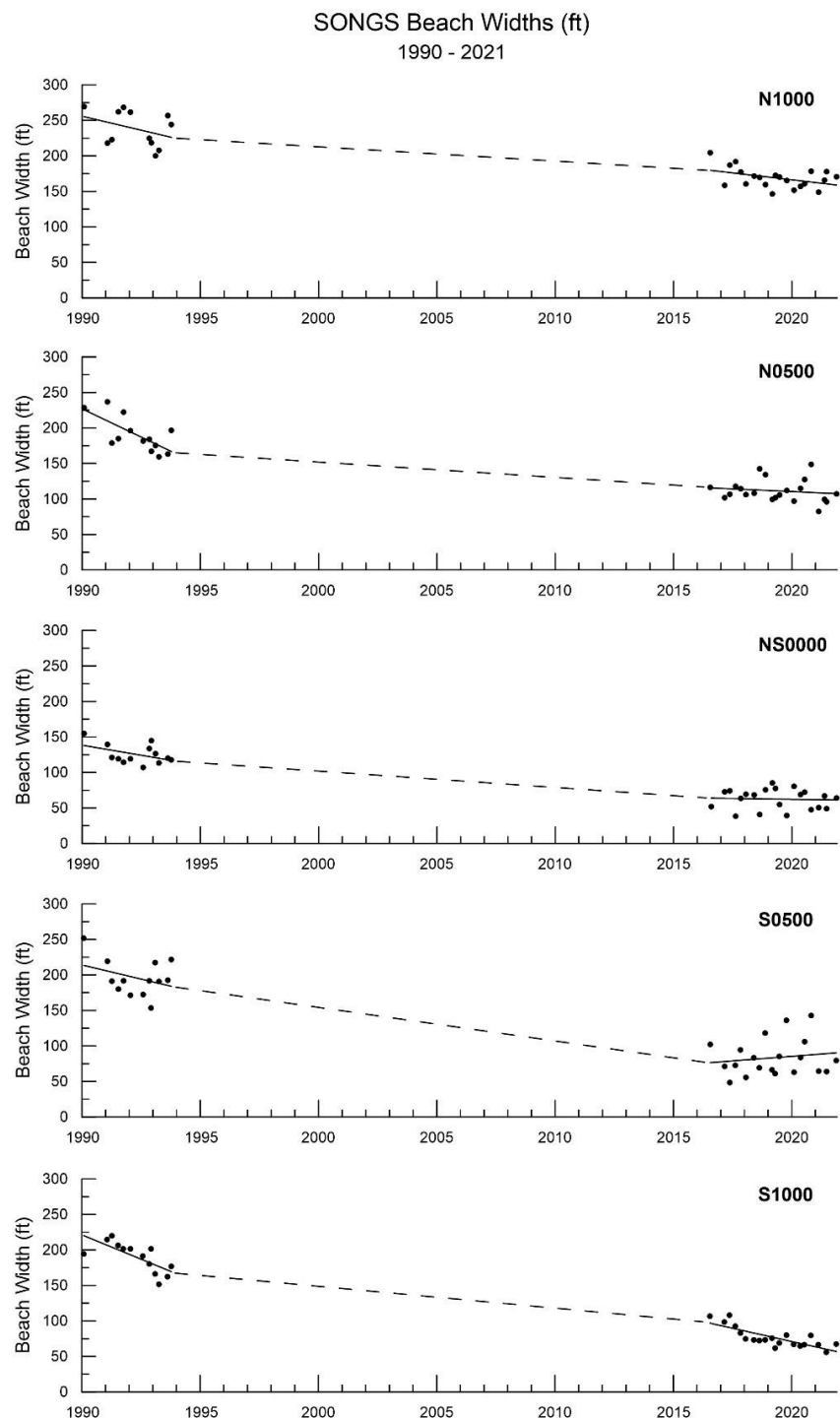


Figure 3-20. Beach width measured between 1991 through 1993 and between 2016 through 2020. Solid lines are the mean of beach width for the referenced periods and dotted lines cover the period where no long-term measurements were carried out. From Appendix E.

Table 3-7. Mean beach widths (ft) at San Onofre, 1990-1993 vs 2017-2022. From Appendix E (Table 7-1).

Profile	1990-1993		2017-2022		Difference in Mean	p-value*
	Mean	Std. Dev	Mean	Std. Dev		
N1000	237.9	25.1	166.2	11.5	71.7	3.57E-07
N0500	190.4	25.0	112.3	16.8	78.1	7.68E-09
NS0000	125.4	13.9	63.9	8.9	61.5	8.65E-13
S0500	195.8	26.0	62.3	13.8	133.5	2.26E-12
S1000	189.8	20.9	31.0	4.2	158.8	4.68E-13



Figure 3-21. Erosion rates for contours at 5, 15, 25, 30, and 50 ft calculated using the DSAS tool from 1998 until 2016.

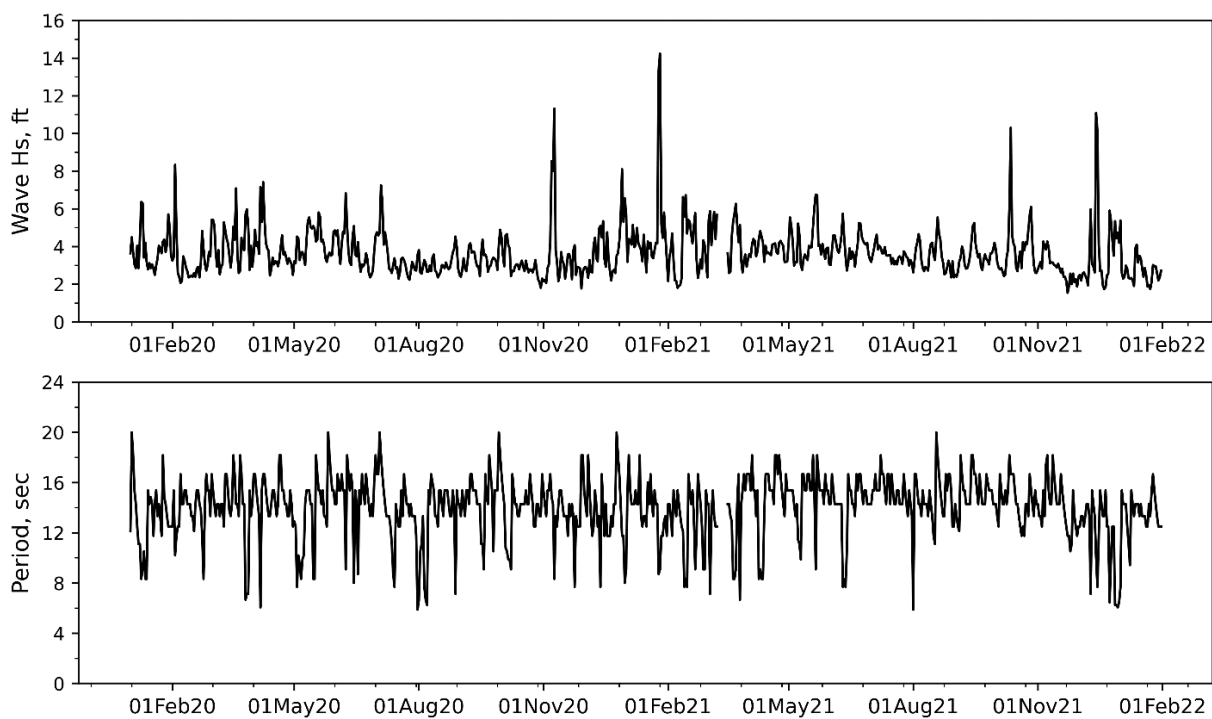


Figure 3-22. Wave height and wave period from 01 January 2020 to 17 February 2022.

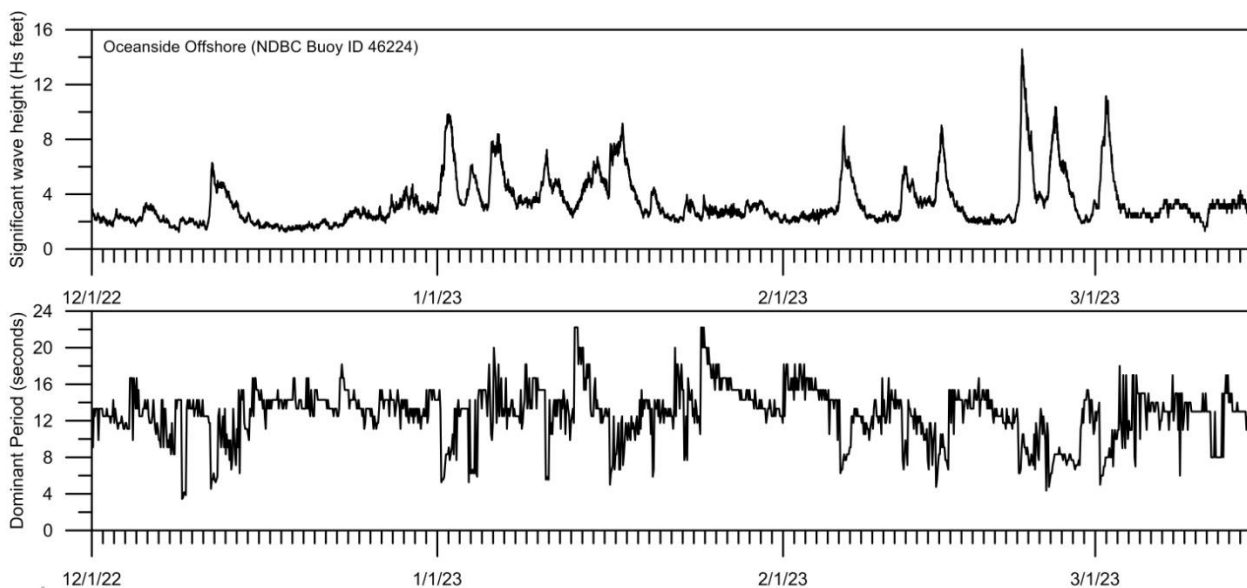


Figure 3-23. Wave height and wave period from 01 December 2022 to 17 March 2023.



Figure 3-24. North portion of the revetment (Range 3) covered by beach sand in 2020 (top), and a small amount of cobbles exposed in 2022.

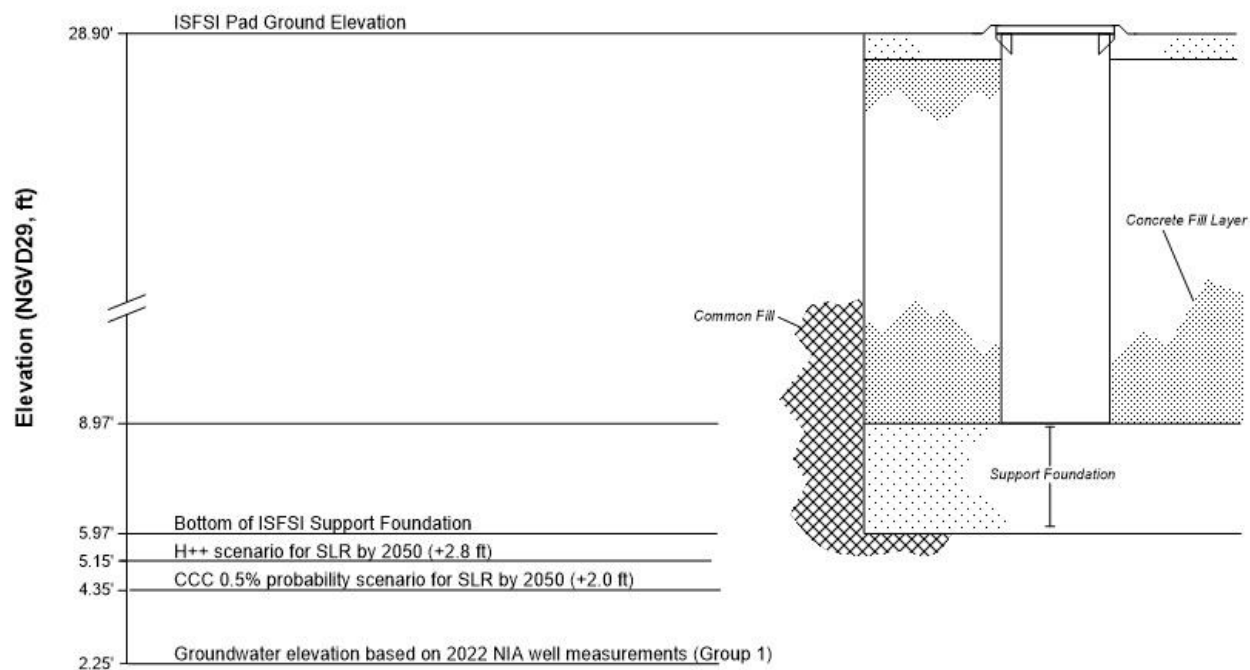


Figure 3-25. Groundwater elevations for 2022 and for the OPC projections in 2050. The CCC projections (2018) for sea level rise are based on OPC projections. From Appendix F.

4.0 RUN-UP AND OVERTOPPING ANALYSIS

Wave run-up is defined as the rush of water up a beach or coastal structure caused by, or associated with, wave-breaking. The run-up elevation, designated R (Figure 4-1), is the maximum vertical height above still water level that the run-up will reach. If the run-up elevation is higher than the beach berm (or back of the beach) elevation, the excess is then representative of overtopping. Run-up elevation is dependent on the incident wave characteristics, beach slope, and porosity, and if a structure is present, on that structure's shape, slope, roughness, permeability, and water depth at the toe. Run-up analysis is important to assess possible flooding and damage to the SONGS revetment, retaining wall, and walkway. The amount of damage is dependent on the run-up elevation and amount of overtopping, as well as on storm wave duration.

4.1 RANDOM WAVE METHOD

Wave run-up (R) is composed of wave setup and swash run-up. The swash run-up is defined as a super elevation of the mean water level and fluctuation about that mean (S). R is given by the equation:

$$R = \eta + S/2 \quad (4-1)$$

where η is the setup and S is swash run-up.

Many small- and large-scale laboratory studies have been conducted to measure run-up values for modeled beaches, sloped dikes, and seawalls (e.g., Hunt 1959; Van der Meer and Janssen 1995; Hedges and Reis 1998). Based on laboratory experiments, Hunt (1959) proposed various formulas for estimating wave run-up, R , on a smooth slope as a function of offshore wave height, H , and the Iribarren number, ζ , such that:

$$R = kH\zeta, \quad (4-2)$$

where k is a constant and ζ is the Iribarren number defined as:

$$\zeta = \frac{\tan\beta}{H_o/L_o} \quad (4-3)$$

where $\tan\beta$ is beach slope, H_o is deepwater wave height, and L_o is deepwater wavelength.

Fewer studies have centered on run-up on beaches (Holland and Holman 1993; Raubenheimer *et al.*, 1995; Ruggiero *et al.*, 2004; Stockdon *et al.*, 2006).

Stockdon *et al.* (2006) considered the contribution from both incident and infra gravity waves, using data from 10 field experiments with varying bathymetries and wave heights. They empirically estimated $R_{2\%}$ by:

$$R_2 = A \quad 0.35 \beta_f H_0 L_0^{1/2} + \frac{H_0 L_0 \quad 0.563 \beta_f^2 + 0.004}{2}^{1/2} \quad (4-4)$$

where β_f is the foreshore beach slope and H_o is the deepwater significant wave height, A is a coefficient equal to 1.1 as estimated by Stockdon, and $R_{2\%}$ is the 2% exceedance level of run-up for each run. The units of the Equation 4-4 are in meters.

The SONGS revetment reduces wave run-up by factor that varies from 0.5 to 0.6 (USACE 1994b, Table 7-2) due to slope roughness and permeability.

4.2 OVERTOPPING

The overtopping rate (Q) is defined as the volume of water that overtops a coastal structure or beach berm along the beach length per unit time and length. The units are volume per second per unit length (ft³/sec-ft or m³/sec-m). Overtopping empirical models are based on laboratory studies of structure overtopping. These models are used to test design specifications intended to limit the overtopping of levees and dikes, and they therefore give conservative values. A beach berm can act in the same manner as these structures in protecting the backshore development from wave attack and flooding.

Wave overtopping values depend on the ratio of freeboard height and wave run-up height. Freeboard R_c is defined as the height of the berm crest above mean water level. In order for waves to overtop a berm, the run-up heights must be greater than the freeboard height. Overtopping is dependent on run-up height and, therefore, dependent on incident wave height and period, and beach slope.

Hedges and Reis (1998) introduced a semi-empirical model (H&R model) based on an overtopping theory for regular waves developed by Kikkawa *et al.* (1968), which assumed that a seawall or beach berm acted as a weir whenever the incident water level exceeded the seawall level and the described instantaneous discharge by the weir formula. The H&R model extended the concept to random waves. Reis *et al.* (2008) compared the H&R model with three other methods used to estimate the overtopping rate for various structures subject to random wave action. The slopes of these structures varied from 1:1 to 1:20, and wave steepness varied from 0.01 to 0.3. The models were: (1) Owen model (Owen, 1980); (2) Van der Meer Janssen model (Van der Meer and Janssen, 1995); and (3) AMAZON Numerical Model (Hu, 2000). The results showed good agreement between the H&R model and the data. There was general agreement between the H&R and AMAZON models, while Owen's model systematically over-predicted the discharges. Van der Meer and Janssen's model gave similar results to the H&R model, except that they over-predicted discharges for some conditions which are outside the ranges of applicability.

The H&R model extending the concept to random waves can be written as:

$$\frac{Q}{gR_{3\max}} = A \left(1 - \frac{R_c}{\gamma R_{\max}} \right)^B \quad \text{for } 0 \leq \frac{R_c}{\gamma R_{\max}} < 1 \quad (4-5)$$

and

$$\frac{Q}{gR_{3\max}} = 0 \quad \text{for} \quad \frac{R_c}{\gamma r R_{\max}} \geq 1 \quad (4-6)$$

where g is gravitational acceleration, R_{\max} is the maximum run-up on smooth slope, and γr is a reduction factor to account for rough slope. In this study, R_{\max} is estimated by equation number 9 presented by Reis *et al.* (2008). Additionally, the coefficients of the HR model were given by Reis *et al.* (2008) as:

$$A = \begin{cases} 0.0033 + 0.0025 \ 1/\beta & \text{for } 0.08 \leq \beta \leq 1 \\ 0.0333 & \text{for } 0.05 \leq \beta < 0.083 \end{cases} \quad (4-7)$$

$$B = \begin{cases} 2.8 + 0.65 \ 1/\beta & \text{for } 0.13 \leq \beta \leq 1 \\ 10.2 - 0.275 \ 1/\beta & \text{for } 0.05 \leq \beta < 0.13 \end{cases} \quad (4-8)$$

where β is the beach slope.

4.3 RESULTS

Figure 3-13 shows typical cross sections of the SONGS revetment. The locations of these profiles are shown in Figure 3-9. The slope (β) of the revetment varies from 0.33 to 0.44. The height of the walkway is about 14 ft (NGVD). The design water level is estimated as 5.5 ft (NGVD). Table 4-1 provides run-up and overtopping results for all design wave and water level conditions, including MSLR under the medium-high scenario for 2020, 2030, 2040, and 2050. Table 4-2 shows these results for the extreme H++ MSLR projection. Tables 4-1 and 4-2 suggest that wave overtopping already occurs (in 2020) for storm wave conditions meeting or exceeding a 10-year return period, that is, waves with 10% probability of occurrence in a given year. This is consistent with observations.

As MSLR progresses, overtopping rates are expected to increase. For large storms, rates are projected to reach 0.5 ft³/sec-ft by 2030 and 1-1.6 ft³/sec-ft by 2050. There is a short segment in the walkway where the concrete wall has been replaced by rails to provide a flow path for the saltwater cooling system during plant operations. This opening in the wall will increase overtopping on the walkway (Figure 4-2). However, it does not represent a significant hazard to pedestrians since the walkway will be closed during storms and there are no more discharges from the system.

4.4 PROBABILITY ANALYSIS

The probability associated with run-up and overtopping is considered in quantitative terms. This risk is defined as the probability that a “T-year” return-period event will occur at least once during a given “n-year” long time period. The run-up results in Tables 4-1 and 4-2 can be used to estimate the risk for any selected “n-year” long time period. The results can also be used to estimate the probability of run-up of a given size during a specified time period. The probability of a T-year run-up in any one year is $P = 1/T$.

In other words, there is a one-percent chance that the 100-year run-up will occur during a given year. The probability is equal to the sum of the probabilities of having one run-up, two run-ups, or n run-up events occurring during n years of interest, or to 1 minus the probability of having no run-ups. The risk can be calculated from Equation 4-9:

$$P = 1 - (1 - 1/T)^n \quad (4-9)$$

Equation 4-9 indicates that there is a 63% chance that the 100-year magnitude run-up will occur at least once during any 100-year time interval. Similarly, Equation 4-9 can be used to calculate the risk associated with any T-year run-up during any time period.

Figure 4-3 gives the probability of occurrence of T = 25-year, 50-year and 100-year run-ups in an n-year period based on Equation 4-9.

4.5 DISCUSSION

Observations suggest that over the last decade or longer, the SONGS revetment has adjusted to reach an equilibrium configuration. Under its current condition, the revetment is expected to withstand projected wave forces with acceptable minimum damages that will not impact the integrity of the revetment as a whole.

The walkway elevation at 14 ft (NGVD) is relatively low and will continue to be flooded under large wave conditions that overtop the revetment. However, it should be noted that the results of run-up and overtopping presented in this study are conservative for the following reasons:

1. The results are based on an extreme high water level of 5.5 ft (NGVD) that includes King Tides, El Niño enhancements, and one-foot storm surges. Observations suggest that it is exceedingly unlikely for large storm waves to occur precisely at the time of peak high (King) tides (e.g., Elwany and Flick, 1999; Flick 1998 and 2016; Young *et al.* 2018).
2. Figure 4-4 illustrates the joint probability distribution between significant wave height and water level between 1976-1994, a period characterized by large wave events occurring between 1981 and 1984. Figure 4-3 shows that the probability of 50-year and 100-year waves occurring in the next 30 years is 0.45 and 0.28, respectively. Multiplying these probabilities by the probability of larger waves occurring at high tides will lead to an extremely low probability of occurrence.

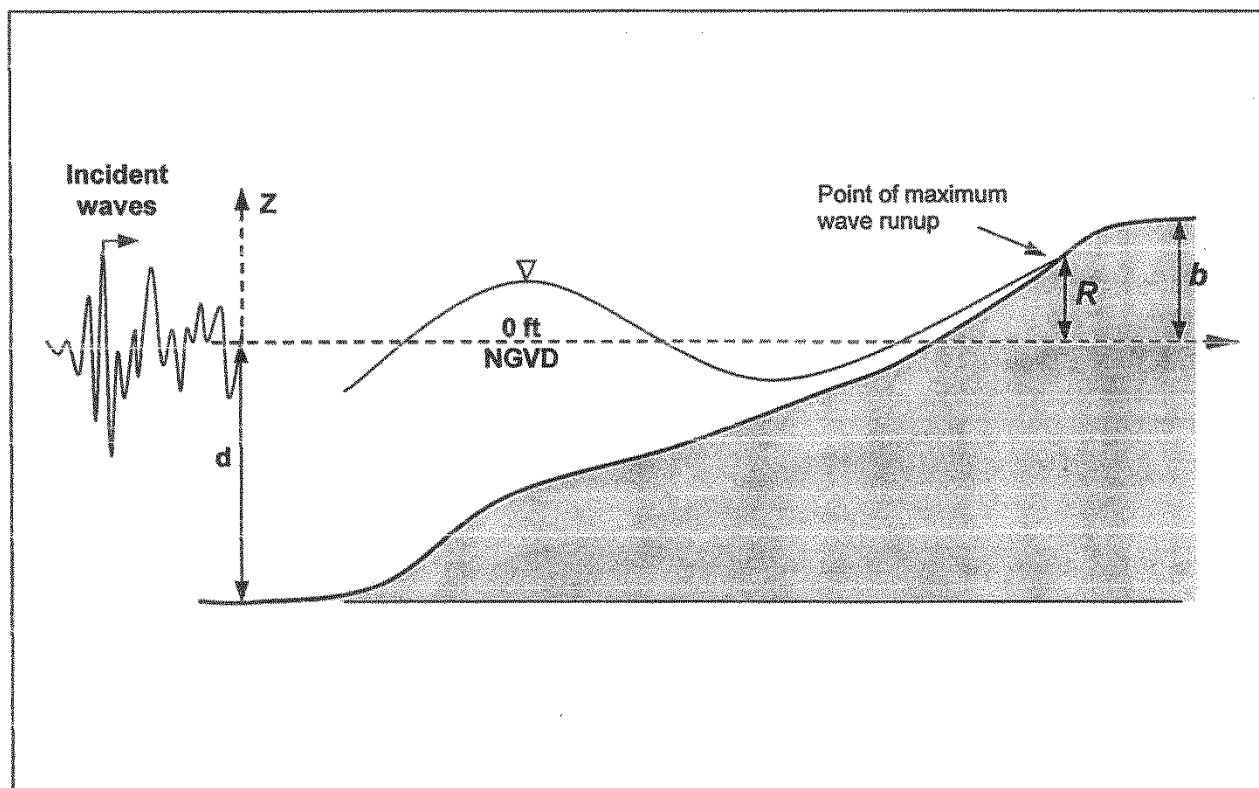


Figure 4-1. Wave run-up on a slope. R is the run-up elevation; b is the height of the beach berm. If $R > b$, then overtopping will occur.

Table 4-1. Run-up and overtopping summary for Medium-High Risk Aversion.

Year	Return Period (yr)	HS (m)	Tp (Sec)	Sea Level Rise (ft)	Run-up (ft)	Run-up Elevation (ft)	Overtopping Rate (ft³/sec-ft)
2020	2	2	9	0	5.27	10.77	0.00
	5	2.4	12	0	7.23	12.73	0.00
	10	2.8	12	0	7.81	13.31	0.01
	25	3.2	17	0	10.58	16.08	0.18
	50	3.5	17	0	11.06	16.56	0.28
	100	3.8	16	0	11.09	16.59	0.32
2030	2	2	9	0.9	5.27	11.67	0.00
	5	2.4	12	0.9	7.23	13.63	0.01
	10	2.8	12	0.9	7.81	14.21	0.04
	25	3.2	17	0.9	10.58	16.98	0.34
	50	3.5	17	0.9	11.06	17.46	0.49
	100	3.8	16	0.9	11.09	17.49	0.56
2040	2	2	9	1.3	5.27	12.07	0.00
	5	2.4	12	1.3	7.23	14.03	0.02
	10	2.8	12	1.3	7.81	14.61	0.06
	25	3.2	17	1.3	10.58	17.38	0.44
	50	3.5	17	1.3	11.06	17.86	0.62
	100	3.8	16	1.3	11.09	17.89	0.71
2050	2	2	9	2	5.27	12.77	0.00
	5	2.4	12	2	7.23	14.73	0.05
	10	2.8	12	2	7.81	15.31	0.12
	25	3.2	17	2	10.58	18.08	0.69
	50	3.5	17	2	11.06	18.56	0.94
	100	3.8	16	2	11.09	18.59	1.05

Table 4-2. Run-up and overtopping summary for Extreme Risk Aversion (H++).

Year	Return Period (yr)	HS (m)	Tp (Sec)	Sea Level Rise (ft)	Run-up (ft)	Run-up Elevation (ft)	Overtopping Rate (ft³/sec-ft)
2020	2	2	9	0	5.27	10.77	0.00
	5	2.4	12	0	7.23	12.73	0.00
	10	2.8	12	0	7.81	13.31	0.01
	25	3.2	17	0	10.58	16.08	0.18
	50	3.5	17	0	11.06	16.56	0.28
	100	3.8	16	0	11.09	16.59	0.32
2030	2	2	9	1.1	5.27	11.87	0.00
	5	2.4	12	1.1	7.23	13.83	0.02
	10	2.8	12	1.1	7.81	14.41	0.05
	25	3.2	17	1.1	10.58	17.18	0.39
	50	3.5	17	1.1	11.06	17.66	0.55
	100	3.8	16	1.1	11.09	17.69	0.63
2040	2	2	9	1.8	5.27	12.57	0.00
	5	2.4	12	1.8	7.23	14.53	0.04
	10	2.8	12	1.8	7.81	15.11	0.10
	25	3.2	17	1.8	10.58	17.88	0.61
	50	3.5	17	1.8	11.06	18.36	0.84
	100	3.8	16	1.8	11.09	18.39	0.94
2050	2	2	9	2.8	5.27	13.57	0.01
	5	2.4	12	2.8	7.23	15.53	0.12
	10	2.8	12	2.8	7.81	16.11	0.24
	25	3.2	17	2.8	10.58	18.88	1.12
	50	3.5	17	2.8	11.06	19.36	1.47
	100	3.8	16	2.8	11.09	19.39	1.62



Figure 4-2. Exposed area in the walkway wall.

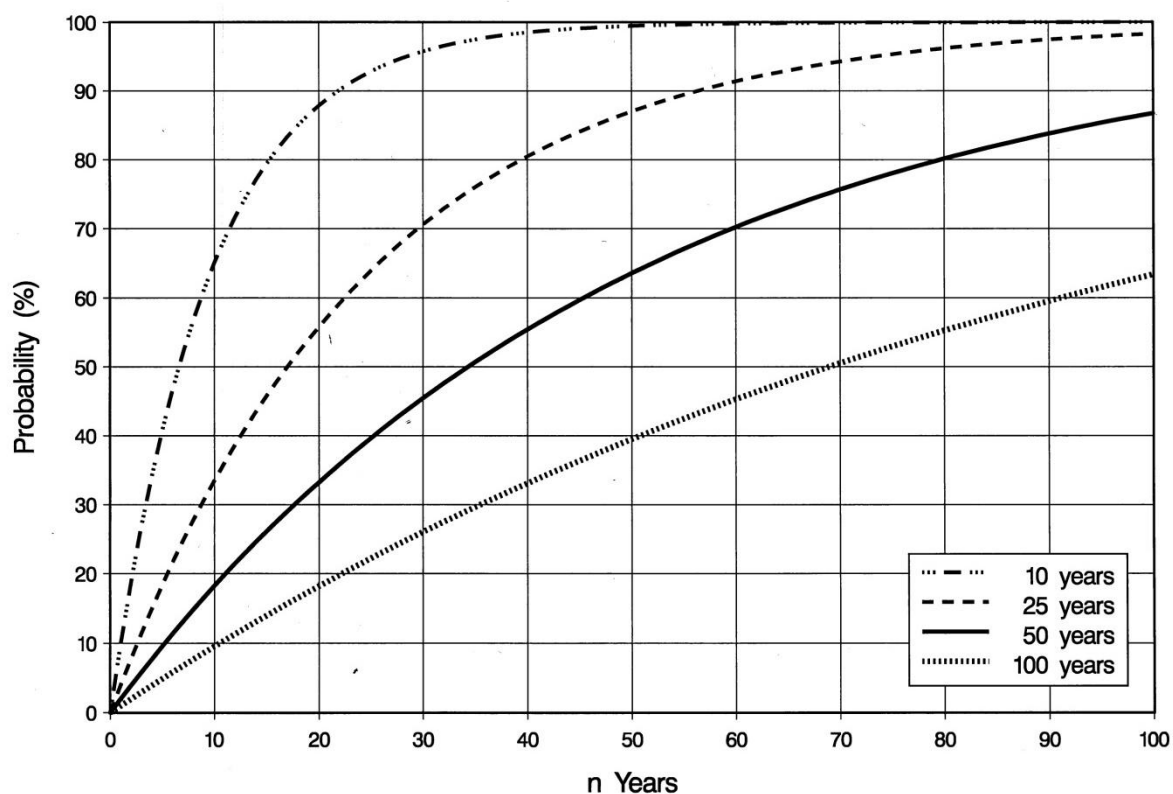


Figure 4-3. Probability of 10-, 25-, 50-, and 100-year waves return period to occur in the next 100 years.

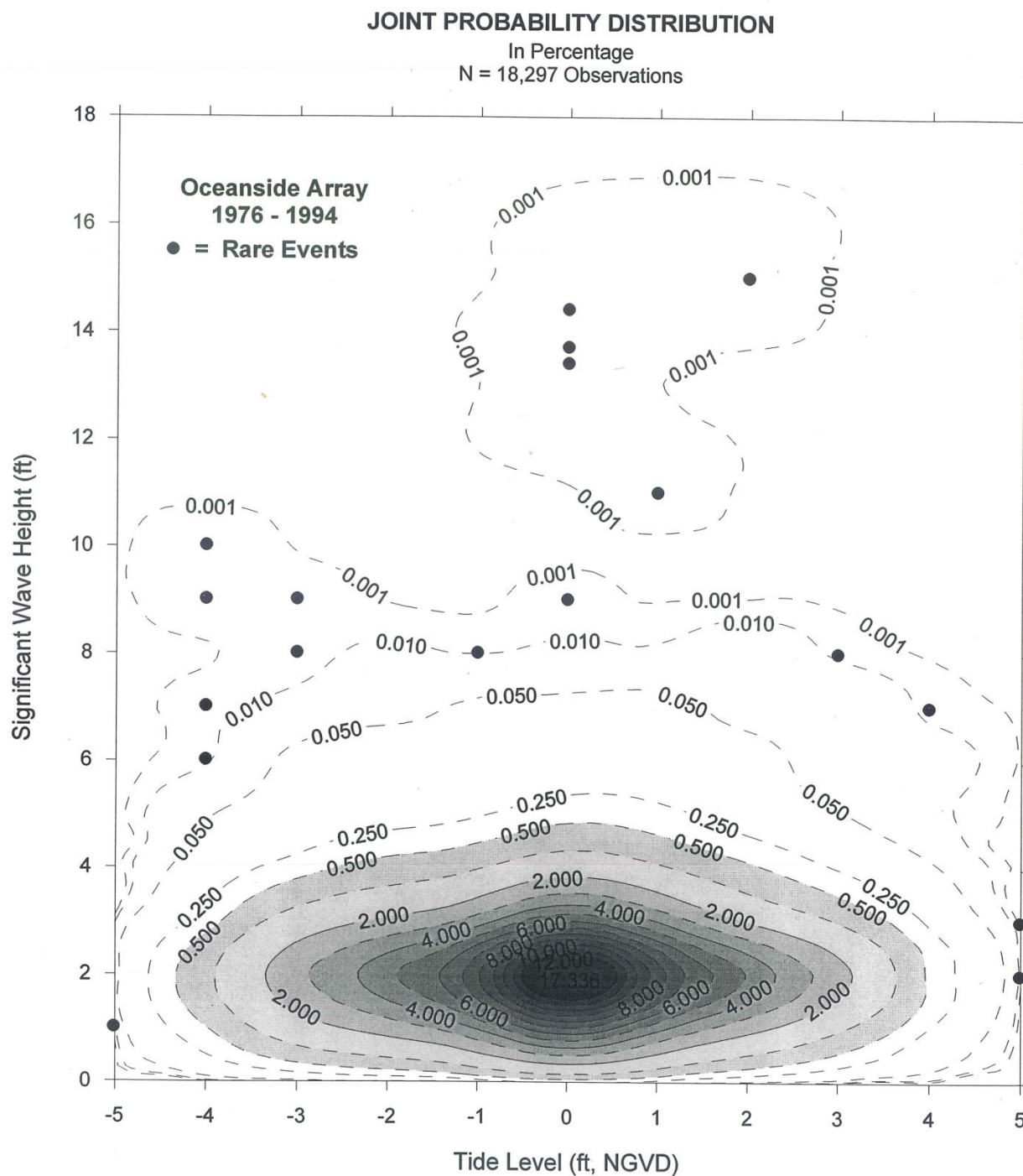


Figure 4-4. Joint Probability distribution between significant wave height and tide level. From Elwany and Flick (1999).

5.0 CONCLUSIONS

The objective of this report is to provide information related to sea level rise vulnerability, structural integrity, and the adaptive capacity of the Lease Premises and the structures therein. We summarize the present knowledge of MSLR using the latest state and federal agency guidelines, especially OPC (2018). We also evaluate the current SONGS revetment and walkway exposure and vulnerability to wave and high-water level events by gauging their current condition and examining storm data from the past year. We review the revetment stability by evaluating structural changes within the past year and comparing the weight of its rocks to the design weight needed to withstand wave forces for various design waves return periods.

The OPC (2018) and CCC (2015, updated 2018) probability-based MSLR scenarios evaluated in this study are unchanged from last year and the most current existing MSLR guidance for the State of California. Projections of future MSLR continue to evolve as understanding of key climate change processes improves. Of notable concern are the possible ranges and rates of glacial ice loss in Greenland and Antarctica (e.g., DeConto and Pollard 2016). However the IPCC (2021; 2022) and NOAA (2022) estimates are lower than those for OPC (2018) and CCC updated projection in 2018. It likely the new guidance from OPC and CCC expected to be published late in 2023 or early 2024, these estimates would likely be lower than those indicated previously by OPC (2018) and CCC (2018).

Section 2.2.2 discusses IPCC (2021) MSLR projections in detail. The OPC, IPCC mid-range, and IPCC mid to high range MSLR projections for 2000, 2030 and 2050 are given in Tables 2-2 through 2-3, respectively. It is apparent that the IPCC (2021; IPCC 2022) projections more closely fit the data from 2000-2021 compared to the OPC (2018) scenarios. For the extreme trajectory (“SSP5-8.5-low confidence”), rises 0.6-1.4 ft by 2050, at most half that of the analogous OPC (2018) H++.

Estimates from the NOAA technical report (2022) are presented in Tables 2-5 and 2-6. These estimate were lower than OPC (2018) medium-high and H++ scenarios and within the range of IPCC (2021; 202) projections for global MSLR. It is expected in 2023-2025 future guidelines from state and federal agencies will publish. The studies completed in last few years will be the basis for the agencies guidelines.

Future MSLR is highly uncertain, especially after about 2050, for several reasons. The largest unknown is what mitigation strategies humans will employ to decrease the rates and amounts of greenhouse gas (GHG) emitted and ultimately resident in the atmosphere. Second, the climate sensitivity, or amount and rate of warming for a given increase in GHGs is not precisely known. In particular, polar ice response to existing and future warming is not yet reliably predictable.

The CCC continued commitment to coastal access suggests that implementing all feasible means to maintain existing lateral access along the beach fronting SONGS will be both necessary and beneficial. Lateral access depends on keeping the revetment in good condition to protect the

walkway fronting the seawall. The SONGS revetment is currently in good condition and can likely provide wave protection to the retaining wall and walkway through at least 2050.

Appendix A shows comparisons between revetment conditions in 2023 vs 2020. The data were obtained by laser scanner system (Section 3.2.2). The photographs taken during January and February 2023 site visit (Appendix D) were important to this study; they complement the laser scanner survey and show the beach conditions at each of the 21 ranges after the 2021-2023 winter wave storms. The laser scanner survey clearly described the rock shape (sizes) while the photographs highlighted the sand and cobble areas on the beach.

This study finds that the revetment, in its present condition, is likely to tolerate wave forces with acceptable rock movement that will not affect the integrity of the revetment as a whole. The study found that, as designed and with regular maintenance, the revetment should withstand wave forces over the next 30 years and has a high adaptive capacity to MSLR (Section 3.10). The noticeable changes in the revetments were at the north portion of the revetment which protecting the walkway, further away from Units 1, 2 and 3, between Ranges 6 and 7 where few of the rocks were either scoured down or moved due to large waves early January 2023 (Figures A-6 and A-7); these rocks were not shown in the results of the 19 January 2023 laser-scanner survey, or the photos taken during the site visit. No damage to the walkway is expected

The beach prevents toe scouring that can undermine the revetment and cause rock units to settle. When the beach is narrow or water level is unusually high, or both, waves breaking on the revetment can cause dislocation of individual rocks, which contributes to revetment instability.

A San Onofre Beach assessment based on SCE's beach monitoring program is valuable as sea level rise accelerates in the future. MSLR will likely increase both the wave forces on the rocks (due to greater water depth and wave height fronting the revetment), and sand scour undermining that could lower and destabilize the revetment (due to beach retreat). Elwany *et al.* (2017) have addressed the impacts of sea level rise on San Onofre Beach.

Wave overtopping and walkway flooding will occur when high wave events coincide with extreme water levels due to the relatively low elevation of the walkway at 14-15 ft, NGVD. However, occasional flooding is not likely to impact lateral public beach access since this will be normally limited during storms. Furthermore, flood waters will drain from the walkway after each event.

Impacts of groundwater on the ISFSI based on quarterly measurements of the groundwater from 9 coastal wells out of 16 total wells are presented in Appendix F. The OPC (2018) medium-high (0.5%) and H++ SLR scenarios for groundwater elevation for 2050 are 4.35 and 5.15 ft, NGVD (Section 2) and are 1.62 and 0.82 ft lower than the bottom of the ISFSI support foundation, respectively. The ISFSI support foundation is 3 ft thick.

6.0 REFERENCES

- Ahrens J. P., 1981a. *Irregular Wave Runup on Smooth Slopes*. Coastal Engineering Technical Aid No. 81-17. USACE, 26 pp.
- Ahrens J. P., 1981b. *Design of Riprap Revetments for Protection Against Wave Attack*. Technical Paper No. 81-5. USACE, 31 pp.
- Bamber, JUL., M. Oppenheimer, ROE. Kopp, WFP. Aspin all, and RAM. Cooke, 2019. *Ice sheet contributions to future sea-level rise from structured expert judgment*. Proc. Nat. Acad. Sci., 116 (23), 11195-11200.
- Bedsworth, L., D. Cayan, G. Franco, L. Fisher, and S. Zana, 2018. *Statewide Summary Report, California's Fourth Climate Change Assessment*. California Governor's Office of Planning and Research, Scripps Institution of Oceanography, California Energy Commission, and California Public Utilities Commission. Publication Number SUM-CCCA4-2018-013, 133 pp.
- Beckley, BED., NAP. Belinsky, S.A. Holmes, FIG. Lemoyne, R.D. Ray, G.T. Mitchum, S.D. Desai, and S.T. Brown, 2010. *Assessment of the Jason-2 Extension to the TOPEX/Poseidon, Jason-1 Sea-Surface Height Time Series for Global Mean Sea Level Monitoring*. Marine Geodesy, 33(1).
- British Columbia Ministry of Environment, Lands and Parks (BCMELP), 2000. *Riprap Design and Construction Guide*. Public Safety Section Water Management Branch, 12 pp.
- Bromirski, P.D., A.J. Miller, R.E. Flick, and G. Auad, 2011. *Dynamical Suppression of Sea Level Rise Along the Pacific Coast of North America: Indications for Imminent Acceleration*. J. Geophys. Res., 116(C7).
- Bromirski, P.D., A.J. Miller, and R.E. Flick, 2012. *North Pacific Sea Level Trends*. Eos Trans. AGU, 93(27), 249-256.
- Calafat, F.M., D.P. Chambers, and M.N. Tsimplis, 2012: Mechanisms of decadal sea level variability in the east-ern North Atlantic and the Mediterranean Sea. *Journal of Geophysical Research: Oceans*, 117, C09022. <https://doi.org/10.1029/2012JC008285>
- California Coastal Commission (CCC), 2015. *California Coastal Commission Sea Level Rise Policy Guidance: Interpretive Guidelines for Addressing Sea Level Rise in Local Coastal Programs and Coastal Development Permits*, California Coastal Commission, San Francisco, CA, 293 pp.
<http://www.coastal.ca.gov/climate/slrguidance.html>

- California Coastal Commission, 2015, updated 2018. *California Coastal Commission Sea Level Rise Policy Guidance, Interpretive Guidelines for Addressing Sea Level Rise in Local Coastal Programs and Coastal Development Permits*, California Coastal Commission, San Francisco, CA, 307 pp.
- California Coastal Commission (CCC), 2020a. *2021-2025, Protecting California's Coast for Present and Future Generations*, CCC, San Francisco, CA, 32 October 2020, 56 pp. <https://www.coastal.ca.gov/strategicplan/spindex.html>.
- California Coastal Commission (CCC), 2020b. *Sea Level Rise in California: Planning for the Future*, California Coastal Commission, San Francisco, CA, 17 pp. <https://storymaps.arcgis.com/stories/d0c1df224a97418bb4dad129ea4c6d17>.
- California Natural Resources Agency (CNRA) and California Environmental Protection Agency (CEPA), 2020. *Making California's Coast Resilient to Sea Level Rise: Principles for Aligned State Action*, CNRA and CEPA, Sacramento, CA, 29 April 2020, 6 pp. <https://www.adaptationclearinghouse.org/resources/making-california-eyes-coast-resilient-to-sea-level-rise-principles-for-aligned-state-action.html>.
- Cayan, D.R., J. Kalinsky, S. Iacobellis, and D. Pierce (with R. Kopp), 2016. *Creating Probabilistic Sea Level Rise Projections*. Unpublished White Paper, Division of Climate, Atmospheric Sciences, and Physical Oceanography, Scripps Institution of Oceanography, La Jolla, CA, 16 pp.
- Coastal Environments, 2000. *SONGS Unit 1 Deconstruction Marine Impacts Study, Phase I*. Unpublished report submitted to Southern California Edison Company, 24 January 2000, CE Ref. No. 2000-03, 44 pp. plus 2 appendices.
- Coastal Environments Inc., 2020. *2017-2019 Beach Profile Surveys at San Onofre*. Report Submitted to Southern California Edison, Rosemead, CA 91770, 9 March 2020, CE Ref. No. 20-03. 41 pp. and 6 Appendices.
- Coastal Environments Inc., 2021. *2020 Beach Profile Surveys at San Onofre*. Report Submitted to Southern California Edison, Rosemead, CA 91770, 31 January 2021, CE Ref. No. 21-01, 49 pp. and 2 Appendices.
- Coastal Environments, 2021a. *2021 Beach Profile Surveys at San Onofre*. Report Submitted to Southern California Edison, 20 December 2021, CE Ref. No. 21-22, 49 pp. + 2 appendices.
- Church, J.A. and N.J. White, 2011. *Sea-Level Rise from the Late 19th to the Early 21st Century*. *Surv. Geophys.*, 32, 585–602.
- DeConto, R., and D. Pollard, 2016. *Contribution of Antarctica to past and future sea level rise*. *Nature* 531, 591-597.

- DeConto, R.M., D. Pollard, R.B. Alley, I. Velicogna, E. Gasson, N. Gomez, S. Sadai, A. Condrón, D.M. Gilford, E.L. Ashe, R.E. Kopp, D. Li, and A. Dutton, 2021. *The Paris Climate Agreement and future sea-level rise from Antarctica*. Nature 593, 83-89.
- Elwany, H, R Flick and S. Aijaz, 1994. 1993 Beach Profile Surveys at San Onofre, Final Report. Submitted to Southern California Edison, Rosemead, C A 91770, CE Ref. No. 94-07. 32 pp. and 2 Appendices.
- Elwany, H., and R. E. Flick, 1999. *Coastal and Oceanographic Conditions in the Vicinity of the Proposed Manchester Resort Development Oceanside, California*. Coastal Environments Reference No. 99-03, prepared for Manchester Resort, 1 Market Place, San Diego, CA, 61 pp. and 4 Appendices.
- Elwany, H., R. E. Flick, and A.D. Young, 2016. *Coastal Analysis for End-State Planning of San Onofre Nuclear Generating Station, Phase 1*, Coastal Environments Reference No. 16-26, prepared for Southern California Edison Company, Rosemead, CA, 151 pp.
- Elwany, H., R. E. Flick, and A.P. Young, 2017. *Coastal Processes Analysis at San Onofre Nuclear Generating Station, Phase 2*, Coastal Environments Reference No. 17-08, prepared for Southern California Edison, 160 pp.
- Elwany, H. and R.E. Flick, and F. Scarelli, 2020. *San Onofre Nuclear Generating Station (SONGS) Mean Sea Level Rise Impact Assessment*, 2019 Technical Report, Report prepared for Southern California Edison by Coastal Environments, Inc. La Jolla, CA, 30 March 2020, CE-Ref. No. 20-08, 64 pp. and 6 Appendices.
- Elwany, H. and R.E. Flick, and F. Scarelli, 2021. *San Onofre Nuclear Generating Station (SONGS) Mean Sea Level Rise Impact Assessment*, 2020 Technical Report. Report prepared for Southern California Edison by Coastal Environments, Inc. La Jolla, CA, 25 March 2021, CE-Ref. No. 21-07, 76 pp. and 6 Appendices.
- Elwany, H. and R.E. Flick, and F. Scarelli, 2022. *San Onofre Nuclear Generating Station (SONGS) Mean Sea Level Rise Impact Assessment*, 2021 Technical Report. Report prepared for Southern California Edison by Coastal Environments, Inc. La Jolla, CA, 03 March 2022, CE-Ref. No. 21-07, 77 pp. and 6 Appendices.
- Flick, R.E. (ed.), 1994. *Shoreline Erosion Assessment and Atlas of the San Diego Region (2 volumes)*. Sacramento, CA: California Department of Boating and Waterways and San Diego Association of Governments.
- Flick, R. E., 1998. *Comparison of California Tides, Storm Surges, and Sea Level During the El Niño Winters of 1982-83 and 1997-98*. Shore & Beach, 66(3), 7-11.
- Flick, R. E., 2016. *California tides, sea level, and waves*. Shore & Beach, Winter 2015-2016, 84(2), 25-30.

- Flick, R.E., and J.R. Wanetick, 1989. *San Onofre Beach Study*. Unpublished report submitted to Southern California Edison Co., Rosemead, CA, October 1989, SIO Ref. No 89-20. 26 pp. and 25 figures.
- Flick, R. E., 1998. *Comparison of California Tides, Storm Surges, and Sea Level During the El Niño Winters of 1982-83 and 1997-98*, Shore & Beach, 66(3), 7-11.
- Fox-Kemper, B., H.T. Hewitt, C. Xiao, G. Aðalgeirsdóttir, S.S. Drijfhout, T.L. Edwards, N.R. Golledge, M. Hemer, R.E. Kopp, G. Krinner, A. Mix, D. Notz, S. Nowicki, I.S. Nurhati, L. Ruiz, J-B. Sallée, A.B.A. Slangen, and Y. Yu, 2021. *Ocean, Cryosphere and Sea Level Change. In Climate Change 2021: The Physical Science Basis. Contribution of Working Group I to the Sixth Assessment Report of the Intergovernmental Panel on Climate Change*. Masson-Delmotte, V., P. Zhai, A. Pirani, S.L. Connors, C. Péan, S. Berger, N. Caud, Y. Chen, L. Goldfarb, M.I. Gomis, M. Huang, K. Leitzell, E. Lonnoy, J.B.R. Matthews, T.K. Maycock, T. Waterfield, O. Yelekçi, R. Yu, and B. Zhou (eds.), Cambridge University Press.
- Garner, G.G., T. Hermans, R.E. Kopp, A.B.A. Slangen, T. L. Edwards, A. Levermann, S. Nowicki, M.D. Palmer, C. Smith, B. Fox-Kemper, H.T. Hewitt, C. Xiao, G. Aðalgeirsdóttir, S.S. Drijfhout, T.L. Edwards, N.R. Golledge, M. Hemer, R.E. Kopp, G. Krinner, A. Mix, D. Notz, S. Nowicki, I.S. Nurhati, L. Ruiz, J-B. Sallée, Y. Yu, L. Hua, T. Palmer, B. Pearson, 2021. *IPCC AR6 Sea-Level Rise Projections, Version 20210809*. PO.DAAC, CA, USA.
- Griggs, G., J. Arvai, D. Cayan, R. DeConto, J. Fox, H.A. Fricker, R.E. Kopp, C. Tebaldi, and E.A. Whiteman, 2017. *Rising Seas in California: An Update on Sea Level Rise Science*. California Ocean Protection Council Science Advisory Team Working Group, California Ocean Science Trust, 71 pp.
- Hamlington, B.D., T. Frederikse, P.R. Thompson, J.K. Willis, R.S. Nerem, and J.T. Fasullo, 2021: Past, present, and future Pacific sea-level change. *Earth's Future*, 9 (4), e2020EF001839. <https://doi.org/10.1029/2020EF001839>.
- Hedges, T.S., Reis, M.T., 1998. *Random wave overtopping of simple seawalls: a new regression model*. Water, Maritime and Energy Journal, 130(1), pp. 1-10.
- Holland, K. T., and R. A. Holman, 1993. *The statistical distribution of swash maxima on natural beaches*. J. Geophys. Res., 87, 10,271-10, 278.
- Hu, K., 2000. *High-Resolution Finite Volume Methods for Hydraulic Flow Modelling*. Manchester, U.K.: Centre for Mathematical Modelling and Flow Analysis, Manchester Metropolitan University, Doctoral thesis, 194 pp.
- Hunt, I. A., 1959. *Design of Seawalls and Breakwaters*. J. Waterways and Harbors Div., ASCE, Vol. 85, No. WW3.

- Intergovernmental Panel on Climate Change (IPCC), 2013. *Climate Change 2013: The Physical Science Basis*, Contribution of Working Group I to the Fifth Assessment Report of the Intergovernmental Panel on Climate Change. Cambridge University Press, Cambridge, United Kingdom and New York, NY, 1535 pp.
- Intergovernmental Panel on Climate Change (IPCC), 2014. *Climate Change 2014: Synthesis Report*, Contribution of Working Groups I, II and III to the Fifth Assessment Report of the Intergovernmental Panel on Climate Change. Geneva, Switzerland, 151 pp.
- Intergovernmental Panel on Climate Change (IPCC), 2022. *AR6 Synthesis Report: Climate Change 2022*, Sixth Assessment Report of the Intergovernmental Panel on Climate Change. Cambridge University Press, in press.
- Intergovernmental Panel on Climate Change (IPCC), 2021. *Climate Change 2021: The Physical Science Basis*, Contribution of Working Group I to the Sixth Assessment Report of the Intergovernmental Panel on Climate Change. Cambridge University Press, 3949 pp.
- Kikkawa, H., Shi-igai, H. and Kono, T., 1968. *Fundamental Study of Wave Over-Topping on Levees*. Journal of Coastal Engineering in Japan, 11, 107-115.
- Kopp, R. E., R. M. Horton, C. M. Little, J. X. Mitrovica, M. Oppenheimer, D.J. Rasmussen, B. H. Strauss, and C. Tebaldi, 2014. *Probabilistic 21st and 22nd century sea level projections at a global network of tide-gauge sites*. Earth's Future, 2, 383-406.
- Mastrandrea, M.D., C.B. Field, T.F. Stocker, O. Edenhofer, K.L. Ebi, D.J. Frame, H. Held, E. Kriegler, K.J. Mach, P.R. Matschoss, G.-K. Plattner, G.W. Yohe, and F.W. Zwiers, 2010. *Guidance Note for Lead Authors of the IPCC Fifth Assessment Report on Consistent Treatment of Uncertainties*. Intergovernmental Panel on Climate Change (IPCC), 6 pp. <http://www.ipcc.ch>.
- Muis S, I. Apecechea, et al., 2020. *A High-Resolution Global Dataset of Extreme Sea Levels, Tides, and Storm Surges, Including Future Projections*, Front. Mar. Sci., 7, 263, 15 pp.
- National Research Council (NRC), 2012. *Sea-Level Rise for the Coasts of California, Oregon, and Washington: Past, Present, and Future*. National Academy Press, Washington, D.C., 201 pp.
- National Oceanographic and Atmospheric Administration (NOAA), 2022. Global Regional Sea Level Rise Scenarios of United States. Maryland, February 2022. 64 pp. and 2 Appendices. <https://oceanservice.noaa.gov/hazards/sealevelrise/noaa-nos-techrpt01-global-regional-SLR-scenarios-US.pdf>.
- Ocean Protection Council, 2018. *State of California Sea Level Rise Guidance, 2018 Update* (California Natural Resources Agency Ocean Protection Council), 84 pp.

- Ocean Protection Council (OPC), 2020. *Strategic Plan to Protect California's Coast and Ocean 2020–2025*, California Natural Resources Agency Ocean Protection Council, 64 pp.
<https://www.opc.ca.gov/webmaster/ftp/pdf/2020-2025-strategic-plan/OPC-2020-2025-Strategic-Plan-FINAL-20200228.pdf>.
- Owen, M.W., 1980. *Design of Seawalls Allowing for Wave Overtopping*. Report. EX 924, Hydraulics Research Station, Wallingford, UK.
- Raubenheimer, B., R.T. Guza, Steve Elgar, and N. Kobayashi, 1995. *Swash on a gently sloping beach*, J. Geophys. Res., 100, 8751-8760.
- Reis, M. T., Hu, K., Hedges, T. S., and Mase, H., 2008. *A comparison of empirical, semiempirical, and numerical wave overtopping models*. J. Coastal Res., 24(2A), 250-262.
- Ruggiero, Peter & Holman, Robert & Beach, R., 2004. *Wave runup on a high-energy dissipative beach*. Journal of Geophysical Research C: Oceans. 109. 10.1029/2003JC002160.
- Stockdon, H. F., Holman, R. A., Howd, P. A., and Sallenger, A. H., 2006. *Empirical parameterization of setup, swash, and runup*, Coastal Engineering, 53, 573–588.
- Thornton, E. B. and Guza, R. T., 1982. *Energy Saturation and Phase Speeds Measured on a Natural Beach*. Journal of Geophysical Research, 87(C12), 9499-9508.
- Thornton, E. B. and Guza, R. T., 1983. *Transformation of Wave Height Distribution*. Journal of Geophysical Research, 88 (C10), 5925-5938.
- USACOE, 1984. Shore Protection Manual. *Waterways Experiment Station, Coastal Engineering Research Center*, Vicksburg, MS, 2 vols.
- USACOE, 1988. *Historic Wave and Sea Level Data Report: San Diego Region*. Coast of California Storm and Tidal Wave Study, Reference No. 88-6.
- USACOE, 1994a. *Hydraulic Design of Flood Control Channels*. Department of the Army. CECW-EH-D, Engineer Manual 1110-2-1601.
- USACOE, 1994b. *Shore Protection Manual, Volume II*. Department of the Army. Coastal Engineering Research Center.
- USACOE, 1995. *Design of Revetments, Seawalls and Bulkheads*. Department of the Army. Coastal Engineering Manual, Engineer Manual 1110-2-1614.
- Van der Meer, J.W. and J.P.F.M. Janssen, 1995. *Wave runup and wave overtopping at dikes*. In: Wave Forces on Inclined and Vertical Wall Structures. ASCE. Ed. N. Kobayashi and Z. Demirbilek. Ch. 1, p. 1-27.

Young, A.P., R. E. Flick, T.W. Gallien, S. N. Giddings, R.T. Guza, M. Harvey, L. Lenain, B.C. Ludka, W. K. Melville, and W. C. O'Reilly, 2018. *Southern California coastal response to the 2015-2016 El Niño*, J. Geophys. Res: Earth Surface, 123.

APPENDIX A

DIGITAL ELEVATION MODELS (DEM)
FROM 2023 & 2020 REVETMENT SURVEYS



Figure A-1. Locations of 21 transects along the revetment, spaced 100 ft apart.

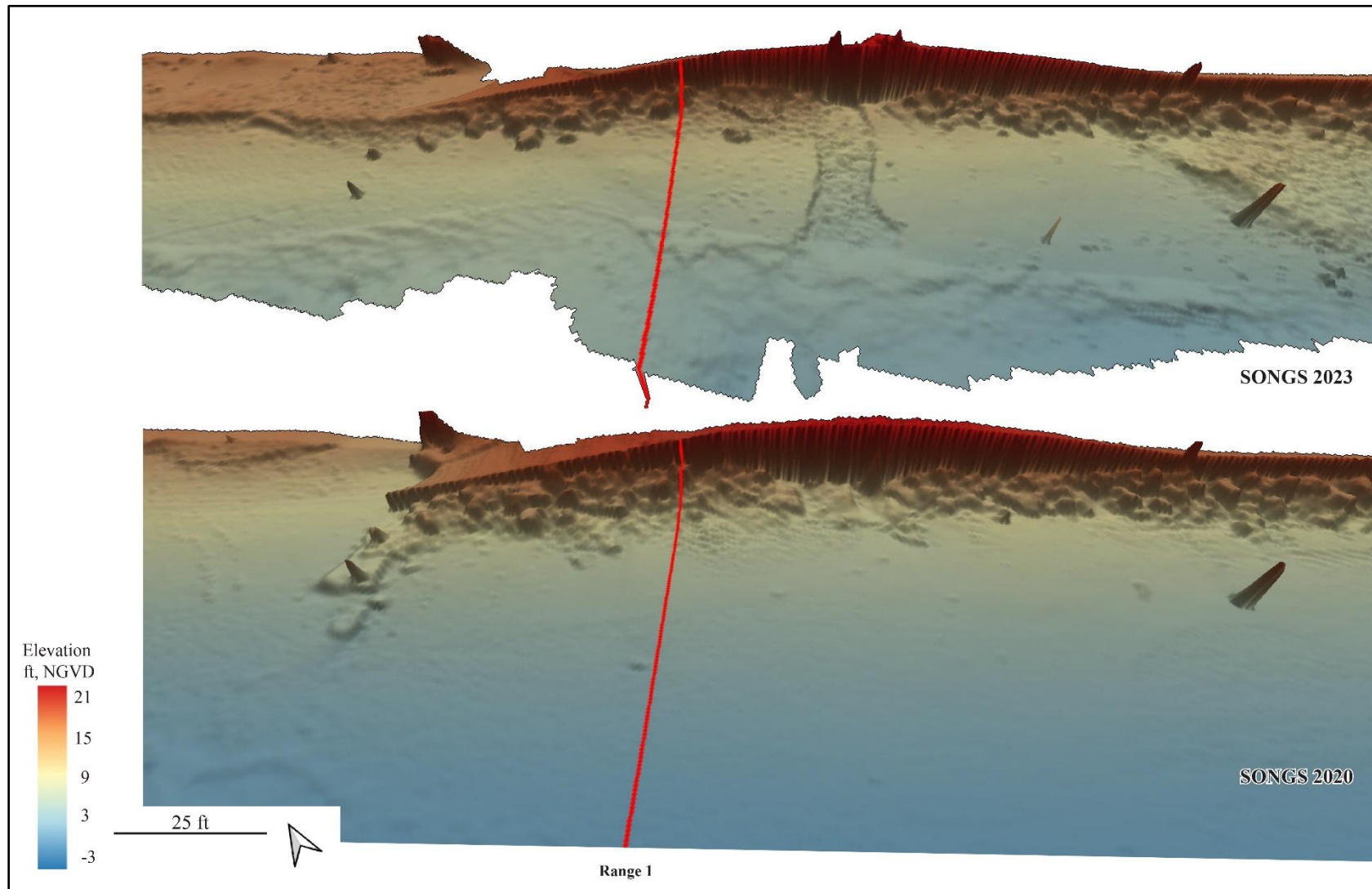


Figure A-2. DEM comparison between 2023 (top) and 2020 (bottom), showing Transect 1 along the SONGS revetment.

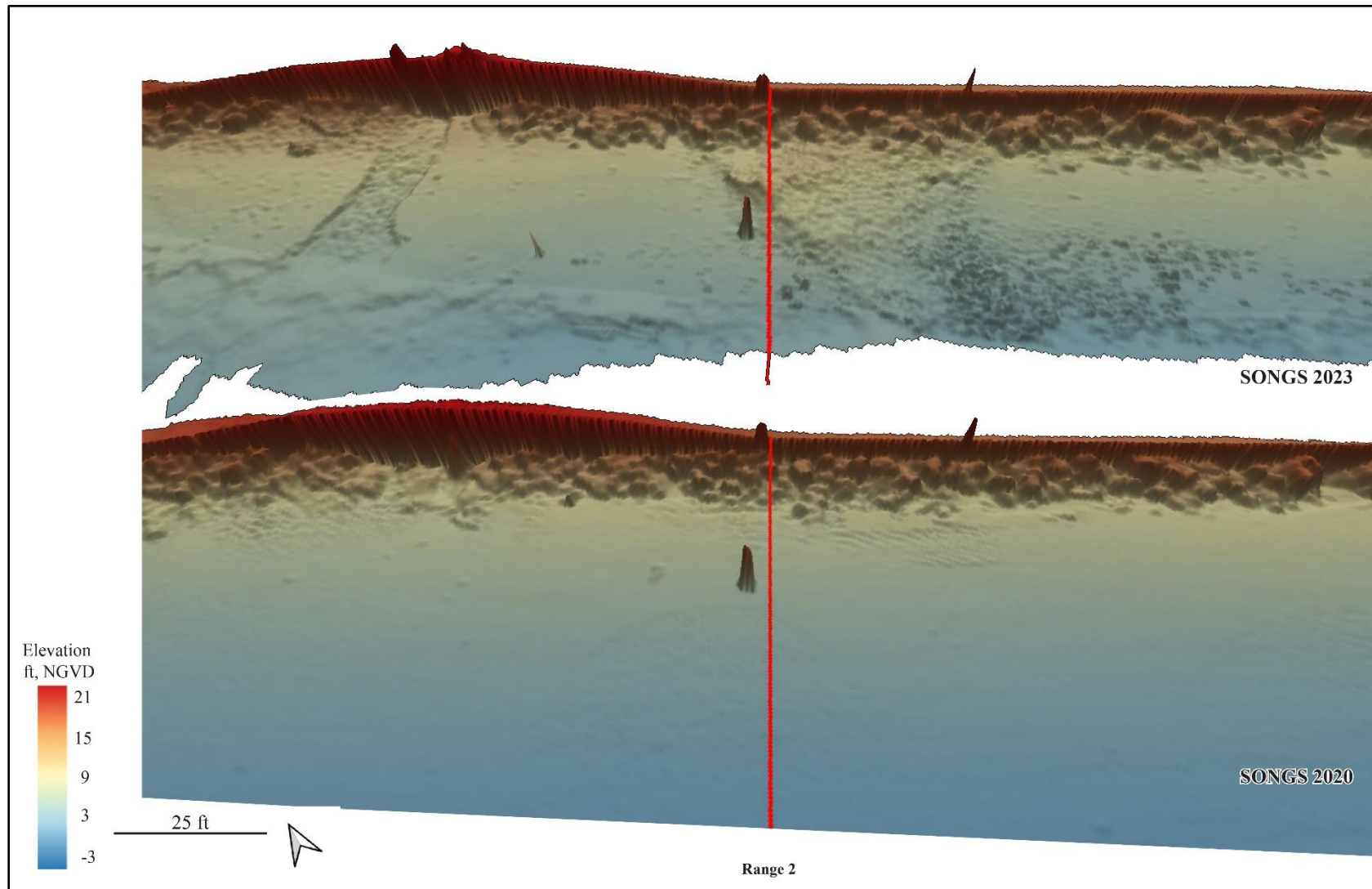


Figure A-3. DEM comparison between 2023 (top) and 2020 (bottom), showing Transect 2 along the SONGS revetment.

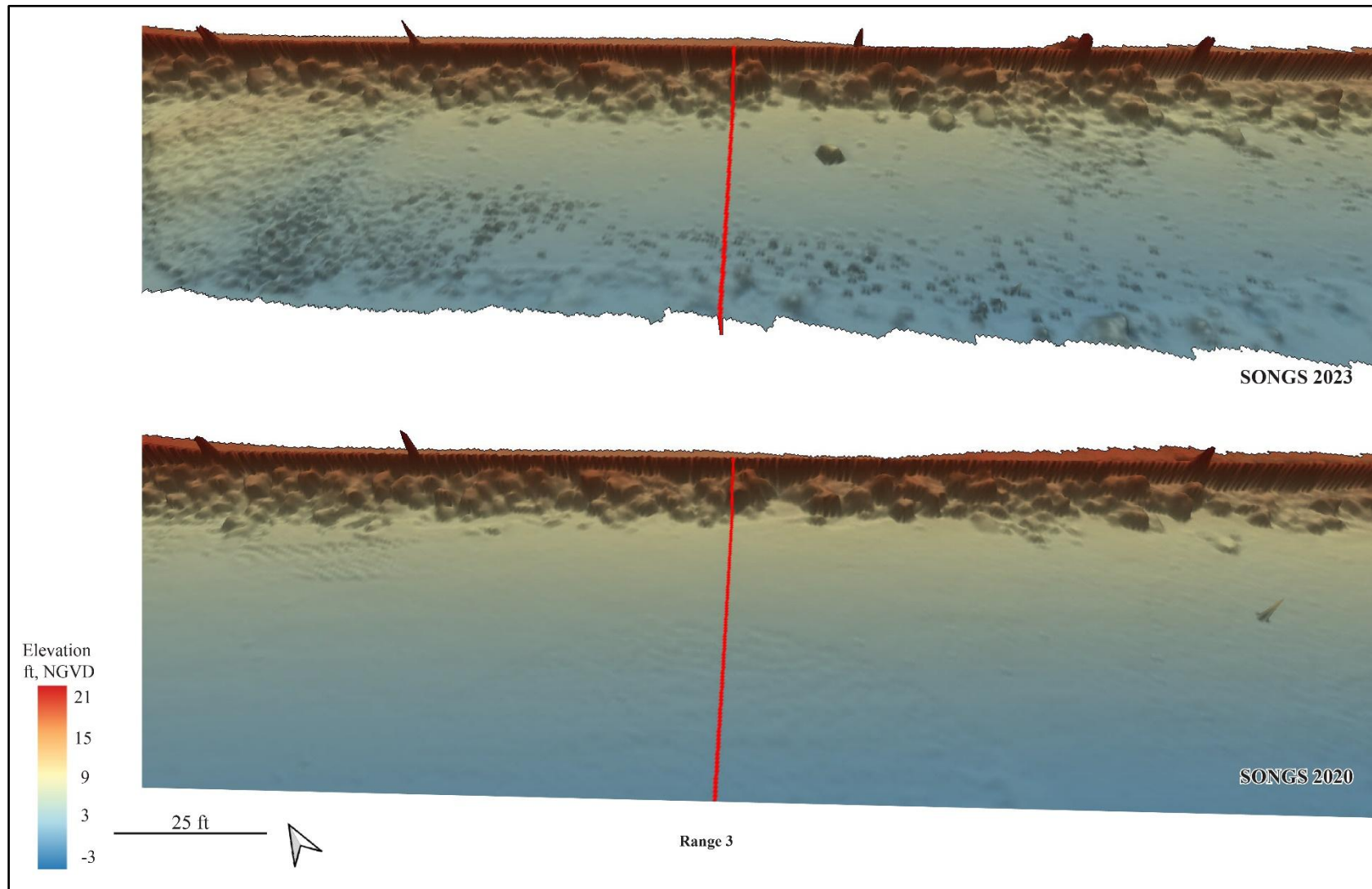


Figure A-4. DEM comparison between 2023 (top) and 2020 (bottom), showing Transect 3 along the SONGS revetment.

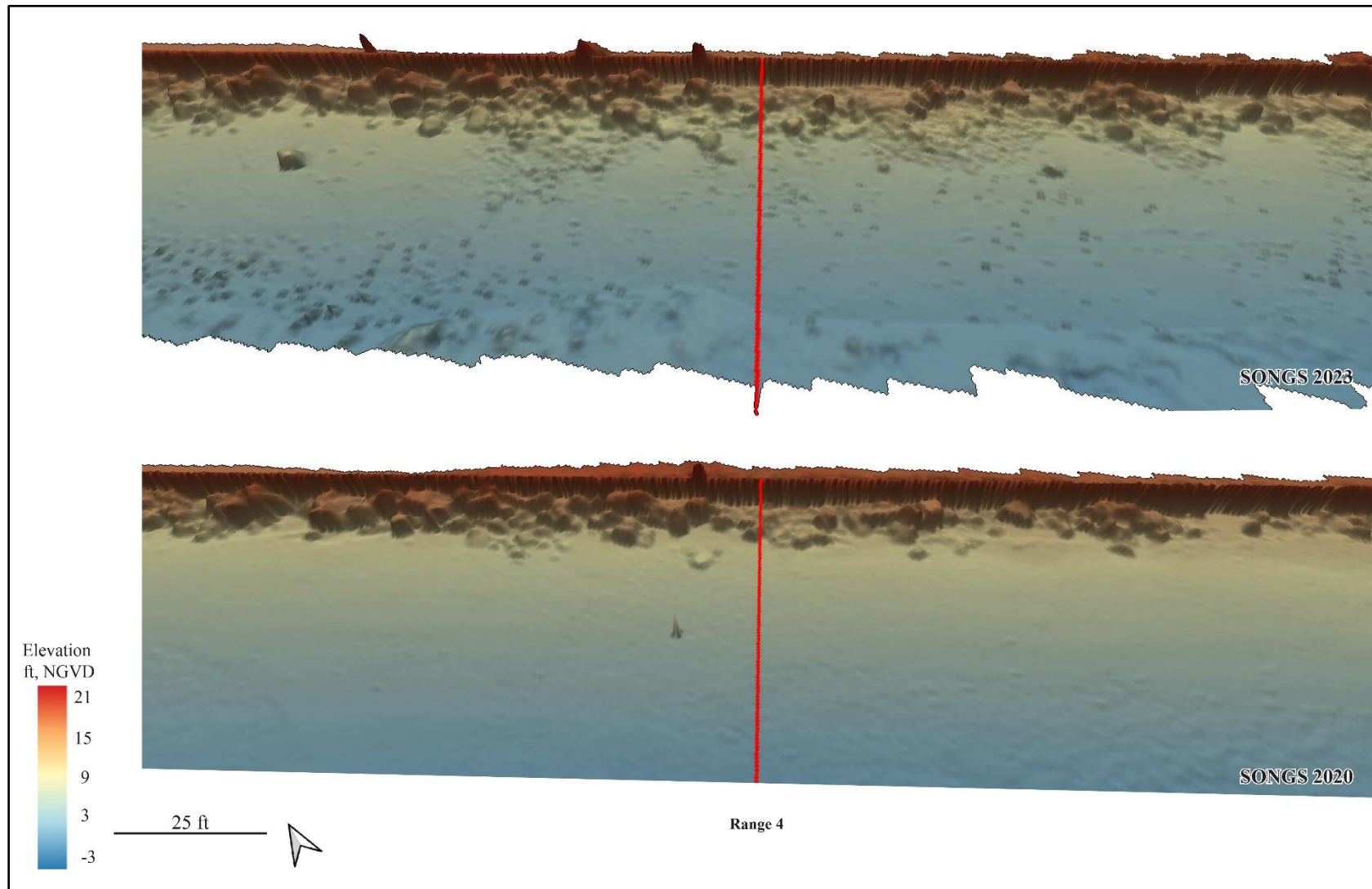


Figure A-5. DEM comparison between 2023 (top) and 2020 (bottom), showing Transect 4 along the SONGS revetment.

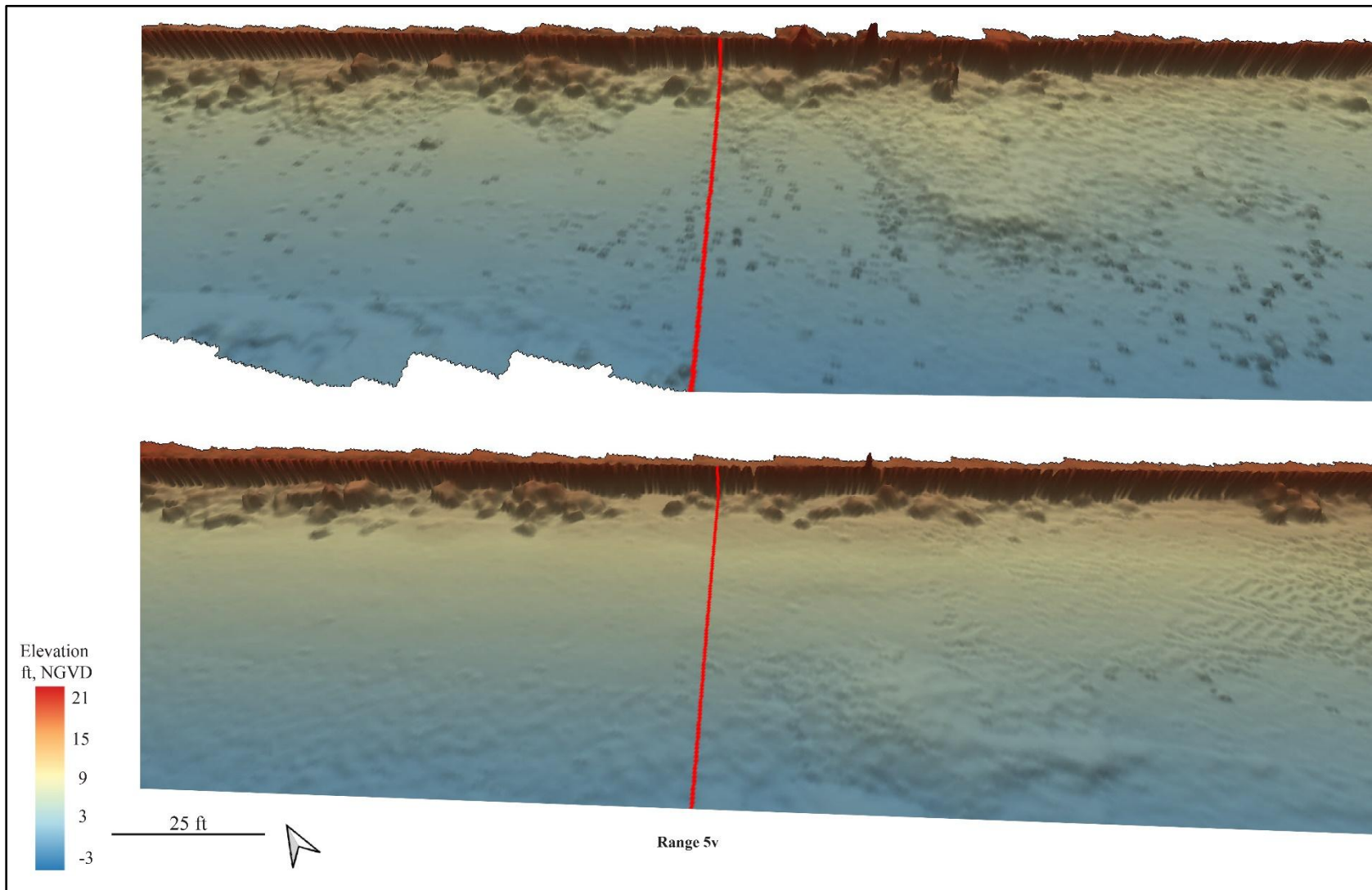


Figure A-6. DEM comparison between 2023 (top) and 2020 (bottom), showing Transect 5 along the SONGS revetment.

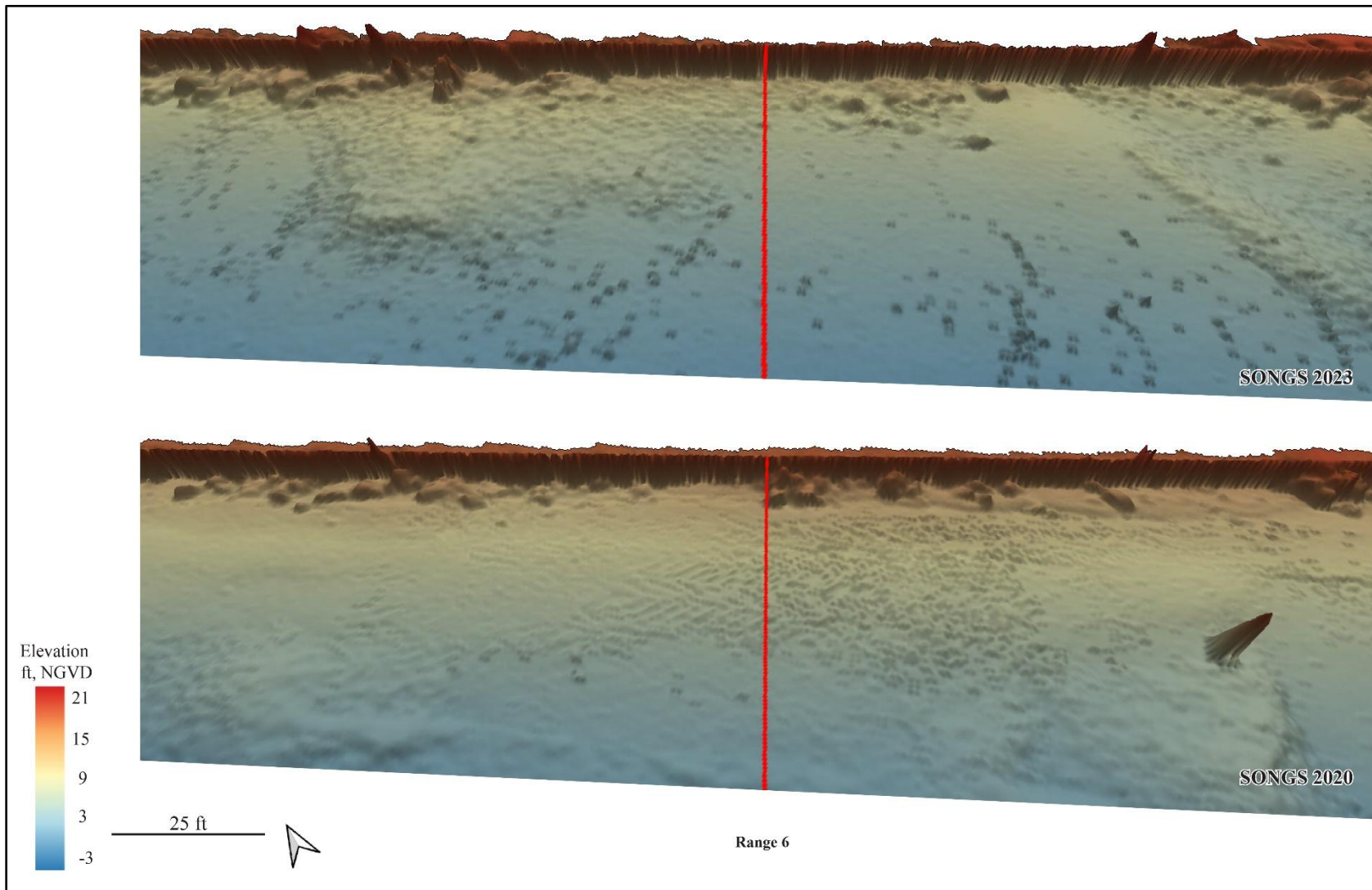


Figure A-7. DEM comparison between 2023 (top) and 2020 (bottom), showing Transect 6 along the SONGS revetment.

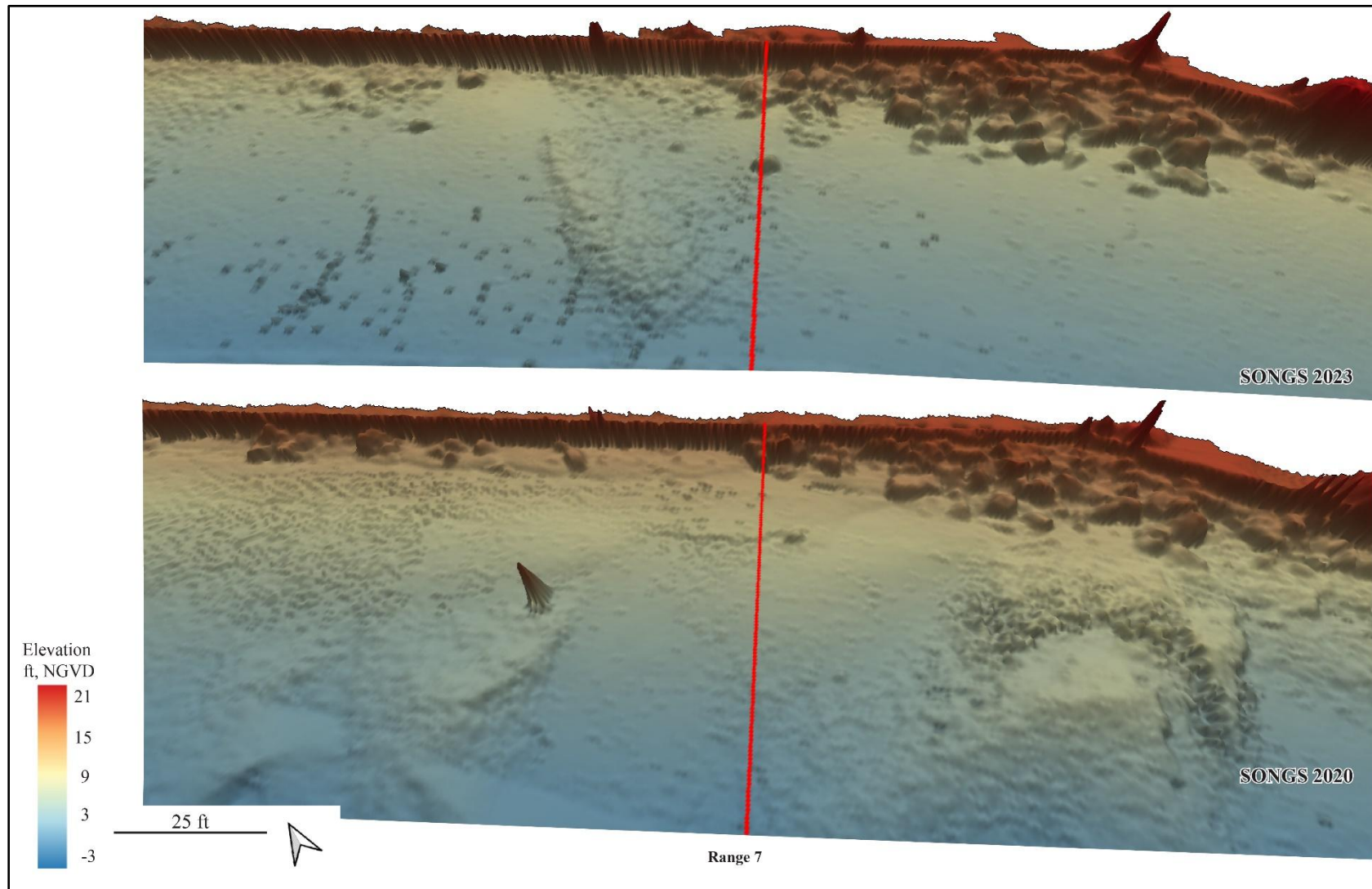


Figure A-8. DEM comparison between 2023 (top) and 2020 (bottom), showing Transect 7 along the SONGS revetment.

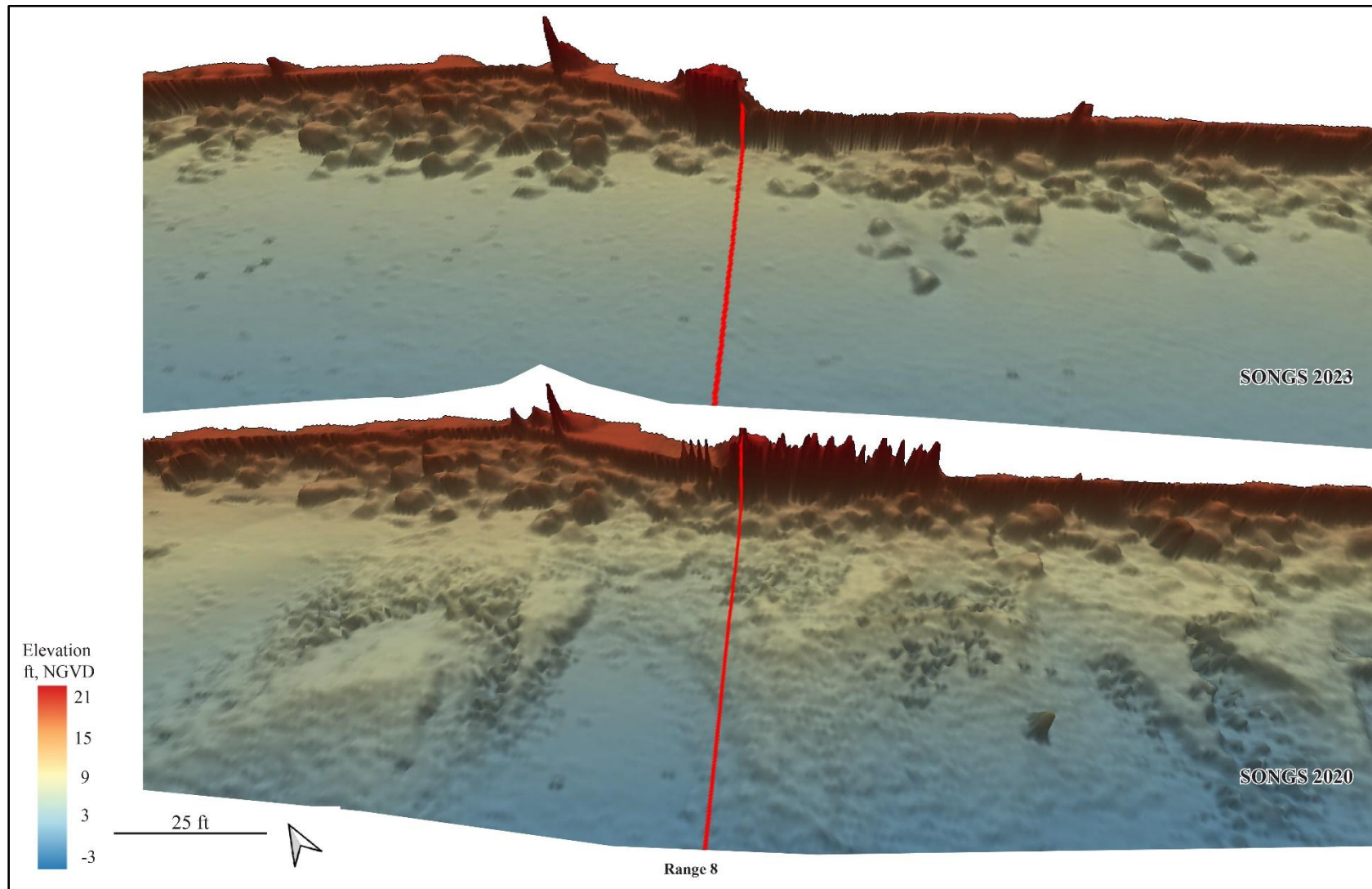


Figure A-9. DEM comparison between 2023 (top) and 2020 (bottom), showing Transect 8 along the SONGS revetment.

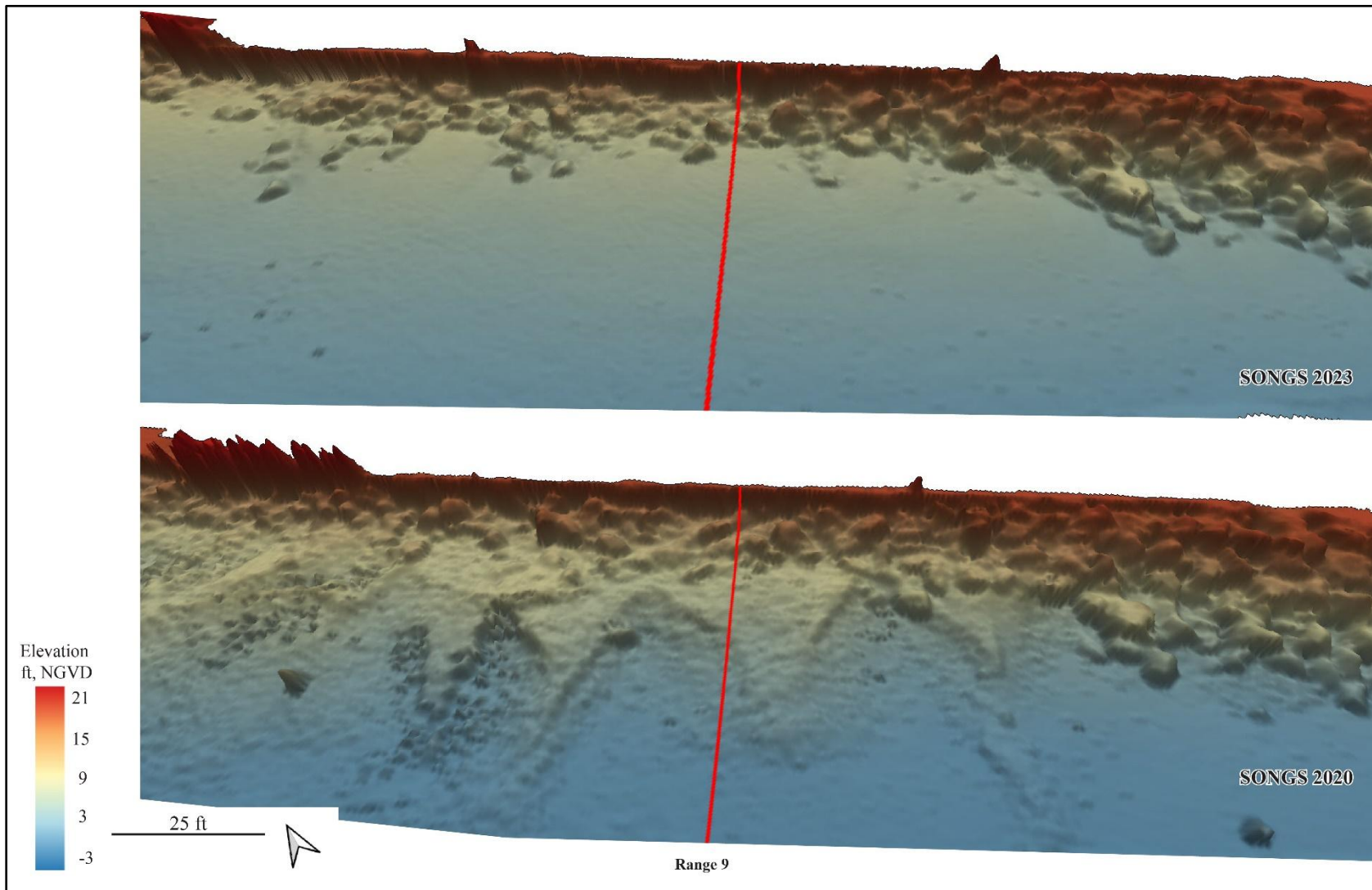


Figure A-10. DEM comparison between 2023 (top) and 2020 (bottom), showing Transect 9 along the SONGS revetment.

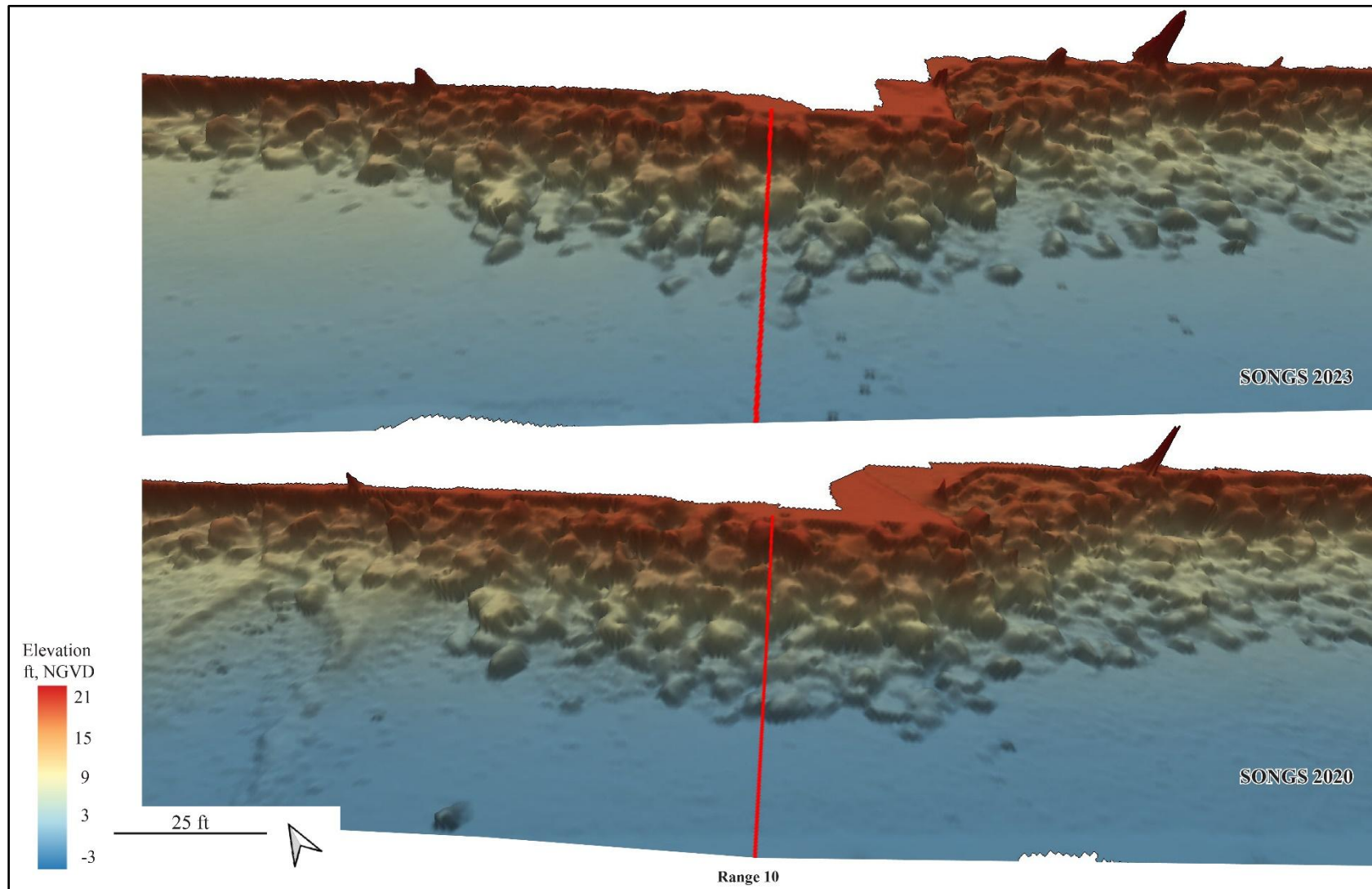


Figure A-11. DEM comparison between 2023 (top) and 2020 (bottom), showing Transect 10 along the SONGS revetment.

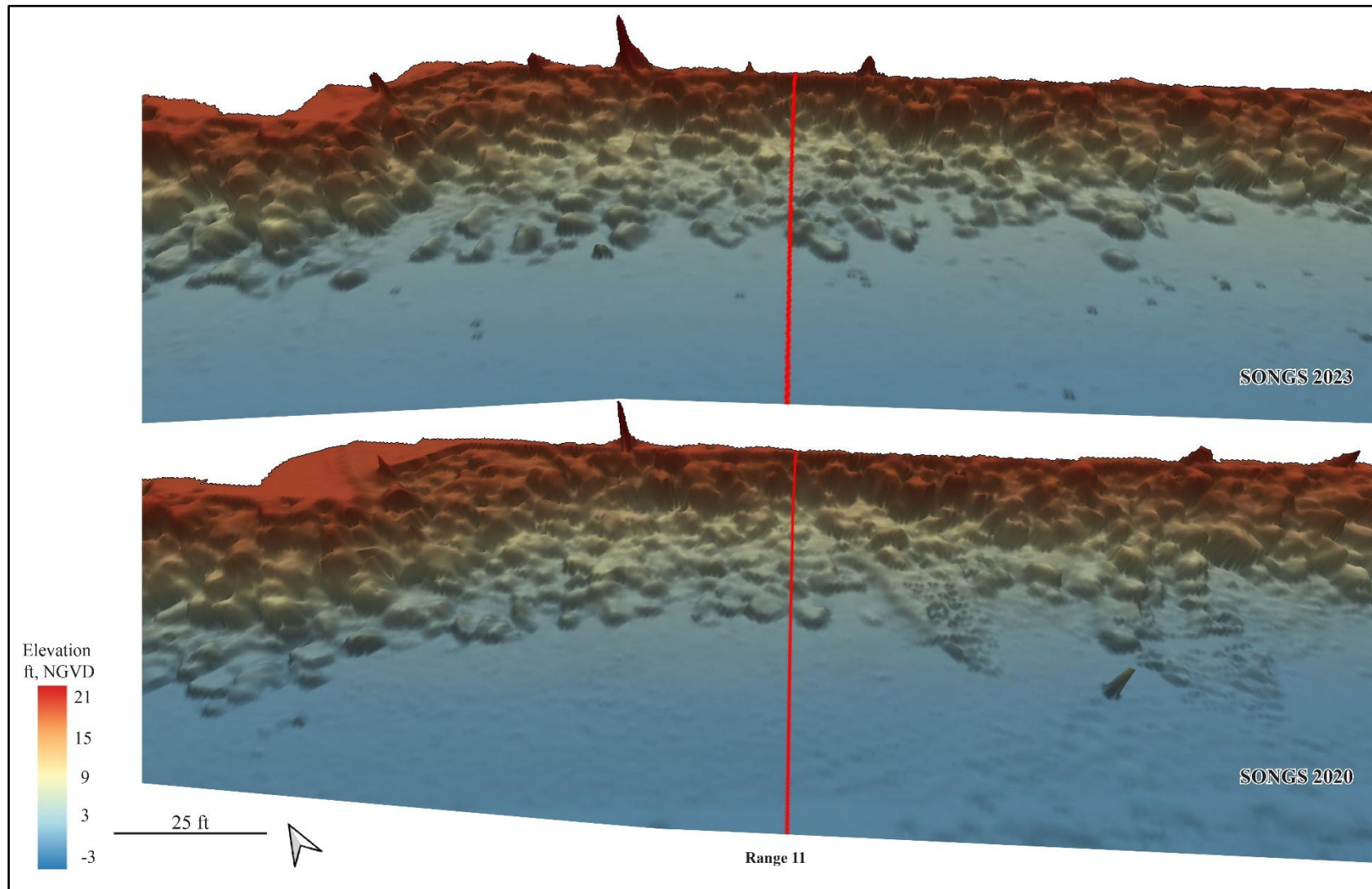


Figure A-12. DEM comparison between 2023 (top) and 2020 (bottom), showing Transect 11 along the SONGS revetment.

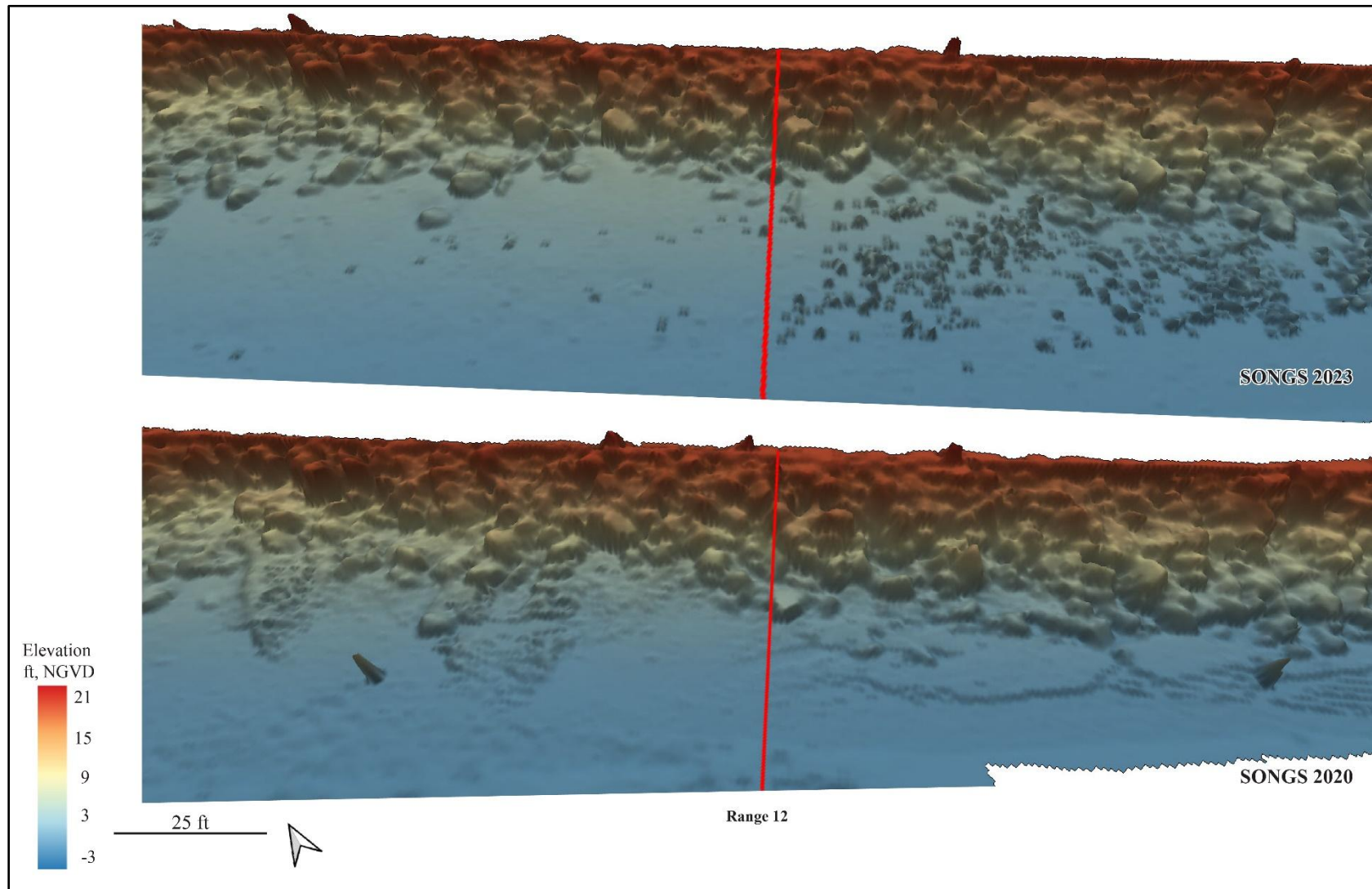


Figure A-13. DEM comparison between 2023 (top) and 2020 (bottom), showing Transect 12 along the SONGS revetment.

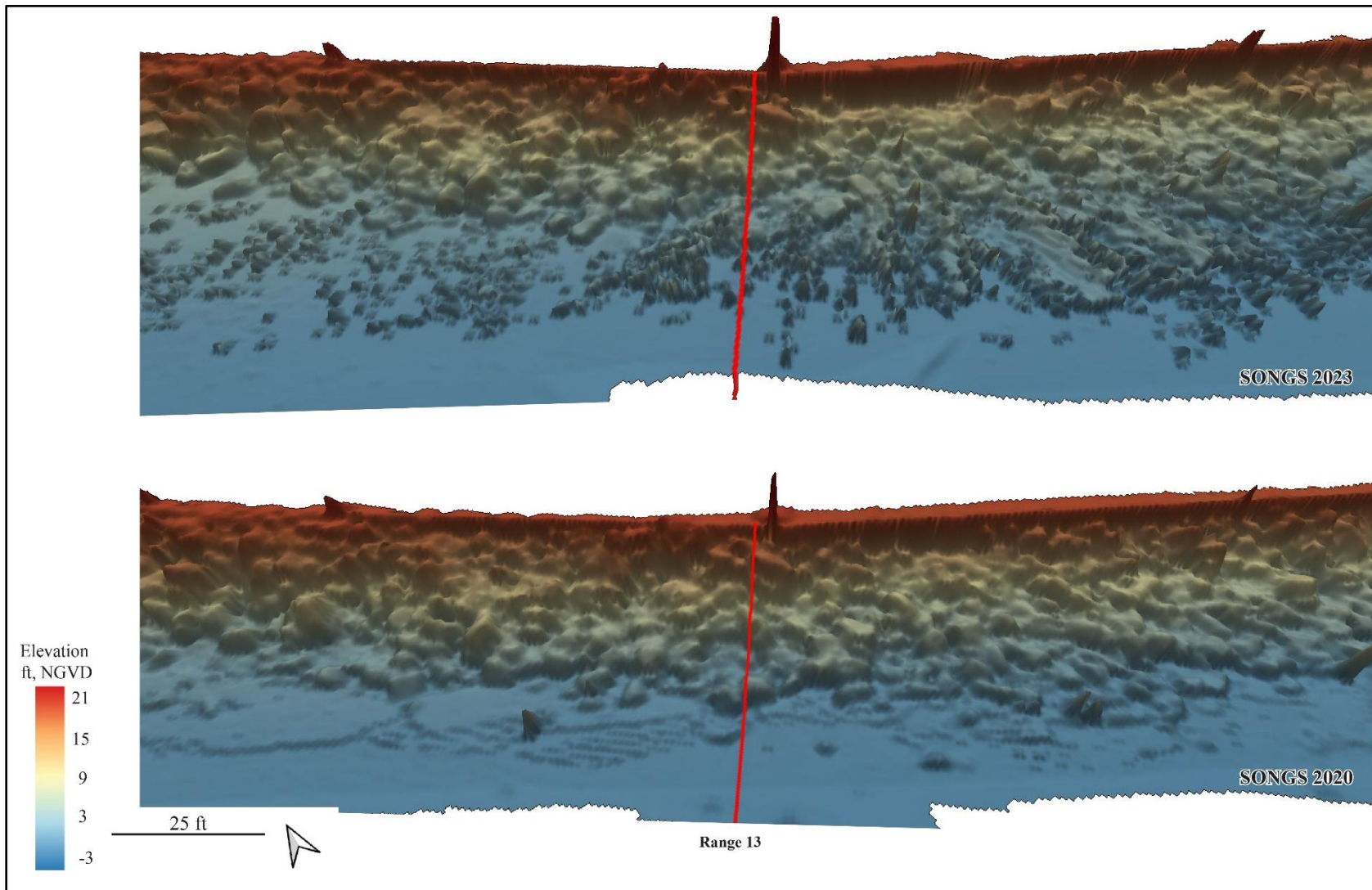


Figure A-14. DEM comparison between 2023 (top) and 2020 (bottom), showing Transect 13 along the SONGS revetment.

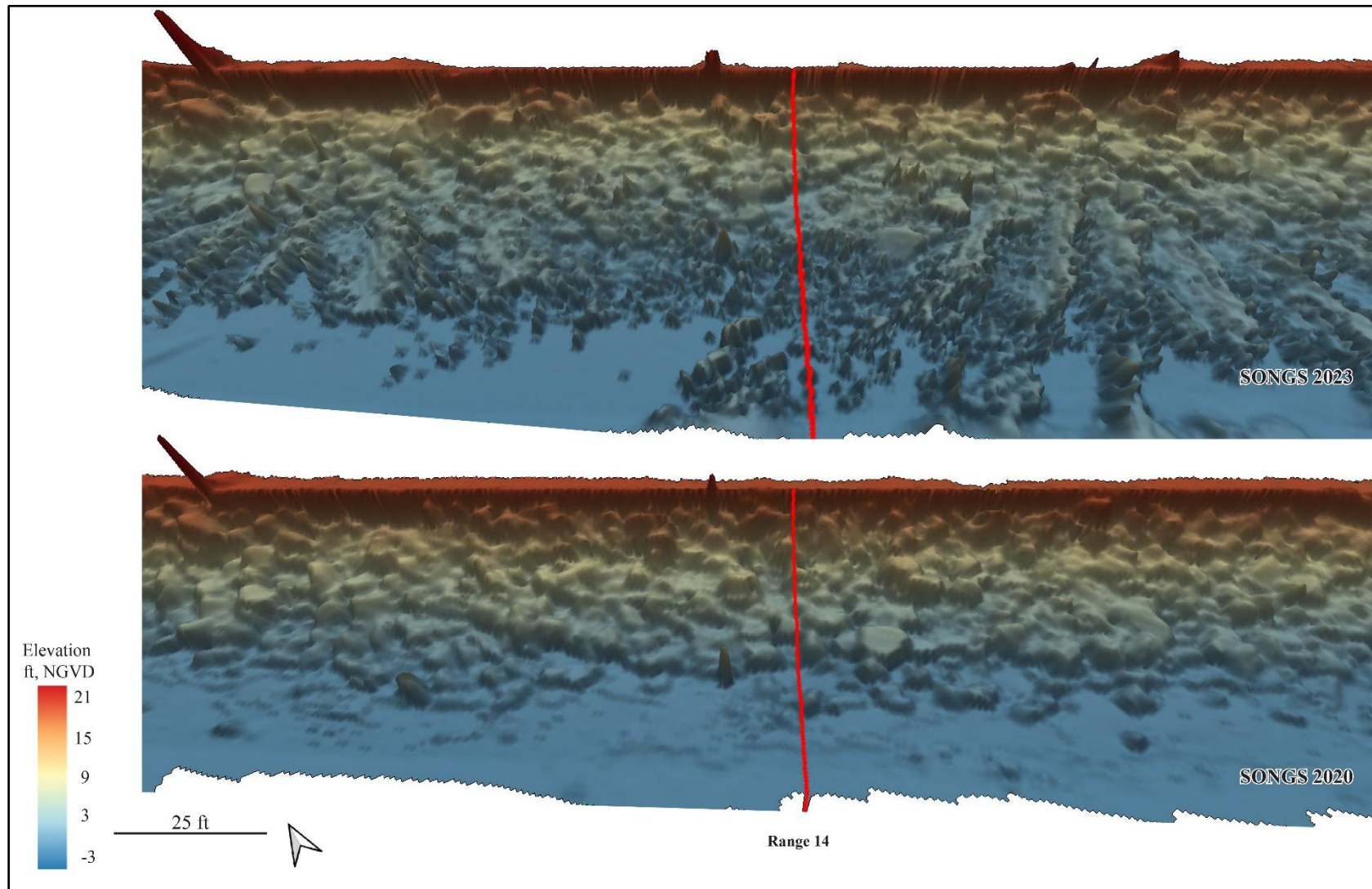


Figure A-15. DEM comparison between 2023 (top) and 2020 (bottom), showing Transect 14 along the SONGS revetment.

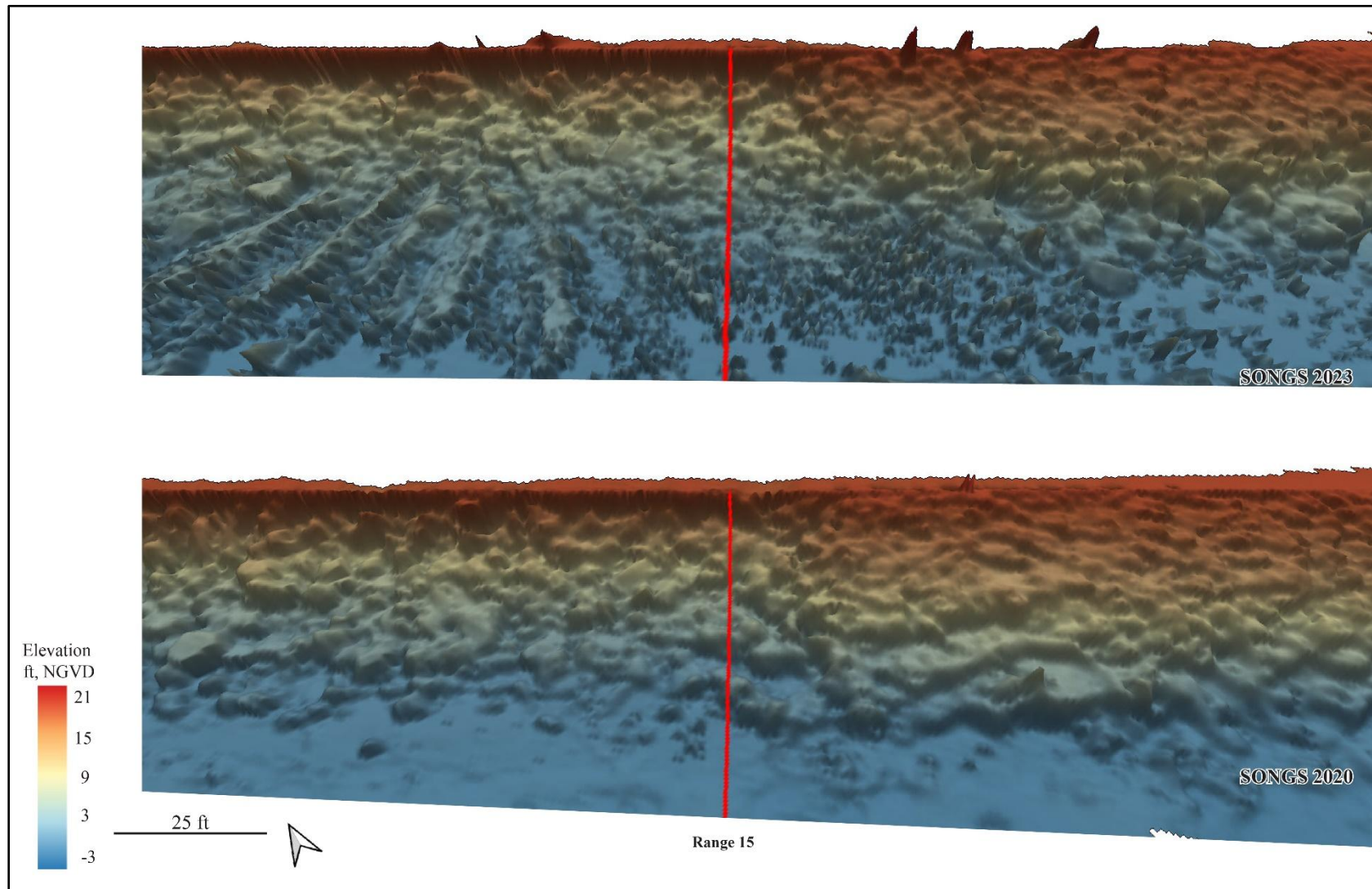


Figure A-16. DEM comparison between 2023 (top) and 2020 (bottom), showing Transect 15 along the SONGS revetment.

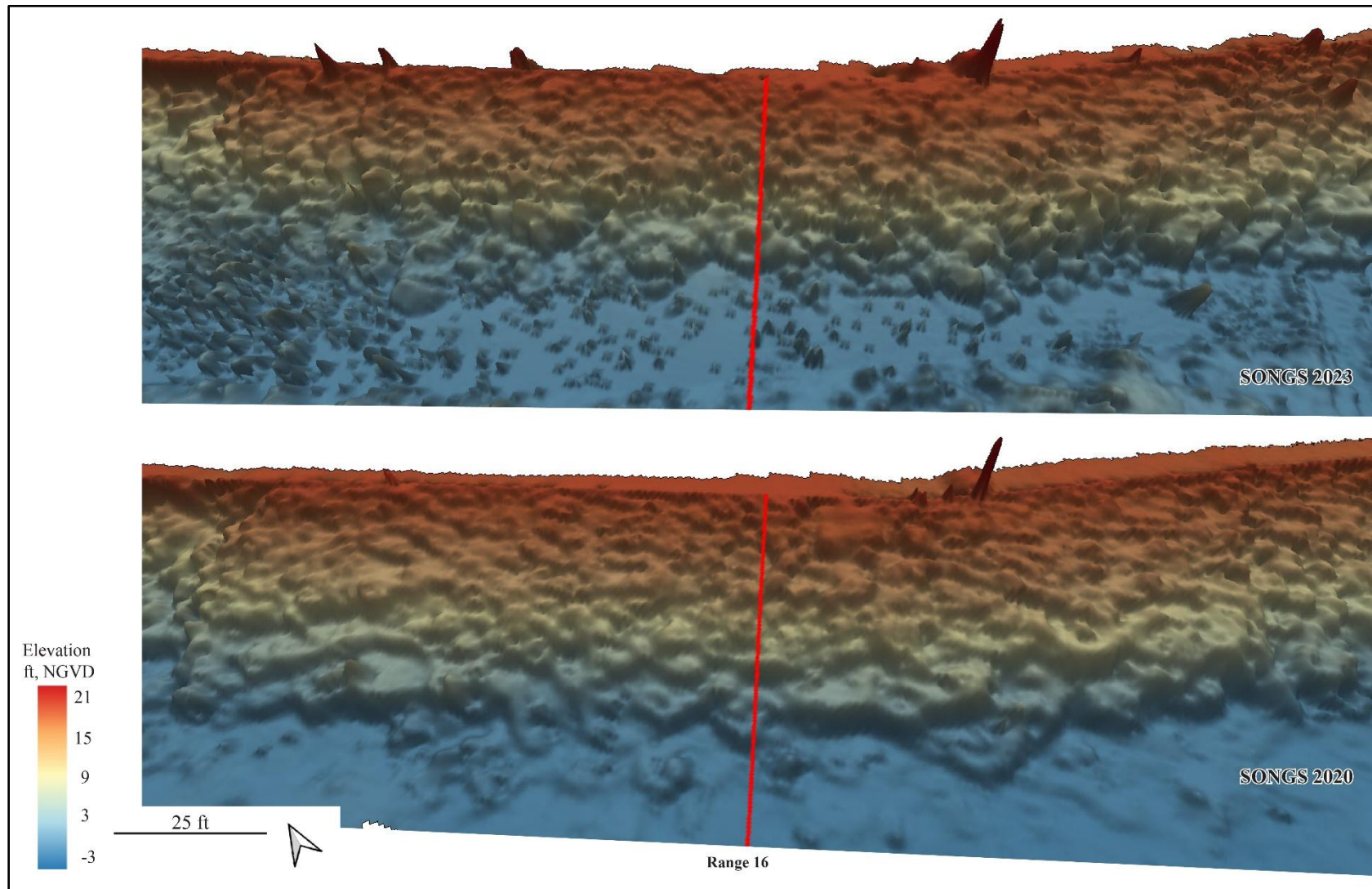


Figure A-17. DEM comparison between 2023 (top) and 2020 (bottom), showing Transect 16 along the SONGS revetment.

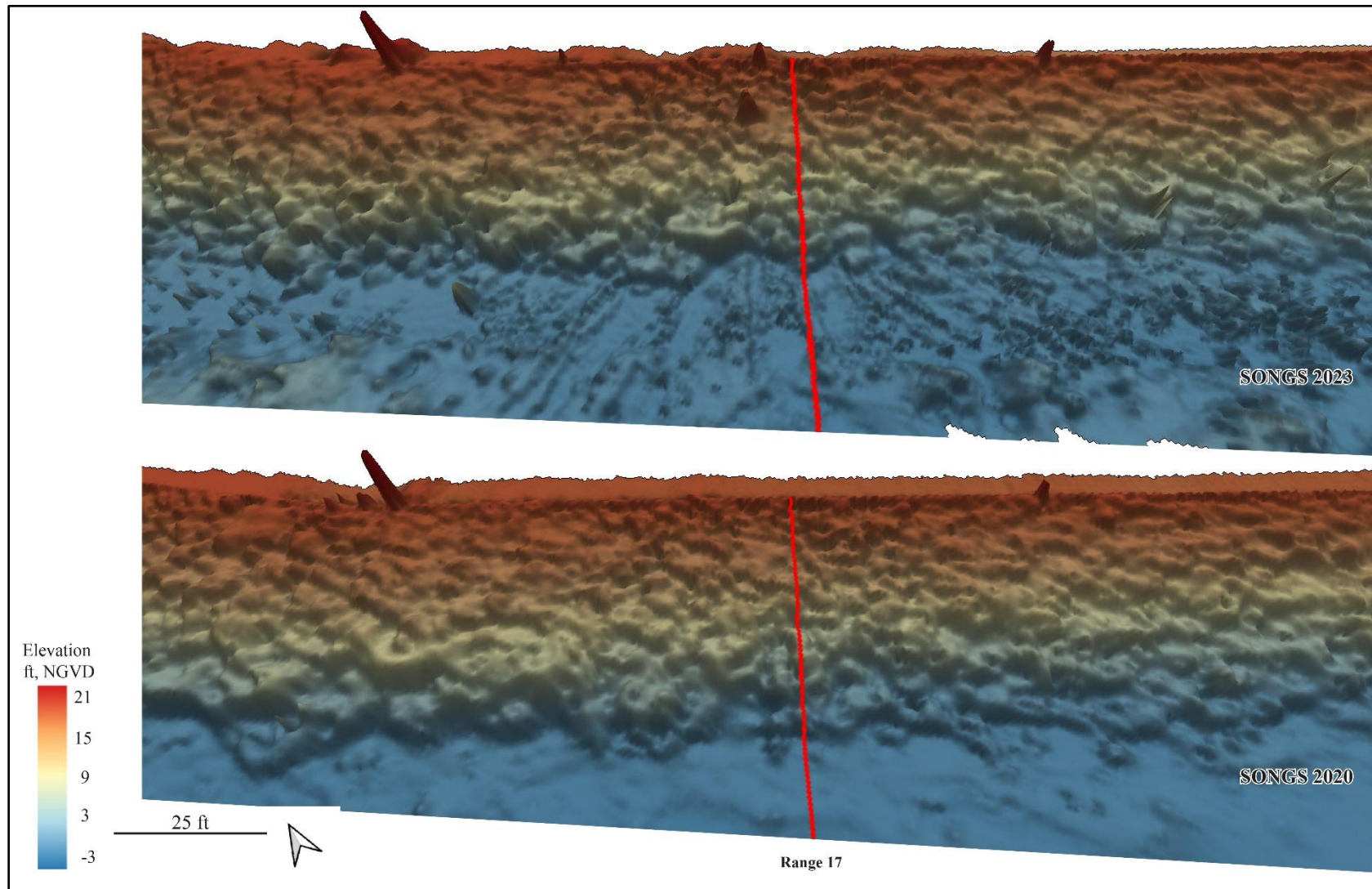


Figure A-18. DEM comparison between 2023 (top) and 2020 (bottom), showing Transect 17 along the SONGS revetment.

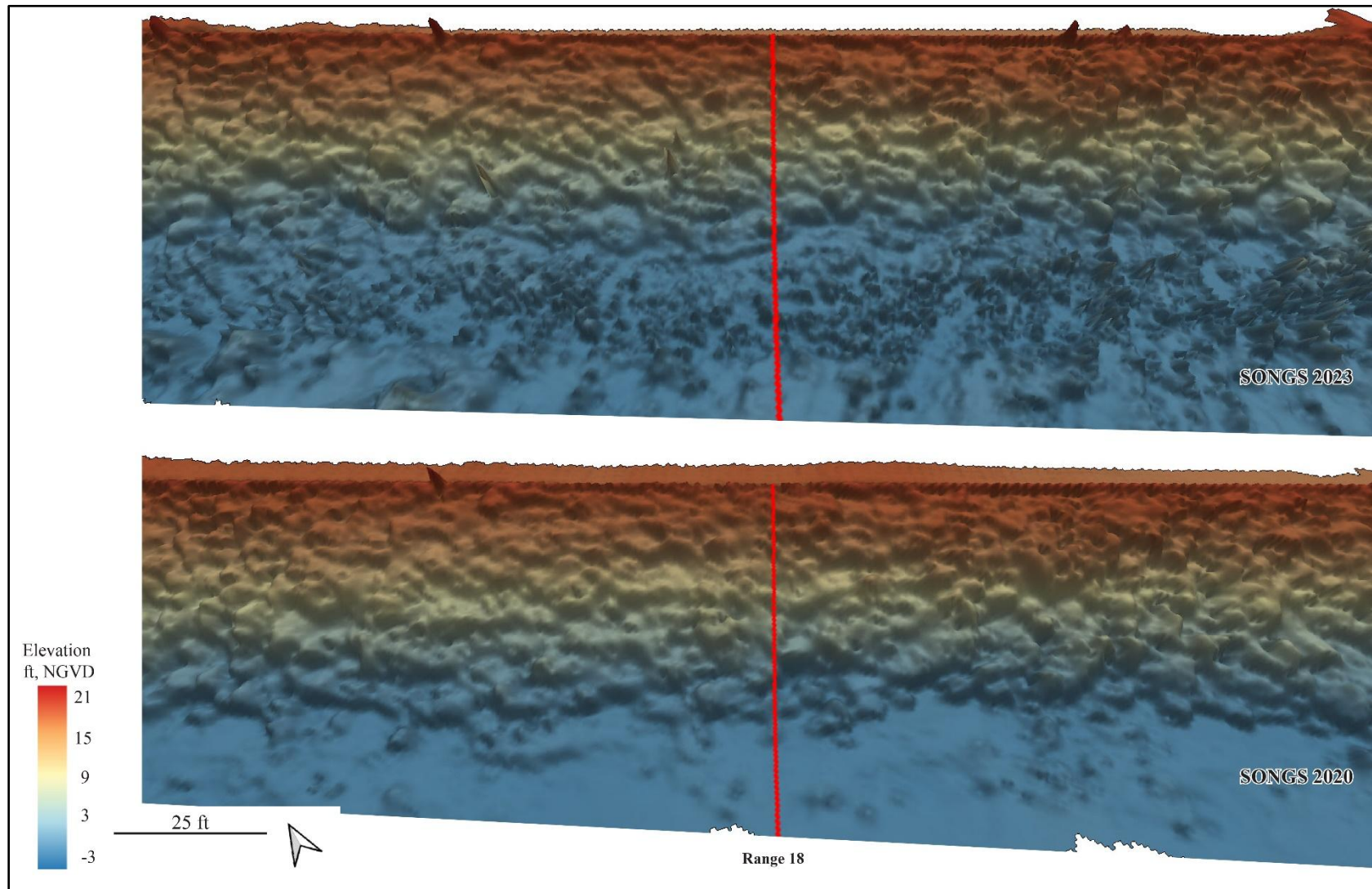


Figure A-19. DEM comparison between 2023 (top) and 2020 (bottom), showing Transect 18 along the SONGS revetment.

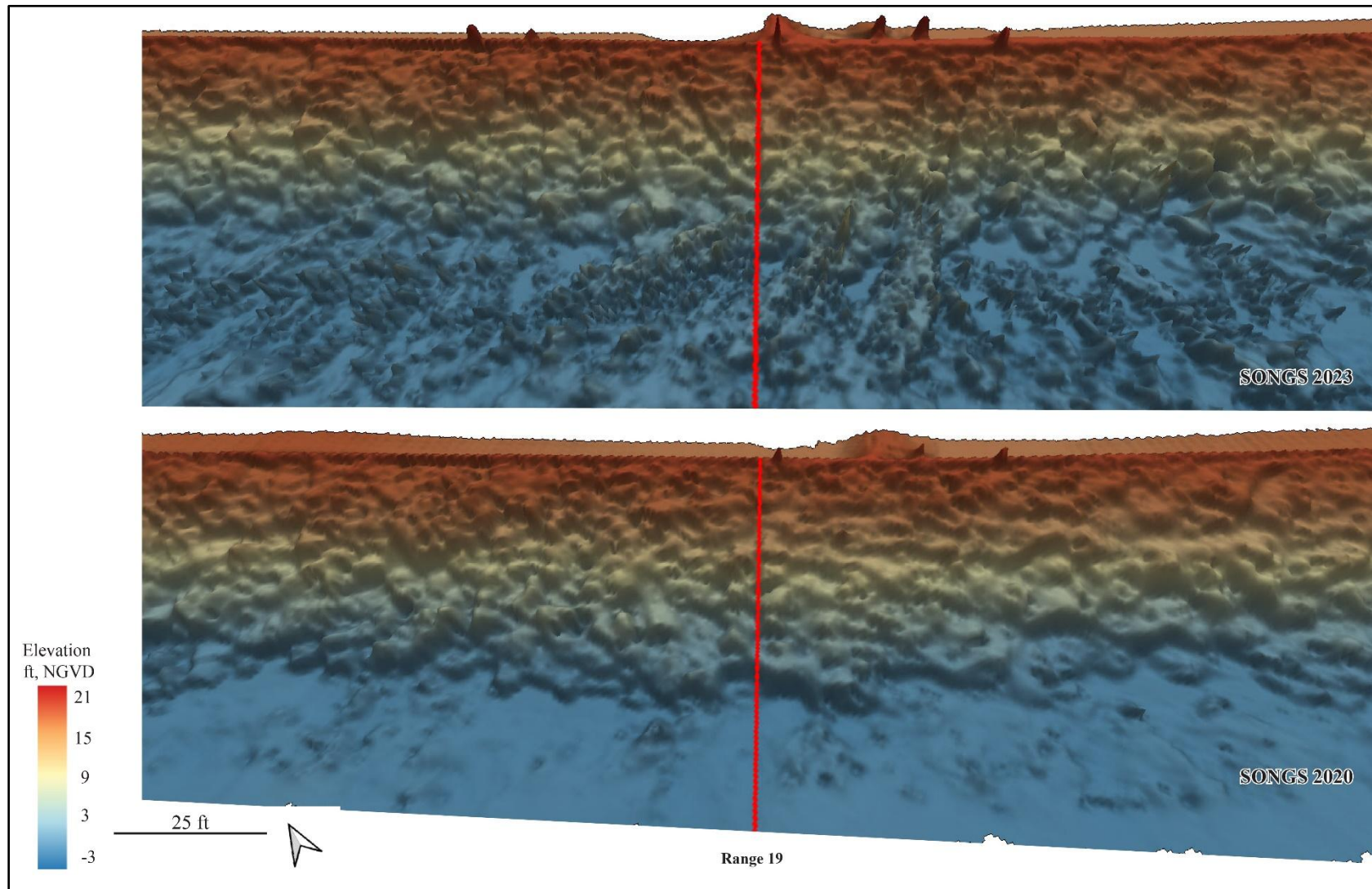


Figure A-20. DEM comparison between 2023 (top) and 2020 (bottom), showing Transect 19 along the SONGS revetment.

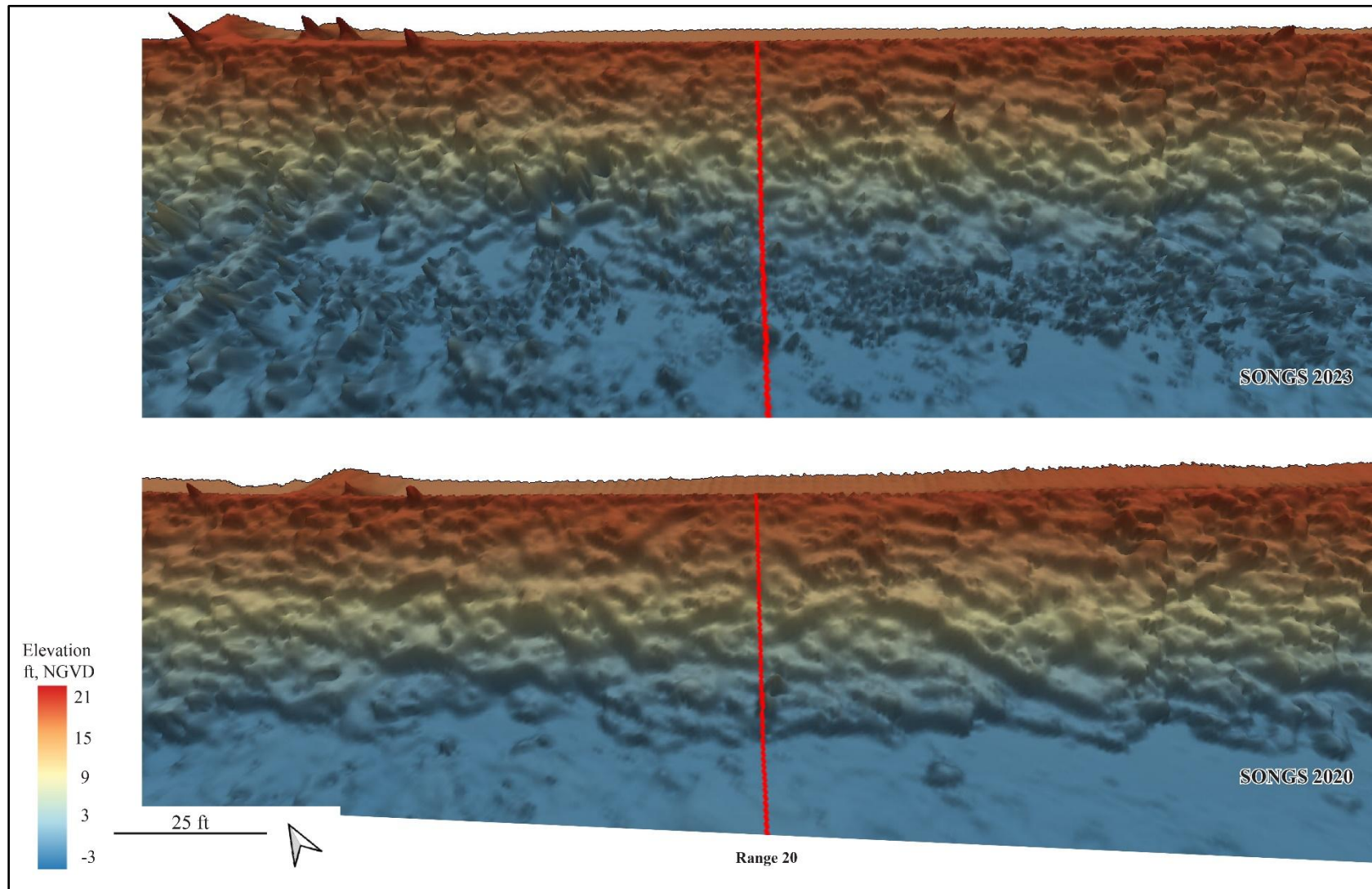


Figure A-21. DEM comparison between 2023 (top) and 2020 (bottom), showing Transect 20 along the SONGS revetment.

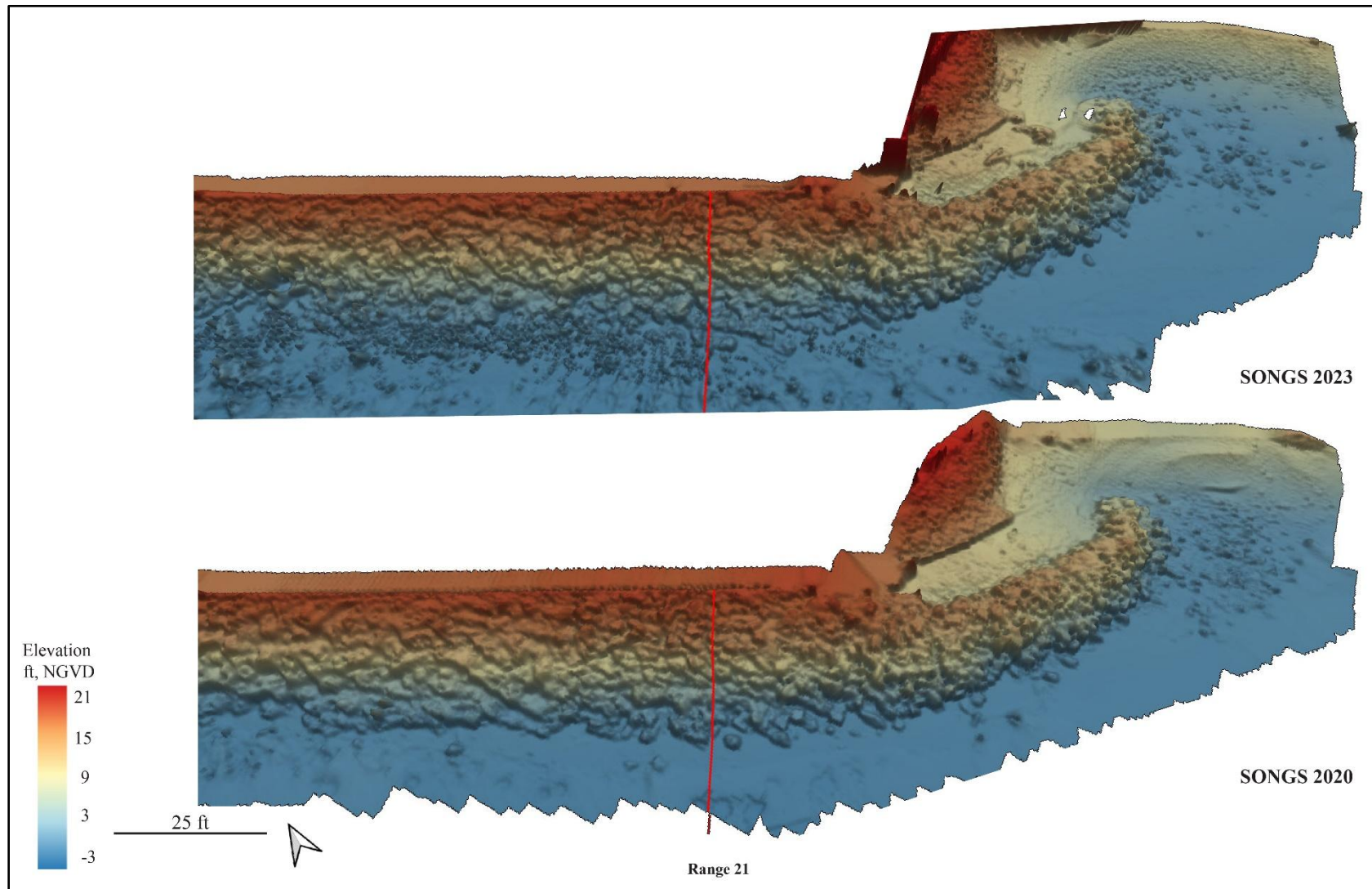


Figure A-22. DEM comparison between 2023 (top) and 2020 (bottom), showing Transect 21 along the SONGS revetment.

APPENDIX B

**CROSS SECTION ELEVATIONS
OF SONGS REVETMENT**

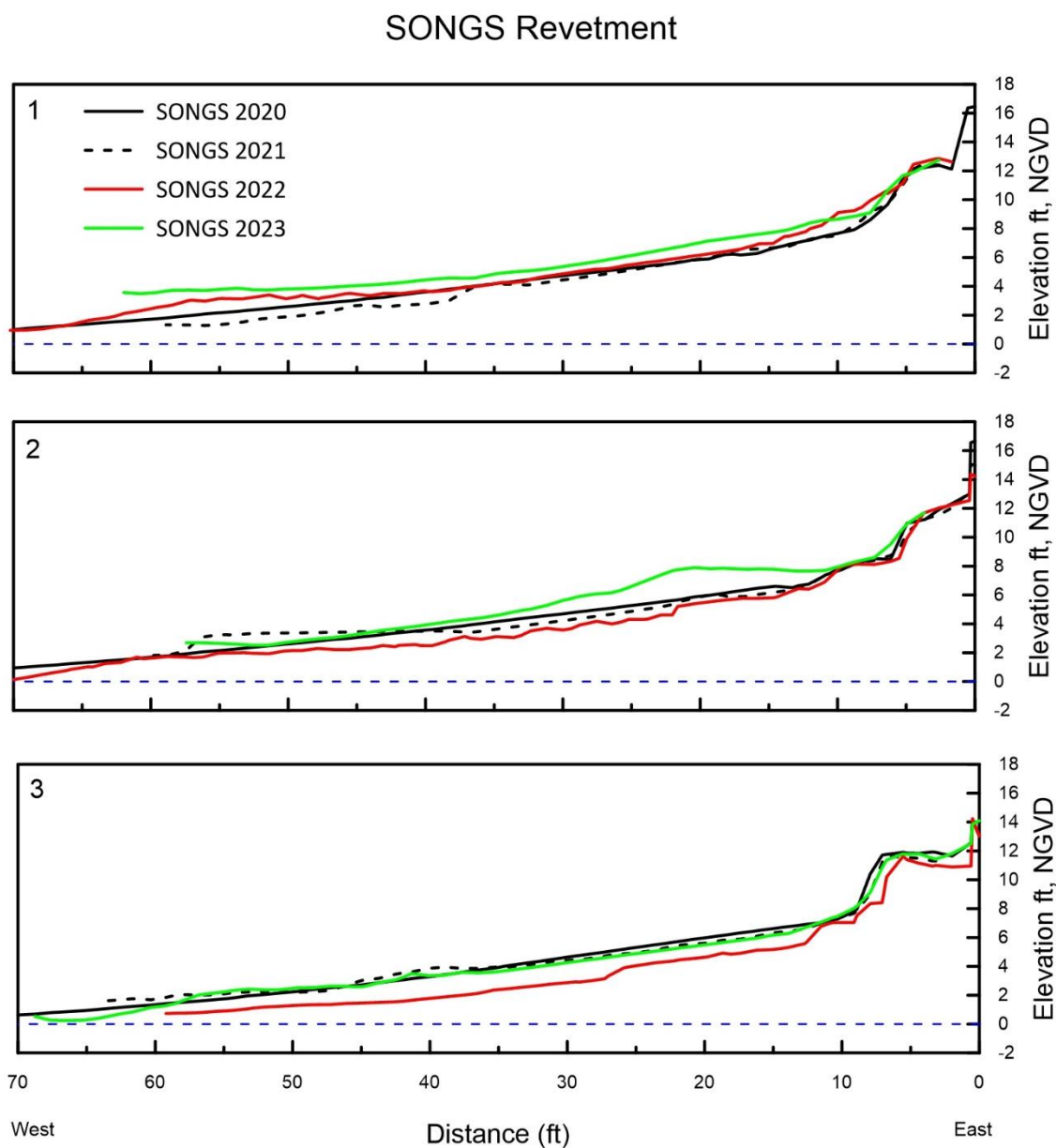


Figure B-1. Cross sections of SONGS revetment along ranges 1-3, surveyed on 19 January 2023, 01 February 2022, 25 February 2021, and 05 March 2020.

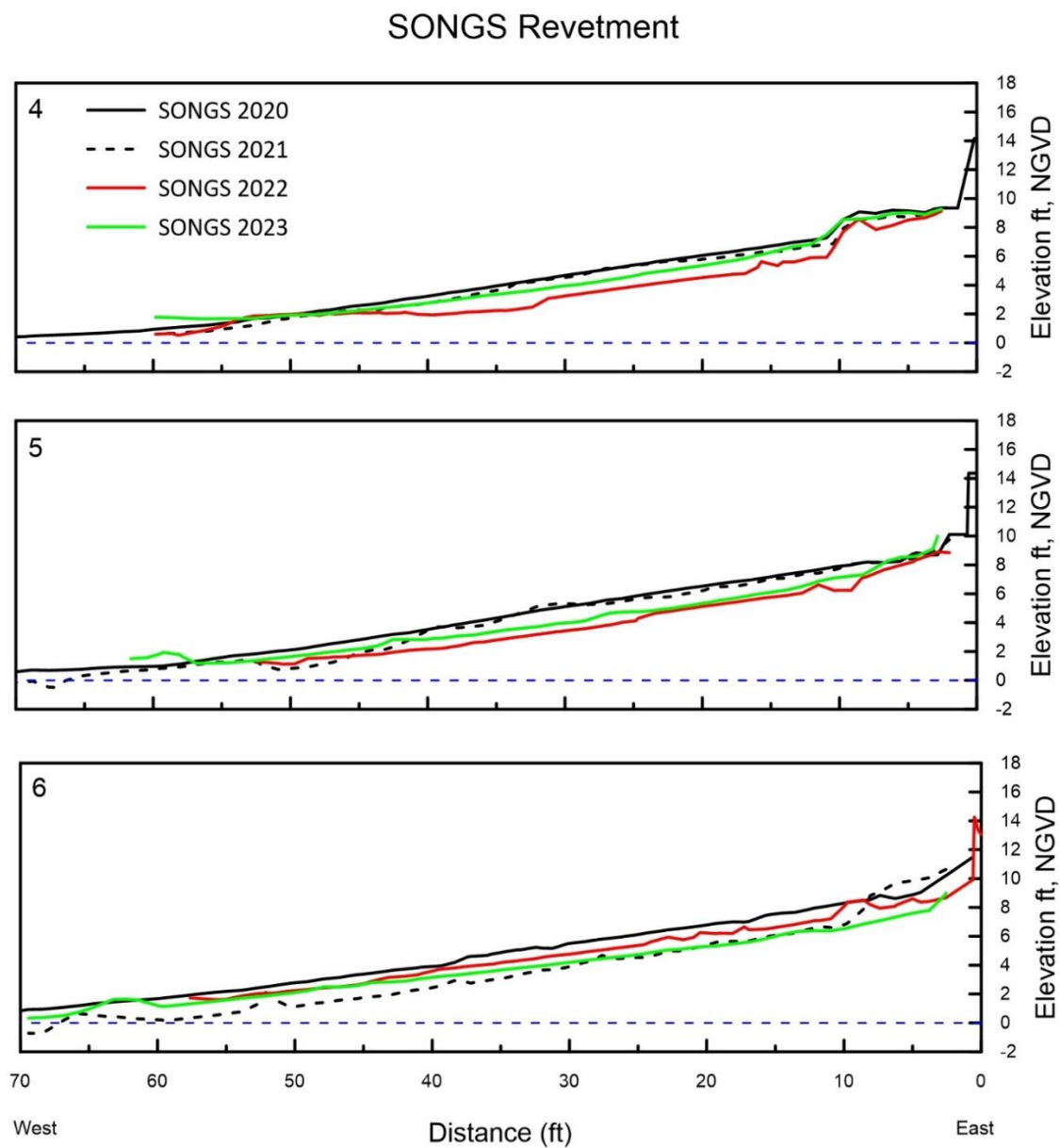


Figure B-2. Cross sections of SONGS revetment along ranges 4-6, surveyed on 19 January 2023, 01 February 2022, 25 February 2021, and 05 March 2020.

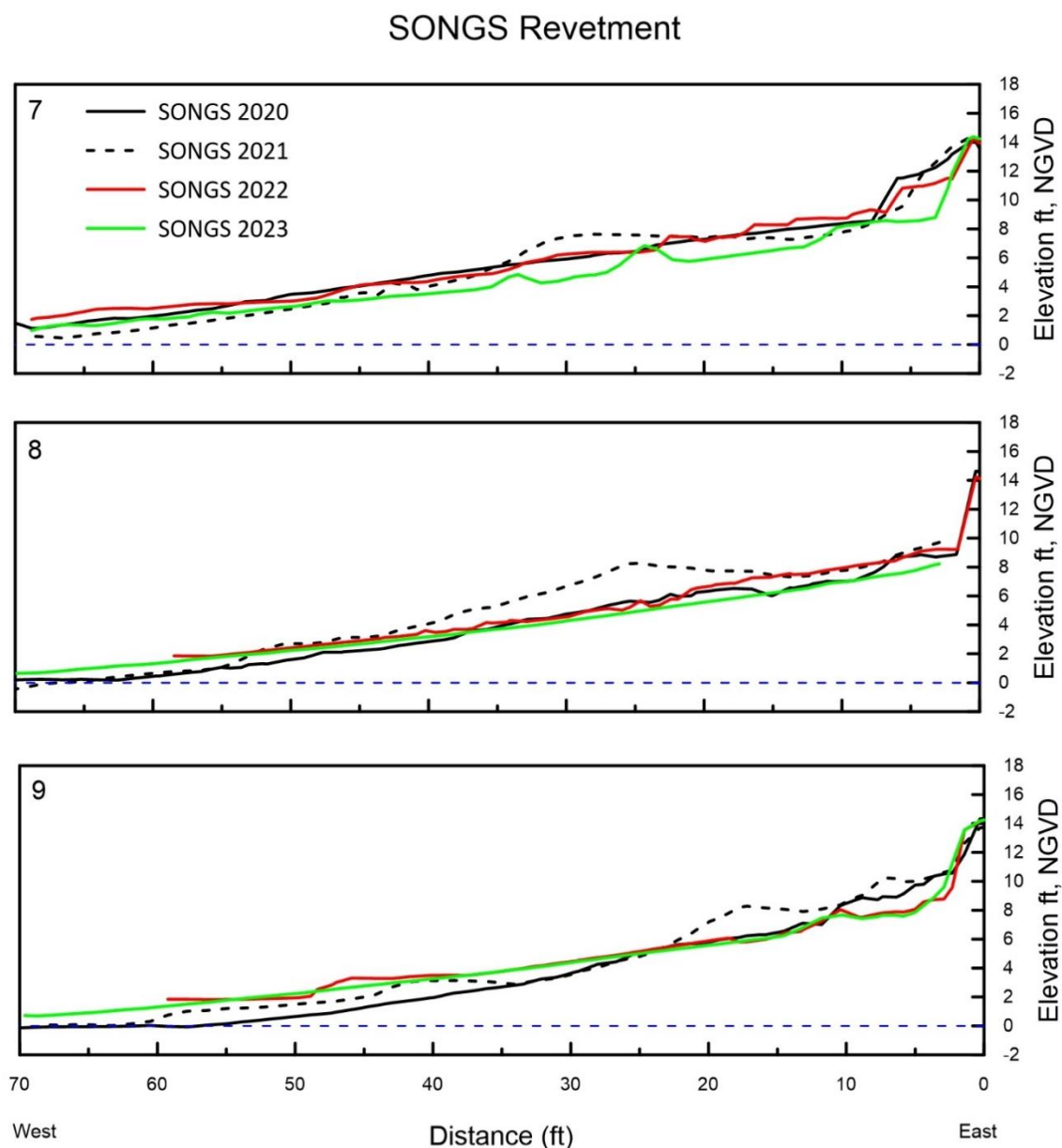


Figure B-3. Cross sections of SONGS revetment along ranges 7-9, surveyed on 19 January 2023, 01 February 2022, 25 February 2021, and 05 March 2020.

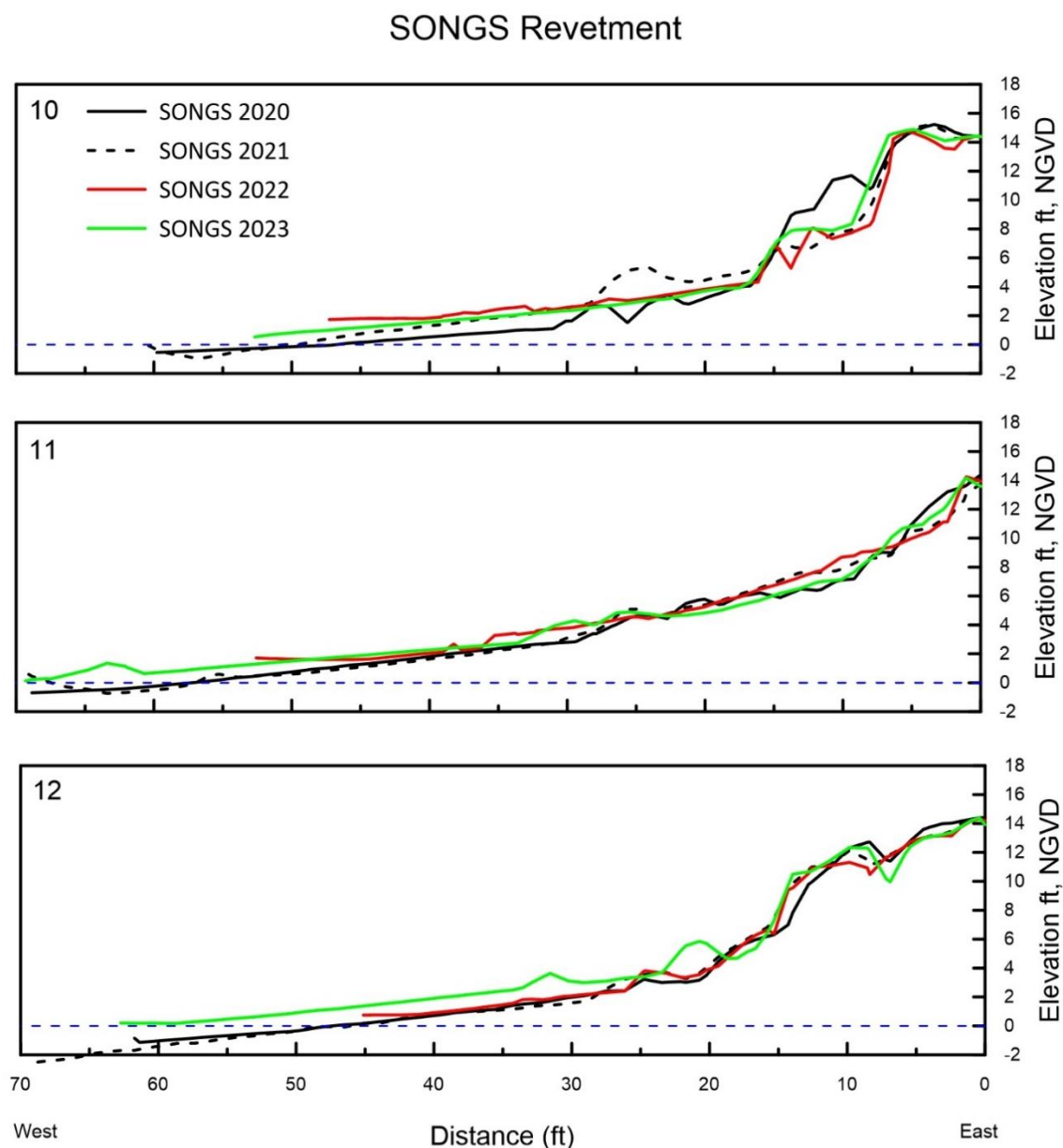


Figure B-4. Cross sections of SONGS revetment along ranges 10-12, surveyed on 19 January 2023, 01 February 2022, 25 February 2021, and 05 March 2020.

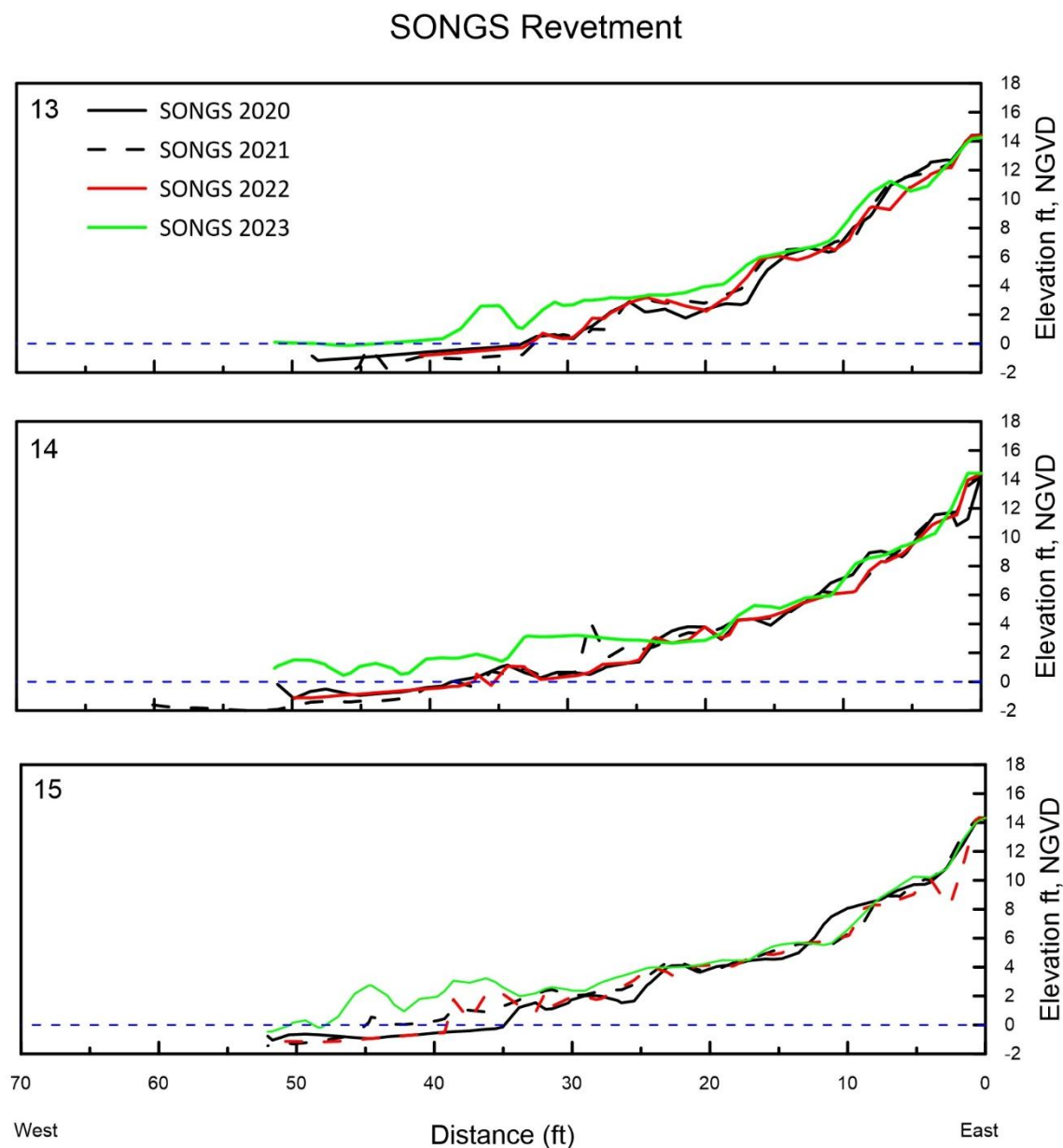


Figure B-5. Cross sections of SONGS revetment along ranges 13-15, surveyed on 19 January 2023, 01 February 2022, 25 February 2021, and 05 March 2020.

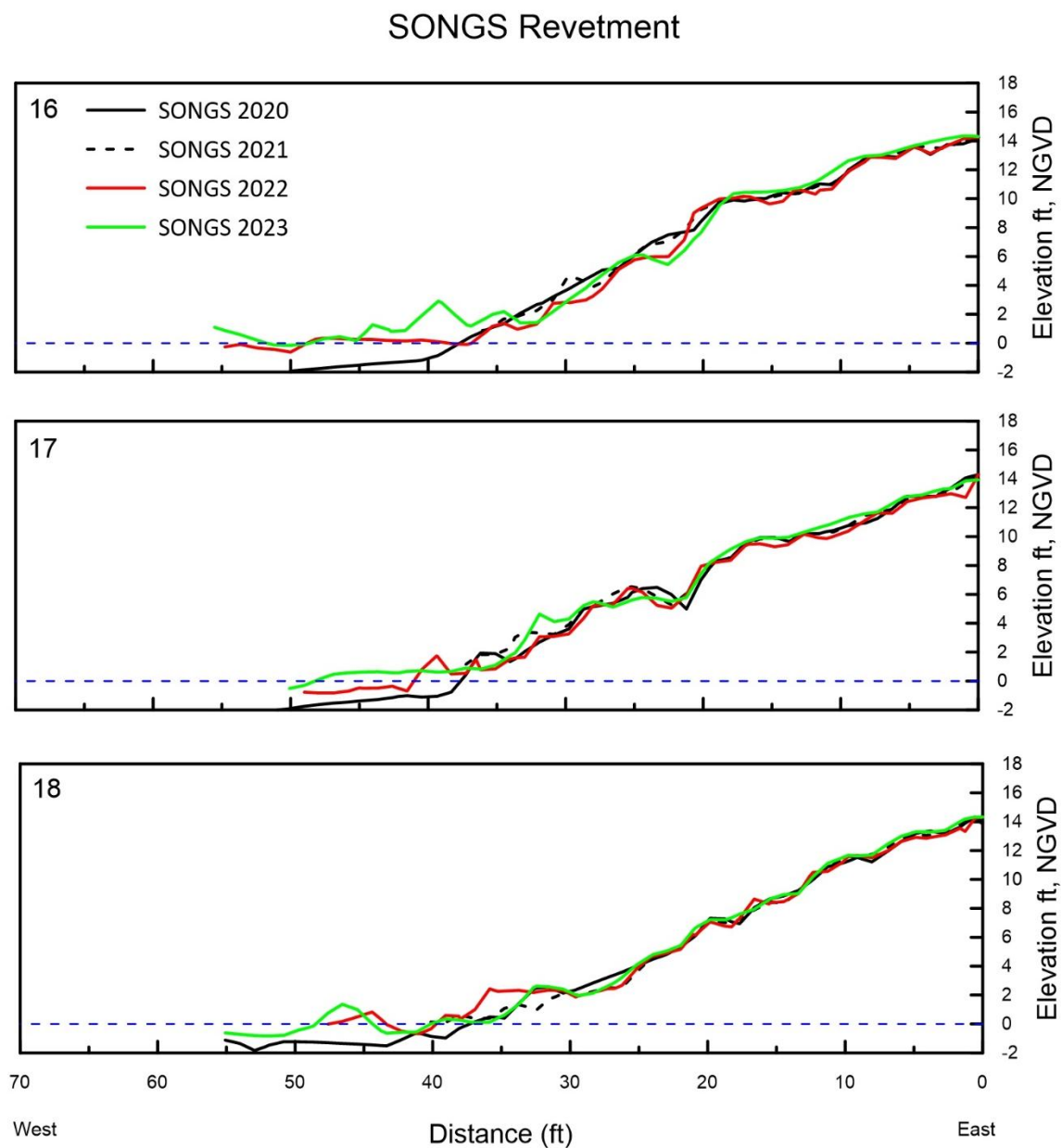


Figure B-6. Cross sections of SONGS revetment along ranges 16-18, surveyed on 19 January 2023, 01 February 2022, 25 February 2021, and 05 March 2020.

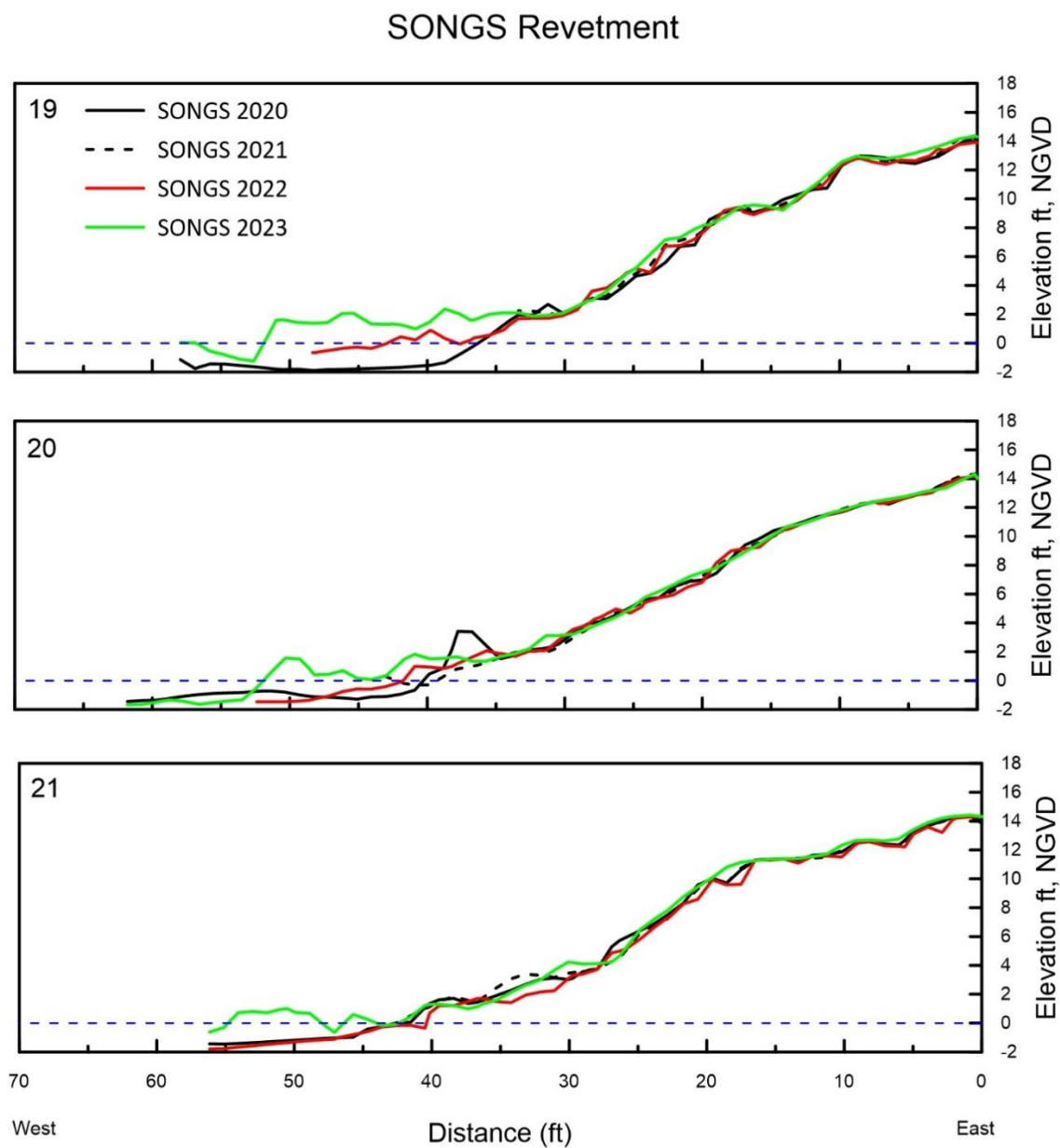


Figure B-7. Cross sections of SONGS revetment along ranges 19-21, surveyed on 19 January 2023, 01 February 2022, 25 February 2021, and 05 March 2020.

APPENDIX C

AERIAL PHOTOGRAPHS
NORTH AND SOUTH SONGS, 2003-2020



Photo C-1. Photograph showing revetment covered by sand and fronted by a wide beach at the northern end of SONGS (10 March 2003).



Photo C-2. Photograph showing waves from north swell attacking SONGS revetment at the southern end of SONGS (10 March 2003).



Photo C-3. Photograph showing waves attacking the revetment and the presence of a sand beach at the northern end of SONGS (26 November 2003).



Photo C-4. Photograph showing waves attacking SONGS revetment at the southern end of SONGS (26 November 2003).

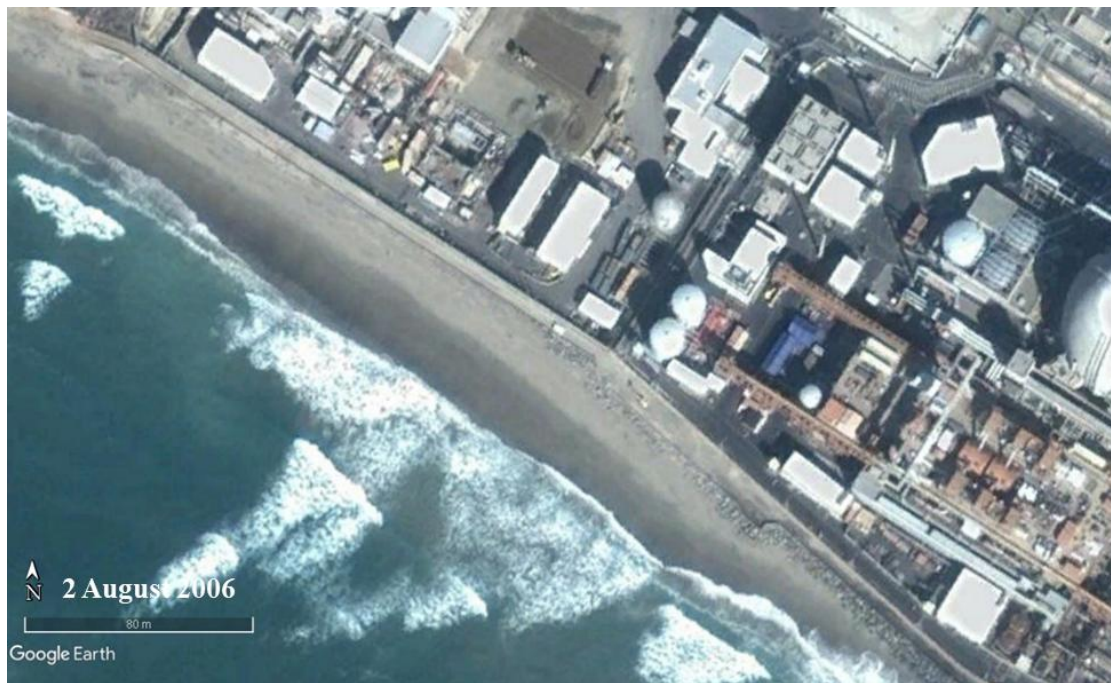


Photo C-5. Photograph showing revetment covered by sand and fronted by a wide beach at the northern end of SONGS (02 August 2006).

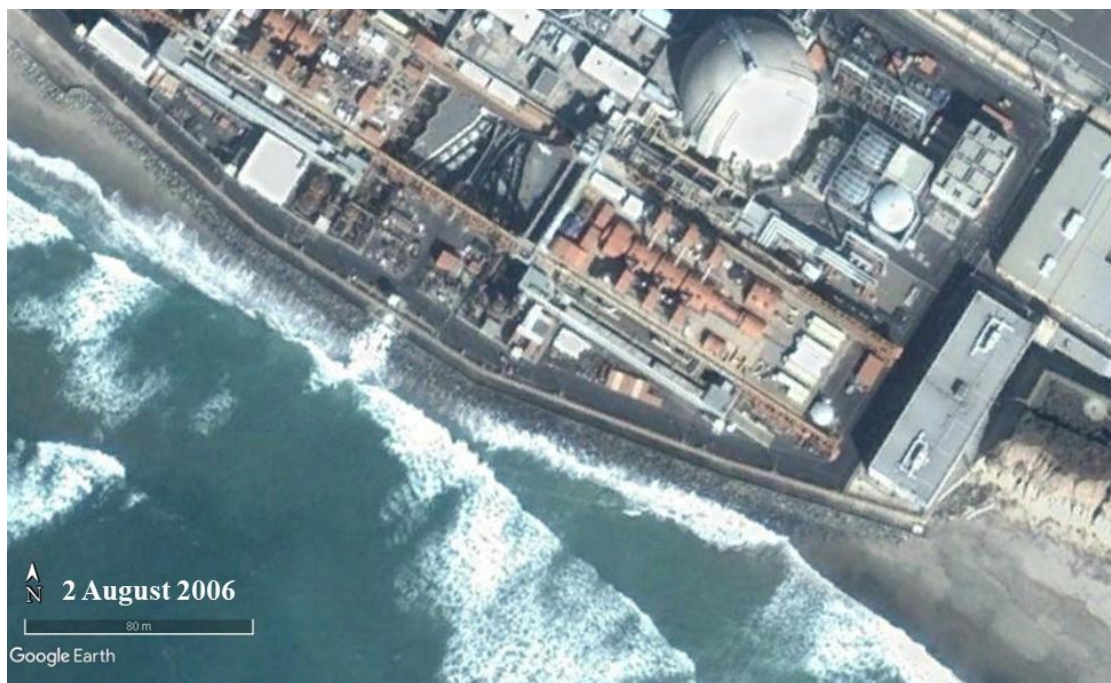


Photo C-6. Photograph showing waves from north swell attacking SONGS revetment at the southern end of SONGS (02 August 2006).

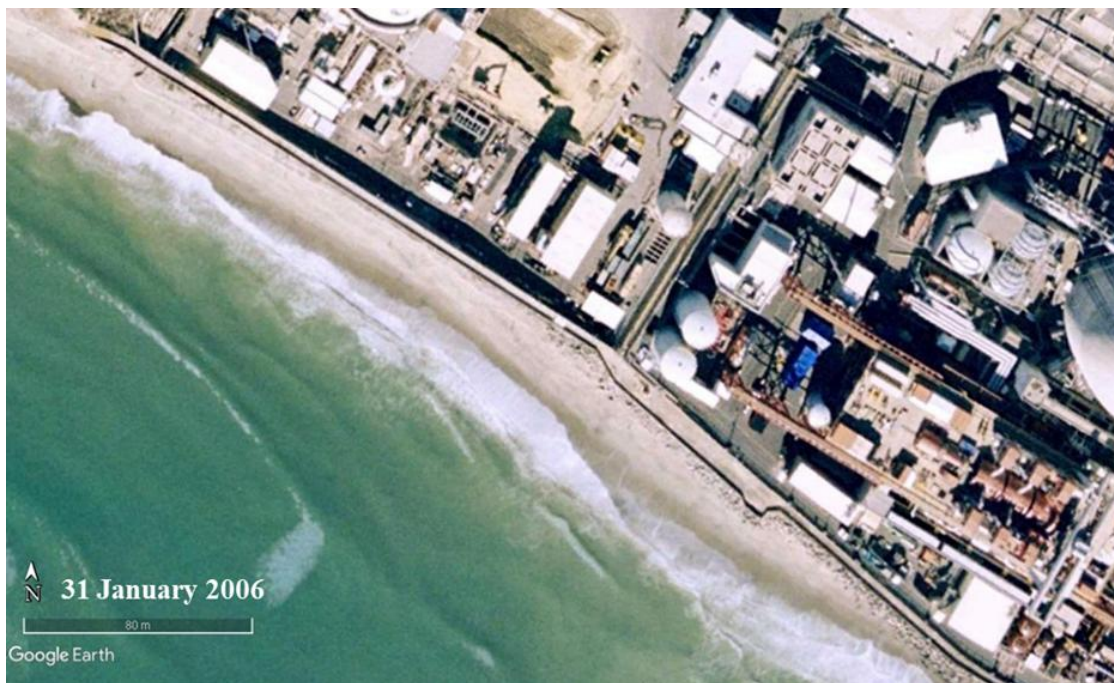


Photo C-7. Photograph showing revetment covered by sand and fronted by a wide beach at the northern end of SONGS (31 January 2006).



Photo C-8. Photograph showing waves from north swell attacking SONGS revetment and refracting towards south at the southern end of SONGS (31 January 2006).

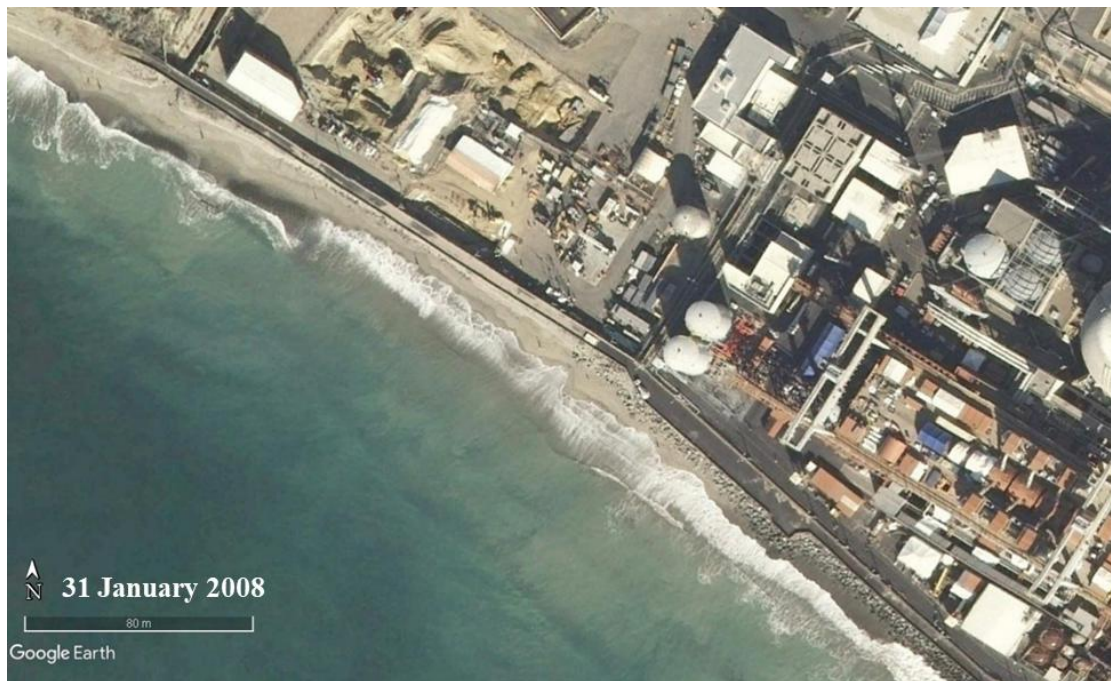


Photo C-9. Photograph showing revetment covered by sand and fronted by a wide beach at the northern end of SONGS (31 January 2008).



Photo C-10. Photograph showing waves attacking SONGS revetment at the southern end of SONGS (31 January 2008).



Photo C-11. Photograph showing revetment covered by sand and fronted by a wide beach at the northern end of SONGS (12 November 2013).



Photo C-12. Photograph showing waves attacking SONGS revetment and refracting towards south at the southern end of SONGS (12 November 2013).



Photo C-13. Photograph showing revetment exposed and fronted by a wide beach at the northern end of SONGS (27 April 2014).

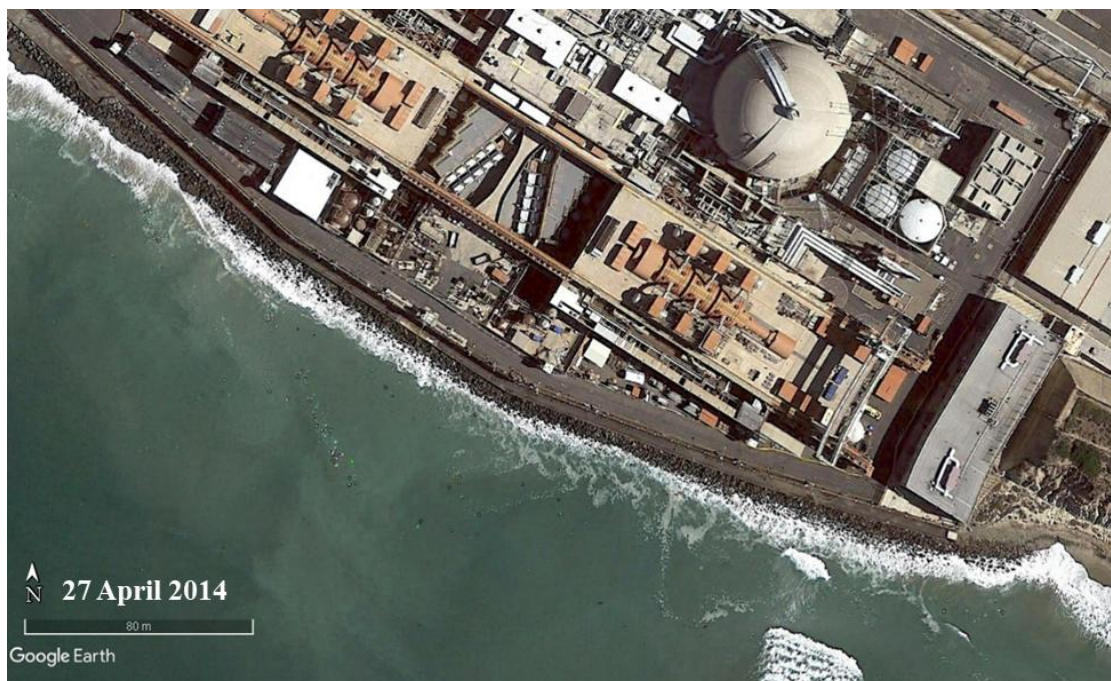


Photo C-14. Photograph showing waves attacking SONGS revetment and refracting towards south at the southern end of SONGS (27 April 2014).

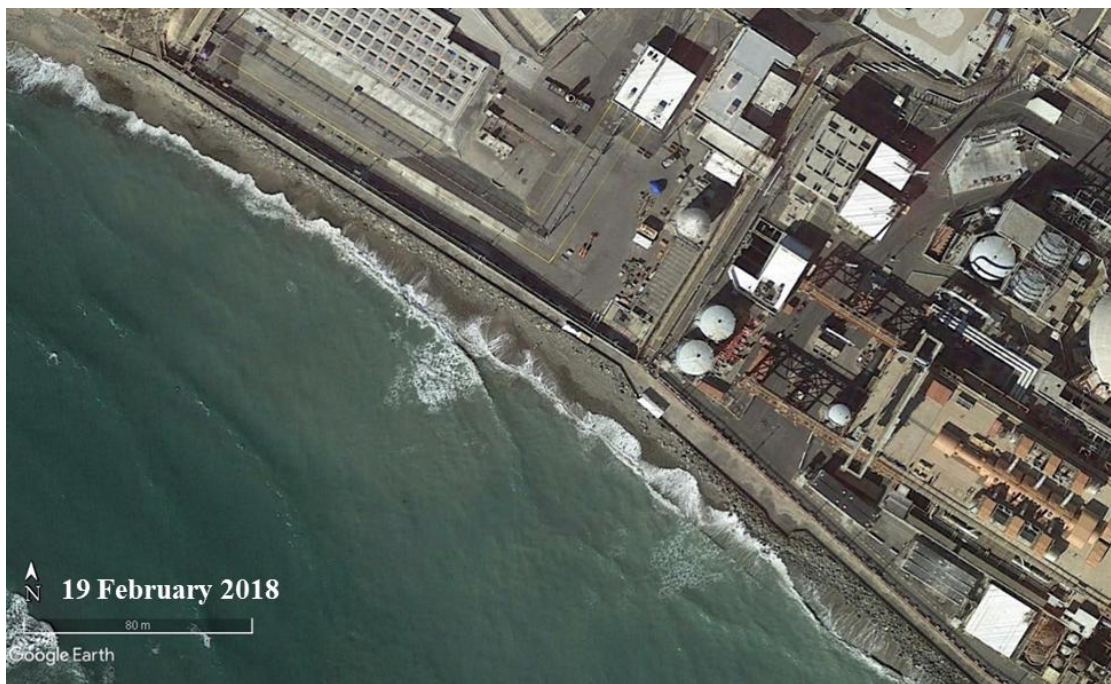


Photo C-15. Photograph showing revetment exposed and fronted by a sand beach at the northern end of SONGS (19 February 2018).

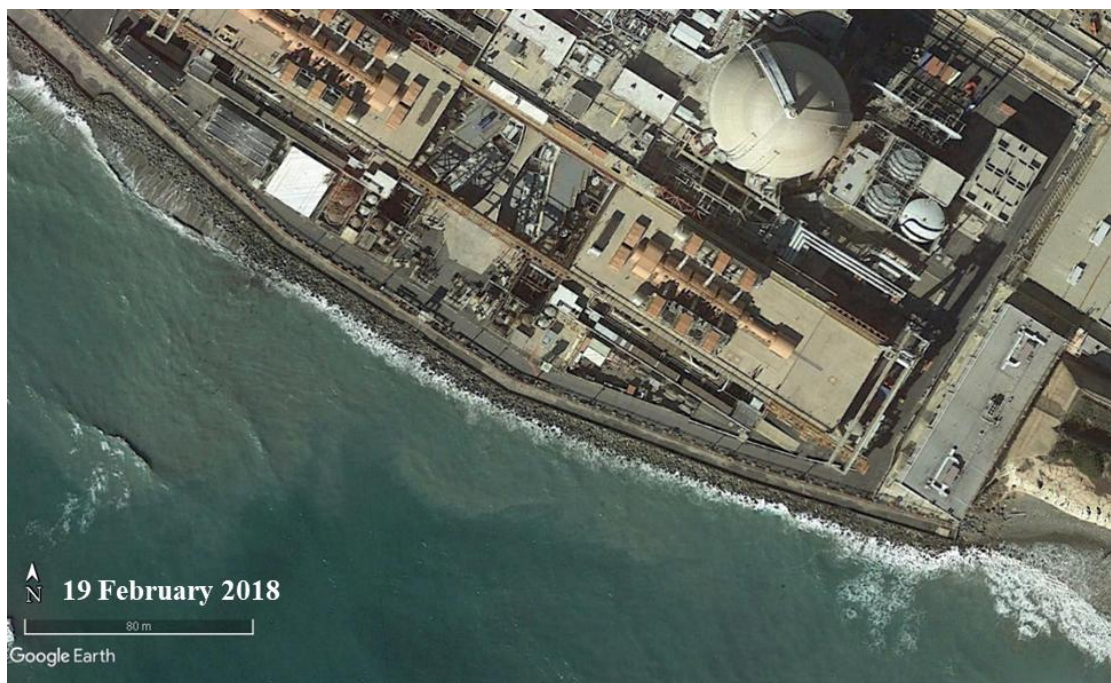


Photo C-16. Photograph showing waves from north swell attacking SONGS revetment and refracting towards south at the southern end of SONGS (19 February 2018).

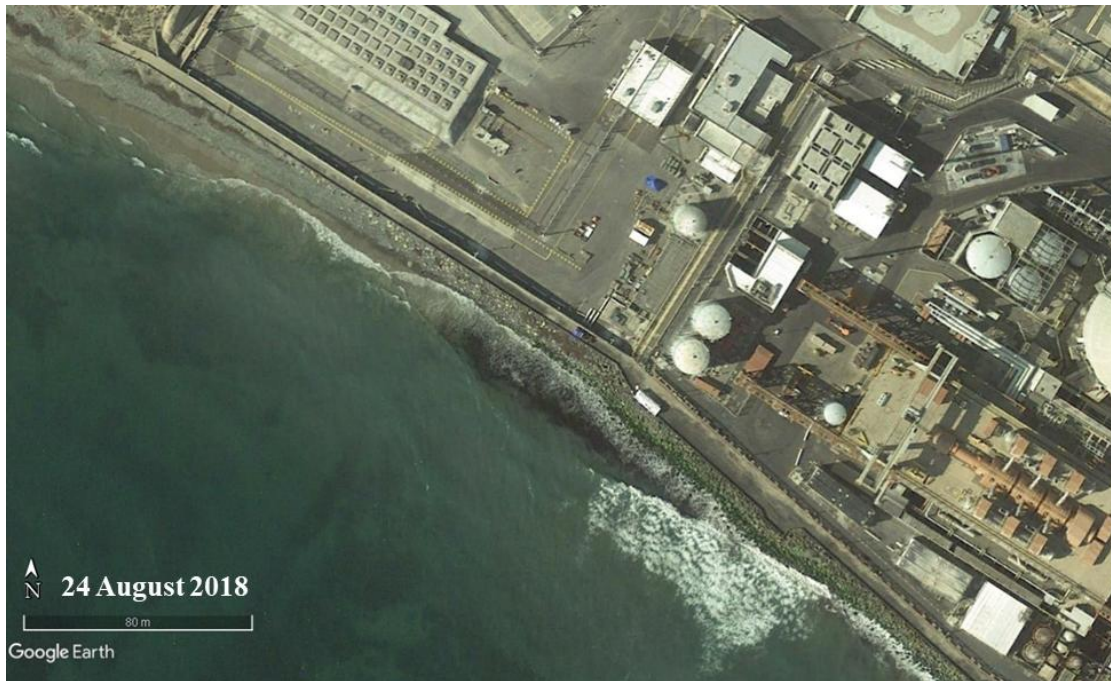


Photo C-17. Photograph showing revetment exposed and fronted by a wide beach at the northern end of SONGS (24 August 2018).



Photo C-18. Photograph showing waves from north swell attacking SONGS revetment and refracting towards south at the southern end of SONGS (24 August 2018).

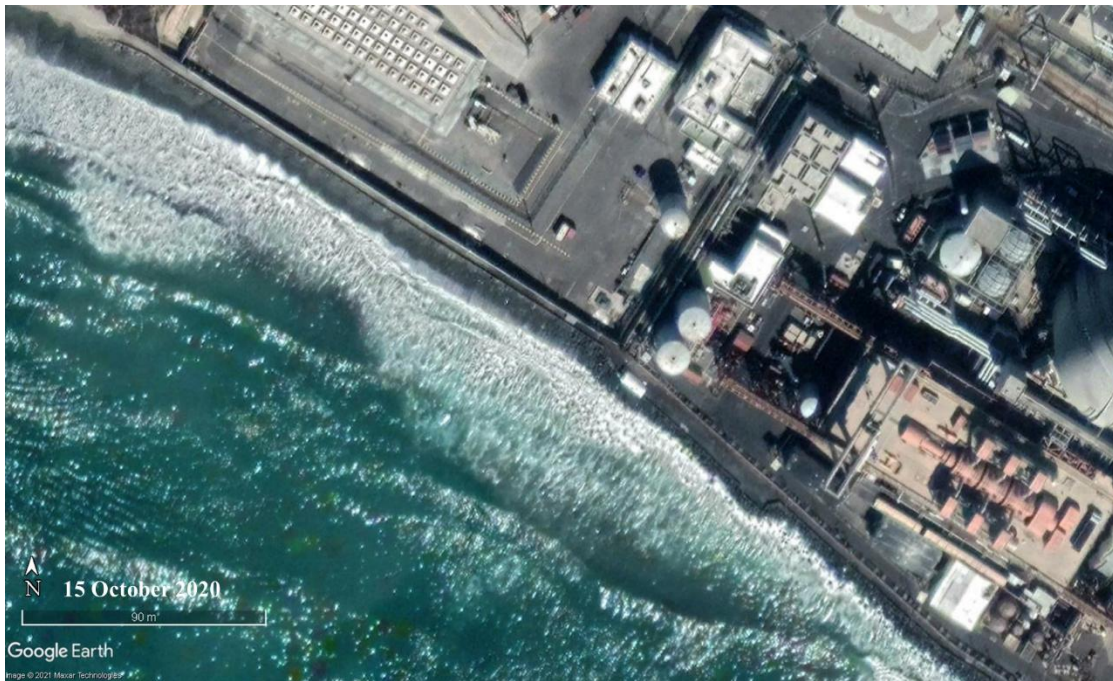


Photo C-19. Photograph showing revetment exposed and fronted by a wide beach at the northern end of SONGS (15 October 2020).



Photo C-20. Photograph showing waves attacking SONGS revetment and refracting towards south at the southern end of SONGS (15 October 2020).

APPENDIX D

PHOTOGRAPHS FROM 2023 & 2020 SURVEYS

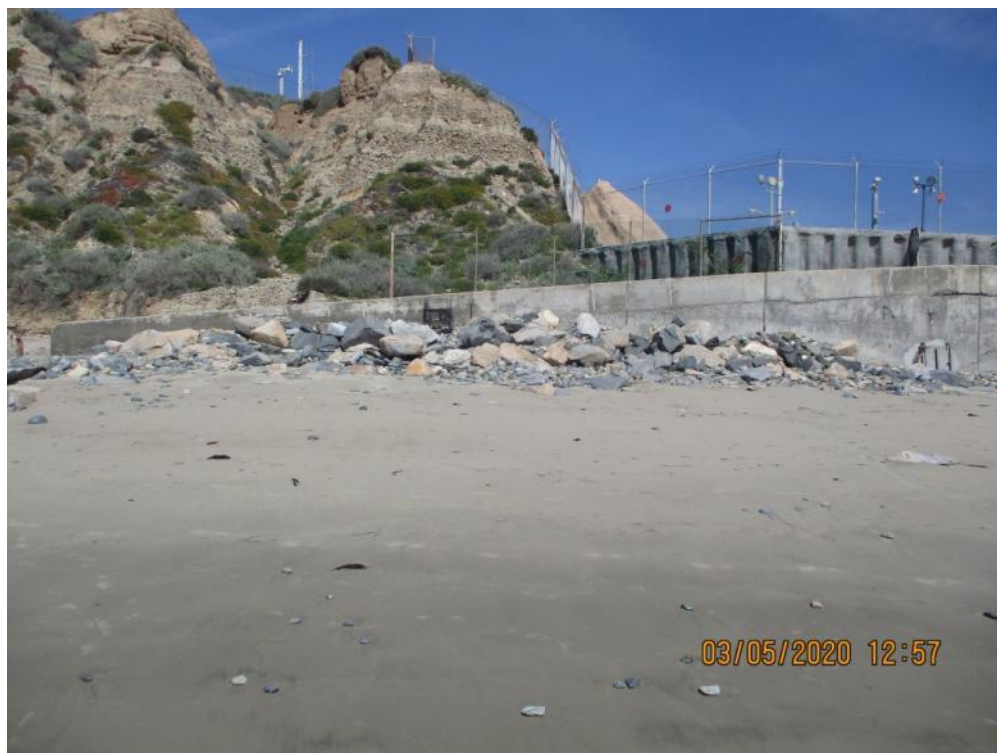


Photo D-1. Photograph for Transect 1 taken on 16 February 2023 (top) and 05 March 2020 (bottom).



Photo D-2. Photograph for Transect 2 taken on 16 February 2023 (top) and 05 March 2020 (bottom).



Photo D-3. Photograph for Transect 3 taken on 16 February 2023 (top) and 05 March 2020 (bottom).



Photo D-4. Photograph for Transect 4 taken on 16 February 2023 (top) and 05 March 2020 (bottom).

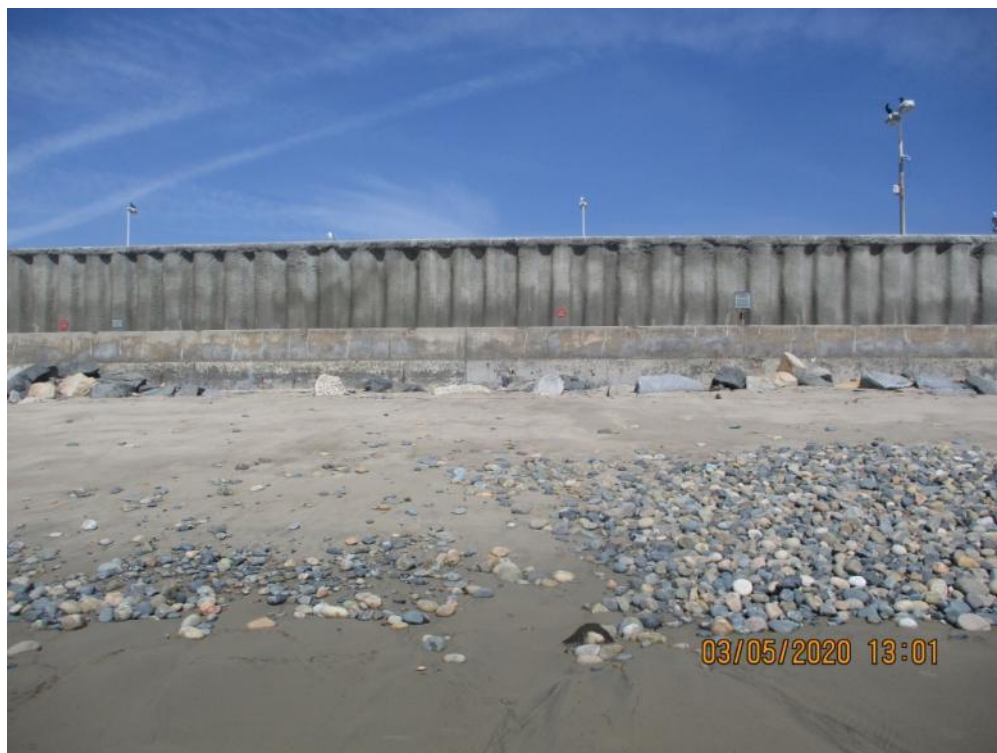
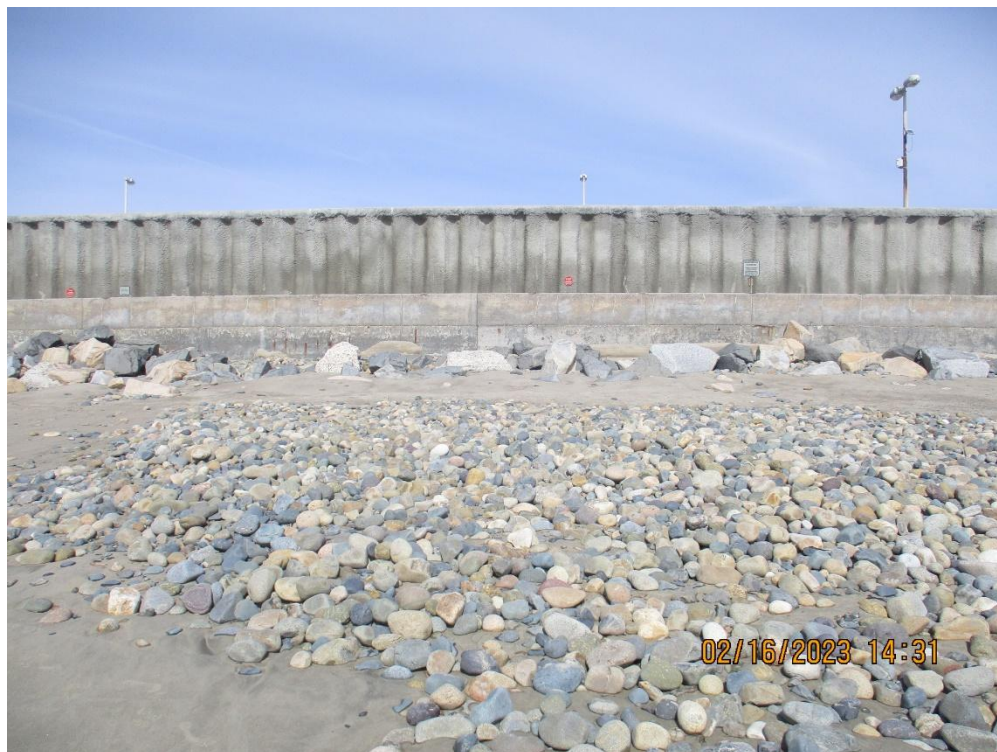


Photo D-5. Photograph for Transect 5 taken on 16 February 2023 (top) and 05 March 2020 (bottom).

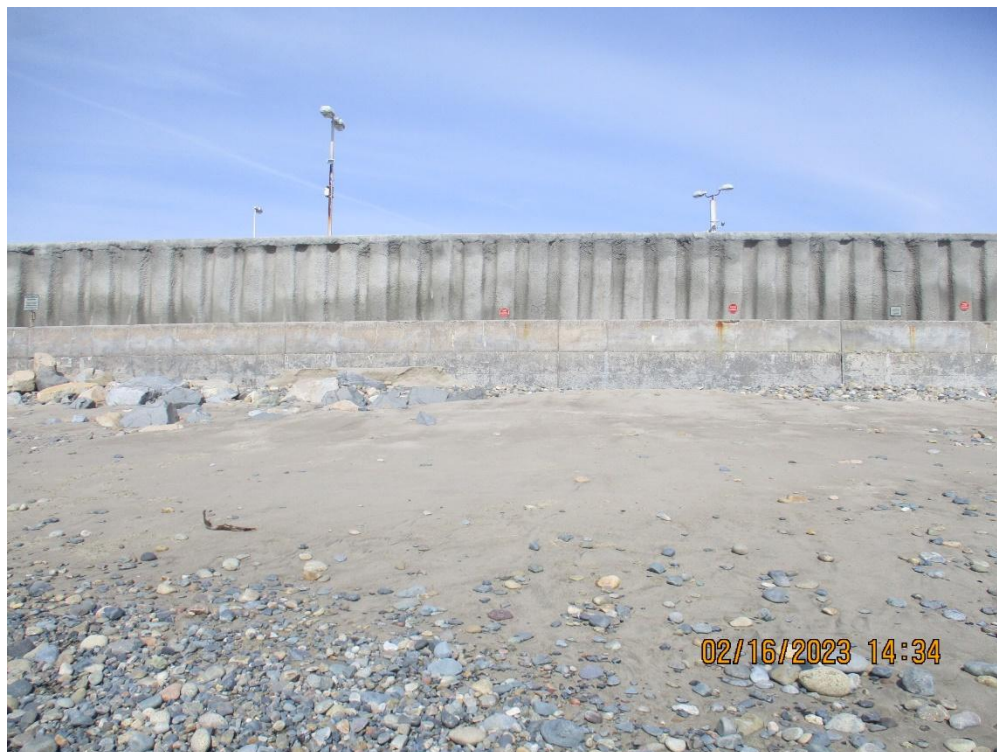


Photo D-6. Photograph for Transect 6 taken on 16 February 2023 (top) and 05 March 2020 (bottom).



Photo D-7. Photograph for Transect 7 taken on 16 February 2023 (top) and 05 March 2020 (bottom).



Photo D-8. Photograph for Transect 8 taken on 16 February 2023 (top) and 05 March 2020 (bottom).



Photo D-9. Photograph for Transect 9 taken on 16 February 2023 (top) and 05 March 2020 (bottom).



Photo D-10. Photograph for Transect 10 taken on 16 February 2023 (top) and 05 March 2020 (bottom).



Photo D-11. Photograph for Transect 11 taken on 16 February 2023 (top) and 05 March 2020 (bottom).



Photo D-12. Photograph for Transect 12 taken on 16 February 2023 (top) and 05 March 2020 (bottom).



Photo D-13. Photograph for Transect 13 taken on 16 February 2023 (top) and 05 March 2020 (bottom).



Photo D-14. Photograph for Transect 14 taken on 16 February 2023 (top) and 05 March 2020 (bottom).



Photo D-15. Photograph for Transect 15 taken on 16 February 2023 (top) and 05 March 2020 (bottom).



Photo D-16. Photograph for Transect 16 taken on 16 February 2023 (top) and 05 March 2020 (bottom).



Photo D-17. Photograph for Transect 17 taken on 16 February 2023 (top) and 05 March 2020 (bottom).



Photo D-18. Photograph for Transect 18 taken on 16 February 2023 (top) and 05 March 2020 (bottom).



Photo D-19. Photograph for Transect 19 taken on 16 February 2023 (top) and 05 March 2020 (bottom).



Photo D-20. Photograph for Transect 20 taken on 16 February 2023 (top) and 05 March 2020 (bottom).

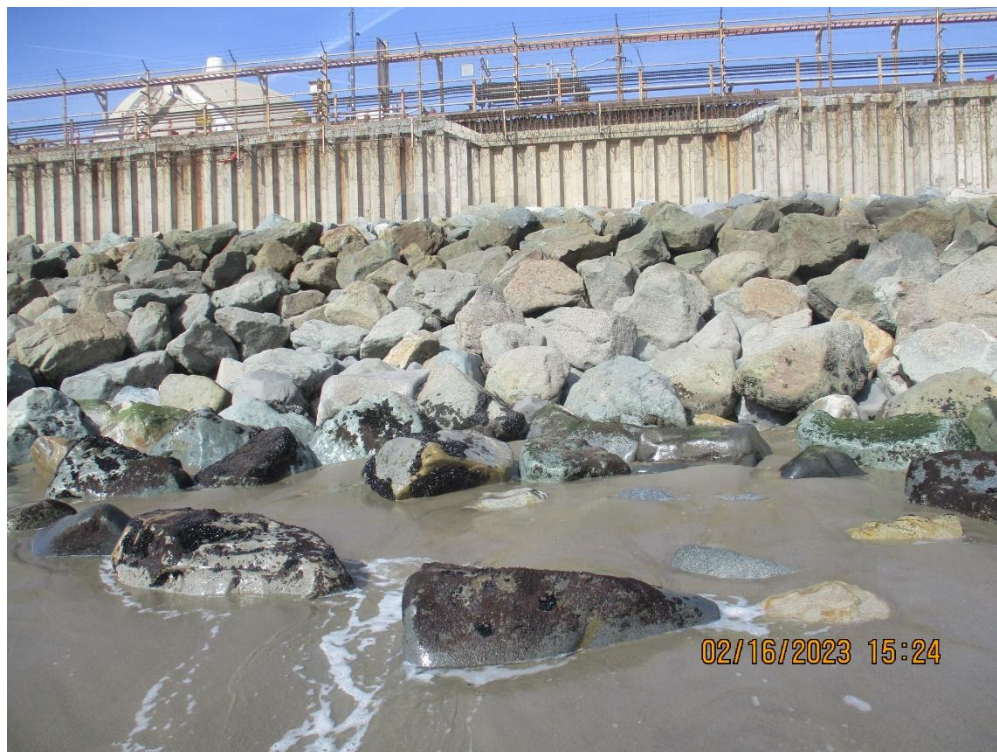


Photo D-21. Photograph for Transect 21 taken on 16 February 2023 (top) and 05 March 2020 (bottom).

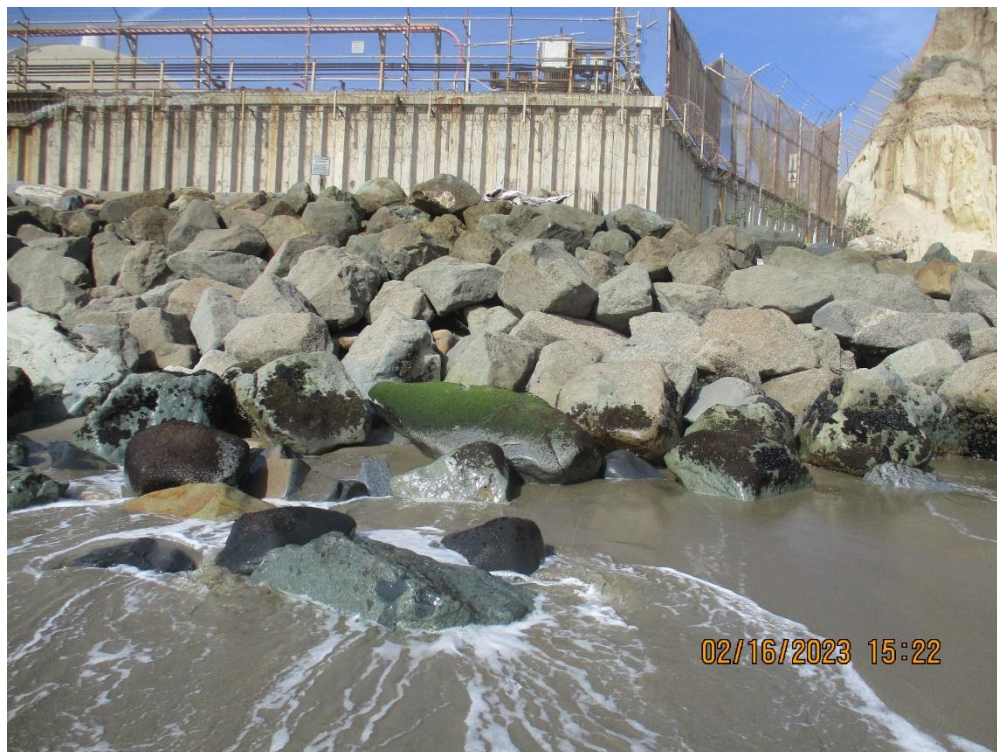


Photo D-22. Photograph showing the start of southern riprap at end of walkway taken on 16 February 2023 (top) and 05 March 2020 (bottom).

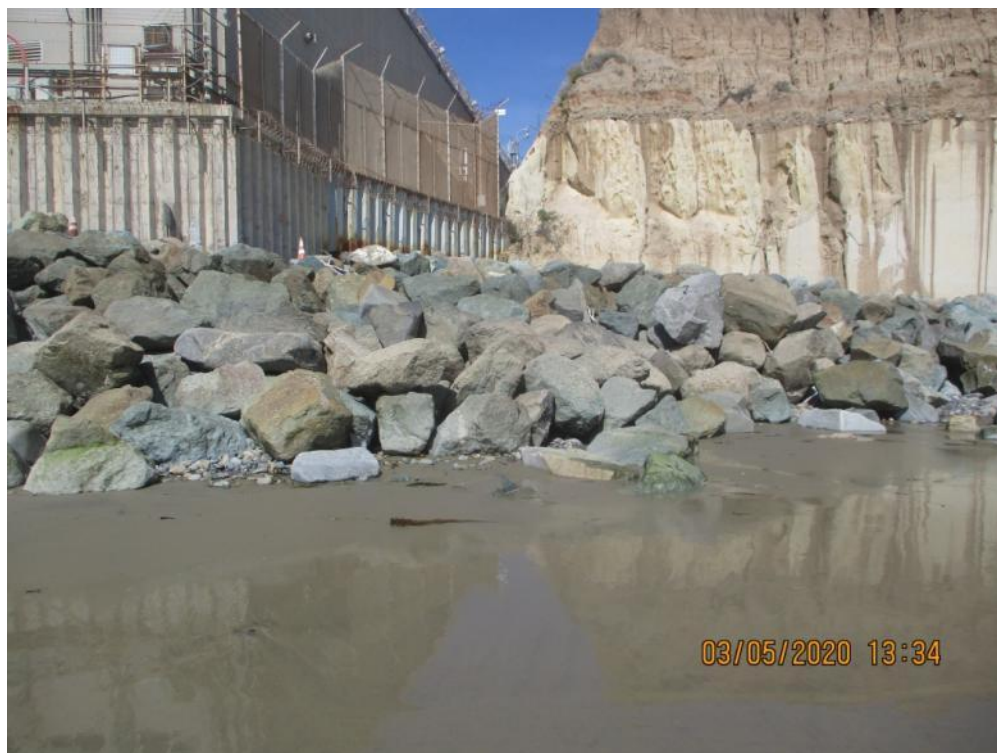


Photo D-23. Photograph showing the middle of southern riprap at end of walkway taken on 16 February 2023 (top) and 05 March 2020 (bottom).



Photo D-24. Photograph showing the end of southern riprap at end of walkway taken on 16 February 2023 (top) and 05 March 2020 (bottom).

APPENDIX E

2022 BEACH PROFILE SURVEYS AT SAN ONOFRE

**SAN ONOFRE NUCLEAR GENERATING STATION (SONGS) UNITS 2 & 3
DECOMMISSIONING PROJECT
2022 BEACH PROFILE SURVEYS AT SAN ONOFRE**



by

M. Hany S. Elwany, Ph.D.
Reinhard E. Flick, Ph.D.
Tim Norall, MS.

Submitted to:

SOUTHERN CALIFORNIA EDISON
2244 Walnut Grove Avenue
Rosemead, CA 91770

COASTAL ENVIRONMENTS, INC.
2166 Avenida de la Playa, Suite E
La Jolla, CA 92037

01 March 2023
CE Reference No. 23-04

TABLE OF CONTENTS

1.0	INTRODUCTION	1
2.0	SURVEY METHOD	4
3.0	2022 BEACH PROFILE SURVEY RESULTS	9
4.0	BEACH PROFILE CHARACTERISTICS	24
5.0	BEACH WIDTH CHANGES FROM 2017 THROUGH 2022	26
6.0	ESTIMATION OF SHORELINE TRENDS AND SEASONAL CYCLES	31
7.0	BEACH PROFILES AND WIDTH FROM 1964 THROUGH 2022.....	37
7.1	BEACH PROFILE HISTORY	37
7.2	BEACH WIDTH DATA	38
8.0	CONCLUSIONS AND RECOMMENDATIONS	47
9.0	REFERENCES	48

LIST OF APPENDICES

Appendix A.	Nearshore Summer and Winter Beach Profiles for 2017-2022	A-1
Appendix B.	Photographs of San Onofre Beach and New Survey Benchmarks Taken in 2022	B-1

LIST OF TABLES

Table 1-1.	Surveys at San Onofre, 2017-2022	2
Table 2-1.	Locations and elevations of benchmarks	7
Table 2-2.	Beach profile start point coordinates, elevations, and alignments.....	8
Table 5-1.	Beach widths (ft) at San Onofre profiles (2017-2022)	29
Table 5-2.	Yearly mean beach widths (ft).....	30
Table 6-1.	Annual beach width changes at San Onofre	34
Table 6-2.	Average beach widths (ft) by season at San Onofre	35
Table 6-3.	Average seasonal beach widths (ft) for March 2017 – October 2022	35
Table 6-4.	Linear regression analysis of beach width, March 2017 – October 2022.....	36
Table 7-1.	Mean beach widths (ft) at San Onofre, 1990-1993 vs. 2017-2022.....	46
Table 7-2.	Estimates of seasonal beach widths changes at San Onofre (ft).....	46

LIST OF FIGURES

Figure 1-1.	Locations of beach profiles surveyed at SONGS	3
Figure 2-1.	Schematic illustration of the beach profile survey method.....	5
Figure 2-2.	Locations of benchmarks at SONGS	6
Figure 3-1.	2022 nearshore beach profile surveys of N1000.....	10
Figure 3-2.	2022 nearshore beach profile surveys of N0500.....	11
Figure 3-3.	2022 nearshore beach profile surveys of N0400'	12
Figure 3-4.	2022 nearshore beach profile surveys of NS0000	13
Figure 3-5.	2022 nearshore beach profile surveys of S0800'	14
Figure 3-6.	2022 nearshore beach profile surveys of S0500	15

Figure 3-7.	2022 nearshore beach profile surveys of S1000	16
Figure 3-8.	2022 offshore beach profile surveys of N1000	17
Figure 3-9.	2022 offshore beach profile surveys of N0500	18
Figure 3-10.	2022 offshore beach profile surveys of N0400'	19
Figure 3-11.	2022 offshore beach profile surveys of NS0000	20
Figure 3-12.	2022 offshore beach profile surveys of S0800'	21
Figure 3-13.	2022 offshore beach profile surveys of S0500	22
Figure 3-14.	2022 offshore beach profile surveys of S1000	23
Figure 4-1.	Typical southern California beach profile	25
Figure 5-1a.	Beach width changes at San Onofre at N1000 – NS0000	27
Figure 5-1b.	Beach width changes at San Onofre at S0800' – S1000	28
Figure 6-1a.	SONGS beach width seasonal cycles at N1000 – NS0000 (2017-2022)	32
Figure 6-1b.	SONGS beach width seasonal cycles at S0800' – S1000 (2017-2022)	33
Figure 7-1.	SONGS area historical shoreline changes, laydown pad locations	39
Figure 7-2.	Beach profile range lines at San Onofre, 1990-1993	40
Figure 7-3.	Beach-width time histories around the time of Units 2 and 3 construction	41
Figure 7-4.	Time history of beach-width changes at San Onofre after removal of Units 2 and 3 laydown pad	42
Figure 7-5.	Historical beach width adjacent to Unit 1, 1928-2000	43
Figure 7-6.	Beach profiles at NS0000, years 2000 and 2016	44
Figure 7-7.	Beach width measured between 1990 through 1993 and between 2016 through 2022	45
Figure A-1.	Nearshore beach profile surveys taken in winter (blue) and summer (red) for N1000	A-2
Figure A-2.	Nearshore beach profile surveys taken in winter (blue) and summer (red) for N0500	A-3
Figure A-3.	Nearshore beach profile surveys taken in winter (blue) and summer (red) for N0400'	A-4
Figure A-4.	Nearshore beach profile surveys taken in winter (blue) and summer (red) for NS0000	A-5
Figure A-5.	Nearshore beach profile surveys taken in winter (blue) and summer (red) for S0800'	A-6
Figure A-6.	Nearshore beach profile surveys taken in winter (blue) and summer (red) for S0500	A-7
Figure A-7.	Nearshore beach profile surveys taken in winter (blue) and summer (red) for S1000	A-8

LIST OF PHOTOGRAPHS

Photo B-1.	Photographs taken in February (top left), June (top right), August (bottom left), and October 2022 (bottom right) looking north from range N1000	B-2
Photo B-2.	Photographs taken in February (top left), June (top right), August (bottom left), and October 2022 (bottom right) looking south from range N1000	B-3
Photo B-3.	Photographs taken in February (top left), June (top right), August (bottom left), and October 2022 (bottom right) looking north from range N0500	B-4

Photo B-4.	Photographs taken in February (top left), June (top right), August (bottom left), and October 2022 (bottom right) looking south from range N0500	B-5
Photo B-5.	Photographs taken in February (top left), June (top right), August (bottom left), and October 2022 (bottom right) looking north from range N0400'	B-6
Photo B-6.	Photographs taken in February (top left), June (top right), August (bottom left), and October 2022 (bottom right) looking south from range N0400'	B-7
Photo B-7.	Photographs taken in February (top left), June (top right), August (bottom left), and October 2022 (bottom right) looking north from range NS0000	B-8
Photo B-8.	Photographs taken in February (top left), June (top right), August (bottom left), and October 2022 (bottom right) looking south from range NS0000	B-9
Photo B-9.	Photographs taken in February (top left), June (top right), and October 2022 (bottom) looking north from range S0800'	B-10
Photo B-10.	Photographs taken in February (top left), June (top right), and October 2022 (bottom) looking south from range S0800'	B-11
Photo B-11.	Photographs taken in February (top left), June (top right), August (bottom left), and October 2022 (bottom right) looking north from range S0500	B-12
Photo B-12.	Photographs taken in February (top left), June (top right), August (bottom left), and October 2022 (bottom right) looking south from range S0500	B-13
Photo B-13.	Photographs taken in February (top left), June (top right), August (bottom left), and October 2022 (bottom right) looking north from range S1000	B-14
Photo B-14.	Photographs taken in February (top left), June (top right), August (bottom left), and October 2022 (bottom right) looking south from range S1000	B-15
Photo B-15.	Benchmark BM04, created on 21 January 2020, is located on the SW corner of Bathroom 4 in the San Onofre State Beach parking lot	B-16
Photo B-16.	Benchmark BM02, created on 21 January 2020, is located on the SW corner of Bathroom 2 in the San Onofre State Beach parking lot	B-16
Photo B-17.	Benchmark BM07, created on 21 January 2020, is located on the NE corner of a concrete structure located south of the San Onofre State Beach parking lot and north of transect N0500	B-17
Photo B-18.	Benchmark BM08, created on 21 January 2020, is marked by a scribed X and located just south of transect NS0000 on top of the seawall.....	B-17
Photo B-19.	Benchmark BM09, created on 21 January 2020, is located on top of the seawall, just south of transect S0800'	B-18
Photo B-20.	Benchmark BM10, created on 21 January 2020, is marked by a metal screw and washer and is located on the walkway south of transect S0800'	B-18
Photo B-21.	Benchmark BM11, created on 21 January 2020, is located on top of the concrete blocks at the southern end of the SONGS walkway	B-19
Photo B-22.	Benchmark BM12, created on 21 January 2020, is located on top of the concrete drainage structure located just north of transect S1000	B-19

SAN ONOFRE NUCLEAR GENERATING STATION (SONGS) UNITS 2 & 3 DECOMMISSIONING PROJECT 2022 BEACH PROFILE SURVEYS AT SAN ONOFRE

1.0 INTRODUCTION

This report summarizes the beach profile survey data collected at San Onofre in 2022 and examines it within the context of recent and historical beach profile data. The goals of this report are to address the recent characteristics of the beach nearby the San Onofre Nuclear Generating Station (SONGS), and to define the short- and long-term erosion and accretion patterns of the beach.

Recent beach characteristics are defined by the 2017, 2018, 2019, 2020, 2021, and 2022 beach measurements, which were carried out quarterly. These measurements capture the beach configuration corresponding to the autumn, winter, spring, and summer seasons, as well as continuing erosion or accretion trends. Additionally, each year the winter and summer beach profile surveys were extended to cover the offshore portion of the beach up to -60 ft water depth. The results of each survey have been presented in reports by Coastal Environments, Inc. (Coastal Environments [CE], 2020a, 2021, 2021a). The longer-term beach change patterns are characterized by comparing the beach widths from these recent surveys to comparable measurements from 1985-1993. The earliest directly comparable data were taken in May 1985, just after the sand release of the SONGS Units 2 and 3 laydown pad (Flick and Wanetick, 1989), and from 1990-1993 (Elwany et al., 1994), 2000 (CE, 2000), and 2016 (CE, 2016).

Data for this study comes from the 24 surveys carried out from March 2017 through October 2022 (Table 1-1). Each survey covered seven profiles (Figure 1-1). Beach profile measurements generally extended to 12 ft below mean sea level (MSL). Two offshore profiles each year extended to 60 ft water depth using a boat-mounted fathometer. Profile elevations are plotted relative to the National Geodetic Vertical Datum 1929 (NGVD), which is 0.44 ft below MSL.

Section 2 of this report presents an overview of the data and how it was collected. In Section 3, the results of the 2022 beach profile surveys at SONGS are presented. The characteristics of SONGS beach profiles and how they relate to typical Southern California beaches are discussed in Section 4. Beach width changes and shoreline trends are discussed in Sections 5 and 6, respectively. Section 7 utilizes the available historical information to better understand beach width fluctuations over a longer time scale and shoreline changes at San Onofre. The conclusions and recommendations are detailed in Section 8. Appendix A shows the nearshore beach profiles carried out in summer and winter for 2017 through 2022. Appendix B presents photographs taken at San Onofre Beach during each survey in 2022, as well as the location of newly established benchmarks.

Table 1-1. Surveys at San Onofre, 2017-2022.

Survey Number	Date	Season
1	01Mar17	Winter
2	19May17	Spring
3	16Aug17	Summer
4	02Nov17	Autumn
5	23Jan18	Winter
6	29May18	Spring
7	22Aug18	Summer
8	18Nov18	Autumn
9	04Mar19	Winter
10	23Apr19	Spring
11	25Jun19	Summer
12	14Oct19	Autumn
13	05Feb20	Winter
14	15May20	Spring
15	17Jul20	Summer
16	27Oct20	Autumn
17	01Feb21	Winter
18	17May21	Spring
19	29Jun21	Summer
20	03Nov21	Autumn
21	28Feb22	Winter
22	08Jun22	Spring
23	11Aug22	Summer
24	06Oct22	Autumn

San Onofre Nuclear Generating Station (SONGS) Units 2 & 3 Decommissioning Project
2022 Beach Profile Surveys at San Onofre

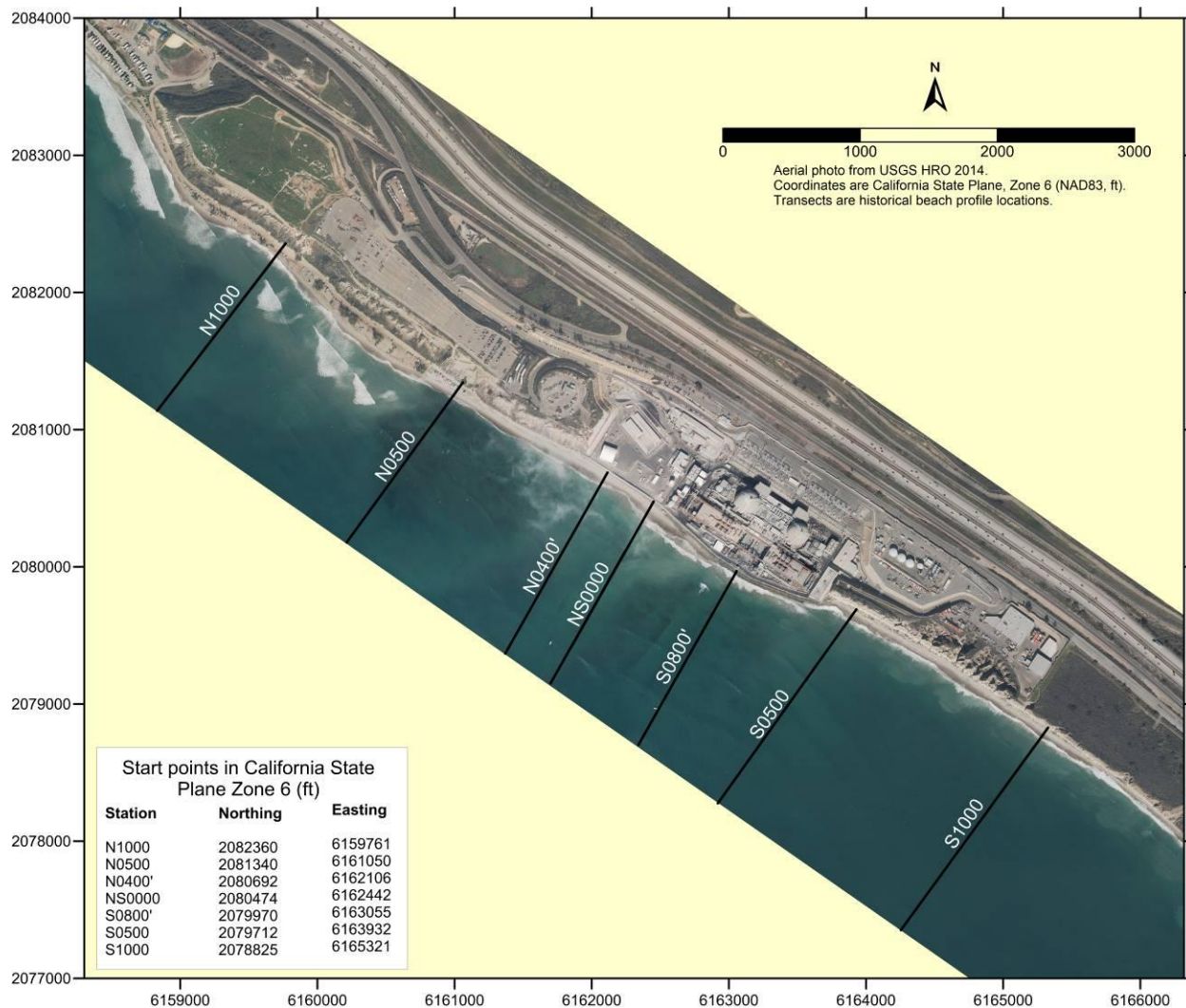


Figure 1-1. Locations of beach profiles surveyed at SONGS.

2.0 SURVEY METHOD

The beach and surf zone were surveyed using a total station (Sokkia SET-610), data logger (Spectra Precision Ranger), and survey rod. The rod holder carries a prism target at the top of a fixed-length pole that reflects an infrared beam sent from the total station. The instrument measures the slant angle and horizontal and vertical distances to the target with an accuracy of approximately 4-6 cm. A handheld electronic field data logger calculates the relative coordinates and elevation using permanent local benchmarks and stores the results. Figure 2-1 illustrates the survey method.

The offshore portions of the profiles were acquired with a digital acoustic echo sounder operated from a 27-ft shallow-draft survey vessel. A Differential Global Positioning System (DGPS) receiver was used to determine the position of each sounding. To improve the accuracy of each position, differential corrections transmitted in real time from U.S. Coast Guard (USCG) beacons were utilized. All systems were interfaced to a laptop computer using the HYDROpro survey package.

At each survey range, the boat traveled from the offshore limit to the surf zone guided by a DGPS navigation system. Soundings were acquired on a near-continuous basis (approximately four to five per second). Vessel positions were recorded at 1-second intervals and merged with the soundings using HYDROpro bathymetric survey software. The calibration of the echo sounder was checked at the beginning and end of each survey session using a standard “bar check” procedure. The merged plots from the 2022 nearshore and offshore profile surveys are presented in Section 3.

All distance measurements on a survey line are made relative to the first reading taken on the starting point of that profile. Starting points were placed as close as practical to the edge or face of the sea cliff. Efforts were made to position the profile starting points used for recent surveys (2017 through 2022) at the same location as those used for all surveys conducted from 1985 to 1993. This enables us to compare the results of the latest surveys with previous data (Flick and Wanetick, 1989; Waldorf, 1989; Elwany et al., 1992, and 1993). The recent survey lines are oriented perpendicular to the mean shoreline using approximately the same fixed bearings as before. The locations of the beach profiles are shown in Figure 2-1.

The horizontal coordinates of the profile starting points were determined by DGPS, and the elevations of these points were determined based on existing benchmarks near SONGS. Figure 2-2 shows the benchmark locations, and Table 2-1 gives their horizontal coordinates and elevations. Table 2-2 gives the horizontal coordinates and elevations of the starting points and the alignment (degrees) of each profile. In January 2020, 11 new benchmarks (BM02 through BM12) were created at SONGS. Photographs displaying these new benchmarks and the surveyed beach profiles are shown in Appendix B.

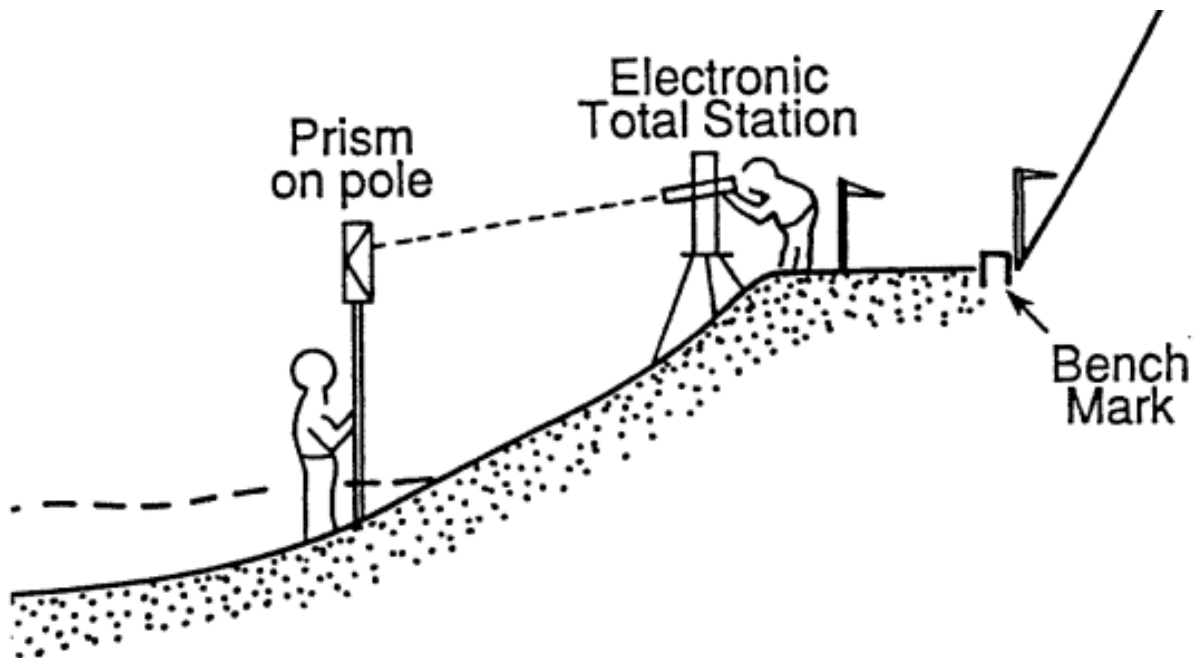


Figure 2-1. Schematic illustration of the beach profile survey method.

San Onofre Nuclear Generating Station (SONGS) Units 2 & 3 Decommissioning Project
2022 Beach Profile Surveys at San Onofre

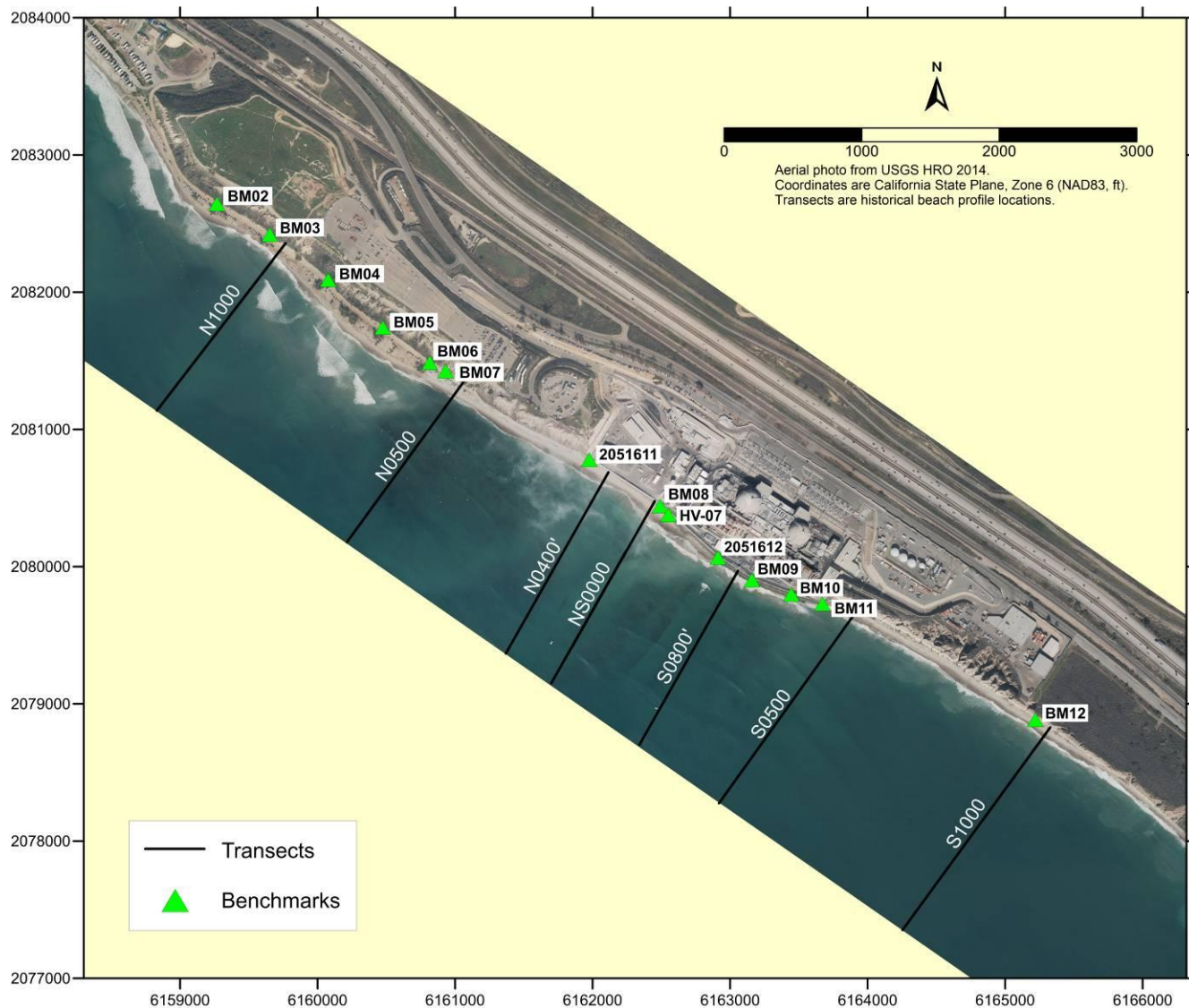


Figure 2-2. Locations of benchmarks at SONGS indicated by green triangular symbols.

Table 2-1. Locations and elevations of benchmarks.

Benchmark	California State Plane Coordinates, Zone 6 (ft), NAD 83		Elevation (ft) NGVD 29
	Easting	Northing	
SO1530	6158825.91 ^a	2083254.09 ^a	17.69
BM02	6159268.34	2082644.35	13.21
BM03	6159653.531	2082419.132	13.072
BM04	6160076.956	2082089.165	16.383
BM05	6160474.686	2081742.329	12.407
BM06	6160816.546	2081485.969	11.542
BM07	6160931.48	2081424.959	19.522
2051611	6161974.95	2080779.78	16.81
BM08	6162490.544	2080441.441	14.298
HV-07	6162550.71	2080377.00	11.47
2051612	6162911.73	2080065.75	11.23
BM09	6163158.671	2079901.588	14.08
BM10	6163444.986	2079797.431	11.065
BM11	6163671.964	2079729.024	11.226
BM12	6165219.354	2078883.841	14.258

^a = Horizontal coordinates determined by GPS.

Table 2-2. Beach profile start point coordinates, elevations, and alignments.

Range	California State Plane Coordinates, Zone 6 (ft), NAD 83		Elevation, NGVD (ft)	Magnetic Heading
	Northing	Easting		
N1000	2082359.92	6159761.45	17.69	205
N0500	2081339.99	6161050.00	15.87	203.5
N0400'	2080691.70	6162106.26	14.32	197
NS0000	2080473.91	6162441.66	14.42	197
S0800'	2079969.71	6163054.98	14.33	197
S0500	2079711.68	6163931.78	varies	203
S1000	2078824.56	6165320.87	varies	203.5

3.0 2022 BEACH PROFILE SURVEY RESULTS

Nearshore beach profiles are performed quarterly along seven profiles at San Onofre (N1000, N0500, N0400', NS0000, S0800', S0500, and S1000). The 2022 beach profile surveys took place on 28 February, 08 June, 11 August, and 06 October, 2022. Figures 3-1 through 3-7 compare the four 2022 nearshore surveys with the November 2021 survey. As described in Section 2, offshore surveys extending to 60 ft water depth are also performed twice each year in spring and fall in order to represent the winter and summer beach profiles respectively. Figures 3-8 through 3-14 display a comparison of the beach profile surveys conducted on 08 June and 06 October 2022. Appendix A compares the summer and winter nearshore surveys for 2017-2022 in order to observe the seasonal fluctuations at SONGS in recent years.

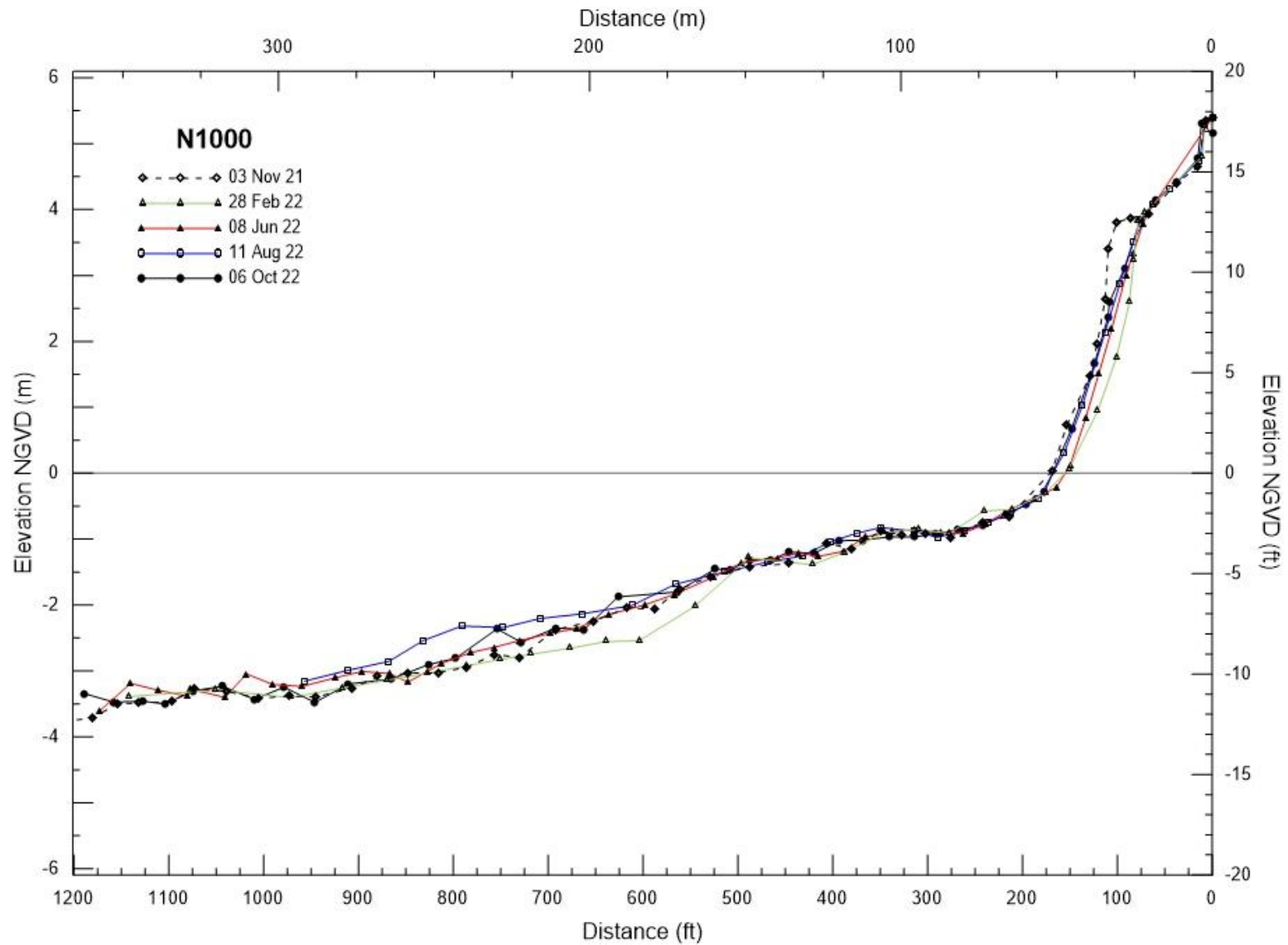


Figure 3-1. 2022 nearshore beach profile surveys of N1000.

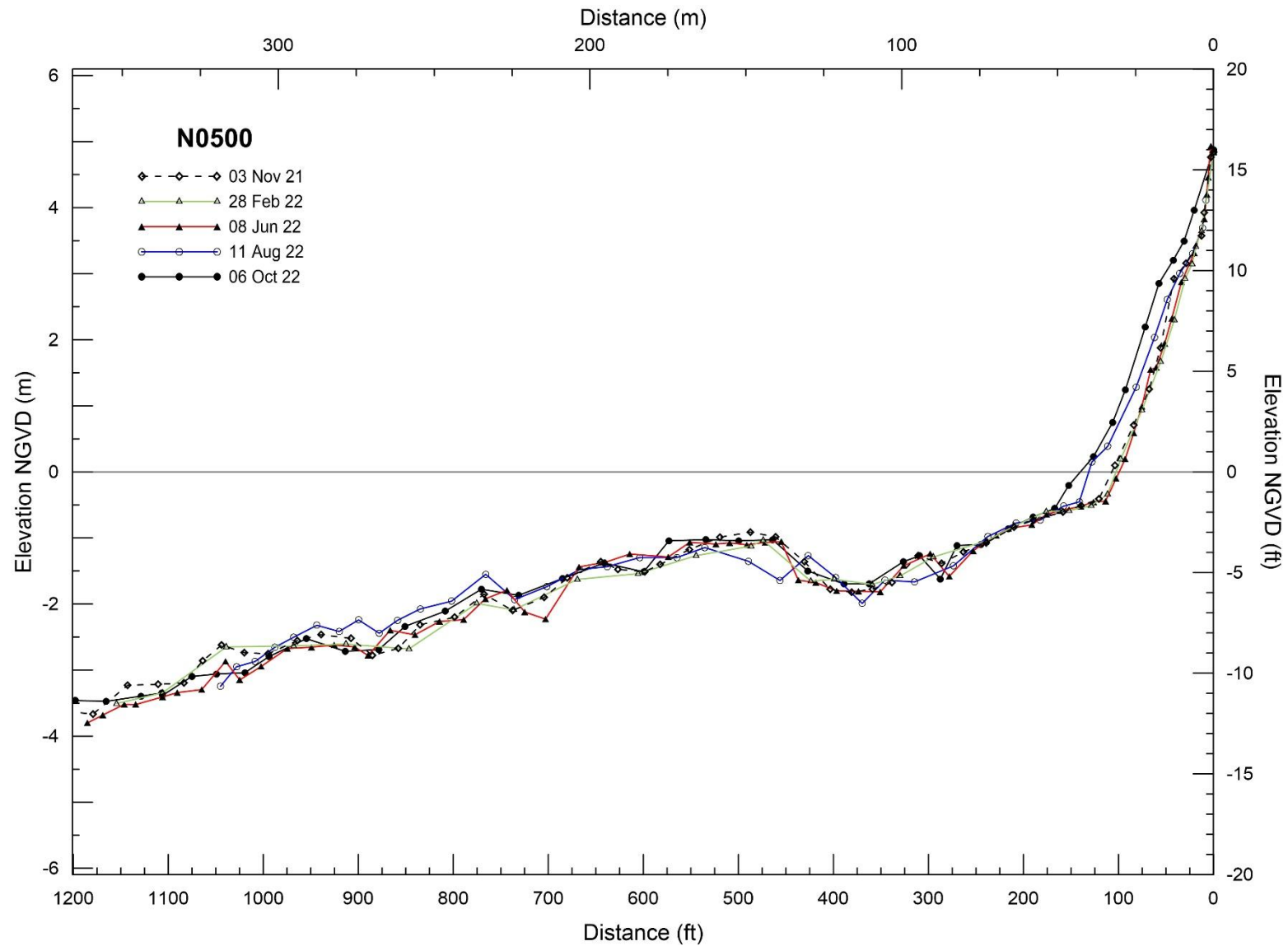


Figure 3-2. 2022 nearshore beach profile surveys of N0500.

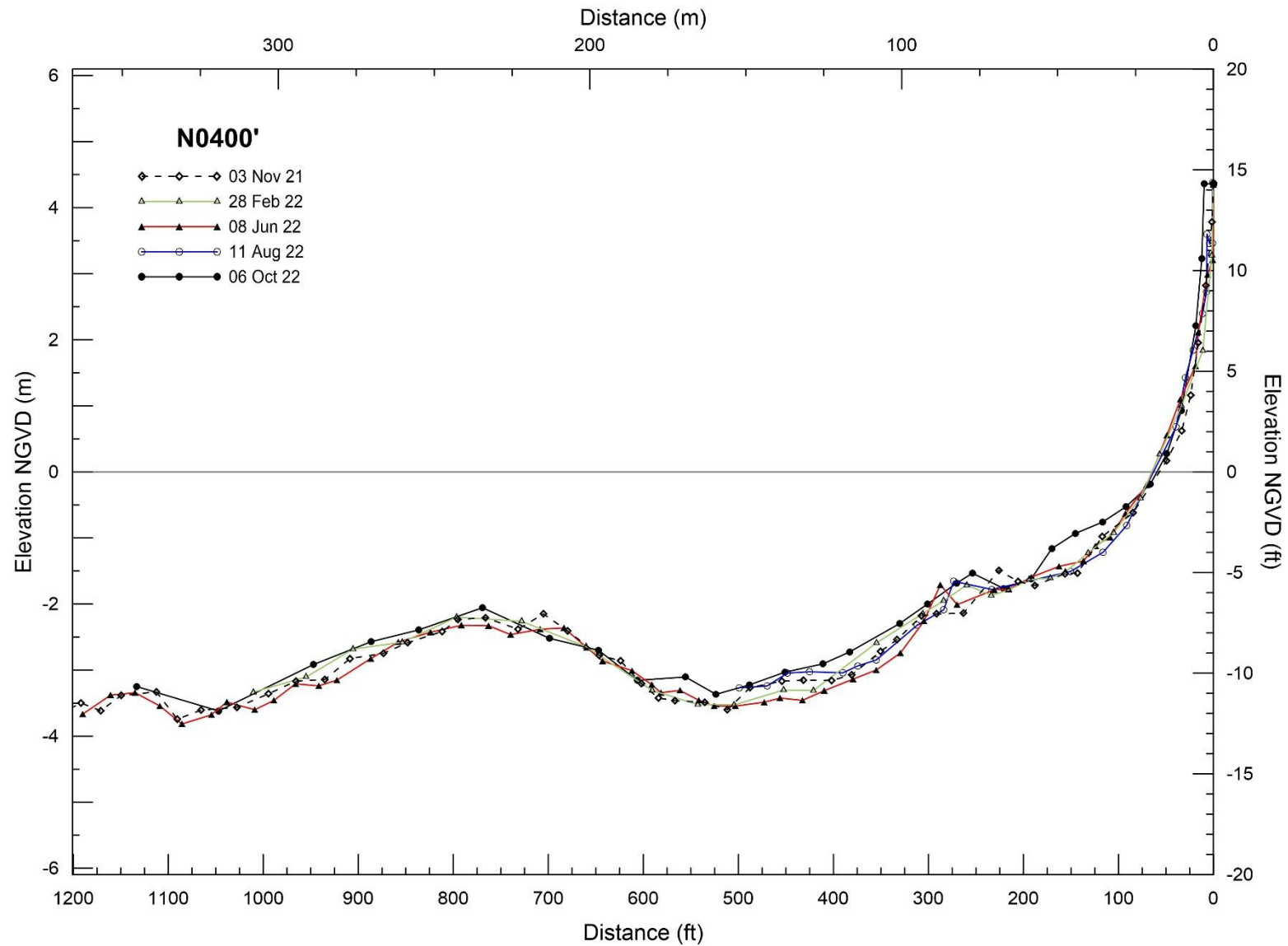


Figure 3-3. 2022 nearshore beach profile surveys of N0400'.

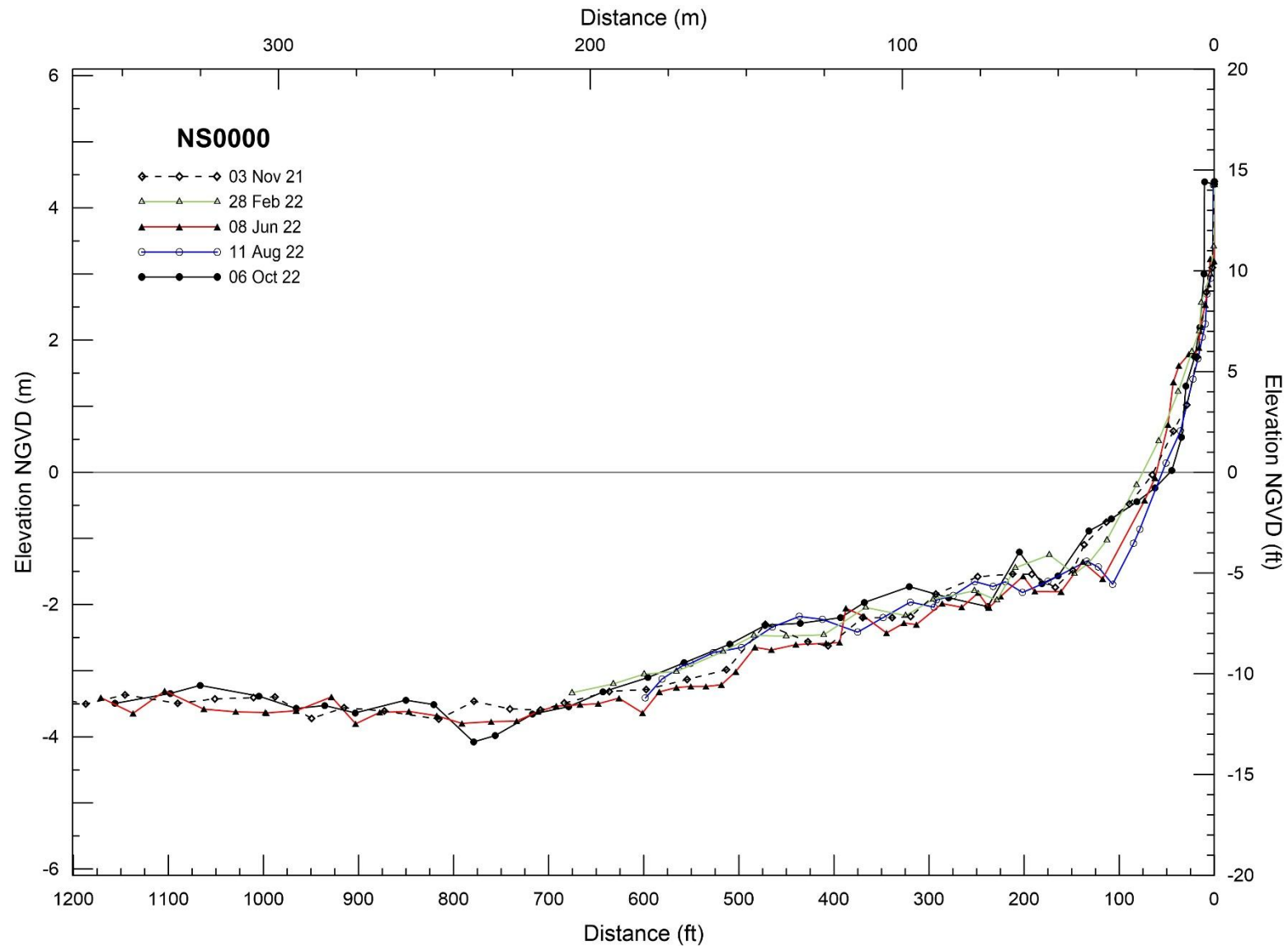


Figure 3-4. 2022 nearshore beach profile surveys of NS0000.

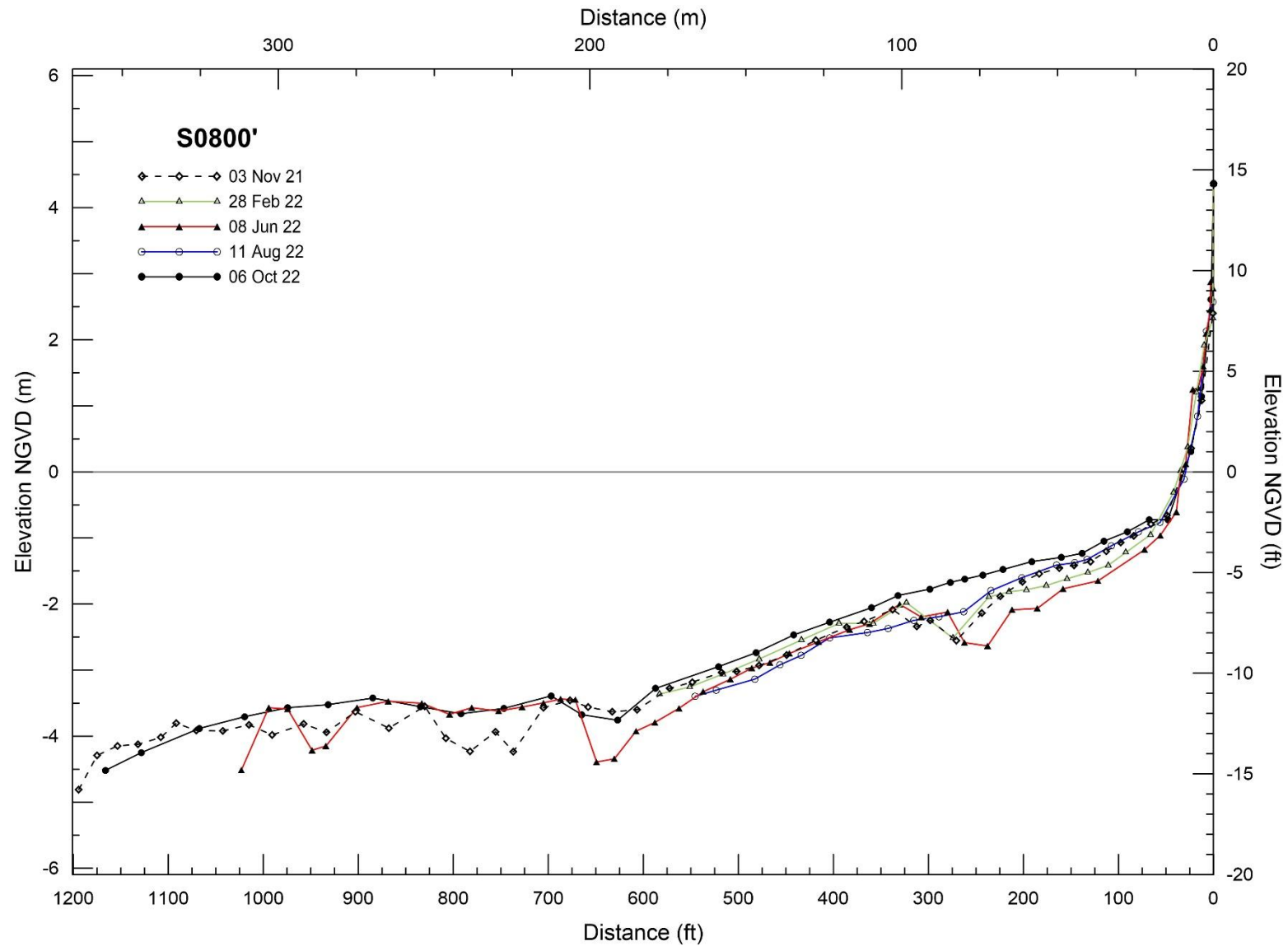


Figure 3-5. 2022 nearshore beach profile surveys of S0800'.

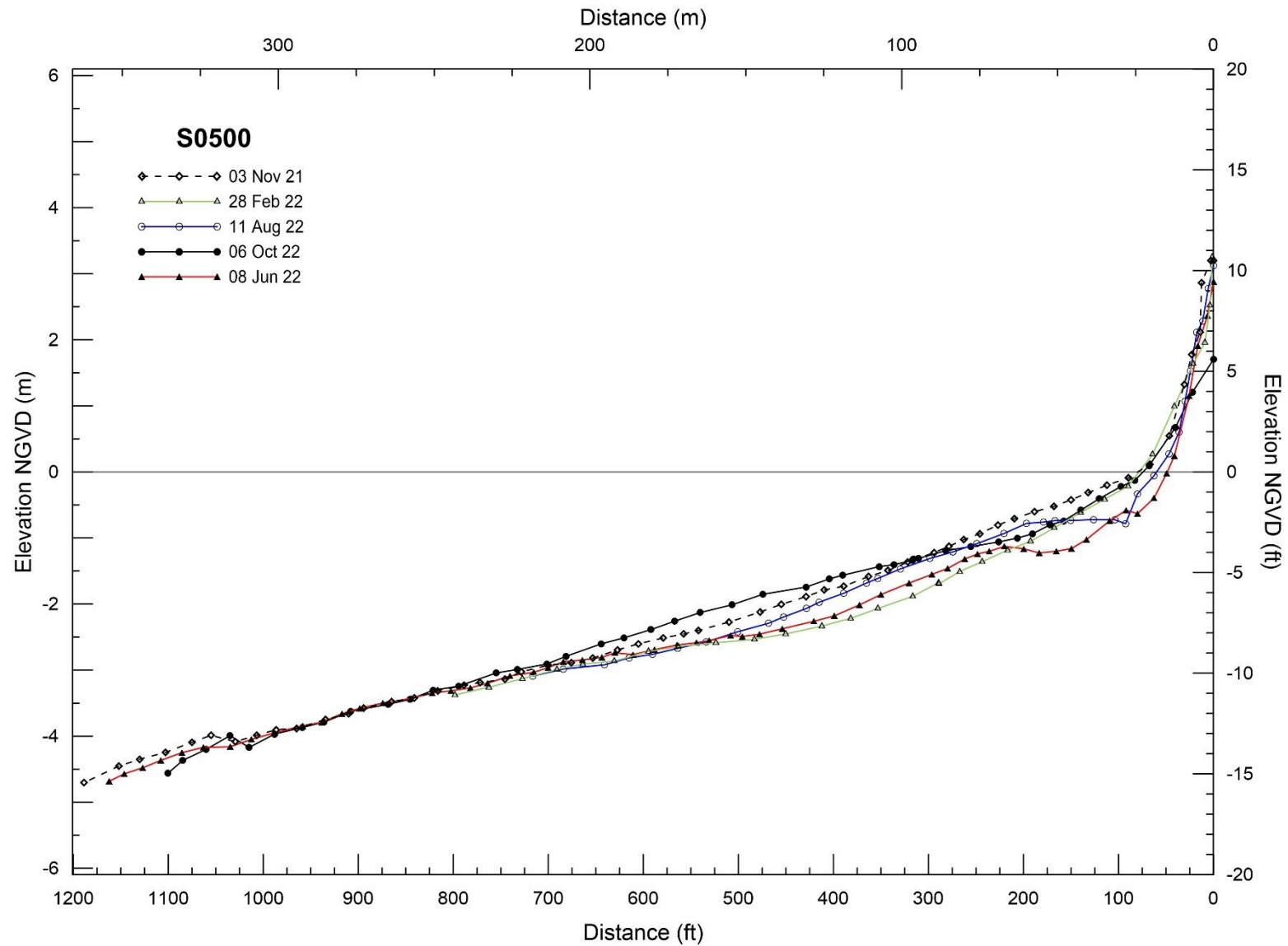


Figure 3-6. 2022 nearshore beach profile surveys of S0500.

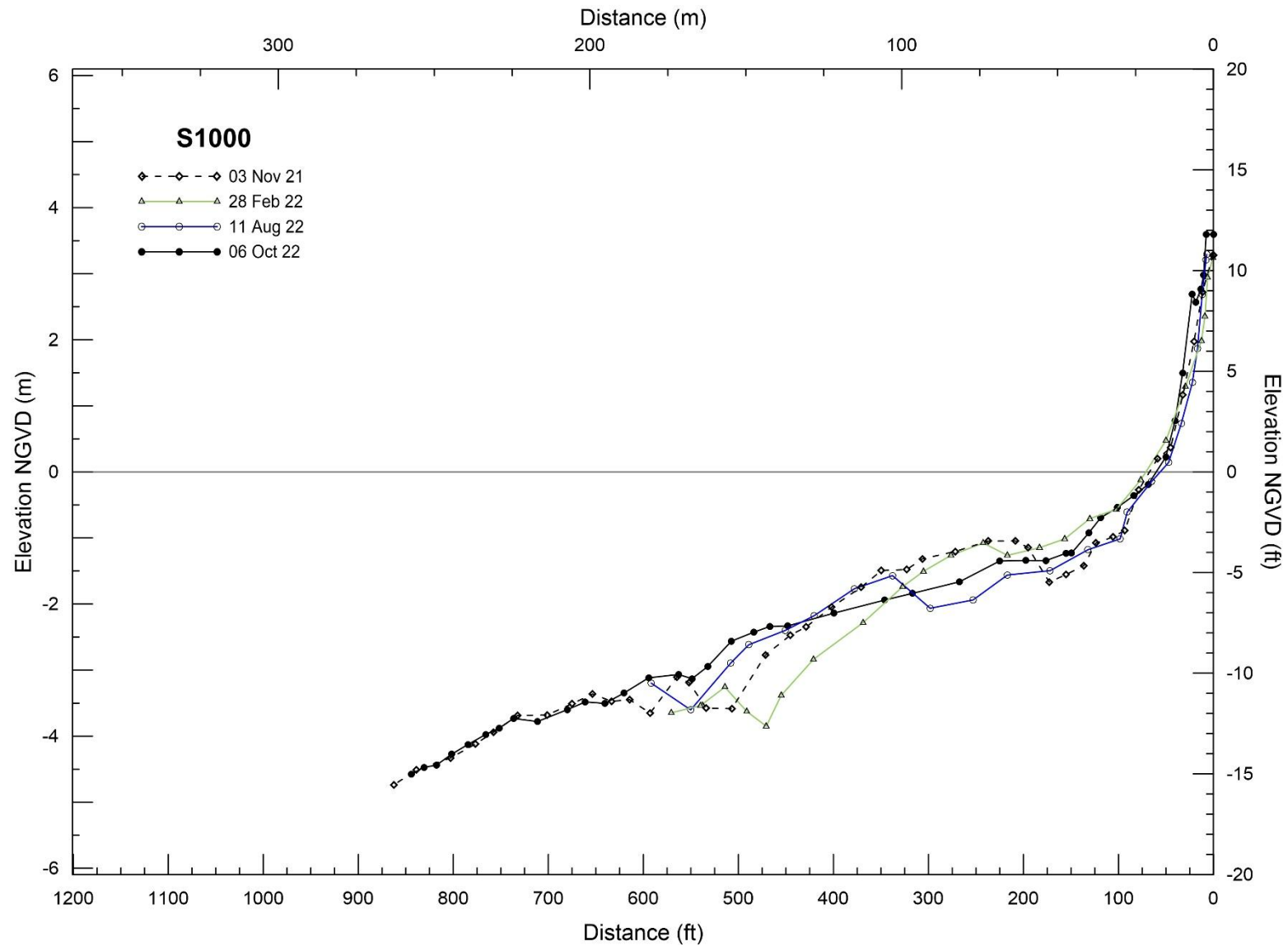


Figure 3-7. 2022 nearshore beach profile surveys of S1000.

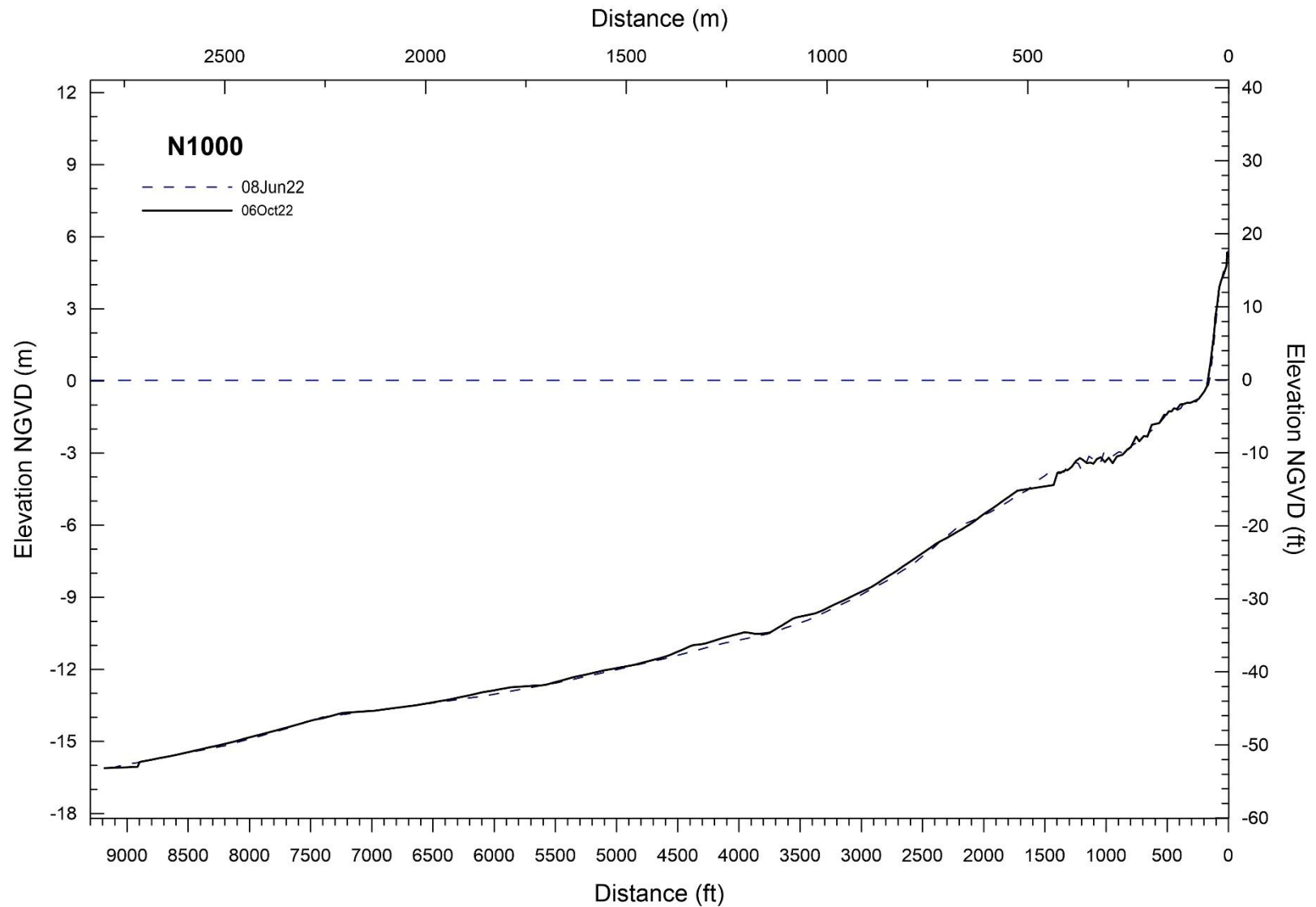


Figure 3-8. 2022 offshore beach profile surveys of N1000.

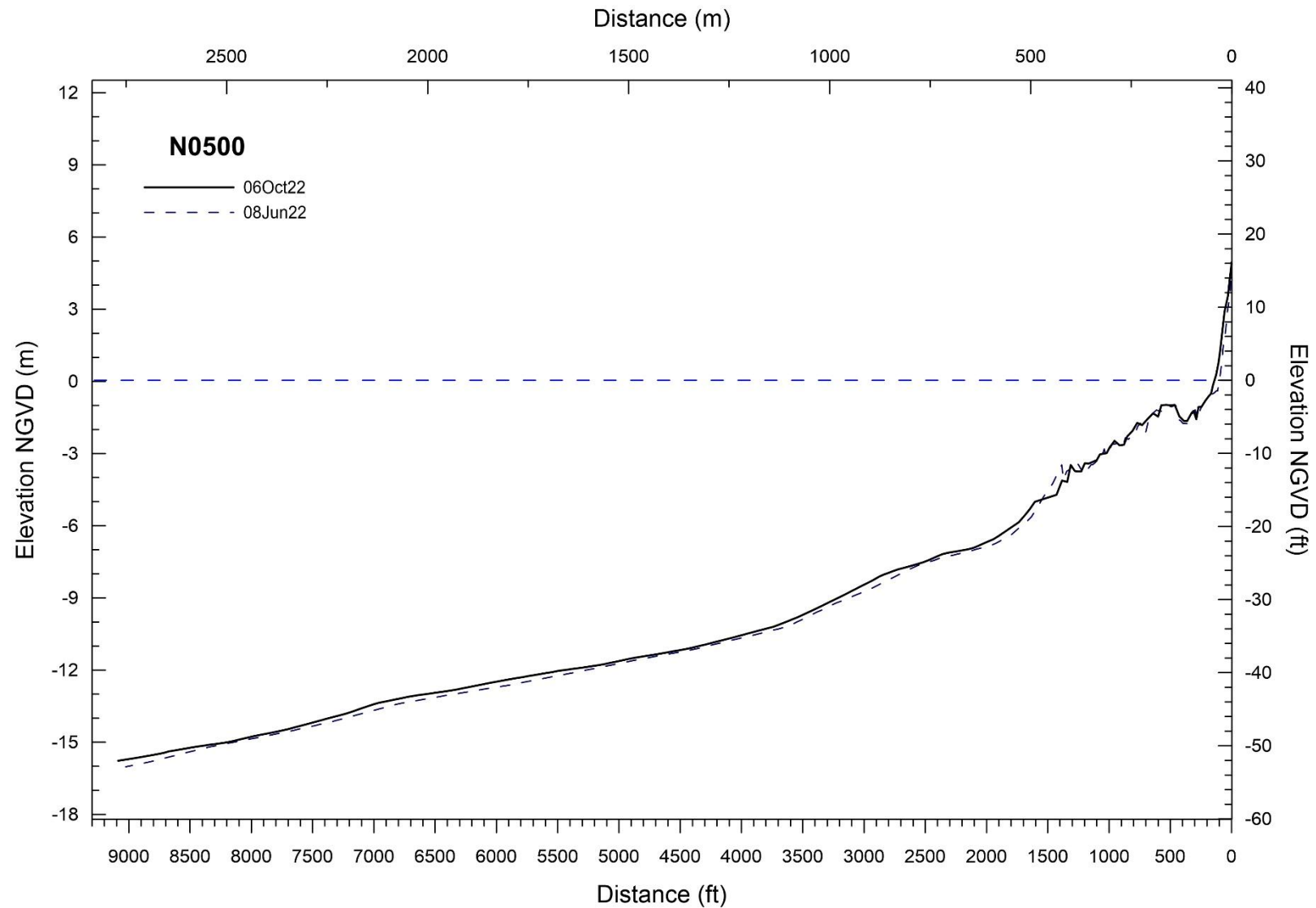


Figure 3-9. 2022 offshore beach profile surveys of N0500.

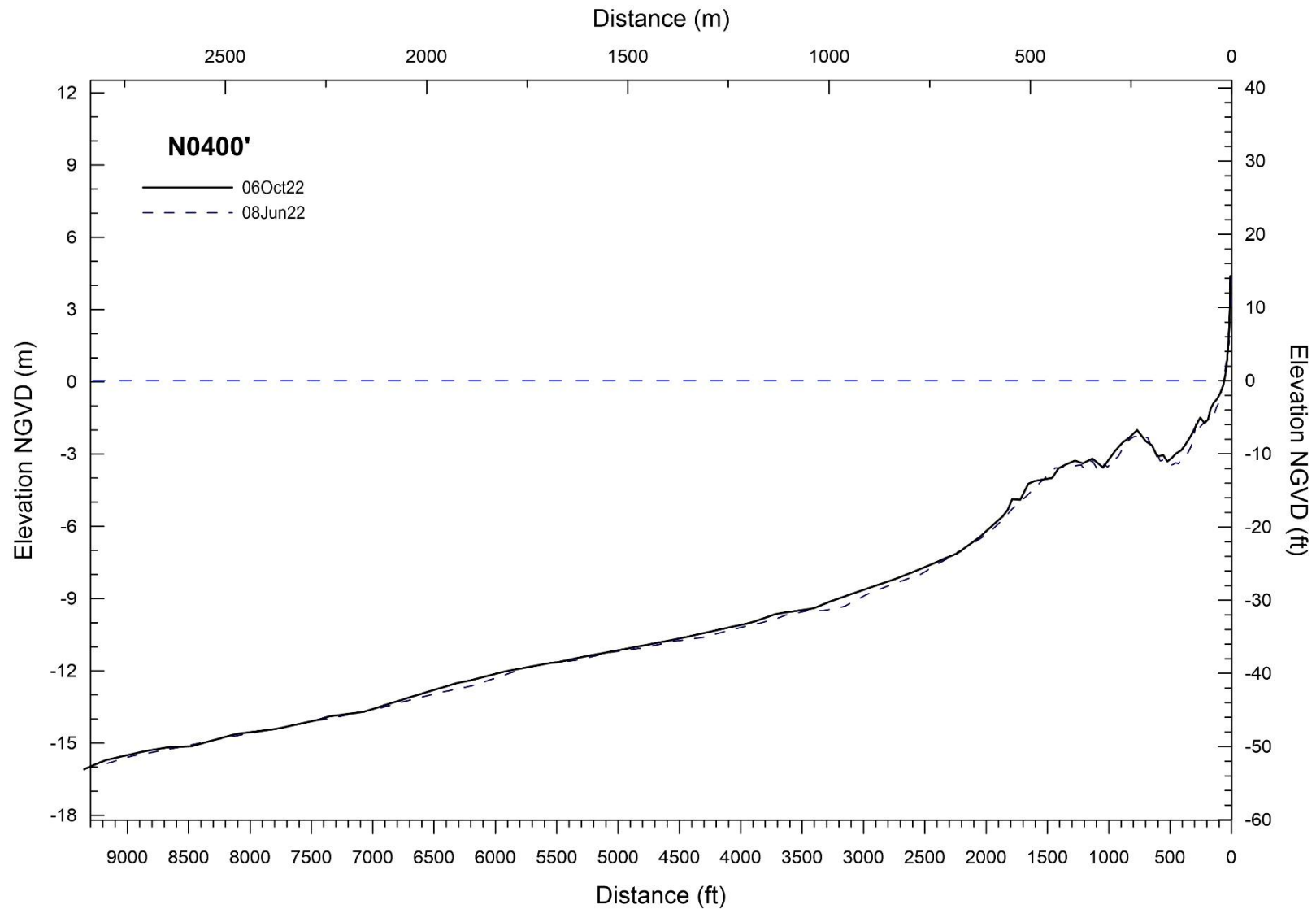


Figure 3-10. 2022 offshore beach profile surveys of N0400'.

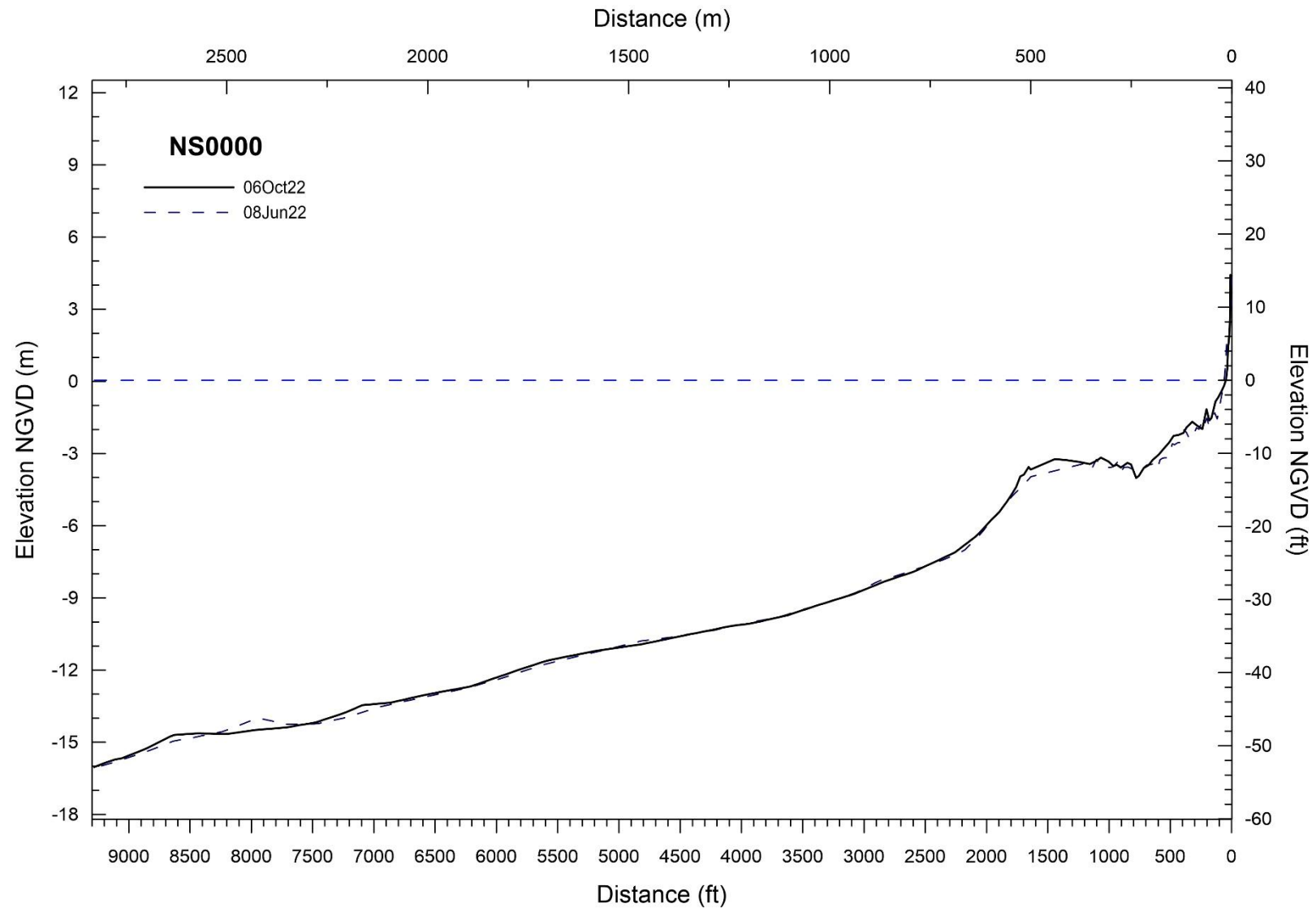


Figure 3-11. 2022 offshore beach profile surveys of NS0000.

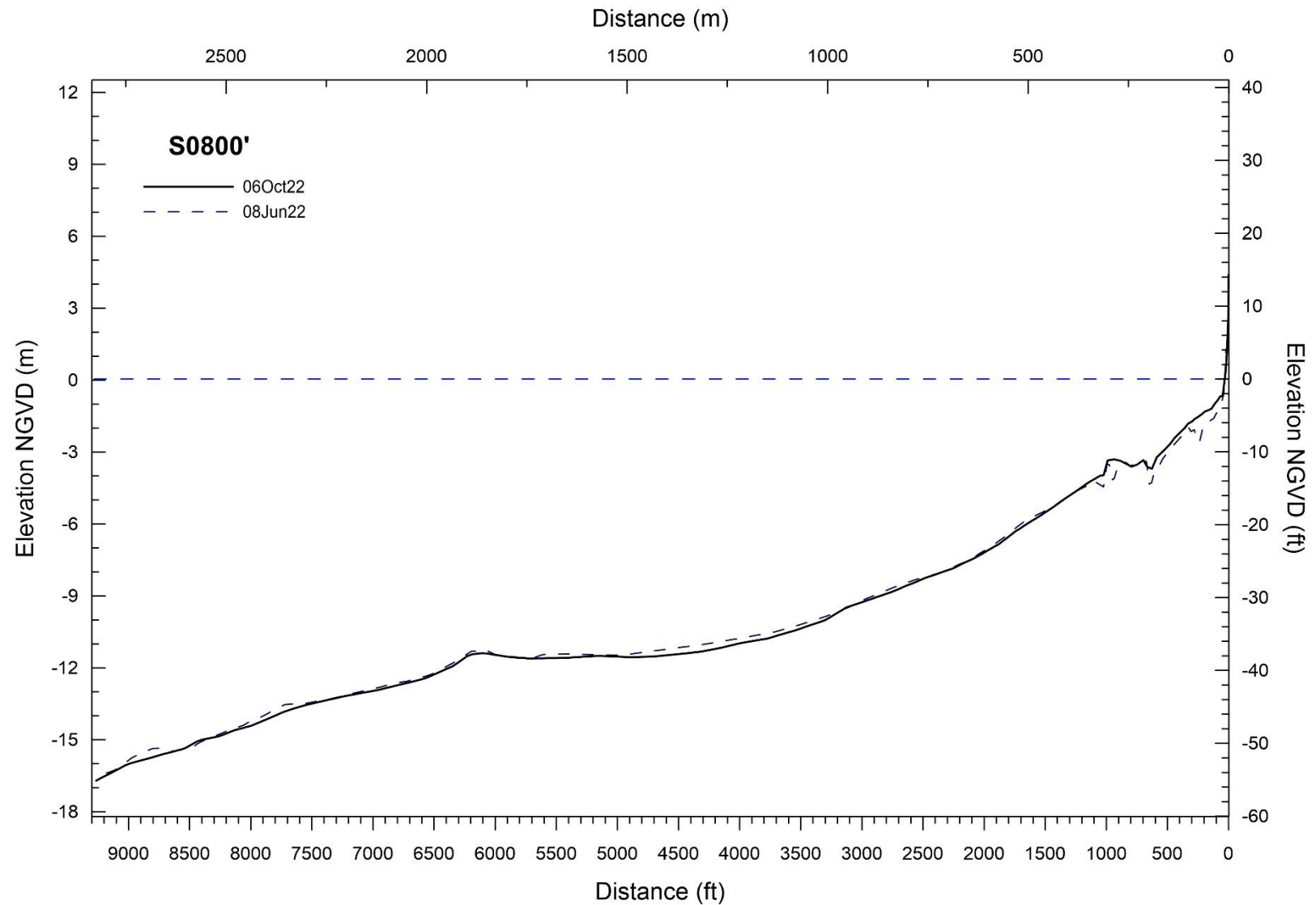


Figure 3-12. 2022 offshore beach profile surveys of S0800'.

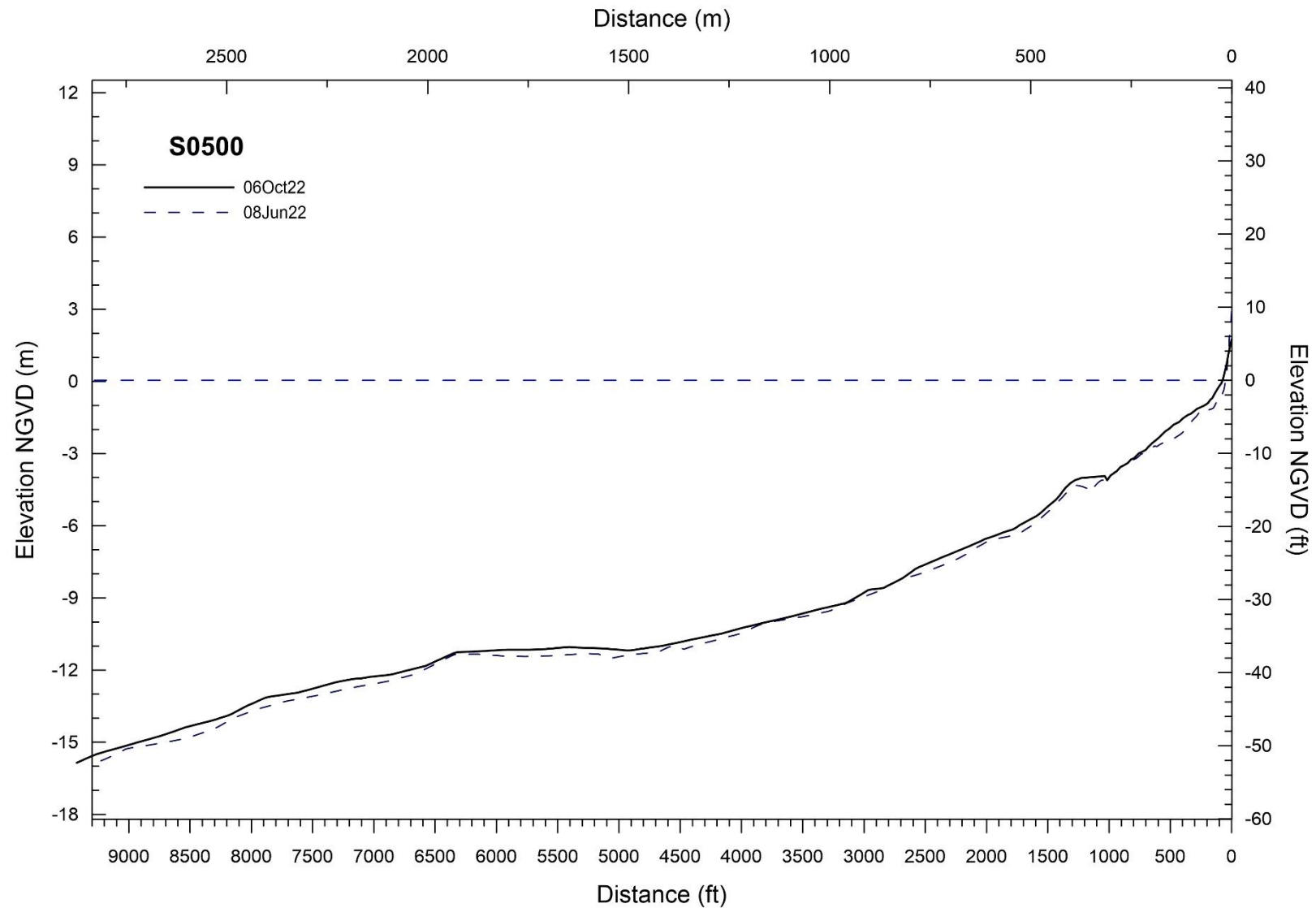


Figure 3-13. 2022 offshore beach profile surveys of S0500.

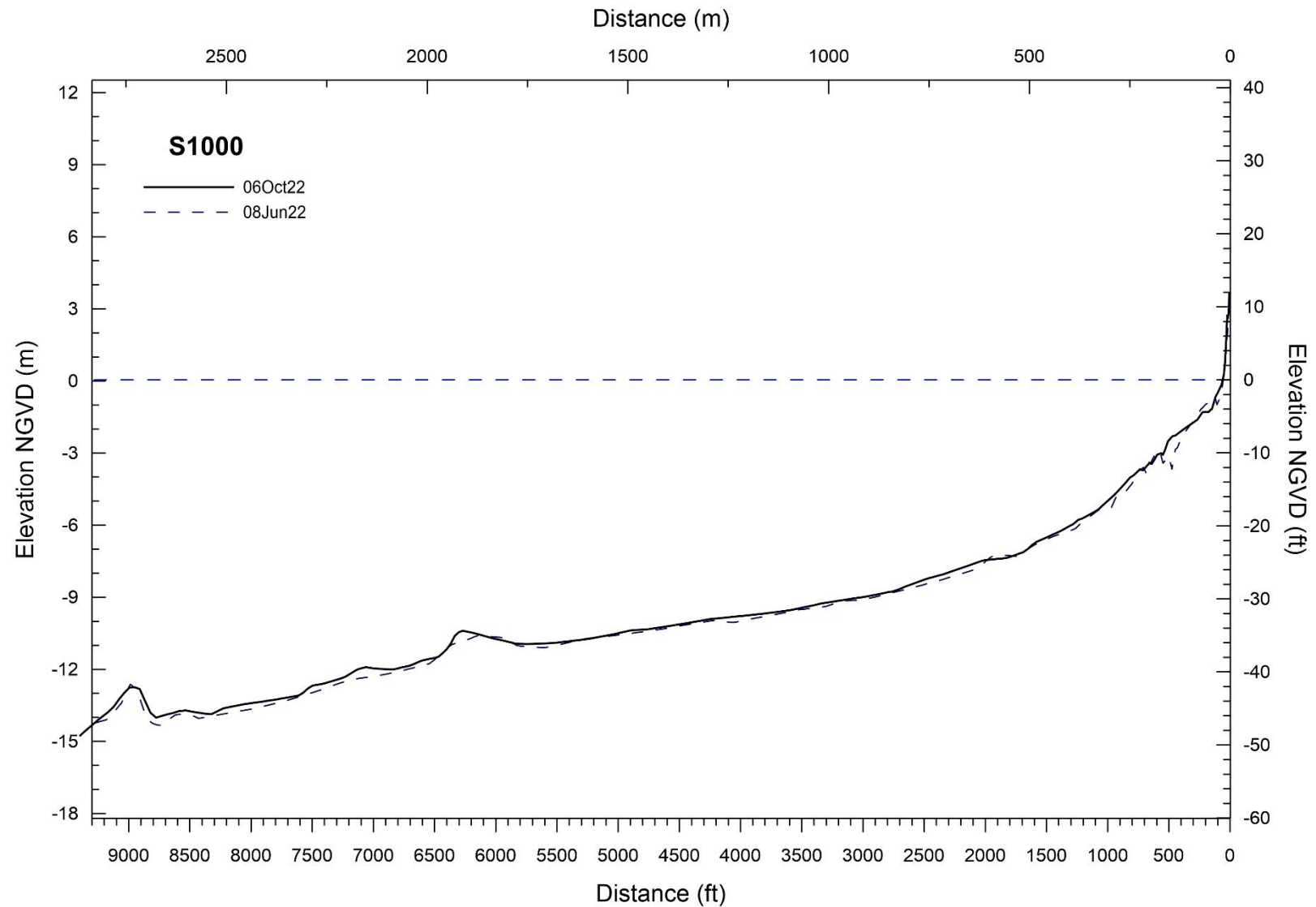


Figure 3-14. 2022 offshore beach profile surveys of S1000.

4.0 BEACH PROFILE CHARACTERISTICS

The beach profiles at San Onofre have much in common with other typical Southern California beaches (Figure 4-1). The characteristics of San Onofre beaches are discussed in detail in *Coastal Analysis for End-State Planning of SONGS, Phase 1* (Elwany et al., 2016). A brief description is given below.

The beaches at San Onofre consist of a relatively thin veneer of medium to coarse sand backed by a sea cliff of varying height. In most places, cobble and bedrock underlay the beach sands at various depths. These depths can vary from zero, where the sand cover is stripped, to several meters where there is an adequate supply of sand to cover the bedrock or the cobble layer.

The subaerial portion of the beach profile extends from the cliff face (or sea wall) to the mean water line. It is distinguished by a narrow to medium width, relatively flat berm, and a moderately steep beach face slope. The berm height and the slope of the beach face both depend on sand grain size and wave climate. The subaerial beach width is defined as the distance from the cliff face (or seawall) to 0 ft NGVD.

The beach berm may contain one or more storm scarps. These are erosional features resulting from large waves that remove sand and cobbles from the beach face and transport them offshore. This represents the normal summer to winter erosion sequence that progressively narrows the berm width and flattens the beach slope. The sand moved offshore often forms into one or more bars, generally in depths less than 10 ft, but seaward of the low tide terrace. The bars act as reservoirs for the sand that is returned to the shore face during the winter to summer accretion phase, coinciding with milder seasonal wave conditions.

The beach berm both in front of, and north and south of SONGS, contain a large amount of cobbles in comparison to many Southern California beaches. These cobble layers are typically covered with sand during the summer and become exposed during winter due to the changing wave climate. The thickness and position of this cobble berm also changes throughout the year and over time (Appendix B pictures).

Berm heights at San Onofre average about 10 ft , and foreshore slopes are about 1:7, vertical to horizontal, or about 8°. Both are fairly uniform longshore. The lack of a winter berm has been common at the sea wall in front of SONGS during the past few years. Lack of sand and occasional high wave activity have resulted in some displacement and settling of the rock riprap, which provides toe protection to the SONGS beach access walkway retaining wall.

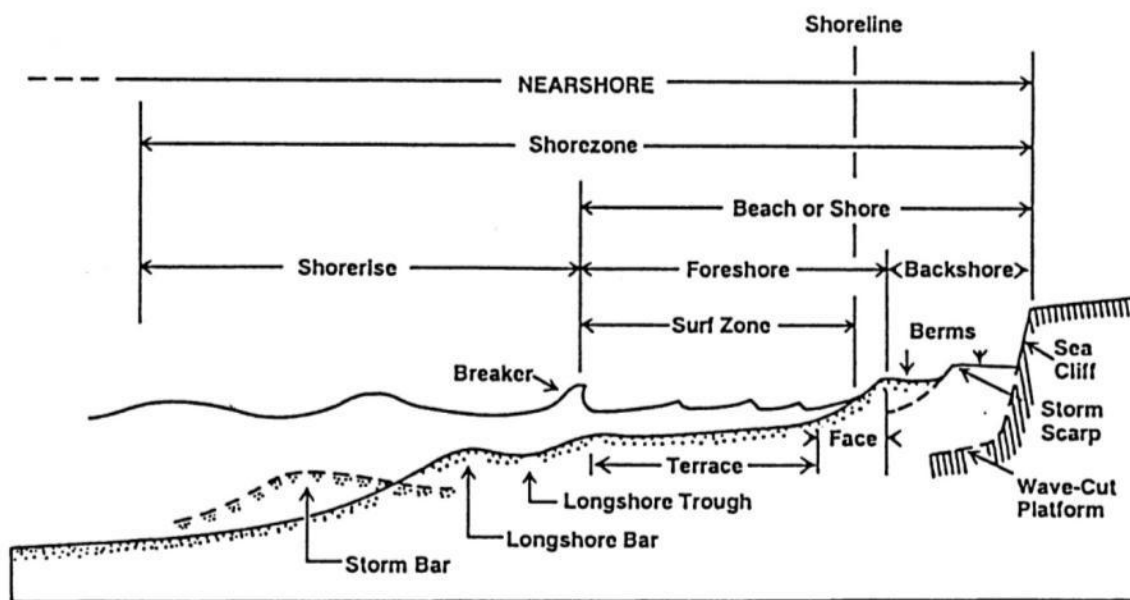


Figure 4-1. Typical Southern California beach profile (Inman, 1980).

5.0 BEACH WIDTH CHANGES FROM 2017 THROUGH 2022

Beach width changes from 2017 through 2022 at seven profiles from N1000 to S1000 are illustrated in Figures 5-1a and 5-1b. The beach width for each survey was computed as the distance from the respective profile's starting point to the intersection of the beach and 0 ft NGVD. Table 5-1 summarizes the beach width observations at each profile for the 24 surveys conducted between March 2017 and October 2022.

Table 5-2 gives the yearly mean beach widths for each profile during this time period. Overall, the northern profiles (N1000 and N0500) consistently display the widest beaches at San Onofre, followed by the profiles south of the power plant (S0500 and S1000). The profiles directly in front of SONGS regularly display the narrowest beaches along all surveyed profiles. The seasonal cycles of these profiles are discussed further in Section 6.

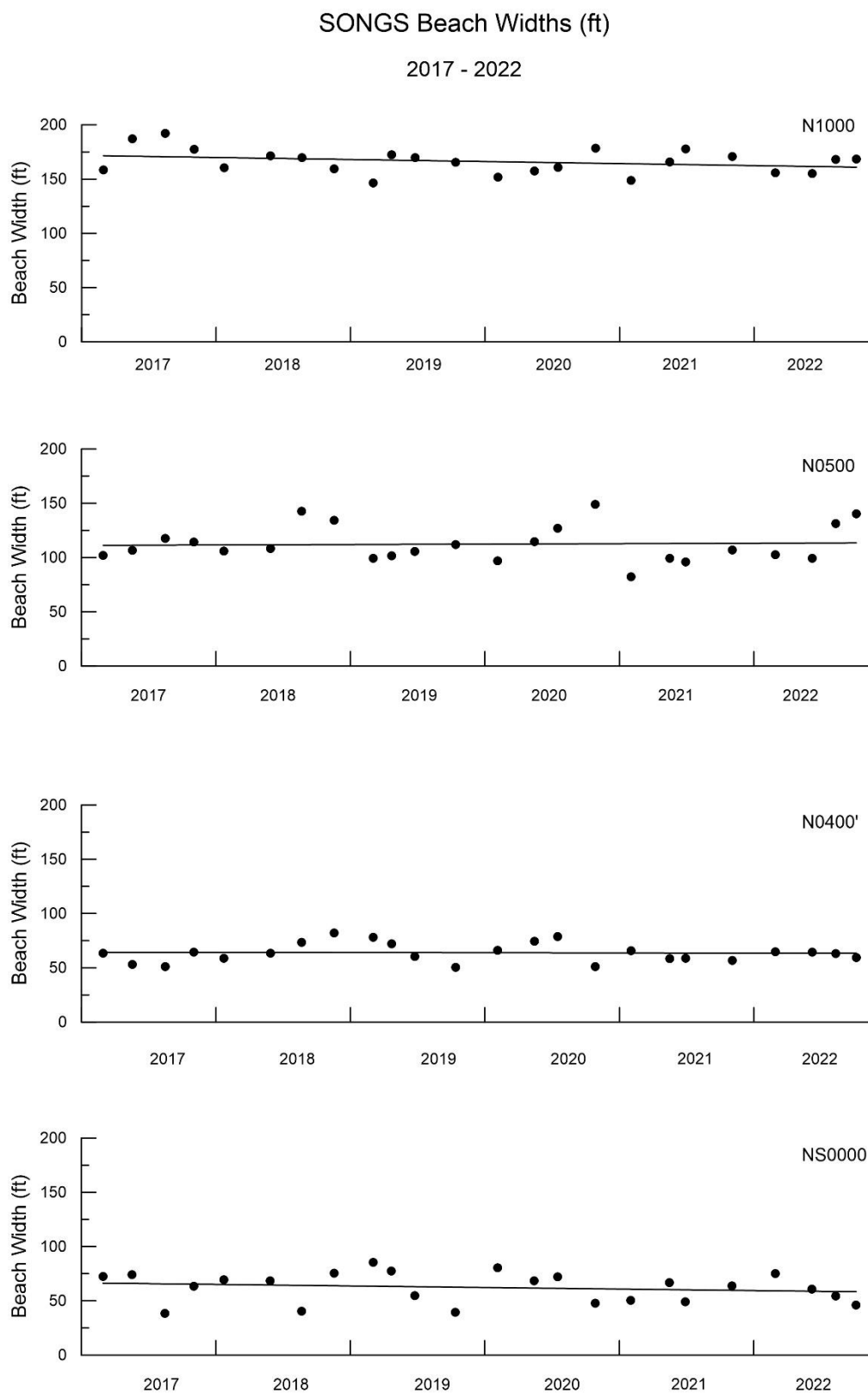


Figure 5-1a. Beach width changes at San Onofre at N1000 – NS0000.

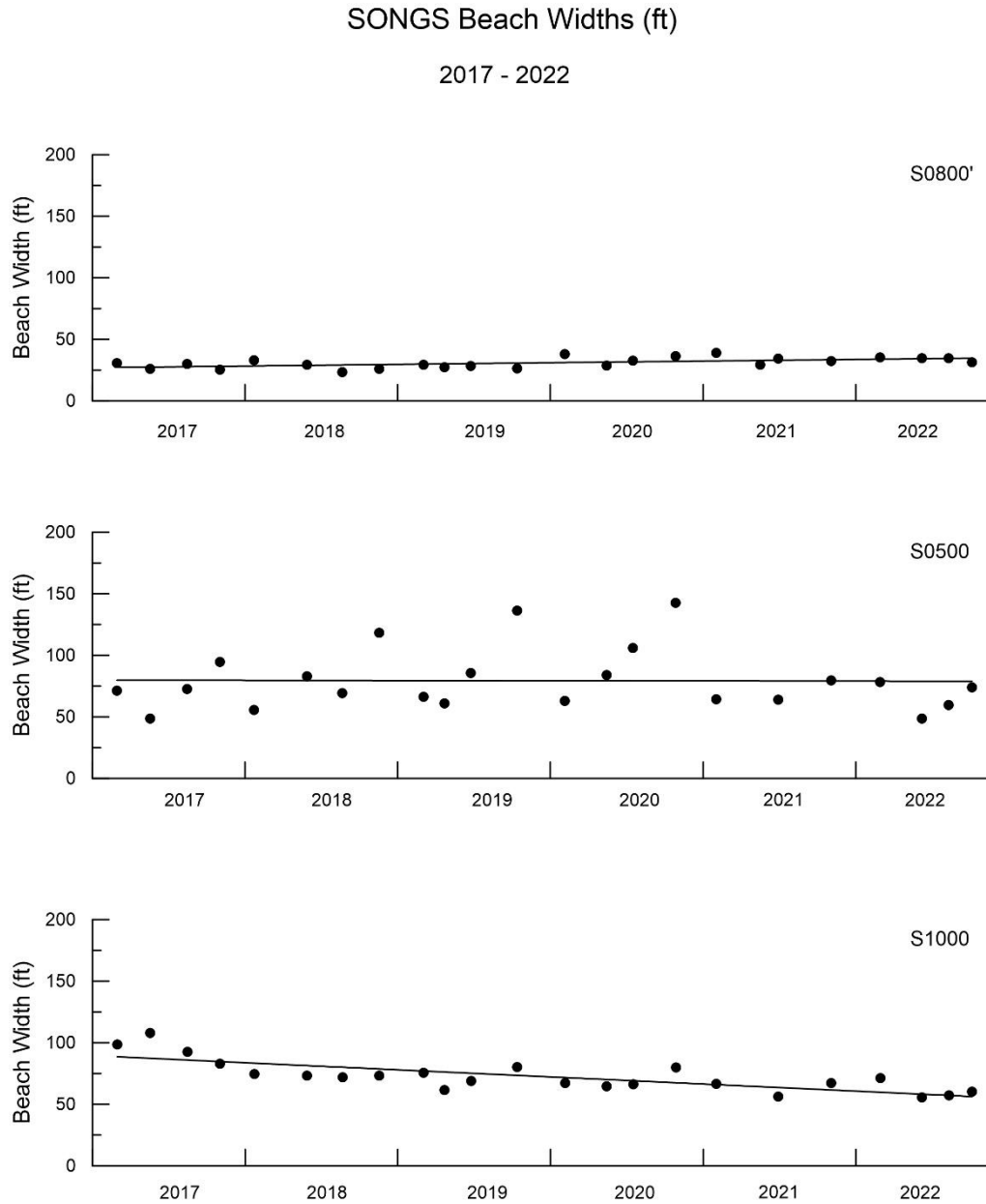


Figure 5-1b. Beach width changes at San Onofre at S0800' – S1000.

Table 5-1. Beach widths (ft) at San Onofre profiles (2017-2022).

Survey Date	Profile						
	N1000	N0500	N0400'	NS0000	S0800'	S0500	S1000
01Mar17	158.6	102.0	63.4	72.4	30.8	71.4	98.6
19May17	187.0	106.5	53.0	74.0	26.1	48.6	107.8
16Aug17	192.1	117.7	51.2	38.4	29.9	72.7	92.7
02Nov17	177.4	114.3	64.4	63.6	25.5	94.6	82.8
23Jan18	160.4	106.1	58.8	69.5	33.0	55.7	74.6
29May18	171.4	108.3	63.5	68.4	29.3	83.1	73.3
22Aug18	169.8	142.6	73.6	40.6	23.4	69.2	72.1
18Nov18	159.3	134.4	82.0	75.5	26.0	118.2	73.4
04Mar19	146.3	99.2	78.1	85.5	29.5	66.3	75.5
23Apr19	172.3	101.8	72.3	77.4	27.5	61.0	61.6
25Jun19	169.9	105.7	60.6	54.9	28.4	85.4	69.0
14Oct19	165.3	112.0	50.4	39.5	26.5	136.2	80.3
05Feb20	151.9	96.9	66.3	80.4	38.2	62.8	67.1
15May20	157.3	114.6	74.4	68.5	28.8	83.9	64.5
17Jul20	160.7	127.2	78.7	72.3	32.9	105.9	66.3
27Oct20	178.4	149.0	51.0	47.8	36.4	142.7	79.7
01Feb21	148.9	82.3	65.9	50.6	39.0	64.3	66.5
17May21	165.8	99.4	58.6	66.9	29.5	N/A	N/A
29Jun21	177.9	96.0	58.9	49.1	34.4	63.9	56.1
03Nov21	170.9	107.0	56.9	63.9	32.5	79.5	67.3
28Feb22	155.6	102.6	64.9	75.2	35.2	78.3	71.1
08Jun22	155.0	99.2	64.6	60.8	34.5	48.6	55.5
11Aug22	168.1	131.3	63.1	54.6	34.5	59.8	57.1
06Oct22	168.3	140.1	59.5	46.3	31.2	74.1	60.2
Max	192.1	149.0	82.0	85.5	39.0	142.7	107.8
Min	146.3	82.3	50.4	38.4	23.4	48.6	55.5
Mean	166.2	112.3	63.9	62.3	31.0	79.4	72.7
Std. Dev	11.5	16.8	8.9	13.8	4.2	25.3	13.2

Table 5-2. Yearly mean beach widths (ft).

Survey Year	Profile						
	N1000	N0500	N0400'	NS0000	S0800'	S0500	S1000
2017	178.8	110.1	58.0	62.1	28.1	71.8	95.5
2018	165.2	122.8	69.5	63.5	27.9	81.5	73.3
2019	163.5	104.7	65.3	64.3	28.0	87.2	71.6
2020	162.1	121.9	67.6	67.3	34.1	98.8	69.4
2021	165.9	96.2	60.1	57.6	33.9	N/A	N/A
2022	161.76	118.30	63.00	59.25	33.87	65.18	60.96
Mean	166.2	112.3	63.9	62.3	31.0	80.9	74.2

6.0 ESTIMATION OF SHORELINE TRENDS AND SEASONAL CYCLES

The shoreline changes at various profiles consist of two components. The first is the seasonal cycle, which is superimposed on the second component: the long-term trend in the beach width. The long-term trends are due to the processes that affect beach width on longer time scales, such as changing wave climates or sand supply changes.

The beach profile data from March 2017 through October 2022 have been used to separate trends in shoreline changes from the yearly seasonal cycle in order to obtain quantitative estimates for the two parameters. The shoreline data from the 24 surveys were regressed against date, and a straight line was fitted to the entire data set (Figures 5-1a and 5-1b). The slope of this line gives the trend and rate (ft/year) of change of the beach width.

These regression values were then used to determine the seasonal shoreline changes. The expected beach width value obtained via linear regression was subtracted from the measured values for each survey date between March 2017 and October 2022. By removing this slope and “detrending” the measured data, the seasonal shoreline cycle for each SONGS profile was determined (Figures 6-1a and 6-1b). The estimate of yearly beach width changes at San Onofre are presented in Table 6-1. These values were determined by taking the difference between the minimum and maximum beach widths for each year. The average annual fluctuation at San Onofre is about 27.54 ft.

Seasonal trends were also evaluated by examining average beach widths by time of year. Table 6-2 displays the average beach width during winter and summer for each year between 2017 and 2022. The winter values were determined by averaging the beach widths measured between February and June of that year, while the summer values averaged beach widths measured between August and October. Table 6-3 shows the overall mean winter and summer beach widths between the years 2017-2022, with summer beaches being on average wider than the winter beaches at SONGS.

In a typical year, southern Californian beaches are widest in the fall, before high-energy winter storms move sediment offshore. Interestingly, the seasonal cycle at NS0000, and to a lesser extent N0400' and S1000, seems to be reversed, in that the beaches are narrower toward the end of summer and widen throughout the winter, while the seasonal cycle at profile S0800' remains relatively constant. This pattern is reflected graphically in Figure 6-1 and quantitatively in Tables 6-2 and 6-3.

Table 6-4 gives the estimates of the observed long-term trends in beach width for 2017 through 2022. Statistical tests were carried out on trends and p-values are presented in Table 6-4. The trend is significantly different from zero on those ranges with p-value < 0.05. The maximum observed trend is an erosion rate of -5.76ft/year along profile S1000. The only other profile with a statistically significant rate of change during this time period is S0800', which displays an accretion rate of 1.35 ft/yr.

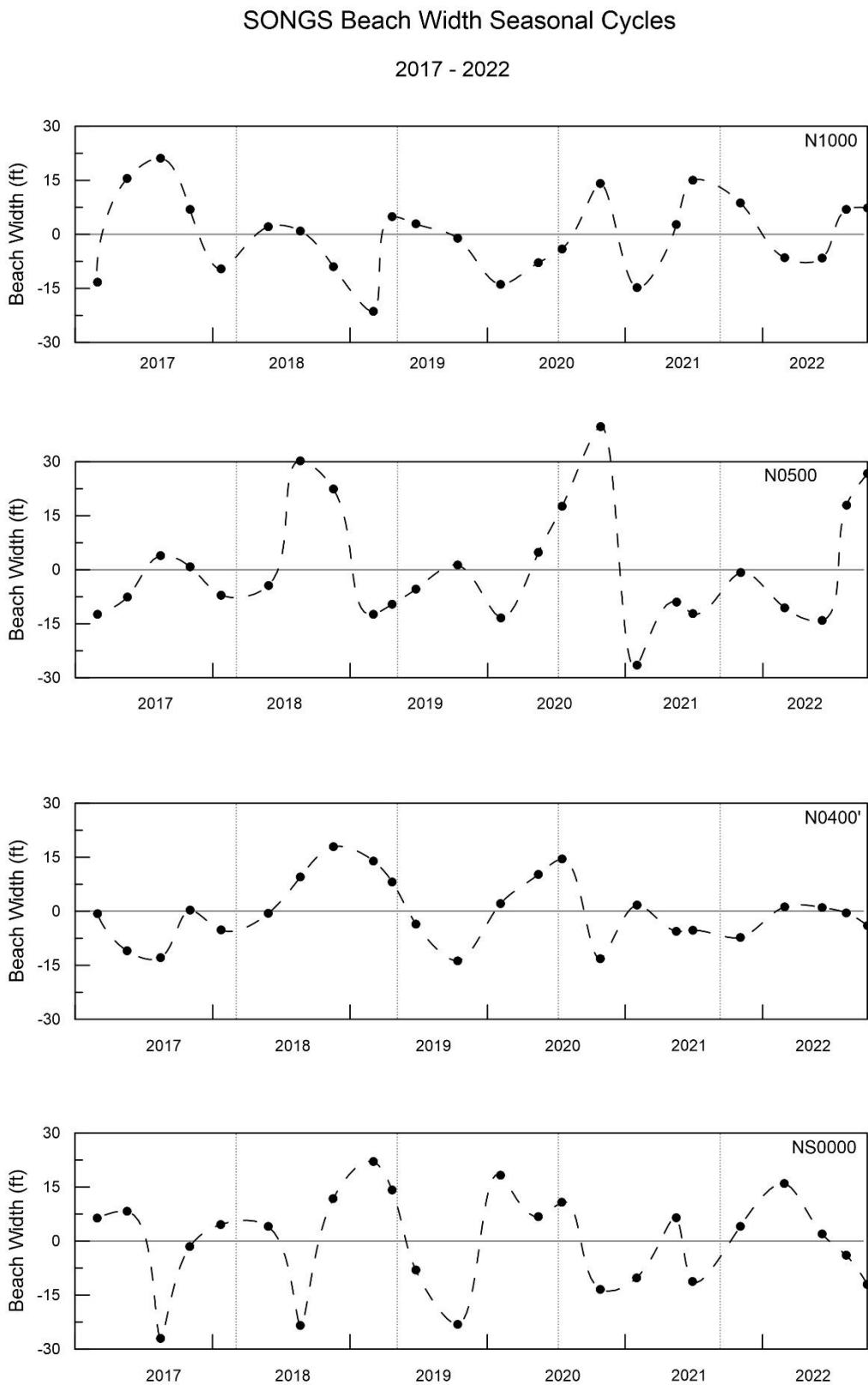


Figure 6-1a. SONGS beach width seasonal cycles at N1000 – NS0000 (2017-2022).

SONGS Beach Width Seasonal Cycles

2017 - 2022

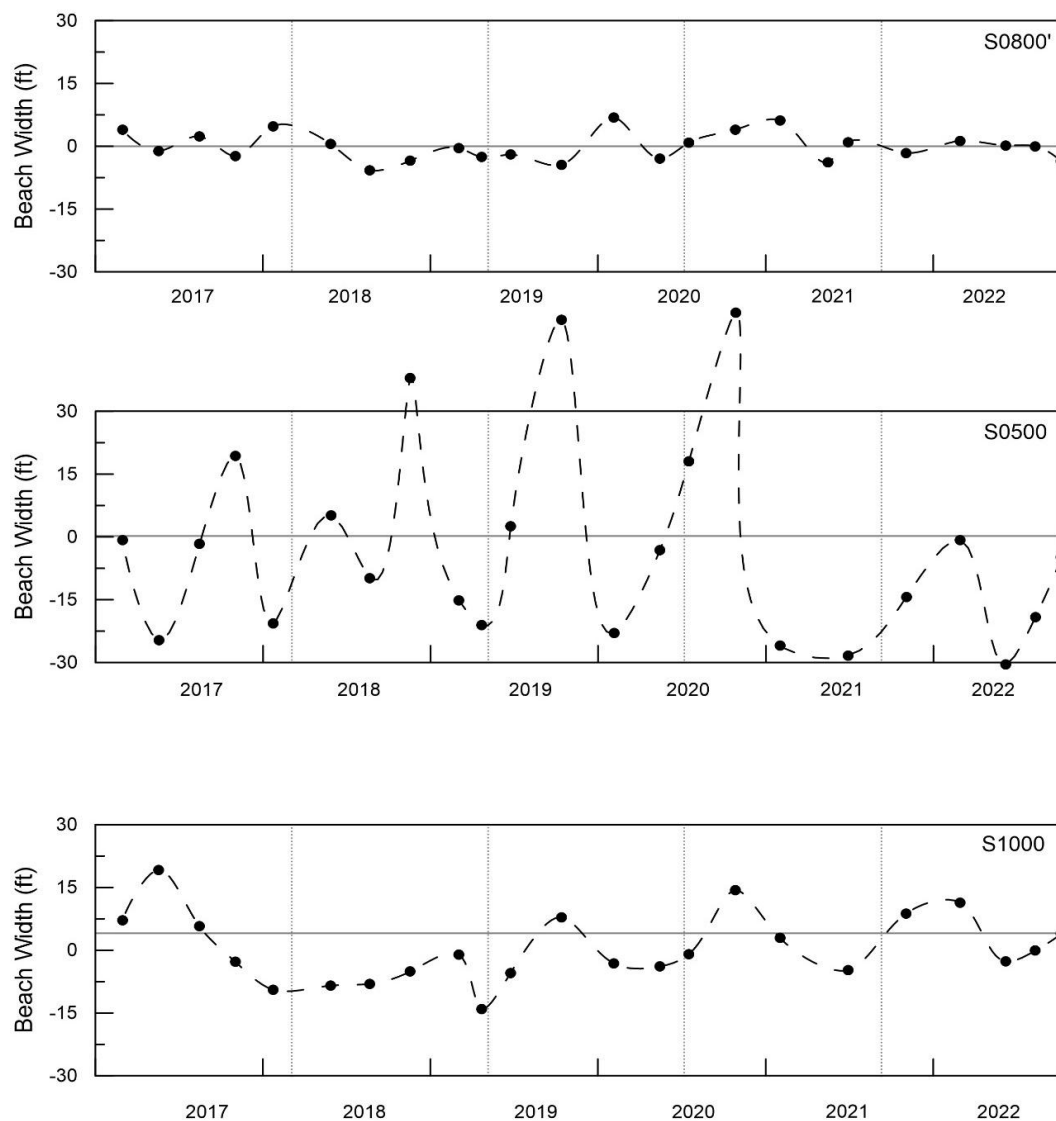


Figure 6-1b. SONGS beach width seasonal cycles at S0800' – S1000 (2017-2022).

Table 6-1. Annual beach width changes at San Onofre.

Profile	Annual Beach Width Change (ft)						Mean
	2017	2018	2019	2020	2021	2022	
N1000	35.30	12.41	26.51	29.33	29.85	13.92	24.03
N0500	13.88	34.19	10.37	49.18	25.79	40.81	31.19
N0400'	13.24	21.41	29.06	28.23	8.97	5.30	17.67
NS0000	35.52	34.93	45.84	32.45	17.67	28.00	32.16
S0800'	6.27	10.46	3.98	9.76	9.97	4.86	11.52
S0500	40.20	51.91	68.99	70.61	N/A	29.67	56.35
S1000	21.46	5.10	22.35	18.68	N/A	14.10	19.86

Table 6-2. Average beach widths (ft) by season at San Onofre.

Profile	2017		2018		2019		2020		2021		2022	
	W ^a	S ^b	W ^a	S ^b	W ^a	S ^b	W ^a	S ^b	W ^a	S ^b	W ^a	S ^b
N1000	172.8	184.7	165.9	164.6	159.3	167.6	154.6	169.5	157.33	174.37	155.29	168.22
N0500	104.2	116.0	107.2	138.5	100.5	108.9	105.8	138.1	90.85	101.53	100.88	135.71
N0400'	58.2	57.8	61.2	77.8	75.2	55.5	70.3	64.9	62.24	57.91	64.73	61.26
NS0000	73.2	51.0	69.0	58.1	81.4	47.2	74.5	60.1	58.75	56.49	68.01	50.48
S0800'	28.4	27.7	31.1	24.7	28.5	27.4	33.5	34.7	34.27	33.44	34.88	32.86
S0500	60.0	83.6	69.4	93.7	63.7	110.8	73.4	124.3	64.33	71.70	63.41	66.95
S1000	103.2	87.8	73.9	72.7	68.6	74.6	65.8	73.0	66.48	61.68	63.31	58.62

^a = averaged beach width values between January and May.

^b = averaged beach width values between June and November.

Table 6-3. Average seasonal beach widths (ft) for March 2017 – October 2022.

Profile	Winter	Summer
N1000	155.29	168.22
N0500	100.88	135.71
N0400'	64.73	61.26
NS0000	68.01	50.48
S0800'	34.88	32.86
S0500	63.41	66.95
S1000	63.31	58.62

Table 6-4. Linear regression analysis of beach width, March 2017 – October 2022.

Profile	Rate of Change (ft/yr)	Intercept (ft)	p-value^a	Trend
N1000	-1.87	171.75	0.1742	Slight Erosion
N0500	0.40	111.15	0.8465	Slight Accretion
N0400'	-0.16	64.40	0.8826	Slight Erosion
NS0000	-1.42	66.57	0.3974	Slight Erosion
S0800'	1.35	26.95	0.0037	Slight Accretion
S0500	-0.16	79.86	0.9601	Slight Erosion
S1000	-5.76	89.51	1.61E-05	Erosion

^a = p-values > 0.05 indicate a statistically non-significant trend (i.e., trend is not different from zero).

^b = p-values < 0.05 indicate a statistically significant trend (i.e., trend is not equal to zero).

7.0 BEACH PROFILES AND WIDTH FROM 1964 THROUGH 2022

The available beach profile data at San Onofre from 1945 through 1998 were used in evaluating the observed changes from 2017 through 2022. There are large gaps in the beach profile data sets where no beach surveys were carried out, but the available information is useful to better understand beach width fluctuations over a long-time scale. Beach width is controlled by waves, sediment supply, beach site location and surroundings, and the beach nearshore and offshore bathymetry.

7.1 BEACH PROFILE HISTORY

Figure 7-1 shows the benchmarks used for historical profiles, in comparison to beach width determined from photographs over time. The earliest beach profile data (1945-1949) for the area were collected by Shepard (1950a, b) at four range lines, three of which are shown in Figure 7-1. The benchmarks for these three surveys are noted as “Crescent” (farthest upcoast), “Fence” (about 4,000 ft [1,200 m] upcoast of Unit 1), and “Surf” (about 660 feet [200 m] upcoast of Unit 1). Shepard’s original survey notes are available in the Scripps Institution of Oceanography (SIO) archives, but efforts to reconstruct the profiles were unsuccessful.

The first set of beach profiles associated with Unit 1 construction was taken on May 15, 1964 and represents the San Onofre State Beach area before the influence of any construction activity, which began in June 1964. A second set of profiles was taken on July 13, 1964, which would also have been before construction activity had any effect. Note that Figure 7-1 also shows the location of the Unit 1 laydown pad (the hatched area), which was in existence from 1964 through 1966. The last set of profiles recorded in this phase of beach measurement, taken on October 29-30, 1970, represents the beach well after the disappearance of the pad’s influence.

The next beach profile study began in 1974 as part of the oceanographic monitoring program for the construction of Units 2 and 3. Benchmarks “B1,” “B3,” “B5,” “B6,” and the remote “B7” (the triangles in Figure 7-1) were established at the beginning of construction for Units 2 and 3. The May 3, 1974 set of profiles represents the “pre-construction beach” in this series. The “B1” line, which is nearest the 1964-1971 “A” line, is shown in Figure 7-1. SCE land survey teams performed these profile surveys, which extend to a depth of -2 to -6 ft (-0.6 to -1.8 m) mean lower low water (MLLW). These profile lines were monitored monthly from 1974 through early 1979.

The larger Units 2 and 3 laydown pad (shown in Figure 7-1, to the right [south] of the Unit 1 pad) was in existence from 1974 through early 1985. The beach profiling work started again in 1985 after the laydown pad had been removed and the sand behind it had been released. The first set of these measurements was taken in May 1985, and this phase of the beach measurement program concluded in September 1987, with nine sets of profiles recorded. An additional survey was carried out by Waldorf (1989) in January 1989. Wading depth profiles were measured every 500 m along the beach, from -6,600 ft (-2,000 m) (north) to +9,900 ft (+3,000 m) (south). These survey lines reached to about -1.5 ft (-0.45 m) depth (MLLW) in the surf zone. The benchmarks for these surveys along the bottom of the cliff face are represented in Figure 7-1 as dots along the beach.

The beach profiling work carried out by CE was started in 1991 and continued through February 1994. Additional surveys were performed along the 1985-1989 range lines at 1650-ft (500 m) intervals (Elwany et al., 1992, 1993, 1994). Up to 14 profile lines were surveyed on a quarterly basis. The locations of these ranges are shown in Figure 7-2. Additional beach profile surveys were carried out by CE in 2000 and 2016 on the same ranges.

7.2 BEACH WIDTH DATA

Massive beach widening at San Onofre was associated with the SONGS construction activity that stretched over 20 years from 1964, when Unit 1 was started, to late 1984, when Units 2 and 3 were completed. Over 1 million cubic meters of sand were placed on the beach while constructing the two temporary laydown pads needed for equipment staging and workspace (Flick and Wanetick, 1989). These laydown pads extended about 70 m seaward of the present-day seawall; even this modest width sufficiently interrupted the longshore transport of sand to widen and stabilize the beaches for several kilometers up-coast.

Most pertinent to this study were the data that documented changes at San Onofre State Beach through the time of construction of Units 1, 2, and 3, and the data gathered after the 1985 removal of the Unit 2 and Unit 3 laydown pad. The SONGS beach surveys showed how the local beach responded to the massive input of sand from construction activities (1985-2000), and provided pre-construction beach conditions. The pre-construction beach width is shown in Figure 7-3.

The post-1985 beach profile data shown in Figure 7-4 documents the return to a narrower state of the beach after completion of construction. Figure 7-5 displays beach width data from 1964-2000, which documents the beach widening due to the placement of the laydown pads and the subsequent beach narrowing back to its natural configuration. A comparison of the 2000 and 2016 beach profiles at NS0000 is shown in Figure 7-6, which further displays the long-term erosional trend seen after construction activities at SONGS.

Figure 7-7 shows the beach widths measured at N1000, N0500, NS0000, S0500, and S1000 during the time periods of 1990-1993 and 2017-2022. The solid line is the mean of beach width for the referenced periods. The dotted lines cover the period where no long-term measurements were carried out. Table 7-1 displays these mean beach widths.

The change in mean beach widths between these two time periods (1990-1993 and 2017-2022) was evaluated with a two-tailed t-test, and the resulting p-values for all transects were less than 0.01 (Table 7-1). This indicates that all profiles displayed a statistically significant erosional trend ($p\text{-value} < 0.05$) between these two time periods. The long-term average erosion rate at San Onofre beach is between 2.0 and 3.7 ft/year.

The beach at San Onofre State Beach, which extends 1 km north and south from SONGS, has retreated considerably and subsequently has caused the cliffs to retreat by about 1.34 ft/year (Hapke & Reed, 2007) due to wave action. Table 7-2 gives the estimated average winter-summer seasonal cycle for the beach width data collected during 1990-1993 (34.5 ft) and 2017-2022 (32.74 ft).

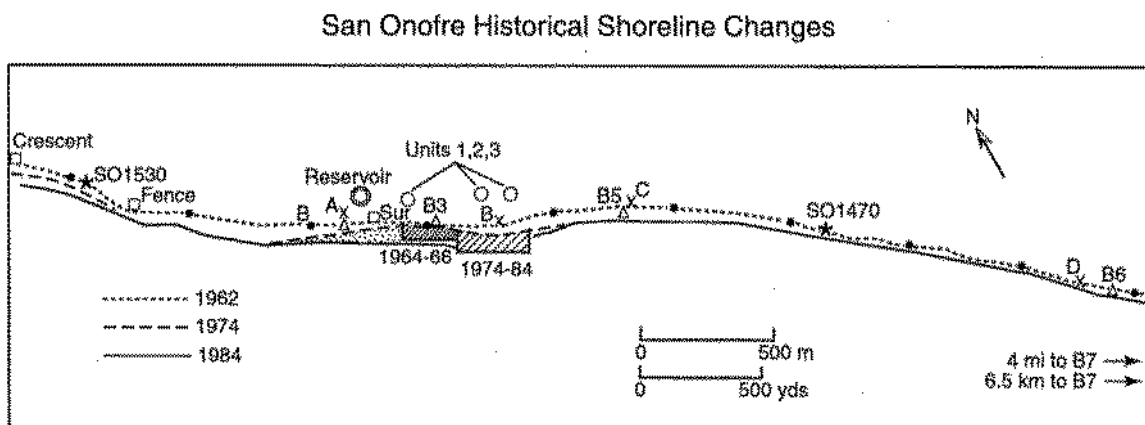


Figure 7-1. SONGS area historical shoreline changes, laydown pad locations (bracketed hatch marks labeled 1964-66 are for Unit 1; those labeled 1974-84 are for Units 2 and 3), and fillet beach (stippled). The shorelines in this figure are an approximation of MHHW traced from photographs for 1962, 1974, 1984. The fillet beach is a salient, perimeter beach. Benchmark designations for early profiles: Crescent, Fence, and Surf, 1940s; A-D, 1984-86; B1-B7, 1974-85. Flick et al. (2010).

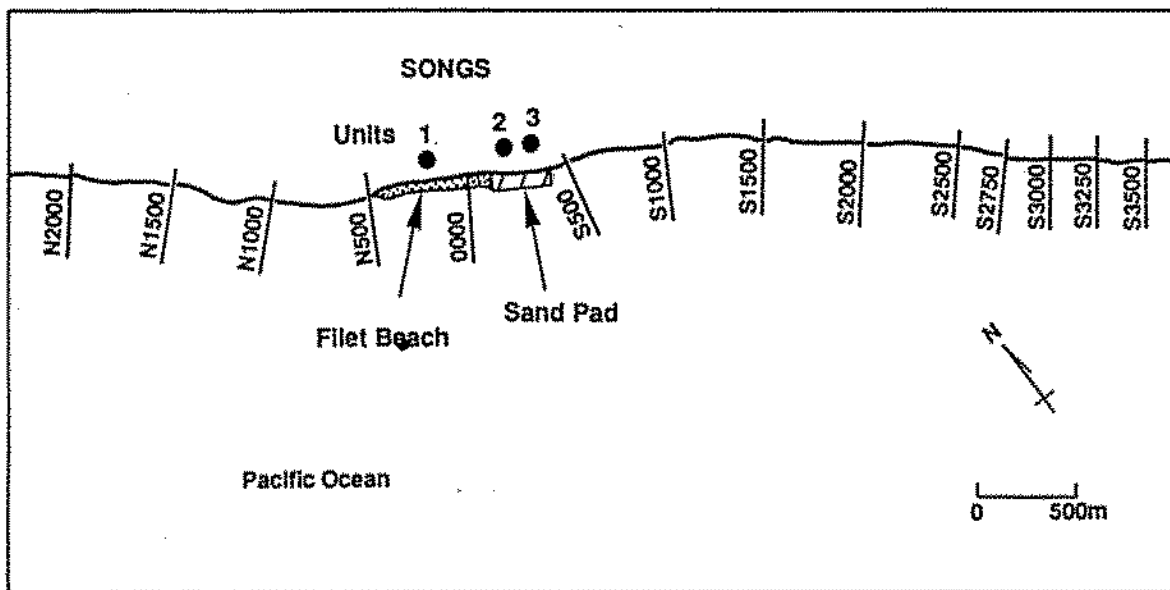


Figure 7-2. Beach profile range lines at San Onofre, 1990-1993.

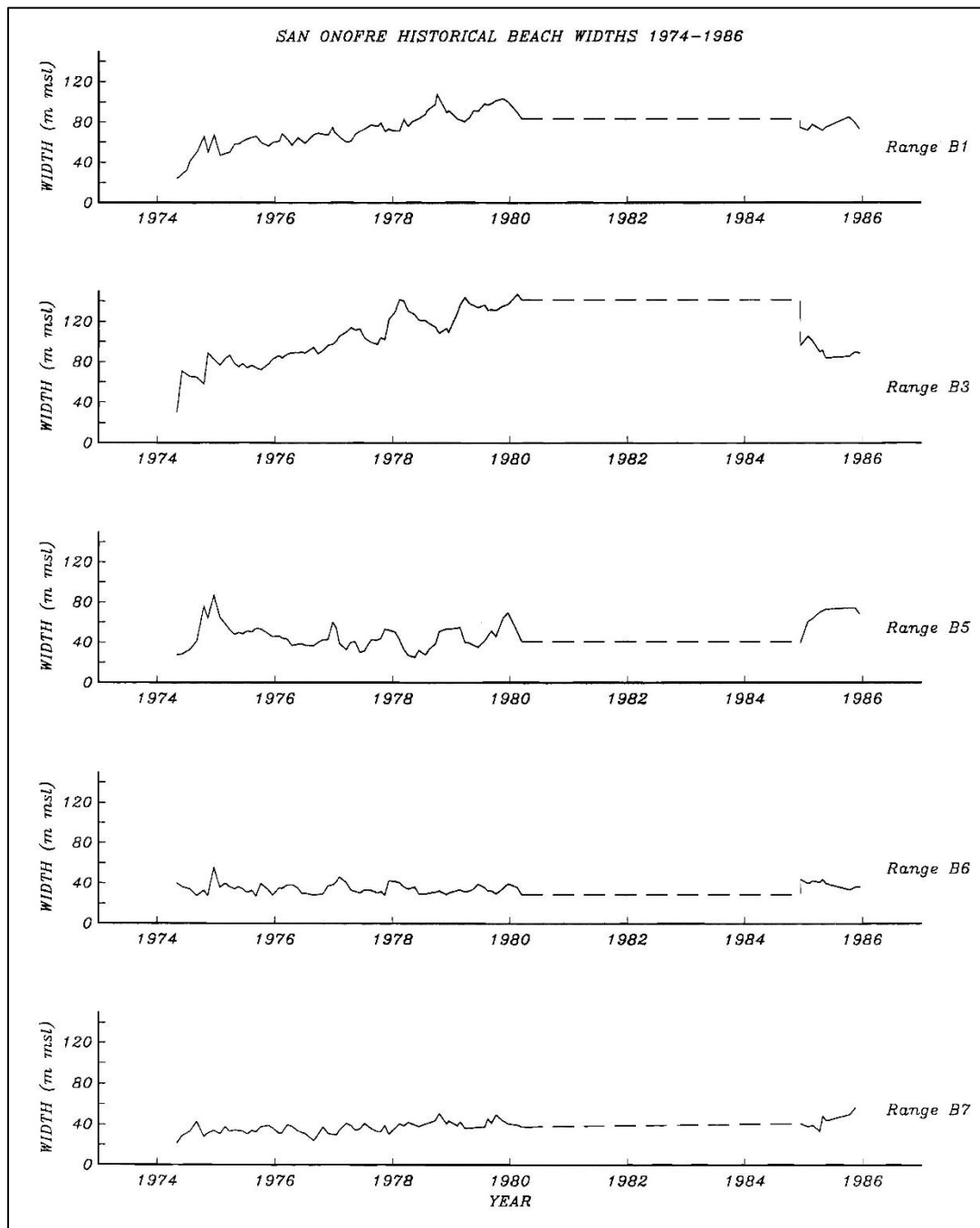


Figure 7-3. Beach-width time histories around the time of Units 2 and 3 construction. Broken lines show time of missing data.

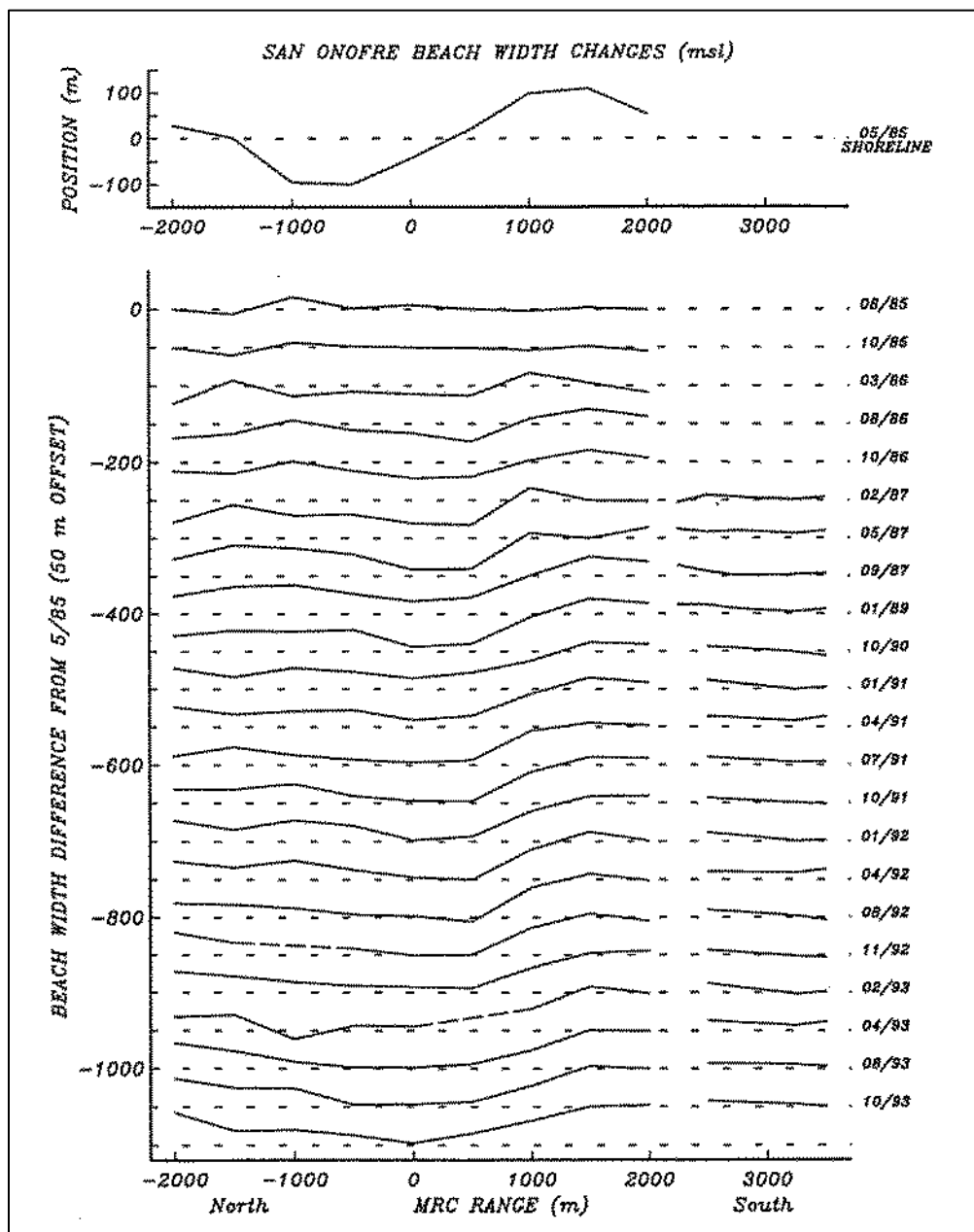


Figure 7-4. Time history of beach-width changes at San Onofre after removal of Units 2 and 3 laydown pad. Changes for dates (month/year) at right relative to May 1985 survey (top panel). Numbers on left axis are dummy values to position lines vertically; each line is plotted relative to the dotted line, which represents the May 1985 survey.

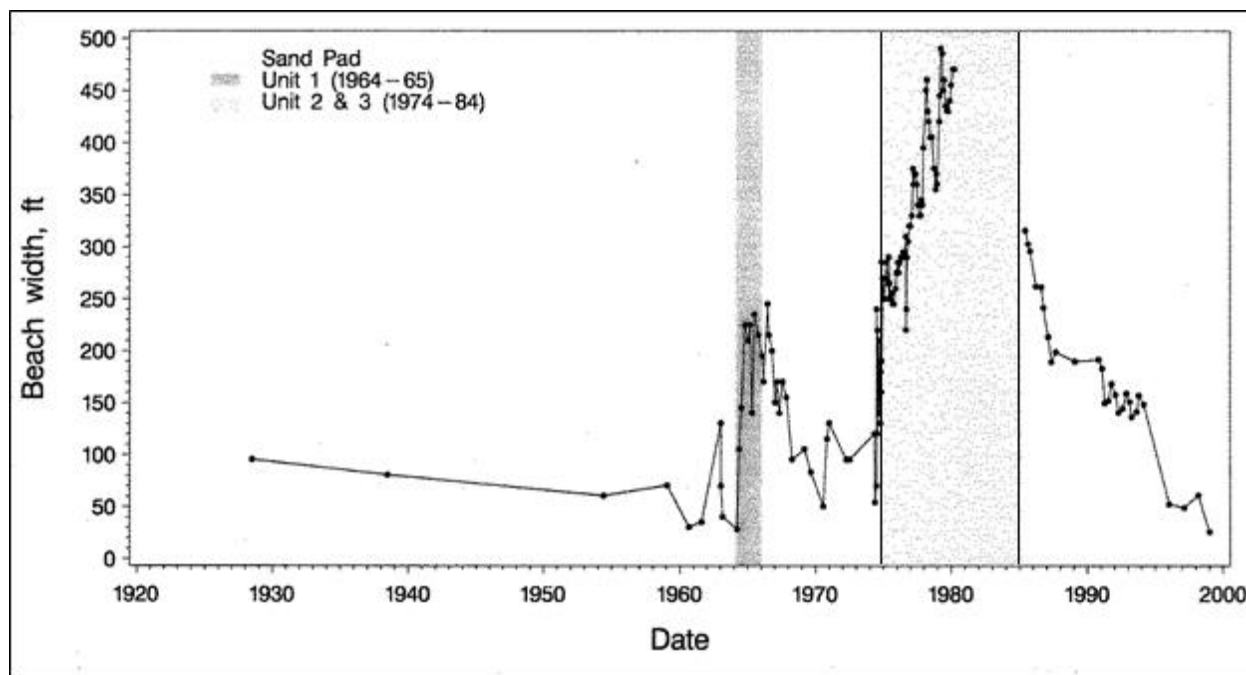


Figure 7-5. Historical beach width adjacent to Unit 1, 1928-2000. Shaded columns show periods when laydown pads were present.

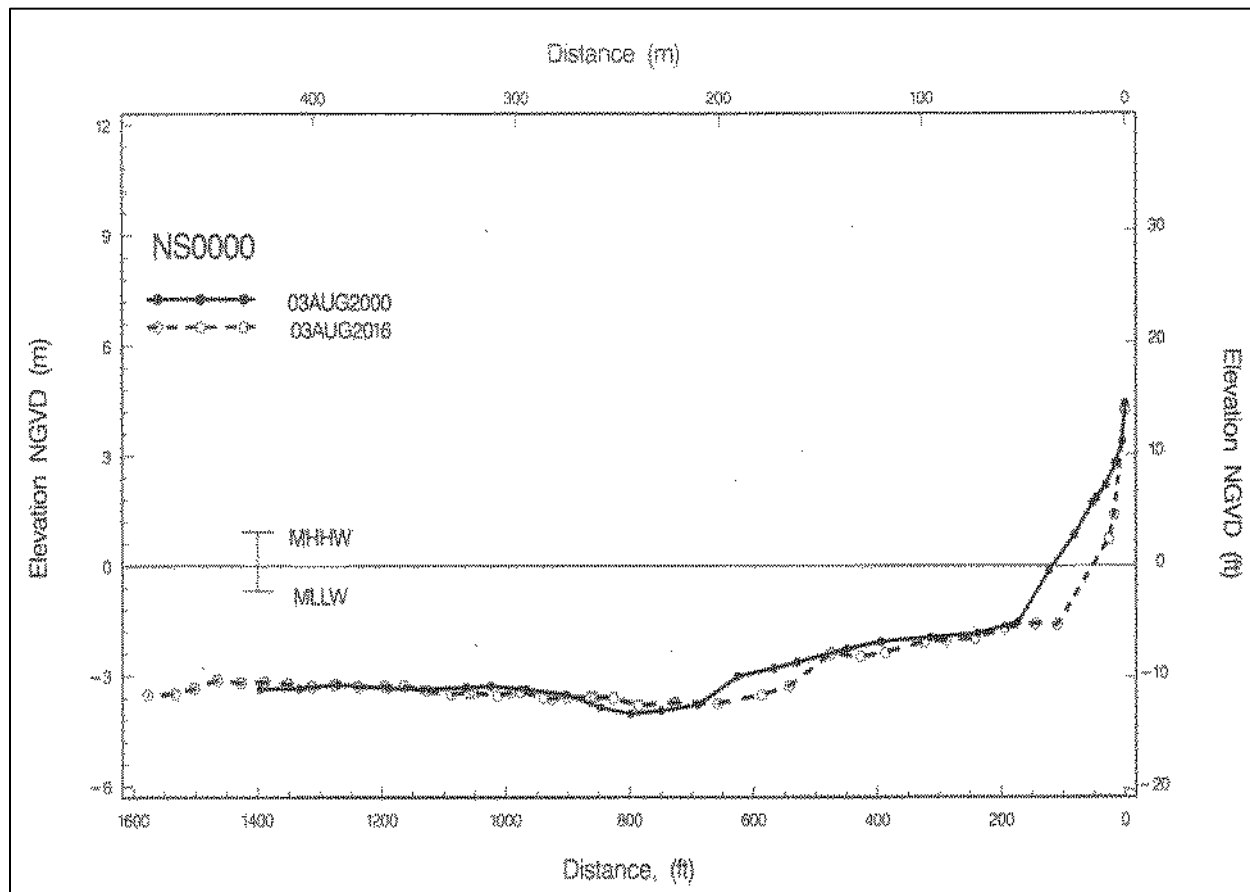


Figure 7-6. Beach profiles at NS0000, years 2000 and 2016.

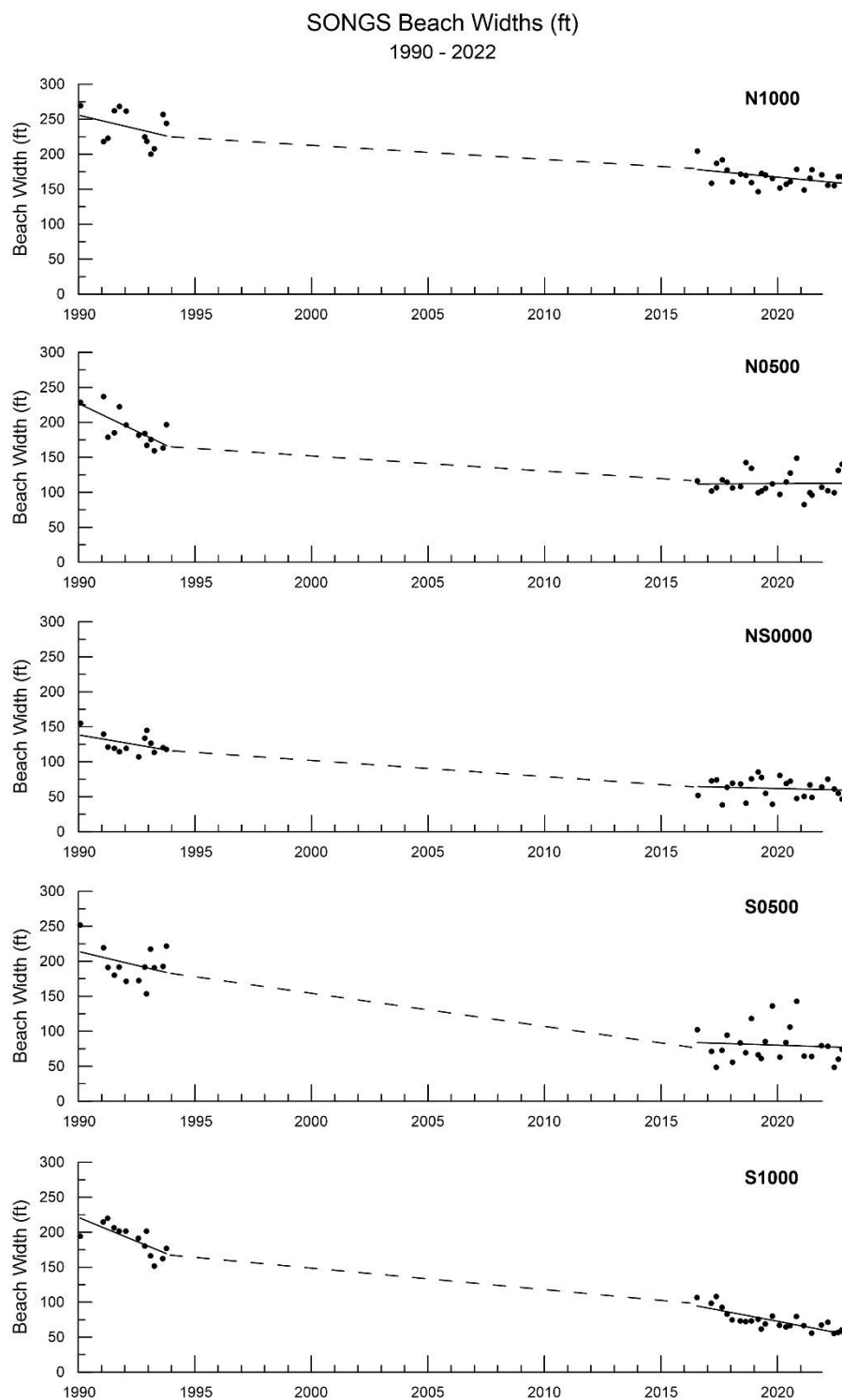


Figure 7-7. Beach width measured between 1990 through 1993 and between 2016 through 2022. Solid lines are the mean of beach width for the referenced periods and dotted lines cover the period where no long-term measurements were carried out.

Table 7-1. Mean beach widths (ft) at San Onofre, 1990-1993 vs. 2017-2022.

Profile	1990-1993		2017-2022		Difference in Mean	p-value*
	Mean	Std. Dev	Mean	Std. Dev		
N1000	237.9	25.1	166.2	11.5	71.7	3.57E-07
N0500	190.4	25.0	112.3	16.8	78.1	7.68E-09
NS0000	125.4	13.9	63.9	8.9	61.5	8.65E-13
S0500	195.8	26.0	62.3	13.8	133.5	2.26E-12
S1000	189.8	20.9	31.0	4.2	158.8	4.68E-13

Table 7-2. Estimates of seasonal beach widths changes at San Onofre (ft).

Survey Period	Profiles					
	N1000	N0500	NS0000	S0500	S1000	Mean
1990-1993	51.6	38.8	23.9	36.2	30.2	34.5
2017-2022	24.0	31.2	32.2	56.4	19.9	32.74

8.0 CONCLUSIONS AND RECOMMENDATIONS

Construction activities at SONGS over the 20-year period from 1965 to 1984 resulted in substantial increases in beach width adjacent to and north of the plant. These increases were primarily a result of the large quantities of excavated sand being placed on the beach and the Unit 1 and Units 2 and 3 laydown pad structures that served to retain the fill. Since the removal of the Units 2 and 3 laydown pad in 1985, the beaches adjacent to and north of SONGS have experienced dramatic narrowing and returned to their pre-construction configuration (Figures 7-4 and 7-5).

Generally, San Onofre Beach retreats moderately by a rate of about 2-4 ft/year. In the period between 1993 and 2022, this is due to limited sand supply from the surrounding creeks and rivers. Since the end of the last wet period in 1998, sediment flows from the surrounding waterways have been considerably reduced.

In the long term, the heavily used beach access and parking at San Onofre State Beach just north of SONGS is likely to suffer sustained erosion as this area continues to return to its more natural, pre-construction beach width. Because of the heavy use and intense public interest in this area, continued monitoring should take place. The information gathered will be very valuable to guide any future decisions concerning management options.

The amplitude of the seasonal cycles in beach width is distinguishable from the net advance or retreat. The average annual cycle varies between 28 to 35 ft (Sections 6&7).

The changes of the beach width and profile are controlled by the waves, sand supply, topography of the site (presence of headland and coastal protection structures), and nearshore and offshore bathymetry. In Southern California, the presence of the offshore islands, the complex bathymetry offshore, and the presence of cobbles and/or bedrocks in the nearshore can cause a single, straight beach to experience various beach width changes along different stretches of the same beach. Monitoring the beaches continues to be a good tool to understand and manage these changes.

The beach profile surveys, and photography programs sponsored by SCE since 1964 have provided valuable information and understanding of the response at San Onofre to beach filling and the construction of stabilizing structures. This insight will be valuable as sea level rise accelerates in the future.

9.0 REFERENCES

- CDIP, 1992. *Coastal Data Information Program, Multi-Year Report: Vol. I, 1975-1991*. Scripps Institution of Oceanography, SIO Ref. No. 91-32. 295 pp. + 2 appendices.
- Coastal Environments, 2000. *SONGS Unit 1 Deconstruction Marine Impacts Study, Phase I*. Unpublished report submitted to Southern California Edison Company, 24 January 2000, CE Ref. No. 2000-03, 44 pp. + 2 appendices.
- Coastal Environments, 2020a. San Onofre Nuclear Generating Station (SONGS) Units 2 & 3 Decommissioning Project, 2017-2019 Beach Profile Surveys at San Onofre. Submitted to Southern California Edison, 17 February 2020, CE Ref. No. 20-03, 41 pp. + 6 appendices.
- Coastal Environments, 2021. San Onofre Nuclear Generating Station (SONGS) Units 2 & 3 Decommissioning Project, 2020 Beach Profile Surveys at San Onofre. Submitted to Southern California Edison, 31 January 2021, CE Ref. No. 21-01, 49 pp. + 2 appendices.
- Coastal Environments, 2021a. San Onofre Nuclear Generating Station (SONGS) Units 2 & 3 Decommissioning Project, 2021 Beach Profile Surveys at San Onofre. Submitted to Southern California Edison, 20 December 2021, CE Ref. No. 21-22, 49 pp. + 2 appendices.
- Elwany, M. H. S., and R. E. Flick, 1992. *1991 Beach Profile Survey at San Onofre*. Unpub. Report, Southern California Edison Co., CE Ref. No. 92-1. 24 pp. + 1 appendix.
- Elwany, H., R. Flick, W. Waldorf, and J. Wanetick, 1993. *1992 Beach Profile Survey at San Onofre*. Report submitted to Southern California Edison Co., 20 April 1993, CE Ref. No. 93-7. 26 pp. + appendices.
- Elwany, H., R. Flick, and Samia Aijaz, 1994. *1993 Beach Profile Survey at San Onofre*. Final Report submitted to Southern California Edison Co., 1 July 1994, CE Ref. No. 94-7. 32 pp. + 2 appendices.
- Elwany, H., R.E. Flick, and A.D. Young, 2016. *Coastal Analysis for End-State Planning of San Onofre Nuclear Generating Station, Phase 1*. Report prepared for Southern California Edison by Coastal Environments, La Jolla, CA, CE Reference No. 16-26, 151 pp.
- Flick, R.E., and J.R. Wanetick, 1989. *San Onofre Beach Study*. Unpublished report submitted to Southern California Edison Co., Rosemead, CA, October 1989, SIO Ref. No. 89-20. 26 pp. + 25 figures.
- Flick, R., J.R. Wanetick, M.H. Elwany, R.S. Grove, and B.W. Waldorf, 2010. Beach changes from construction of San Onofre Nuclear Generating Station, 1964-1989. *Shore & Beach*, 78(4): 12-25.

Hapke, C.J. and D. Reid, 2007. *National Assessment of Shoreline Change, Part 4: Historical Coastal Cliff Retreat along the California Coast*. USGS Report 2007-1133.

Inman, D.L., 1980. Man's Impact on the California Coast Zone. Report submitted to State of California, The resources Agency, Department of Boating & Waterways, p. 18.

Waldorf, B.W., 1989. *Beach Profiles in the Vicinity of the San Onofre Nuclear Generating Station*. Unpublished data report submitted to Southern California Edison Company. 5 pp. + appendices.

APPENDIX A

**NEARSHORE SUMMER AND WINTER
BEACH PROFILES FOR 2017-2022**

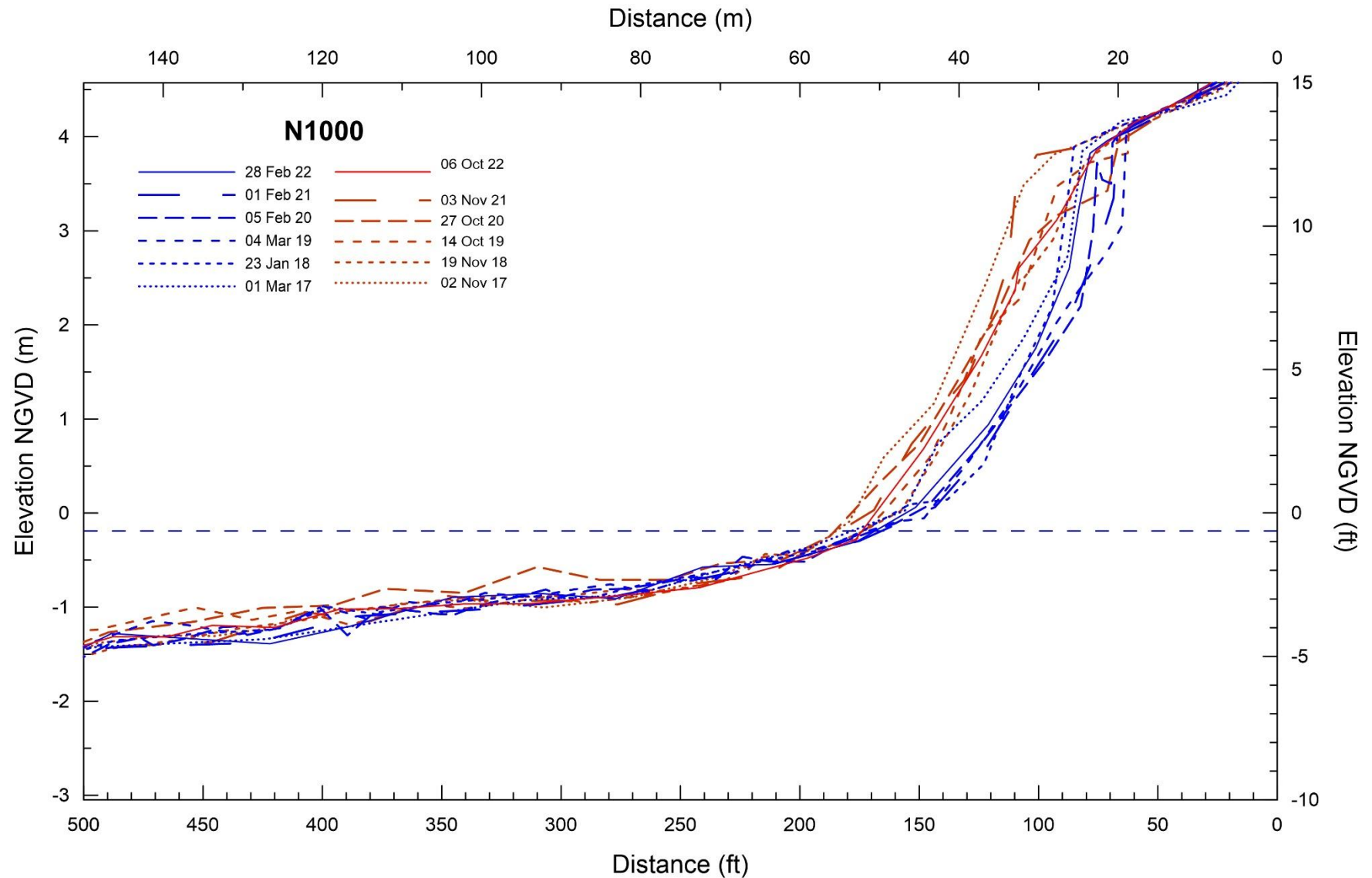


Figure A-1. Nearshore beach profile surveys taken in winter (blue) and summer (red) for N1000.

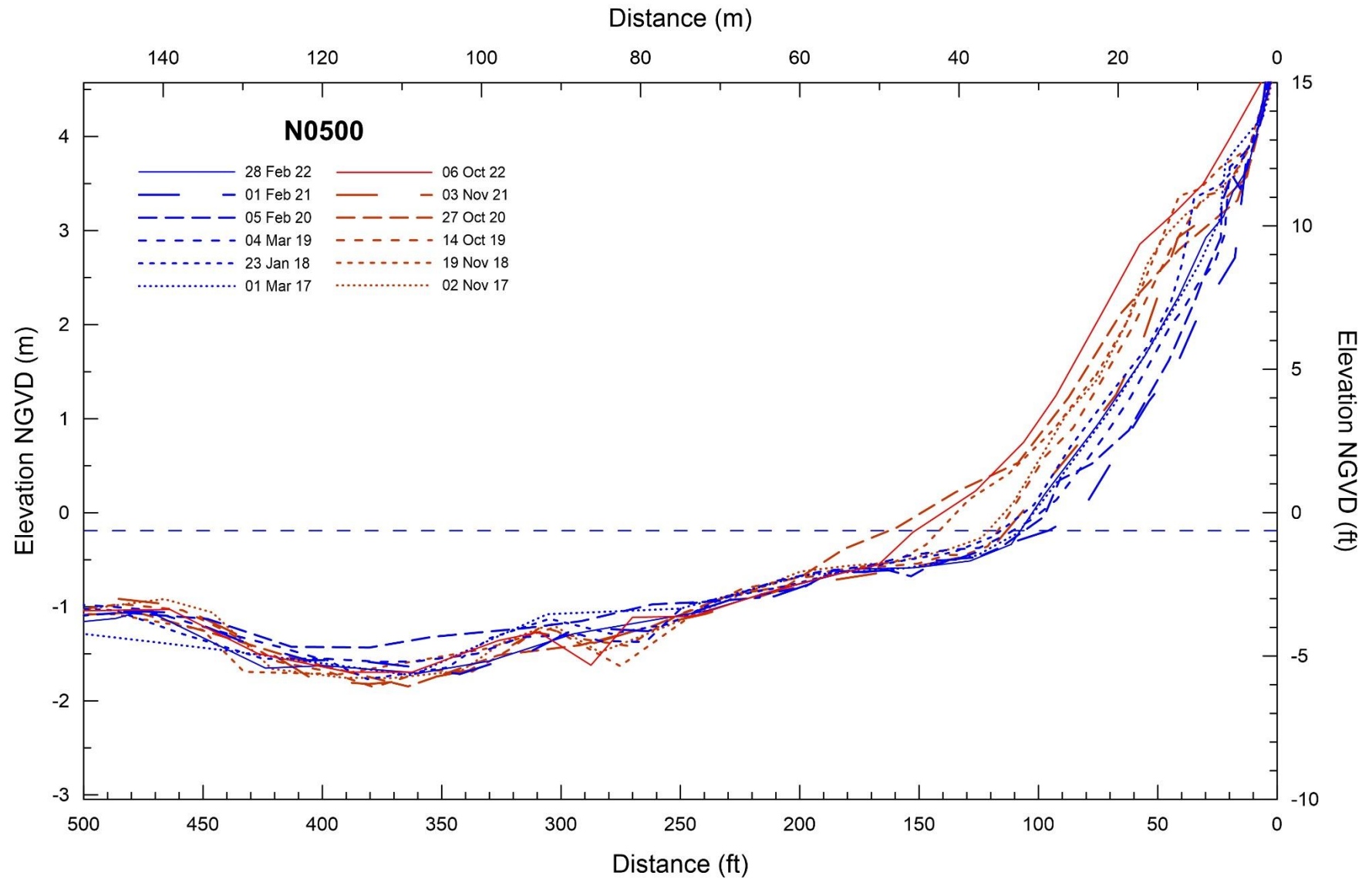


Figure A-2. Nearshore beach profile surveys taken in winter (blue) and summer (red) for N0500.

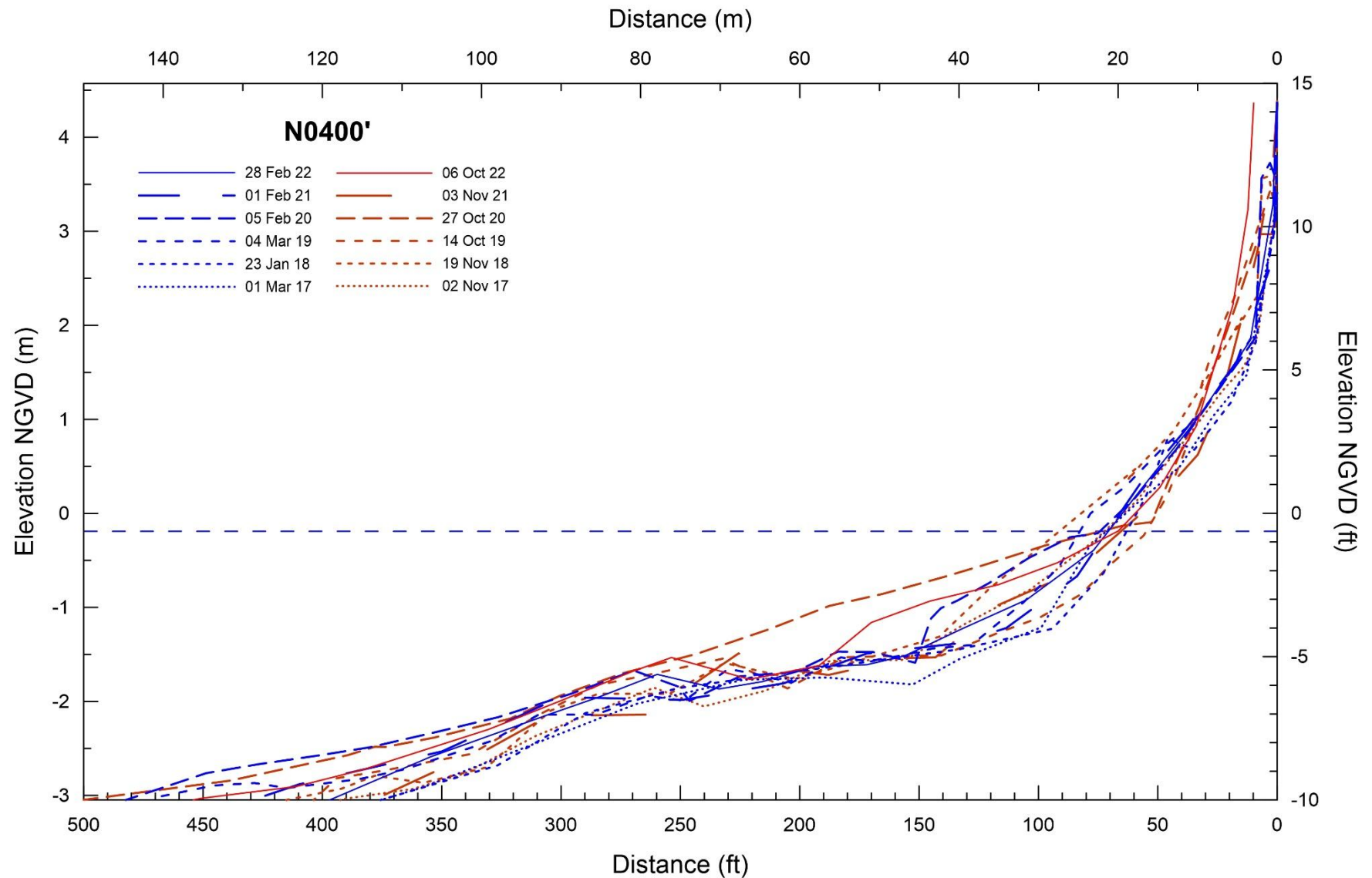


Figure A-3. Nearshore beach profile surveys taken in winter (blue) and summer (red) for N0400'.

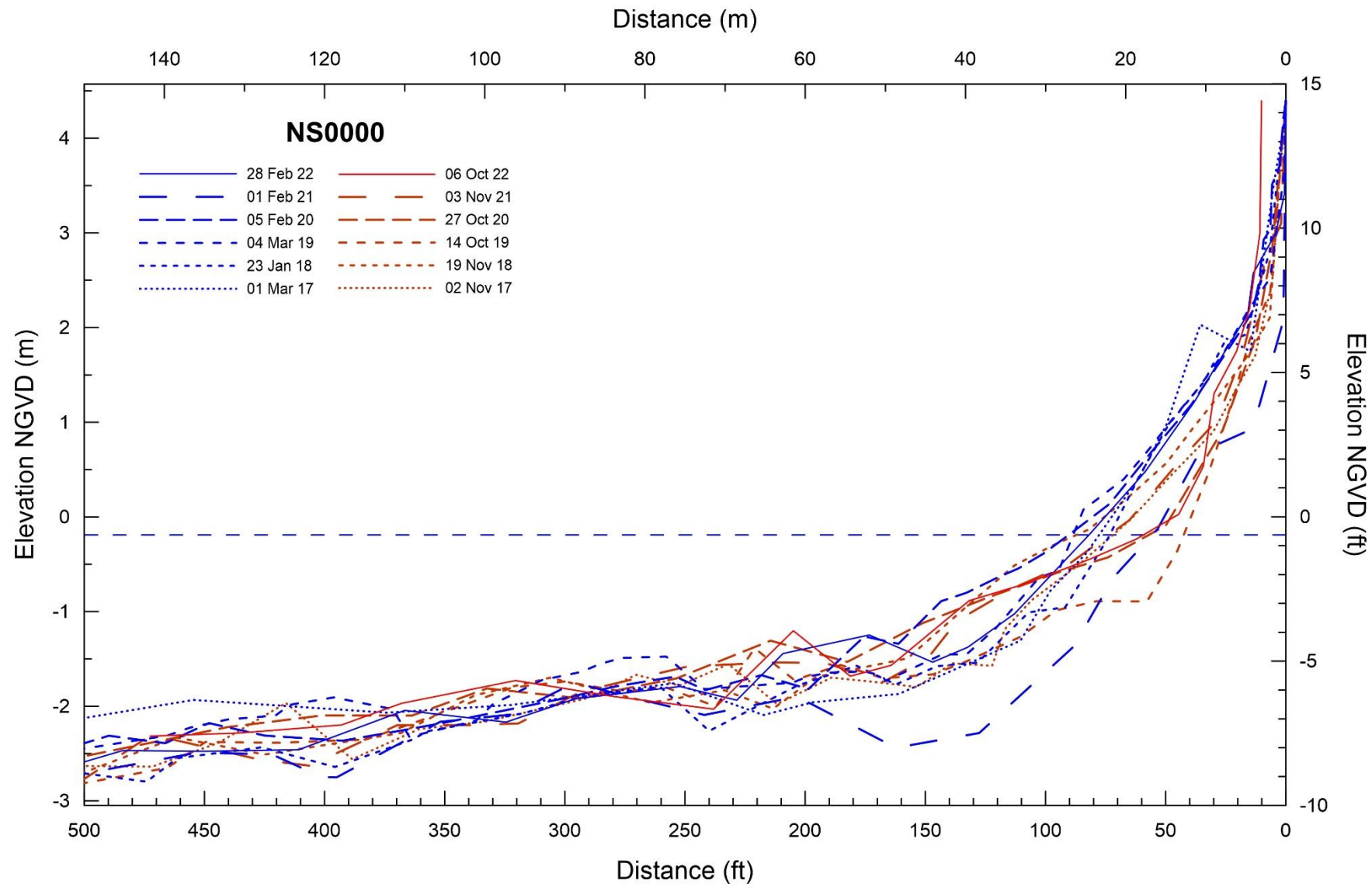


Figure A-4. Nearshore beach profile surveys taken in winter (blue) and summer (red) for NS0000.

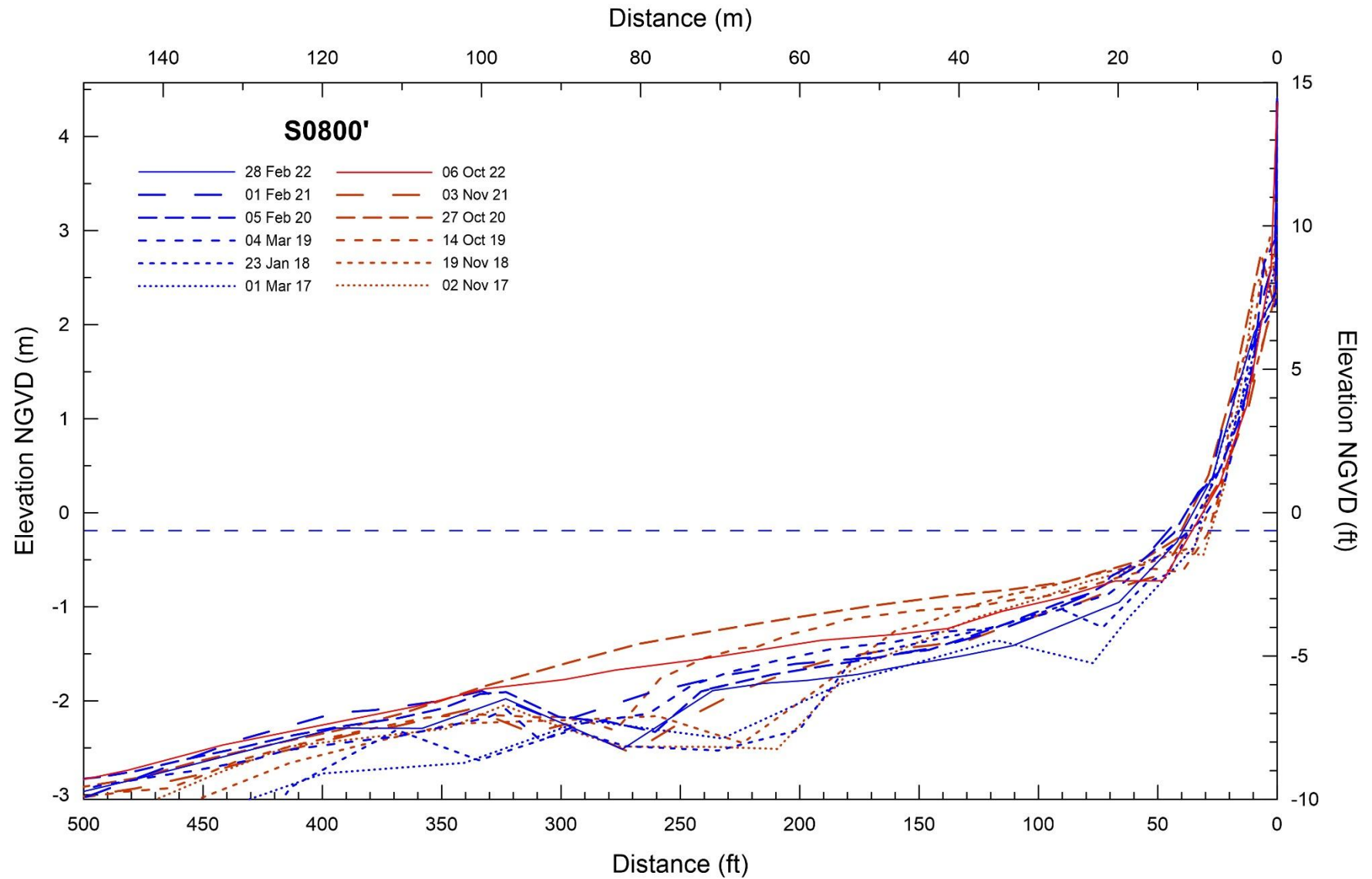


Figure A-5. Nearshore beach profile surveys taken in winter (blue) and summer (red) for S0800'.

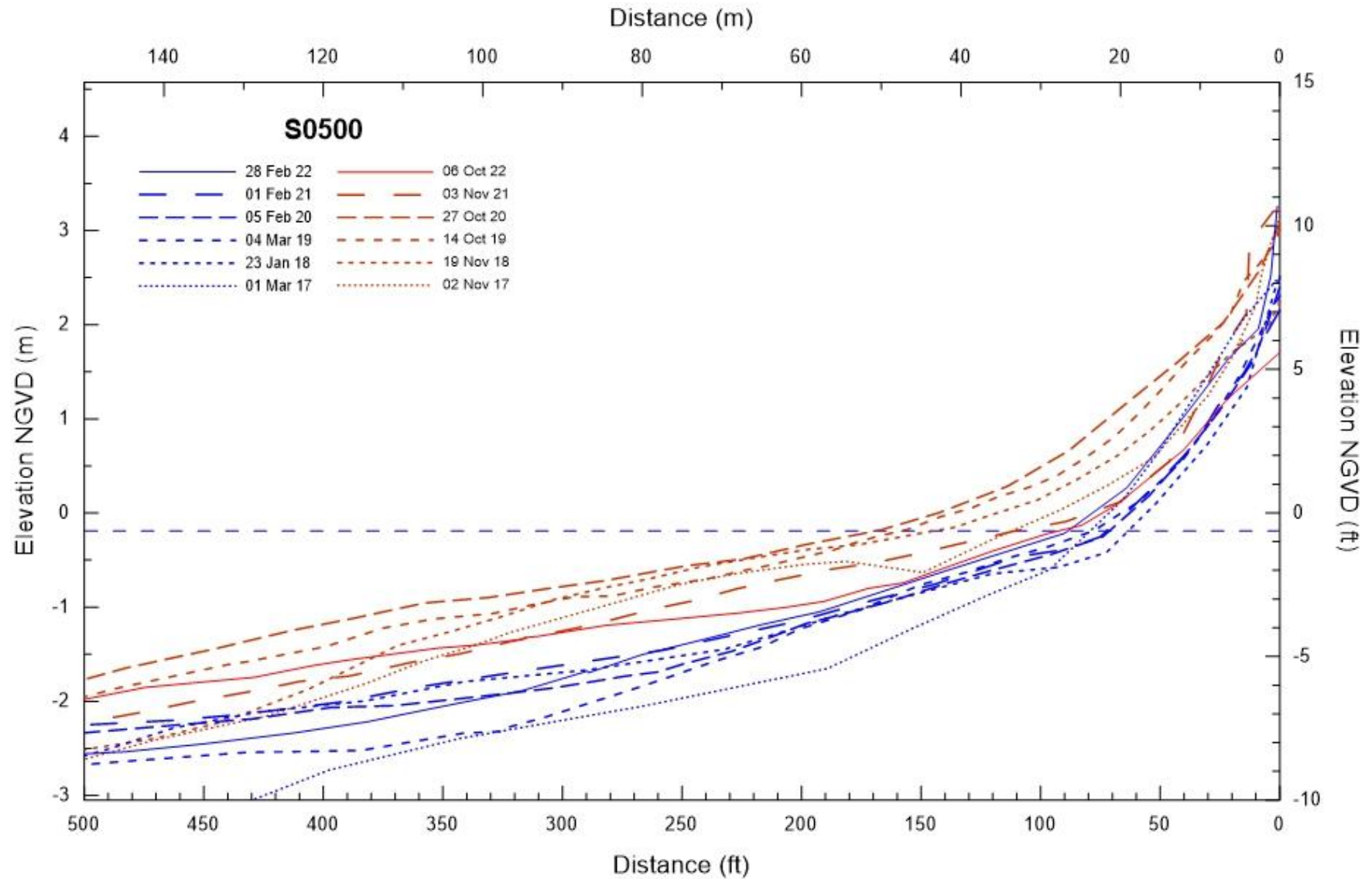


Figure A-6. Nearshore beach profile surveys taken in winter (blue) and summer (red) for S0500.

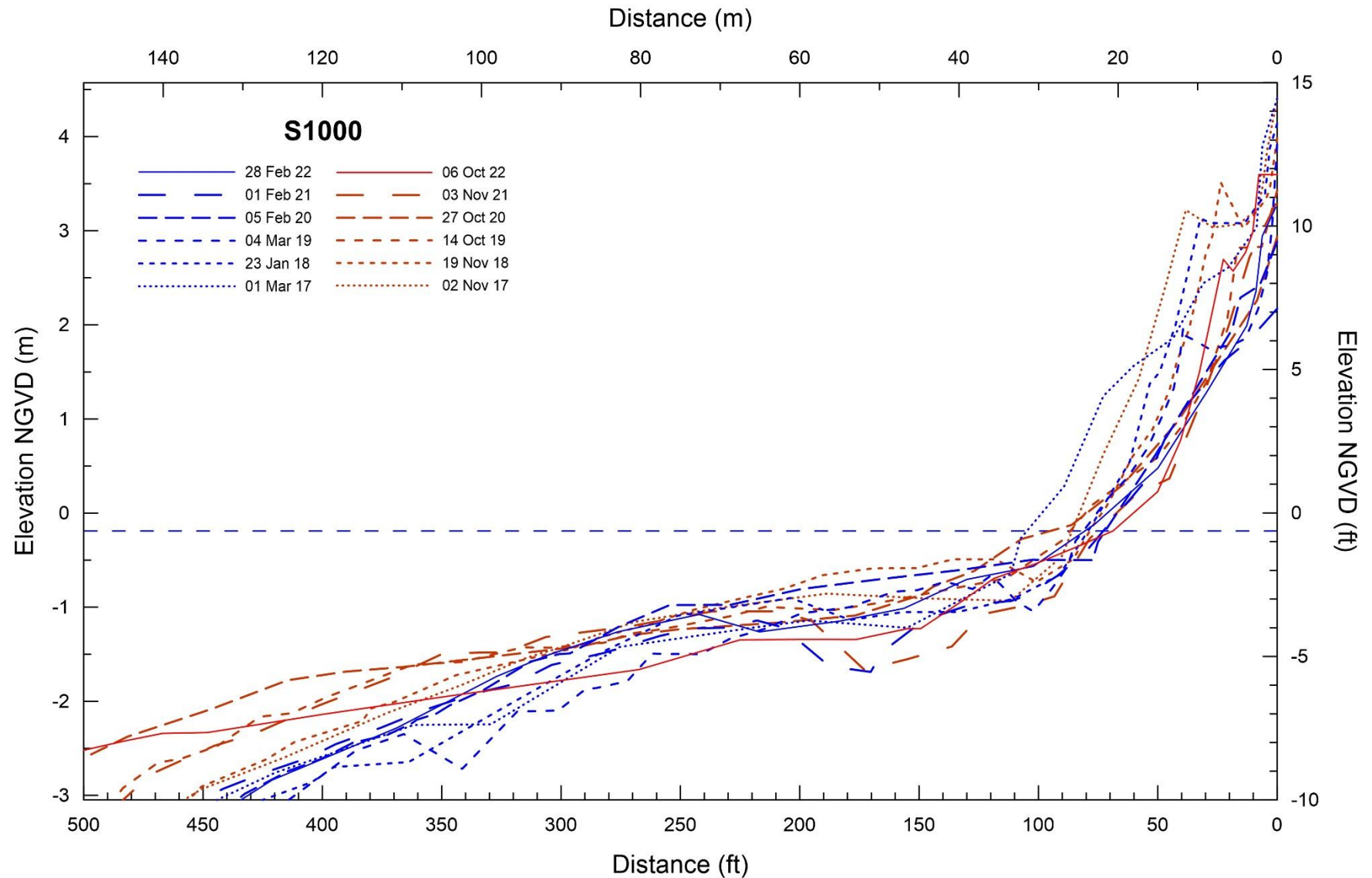


Figure A-7. Nearshore beach profile surveys taken in winter (blue) and summer (red) for S1000.

APPENDIX B

**PHOTOGRAPHS OF SAN ONOFRE BEACH
AND NEW SURVEY BENCHMARKS
TAKEN IN 2022**

San Onofre Nuclear Generating Station (SONGS) Units 2 & 3 Decommissioning Project
2022 Beach Profile Surveys at San Onofre



Photo B-1. Photographs taken in February (top left), June (top right), August (bottom left), and October 2022 (bottom right) looking north from range N1000.

San Onofre Nuclear Generating Station (SONGS) Units 2 & 3 Decommissioning Project
2022 Beach Profile Surveys at San Onofre



Photo B-2. Photographs taken in February (top left), June (top right), August (bottom left), and October 2022 (bottom right) looking south from range N1000.

San Onofre Nuclear Generating Station (SONGS) Units 2 & 3 Decommissioning Project
2022 Beach Profile Surveys at San Onofre



Photo B-3. Photographs taken in February (top left), June (top right), August (bottom left), and October 2022 (bottom right) looking north from range N0500.

San Onofre Nuclear Generating Station (SONGS) Units 2 & 3 Decommissioning Project
2022 Beach Profile Surveys at San Onofre



Photo B-4. Photographs taken in February (top left), June (top right), August (bottom left), and October 2022 (bottom right) looking south from range N0500.

San Onofre Nuclear Generating Station (SONGS) Units 2 & 3 Decommissioning Project
2022 Beach Profile Surveys at San Onofre



Photo B-5. Photographs taken in February (top left), June (top right), August (bottom left), and October 2022 (bottom right) looking north from range N0400'.

San Onofre Nuclear Generating Station (SONGS) Units 2 & 3 Decommissioning Project
2022 Beach Profile Surveys at San Onofre

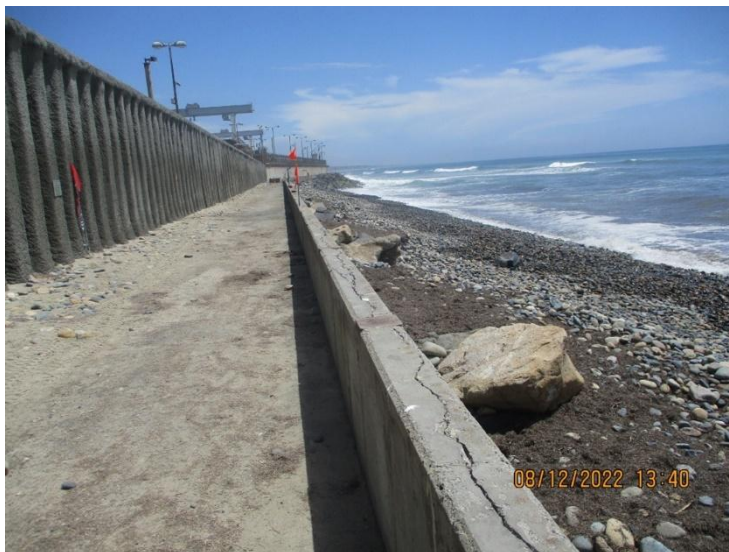
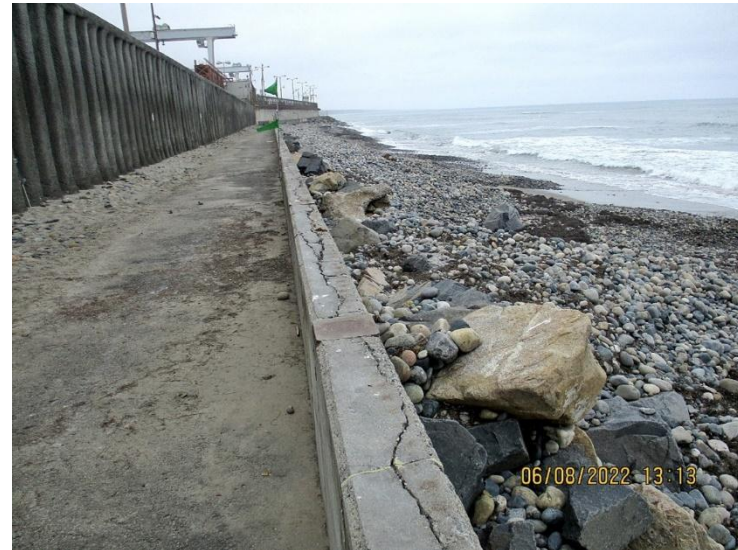


Photo B-6. Photographs taken in February (top left), June (top right), August (bottom left), and October 2022 (bottom right) looking south from range N0400'.

San Onofre Nuclear Generating Station (SONGS) Units 2 & 3 Decommissioning Project
2022 Beach Profile Surveys at San Onofre



Photo B-7. Photographs taken in February (top left), June (top right), August (bottom left), and October 2022 (bottom right) looking north from range NS0000.

San Onofre Nuclear Generating Station (SONGS) Units 2 & 3 Decommissioning Project
2022 Beach Profile Surveys at San Onofre

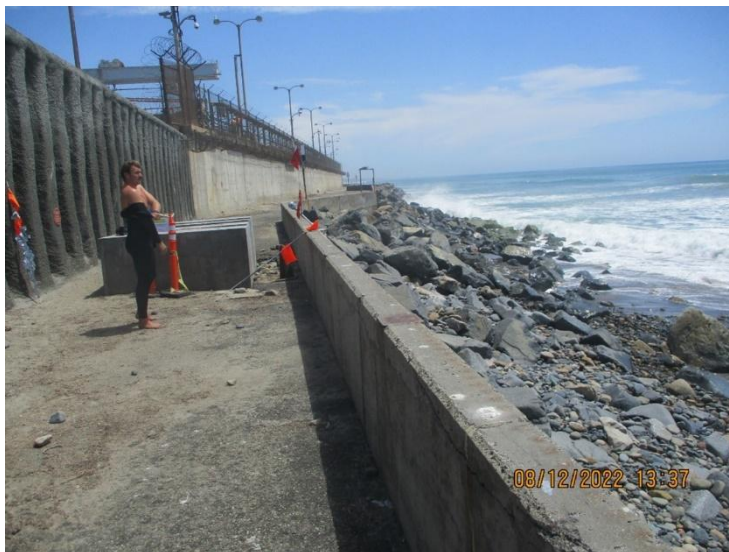


Photo B-8. Photographs taken in February (top left), June (top right), August (bottom left), and October 2022 (bottom right) looking south from range NS0000.

San Onofre Nuclear Generating Station (SONGS) Units 2 & 3 Decommissioning Project
2022 Beach Profile Surveys at San Onofre

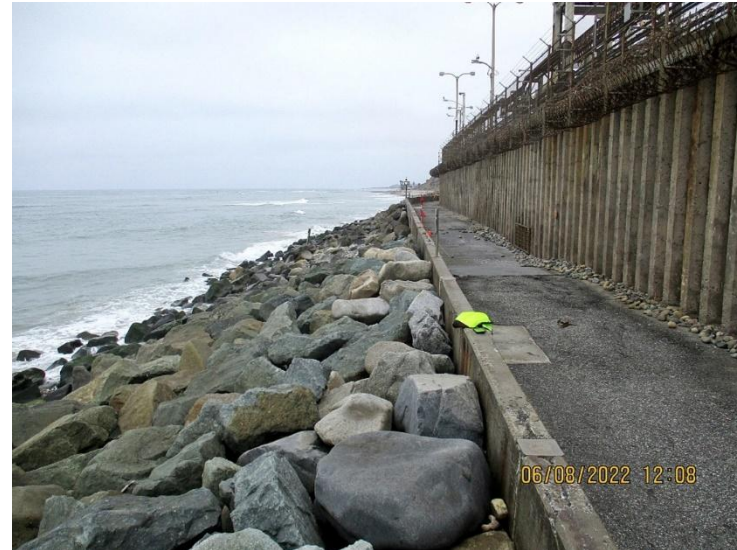
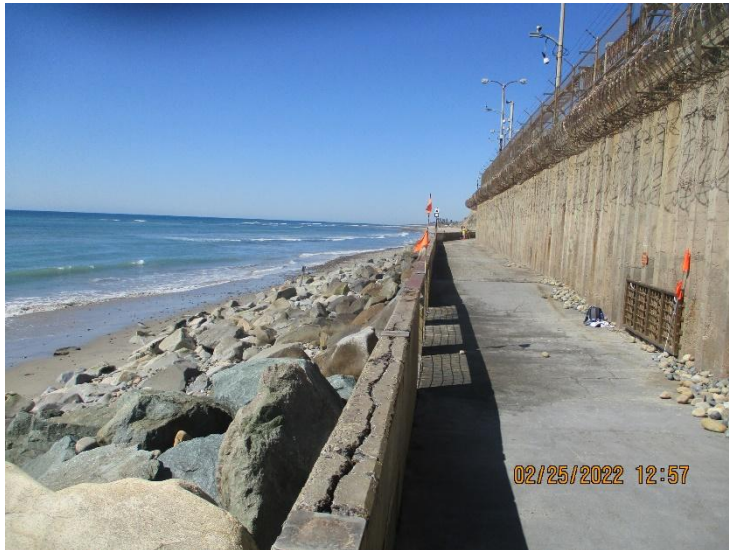


Photo B-9. Photographs taken in February (top left), June (top right), and October 2022 (bottom) looking north from range S0800'.

(top

San Onofre Nuclear Generating Station (SONGS) Units 2 & 3 Decommissioning Project
2022 Beach Profile Surveys at San Onofre



Photo B-10. Photographs taken in February (top left), June (top right), and October 2022 (bottom) looking south from range S0800'.

San Onofre Nuclear Generating Station (SONGS) Units 2 & 3 Decommissioning Project
2022 Beach Profile Surveys at San Onofre

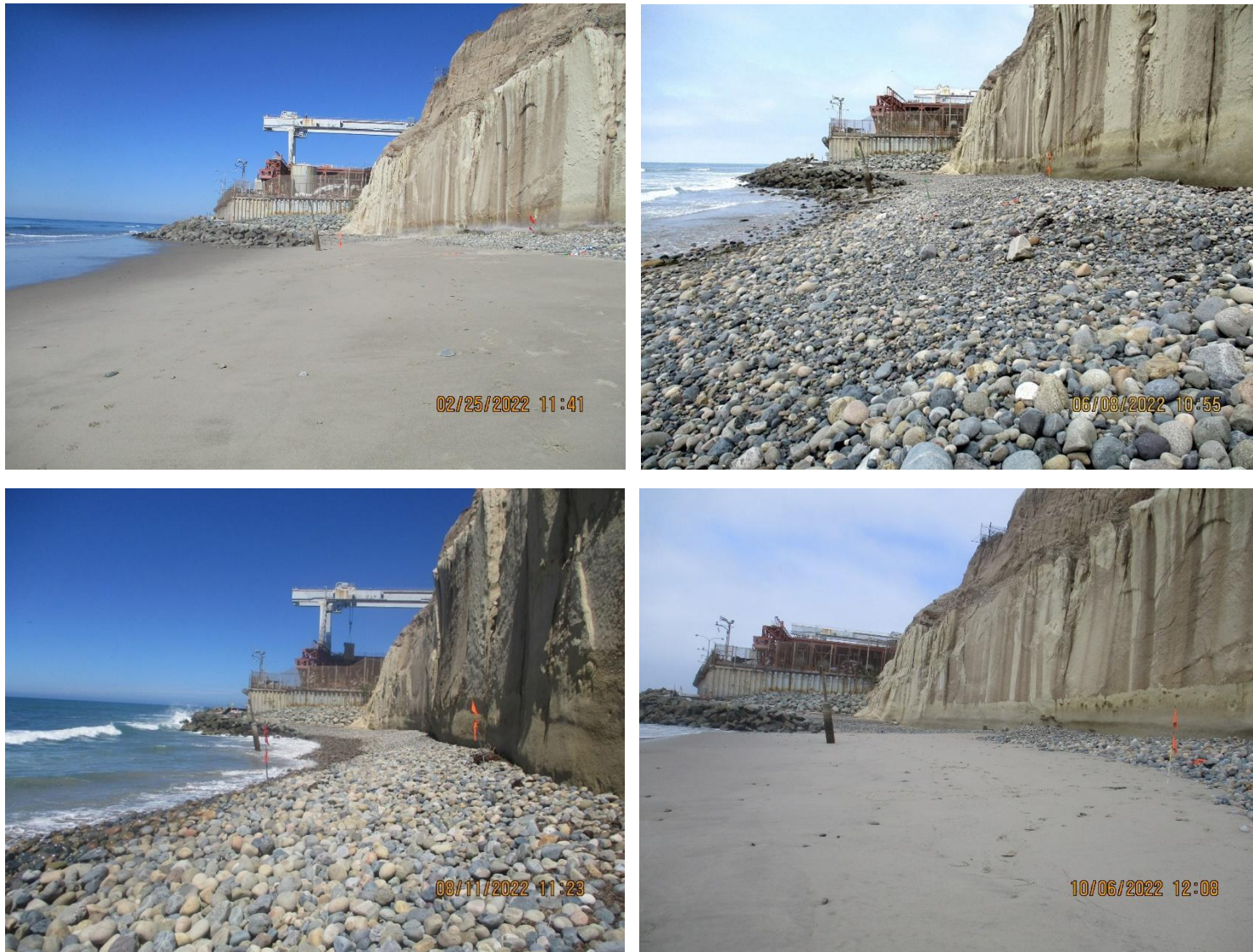


Photo B-11. Photographs taken in February (top left), June (top right), August (bottom left), and October 2022 (bottom right) looking north from range S0500.

San Onofre Nuclear Generating Station (SONGS) Units 2 & 3 Decommissioning Project
2022 Beach Profile Surveys at San Onofre



Photo B-12. Photographs taken in February (top left), June (top right), August (bottom left), and October 2022 (bottom right) looking south from range S0500.

San Onofre Nuclear Generating Station (SONGS) Units 2 & 3 Decommissioning Project
2022 Beach Profile Surveys at San Onofre



Photo B-13. Photographs taken in February (top left), June (top right), August (bottom left), and October 2022 (bottom right) looking north from range S1000.



Photo B-14. Photographs taken in February (top left), June (top right), August (bottom left), and October 2022 (bottom right) looking south from range S1000.



Photo B-15. Benchmark BM04, created on 21 January 2020, is located on the SW corner of Bathroom 4 in the San Onofre State Beach parking lot.



Photo B-16. Benchmark BM02, created on 21 January 2020, is located on the SW corner of Bathroom 2 in the San Onofre State Beach parking lot. Benchmarks BM02 through BM06 are all marked by a scribed X on the concrete foundation.



Photo B-17. Benchmark BM07, created on 21 January 2020, is located on the NE corner of a concrete structure located south of the San Onofre State Beach parking lot and north of transect N0500.



Photo B-18. Benchmark BM08, created on 21 January 2020, is marked by a scribed X and located just south of transect NS0000 on top of the seawall.

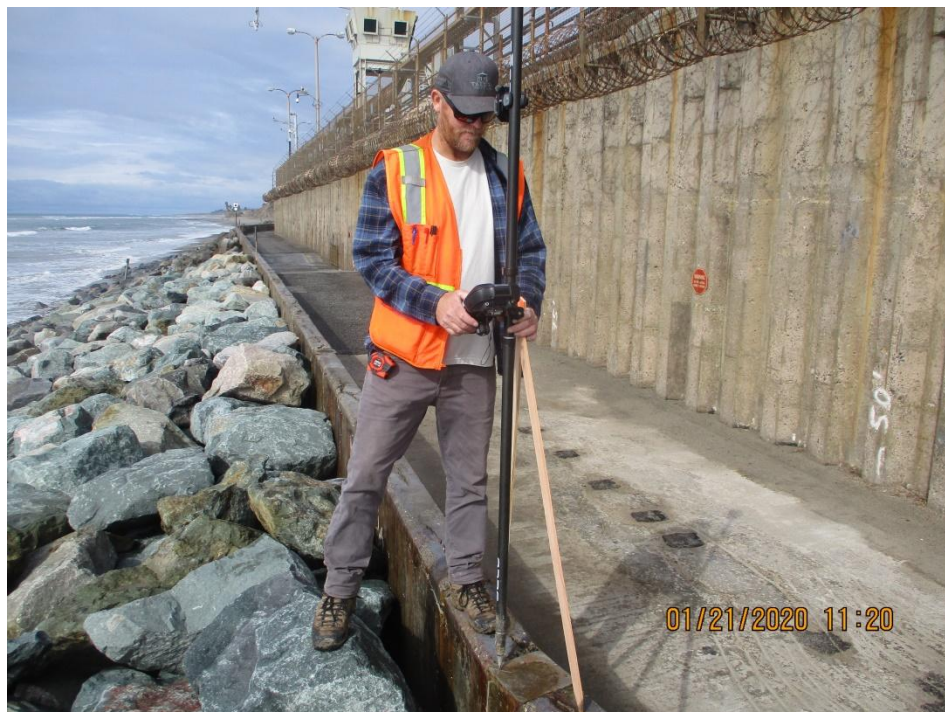


Photo B-19. Benchmark BM09, created on 21 January 2020, is located on top of the seawall, just south of transect S0800'.



Photo B-20. Benchmark BM10, created on 21 January 2020, is marked by a metal screw and washer and is located on the walkway south of transect S0800'. This benchmark has replaced benchmark 2051613.



Photo B-21. Benchmark BM11, created on 21 January 2020, is located on top of the concrete blocks at the southern end of the SONGS walkway.

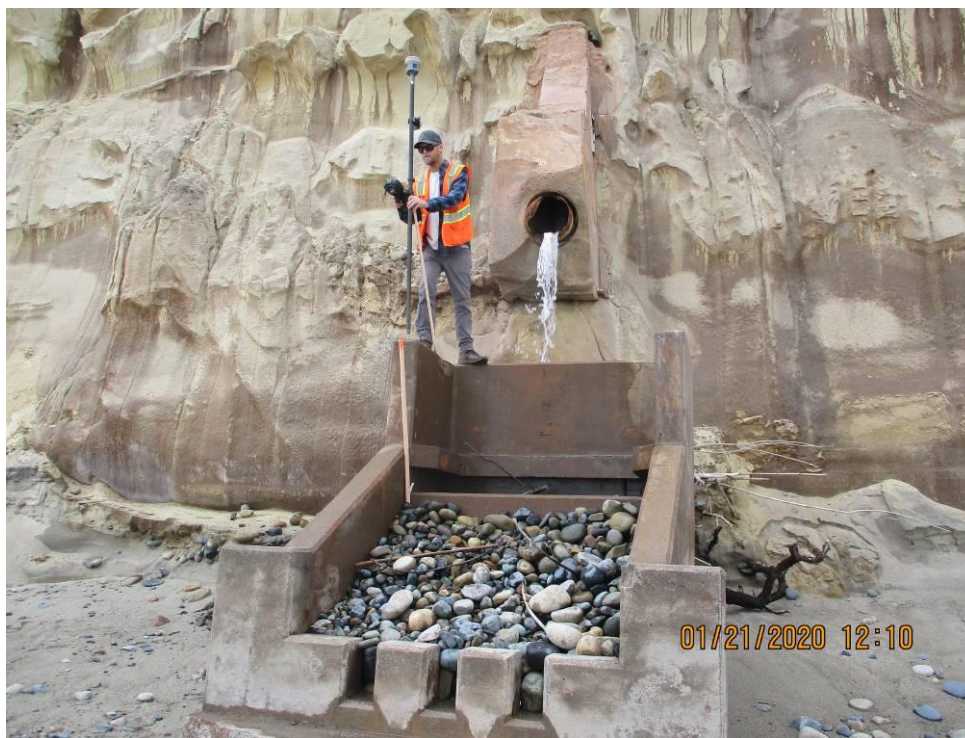


Photo B-22. Benchmark BM12, created on 21 January 2020, is located on top of the concrete drainage structure located just north of transect S1000.

APPENDIX F

2022 GROUNDWATER LEVELS AT SAN ONOFRE GENERATING STATION

**2022 GROUNDWATER LEVELS AT
SAN ONOFRE NUCLEAR GENERATING STATION
SAN ONOFRE, CALIFORNIA**



by

Coastal Environments, Inc.
2166 Avenida de la Playa, Suite E
La Jolla, CA 92037

for

Southern California Edison Company
2244 Walnut Grove Avenue
Rosemead, CA 91770

03 February 2023
CE Reference No. 23-03

TABLE OF CONTENTS

1.0	INTRODUCTION	1
2.0	ANALYSIS METHODS	2
3.0	RESULTS	5
4.0	CONCLUSIONS	14
5.0	REFERENCES	15

LIST OF APPENDICES

Appendix A.	2022 Groundwater and Tidal Data.....	A-1
-------------	--------------------------------------	-----

LIST OF FIGURES

Figure 2-1.	Locations of SONGS groundwater wells.....	3
Figure 2-2.	Locations of Group 1 (NIA) SONGS groundwater wells.....	4
Figure 3-1.	Groundwater elevation of Group 1 (NIA) SONGS wells and daily tides for 2022.....	9
Figure 3-2.	Groundwater elevation of Group 2 (PA) SONGS wells and daily tides for 2022.....	10
Figure 3-3.	Groundwater elevation of Group 3 (OCA) SONGS wells and daily tides for 2022	11
Figure 3-4.	Groundwater elevations (NGVD29) in 2022 and 2050 based on the CCC and H++ SLR projections	12
Figure 3-5.	Groundwater elevations (MLLW, Epoch 1941-1959) in 2022 and 2050 based on the CCC and H++ SLR projections	13

LIST OF TABLES

Table 3-1.	SONGS groundwater well sample data	6
Table 3-2.	Mean SONGS groundwater elevations	8
Table A-1.	SONGS groundwater well and ocean tide elevation data	A-2

2022 GROUNDWATER LEVELS AT SAN ONOFRE NUCLEAR GENERATING STATION SAN ONOFRE, CALIFORNIA

1.0 INTRODUCTION

This report has been compiled per Special Provision 14 (b) in California State Lands Commission Lease No. PRC 6785.1 for the use, maintenance, and decommissioning of exiting offshore improvements associated with the San Onofre Nuclear Generating Station (SONGS). Lease Provision 14 (b) requires, as part of compliance with applicable provisions or standards addressing sea level rise (SLR) that may be required or adopted by local, state, or federal agencies related to and affecting the lease premises, that the Lessee provide an annual summary, including quarterly groundwater elevation data collected from onsite monitoring wells.

In accordance with this requirement, this report compares the quarterly groundwater elevation data from the 16 wells located within SONGS against the coastal tide data to observe any correlation between elevation values. Data for both groundwater and tidal elevations span from January to December 2022.

At coastal discharge boundaries, freshwater and saltwater are typically slow to mix; the less-dense freshwater remains at the top of the water table, riding above the denser saltwater wedge, which extends below the land. Closer to the shoreline, however, daily tidal changes can result in short-term mixing of water sources and directly raise or lower the water table. San Onofre exemplifies one of these shallow coastal aquifers, where tidal effects on groundwater levels were noted in the 2022 groundwater measurements.

Section 2 of this report describes the sources and uses of the SONGS groundwater well and tidal data, as well as how this data was organized to obtain discernable results. Section 3 presents these results both graphically and in table format, while Section 4 discusses them and the relationship between groundwater elevation, daily tides, and SLR at SONGS. Ultimately, this report finds that projected groundwater elevations in 2050 are lower than the Independent Spent Fuel Storage Installation (ISFSI) support foundation by 1.23 and 0.43 ft, respectively, for medium-high and extreme risk aversion scenarios (Section 3).

2.0 ANALYSIS METHODS

Groundwater and well data for the year 2022 were provided by Southern California Edison (SCE) and compared against tidal data gathered by Coastal Environments, Inc. (CE). These include quarterly data from SCE Groundwater Protection Initiative (GPI) wells and other wells where data are collected semiannually or annually. ISFSI pad cross-sections were also provided by SCE. Figures 2-1 and 2-2 show the locations of the sampled wells at SONGS. Individual wells were measured 1 or 4 times within the calendar year. Data provided for the 16 wells located within SONGS included (1) date and time of sample, (2) ground surface elevation of well, (3) measured water depth, and (4) groundwater elevation.

Groundwater elevations were determined by measuring the wells' water depth, defined as the distance from a well's ground surface to its water level. This value was then subtracted from the known ground surface elevation of each well to determine groundwater elevations. Elevation data are presented in NGVD29 (National Geodetic Vertical Datum, 1929) for this report. Unlike MLLW (Mean Lower Low Water) datum values, which vary between tidal epochs, NGVD29 datum values remain fixed. Additionally, NGVD29 lies closer to Mean High Water (MHW) than MLLW, making NGVD29 more useful for representing current sea levels and SLR. Elevation values can be converted between datums by subtracting 2.60 ft from MLLW (Epoch 1941-1959) to get the elevation in NGVD29. Appendix A presents the groundwater measurements for the 16 wells in both datums.

To better examine groundwater trends, each of the 16 wells was assigned to one of three groups based on their elevation and location within SONGS. Group 1 included wells NIA-1, NIA-2, NIA-3, NIA-4, NIA-5, NIA-6, NIA-7, NIA-10, and NIA-11. This clustered group of wells occupies the lowest ground surface elevation and is located between the shoreline and North Industrial Area (Unit 1 remnants and ISFSI). Group 2 includes wells PA-1, PA-2, PA-3, and PA-4, which are at middling ground surface elevations and located between the Unit 2/3 structures and the shoreline. Group 3 includes the remaining wells of OCA-1, OCA-2, and OCA-3, which have the highest ground surface elevations and lie farthest from the shoreline.



Figure 2-1. Locations of SONGS groundwater wells.

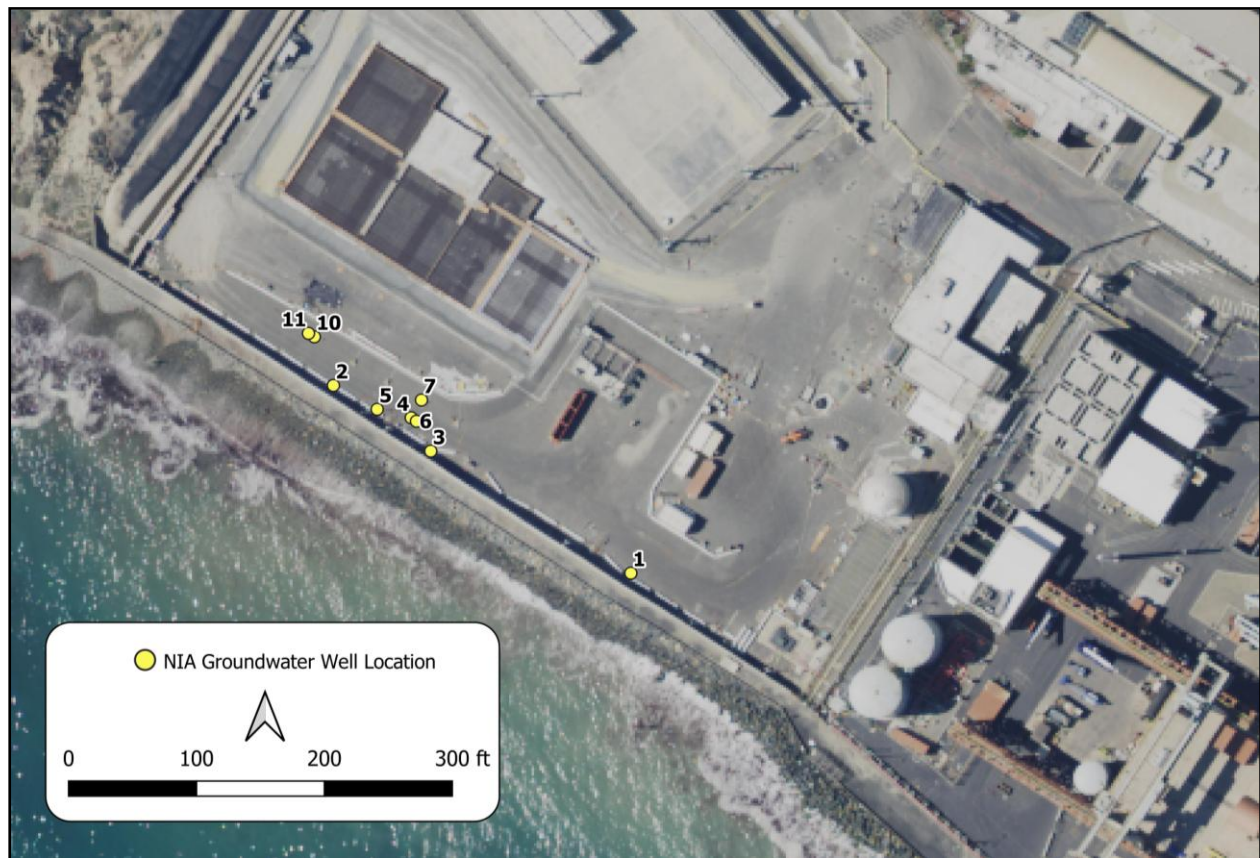


Figure 2-2. Locations of Group 1 (NIA) SONGS groundwater wells.

3.0 RESULTS

Table 3-1 displays the pertinent groundwater well elevation data for all measured samples, as well as the corresponding tidal data. Table 3-2 shows the mean groundwater elevations for each well group. Mean elevations were also calculated for individual wells that were measured more than once in 2022. Standard deviation values were not calculated for wells measured only once during 2022.

Figures 3-1 through 3-3 graphically show the groundwater elevations for each well plotted against the measured daily maximum and minimum tide elevations for 2022. Each figure displays well measurements from one of the three well groups; this allows for a visual comparison of groundwater elevations for wells within similar areas of SONGS.

The Group 1 wells are located just west of the Unit 1 remnants and ISFSI pads, and their ground surface elevations vary from 11.19 to 13.46 ft (NGVD). The 2022 groundwater elevation at these wells varies from 0.36 to 3.90 ft (Table 3-1), and the mean groundwater elevation for these 9 wells is 2.35 ft (Table 3-2). Due to their location within SONGS, Group 1 data were used to determine the distance between groundwater levels and the Holtec UMAX ISFSI support foundation in 2050, where the projection of SLR, according to the Ocean Protection Council (OPC), is 2 ft for a medium-high risk aversion scenario and 2.8 ft for the H++ extreme risk scenario. Figure 3-4 shows these 2050 sea level projections, along with the 2022 groundwater elevations, in comparison to the ISFSI pad. The H++ scenario groundwater elevation for 2050 is 5.15 ft and is lower than the bottom of the Holtec UMAX ISFSI support foundation (5.97 ft, NGVD) by 0.82 ft. The medium-high risk aversion CCC scenario groundwater elevation for 2050 is 4.35 ft, NGVD, and is 1.62 ft lower than the bottom of the ISFSI support foundation. Figure 3-5 is similar to Figure 3-4, but the elevation values are referenced to MLLW (Epoch 1941-1959).

Table 3-1. SONGS groundwater well sample data.

Well Group	Well Description	Sample Date	Sample Time	Surface Ground Elevation (NGVD29, ft)	Groundwater Elevation (NGVD29, ft)	Ocean Tide Level (NGVD29, ft)
Group 1	NIA-1	2-Feb-22	9:32	11.19	3.90	4.29
		20-Apr-22	10:11	11.19	1.97	-1.20
		20-Jul-22	9:40	11.19	2.56	-.80
		8-Dec-22	8:17	11.19	3.13	3.59
	NIA-2	23-Feb-22	9:36	12.80	2.04	-1.25
		19-May-22	8:55	12.80	1.47	-2.33
		1-Aug-22	9:36	12.80	1.91	-0.03
		8-Dec-22	10:12	12.80	3.35	2.52
	NIA-3	25-May-22	11:47	11.25	1.94	-1.35
	NIA-4	25-May-22	13:37	11.58	1.77	-1.34
	NIA-5	26-May-22	11:18	12.08	2.45	-0.34
	NIA-6	25-May-22	12:37	11.59	1.92	-1.50
	NIA-7	1-Jun-22	9:39	12.14	2.28	0.07
	NIA-10	20-Apr-22	8:10	13.46	1.68	-2.78
		20-Jul-22	7:25	13.46	2.56	-0.42
	NIA-11	26-May-22	10:15	13.46	2.70	0.45
Group 2	PA-1	3-Feb-22	7:35	26.21	1.91	1.75
		21-Apr-22	7:07	26.21	1.66	-2.75
		21-Jul-22	14:09	26.21	1.87	1.60
		18-Oct-22	7:56	26.21	1.90	1.68
	PA-2	3-Feb-22	13:08	26.91	2.12	0.84
		21-Apr-22	8:42	26.91	0.64	-2.93
		21-Jul-22	10:25	26.91	0.97	-0.14
		20-Oct-22	7:31	26.91	1.07	2.22
	PA-3	3-Feb-22	9:30	26.72	1.04	3.40
		21-Apr-22	11:40	26.72	1.01	-1.09
		21-Jul-22	8:37	26.72	1.40	0.01
		19-Oct-22	8:40	26.72	1.18	1.74
	PA-4	3-Feb-22	10:30	26.34	2.94	3.40
		21-Apr-22	13:20	26.34	0.36	-0.02
		21-Jul-22	6:55	26.34	1.27	0.47
		19-Oct-22	11:25	26.34	1.47	0.73

Table 3-1, cont. SONGS groundwater well sample data.

Well Group	Well Description	Sample Date	Sample Time	Surface Ground Elevation (NGVD29, ft)	Groundwater Elevation (NGVD 29, ft)	Ocean Tide Level (NGVD29, ft)
Group 3	OCA-1	7-Feb-22	13:19	45.09	3.44	0.18
		25-Apr-22	14:42	45.09	3.14	-1.83
		25-Jul-22	7:40	45.09	3.53	0.81
		7-Dec-22	11:26	45.09	3.51	0.32
	OCA-2	7-Feb-22	10:22	113.79	3.37	-0.41
		25-Apr-22	12:16	113.79	3.23	-2.74
		25-Jul-22	10:59	113.79	3.55	1.15
		7-Dec-22	9:28	113.79	3.45	2.87
	OCA-3	7-Feb-22	8:16	103.10	2.16	-0.68
		25-Apr-22	7:54	103.10	2.25	1.25
		25-Jul-22	14:05	103.10	2.32	0.44
		24-Oct-22	9:51	103.10	2.85	3.18

Table 3-2. Mean SONGS groundwater elevations.

Well Group	Well Description	Surface Ground Elevation (NGVD29, ft)	Mean Groundwater Level (NGVD29, ft)		Standard Deviation (ft)	
			Well	Group	Well	Group
Group 1	NIA-1	11.19	2.89	2.35	0.82	0.66
	NIA-2	12.80	2.19		0.81	
	NIA-3	11.25	1.94		N/A	
	NIA-4	11.58	1.77		N/A	
	NIA-5	12.08	2.45		N/A	
	NIA-6	11.59	1.92		N/A	
	NIA-7	12.14	2.28		N/A	
	NIA-10	13.46	2.12		.62	
	NIA-11	13.46	2.70		N/A	
Group 2	PA-1	26.21	1.84	1.43	0.12	0.63
	PA-2	26.91	1.20		0.64	
	PA-3	26.72	1.16		0.18	
	PA-4	26.34	1.51		1.07	
Group 3	OCA-1	45.09	3.41	3.07	0.18	0.54
	OCA-2	113.79	3.40		0.14	
	OCA-3	103.10	2.40		0.31	

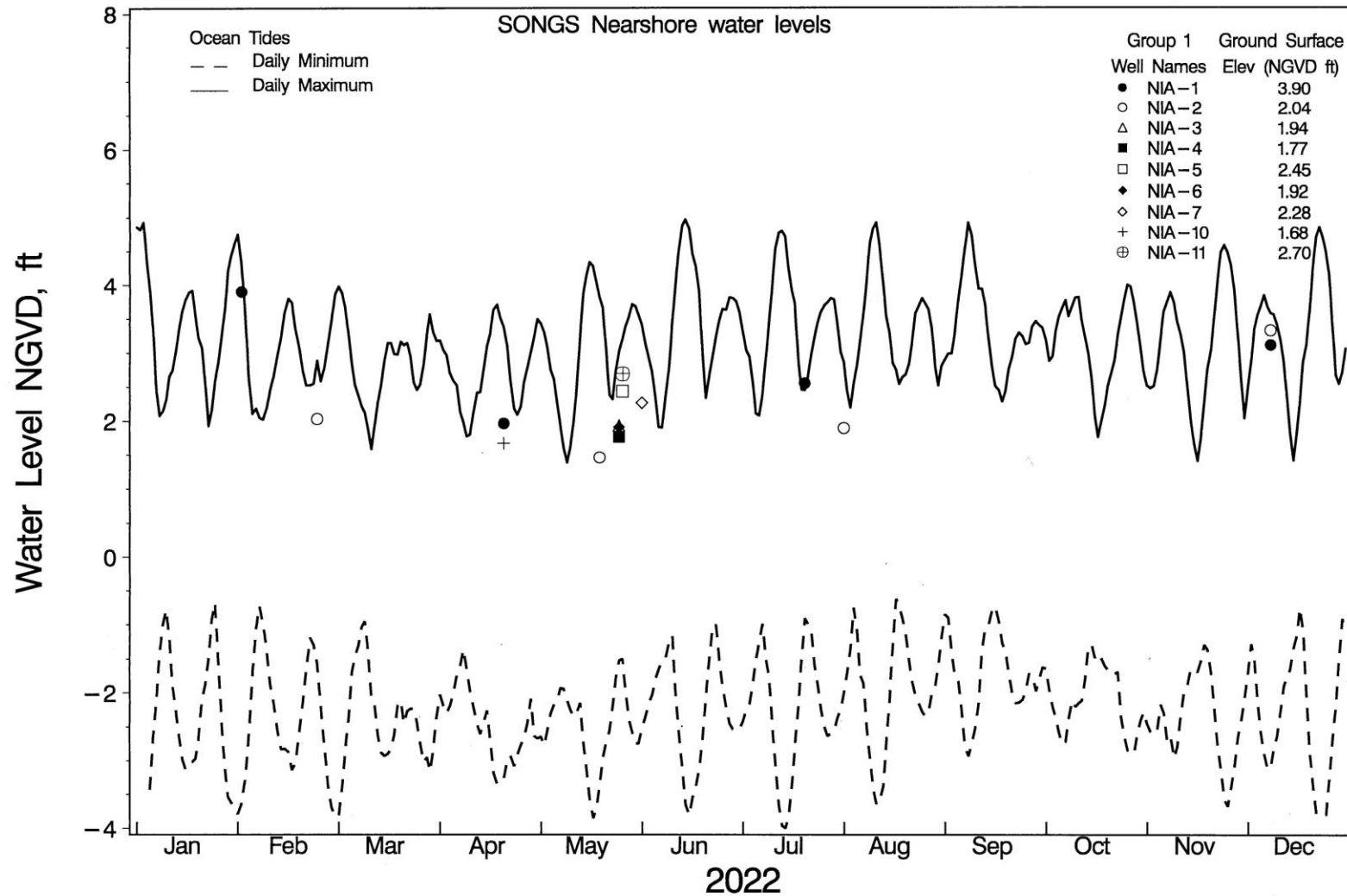


Figure 3-1. Groundwater elevation of Group 1 (NIA) SONGS wells and daily tides for 2022.

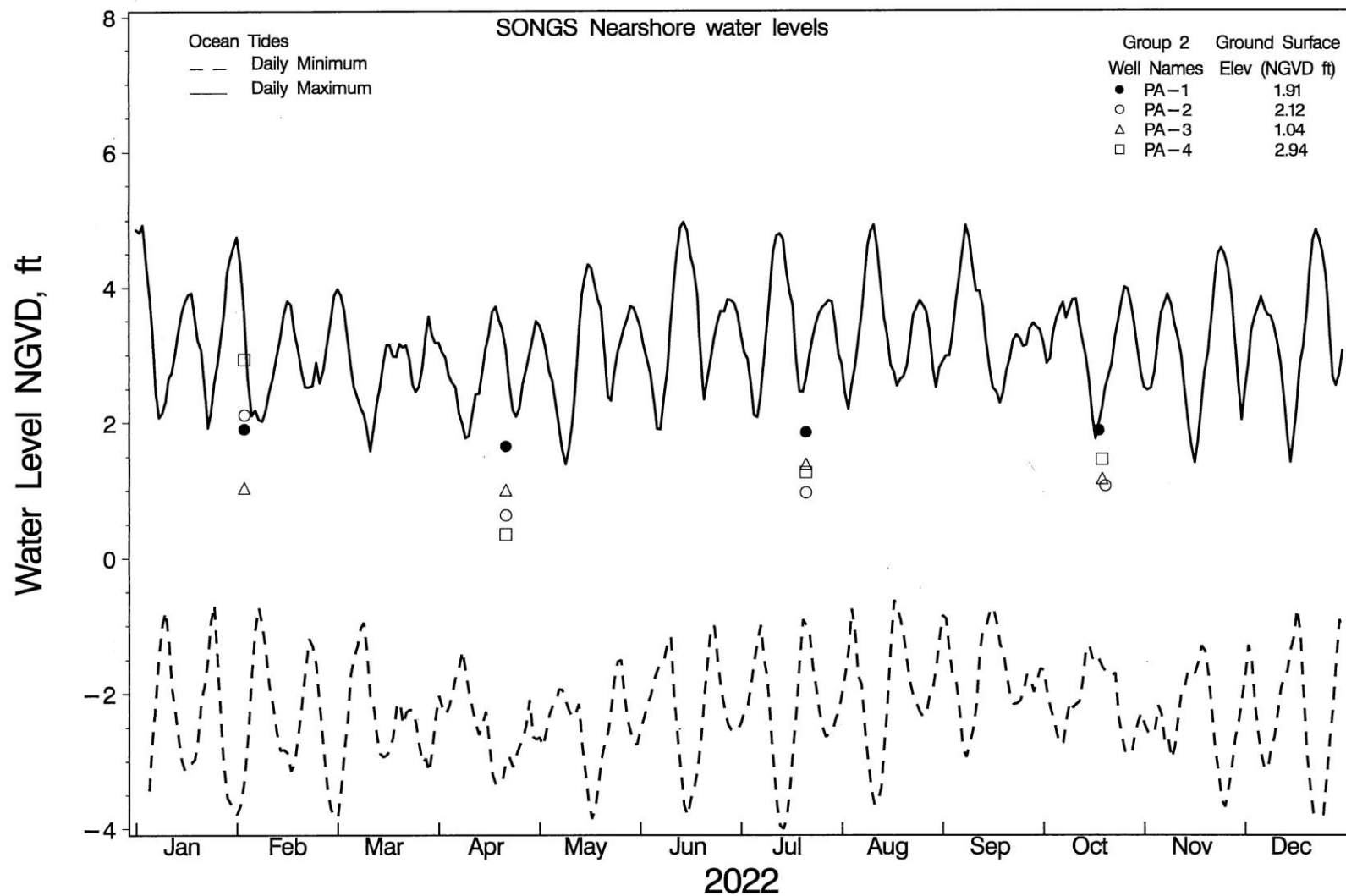


Figure 3-2. Groundwater elevation of Group 2 (PA) SONGS wells and daily tides for 2022.

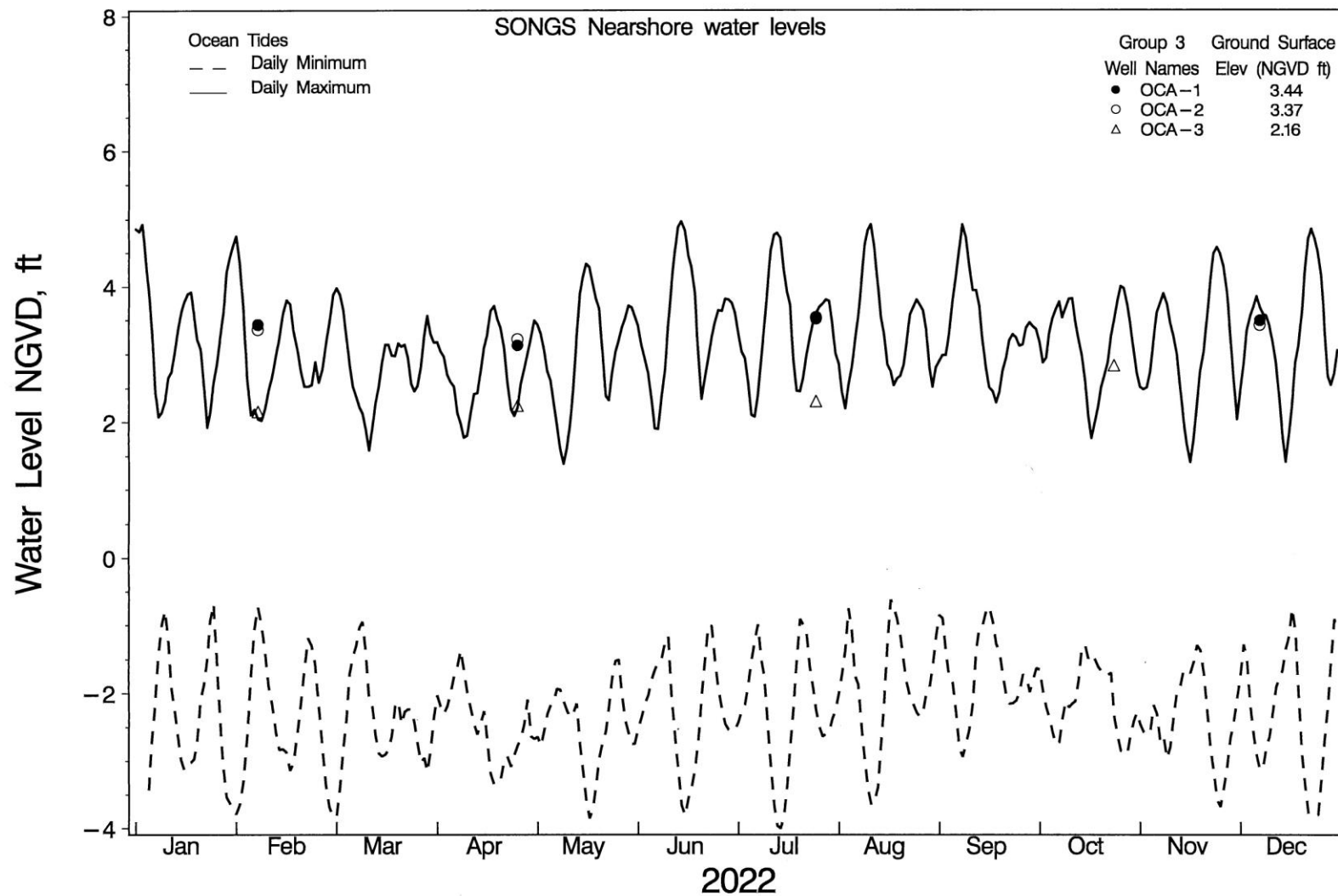


Figure 3-3. Groundwater elevation of Group 3 (OCA) SONGS wells and daily tides for 2022.

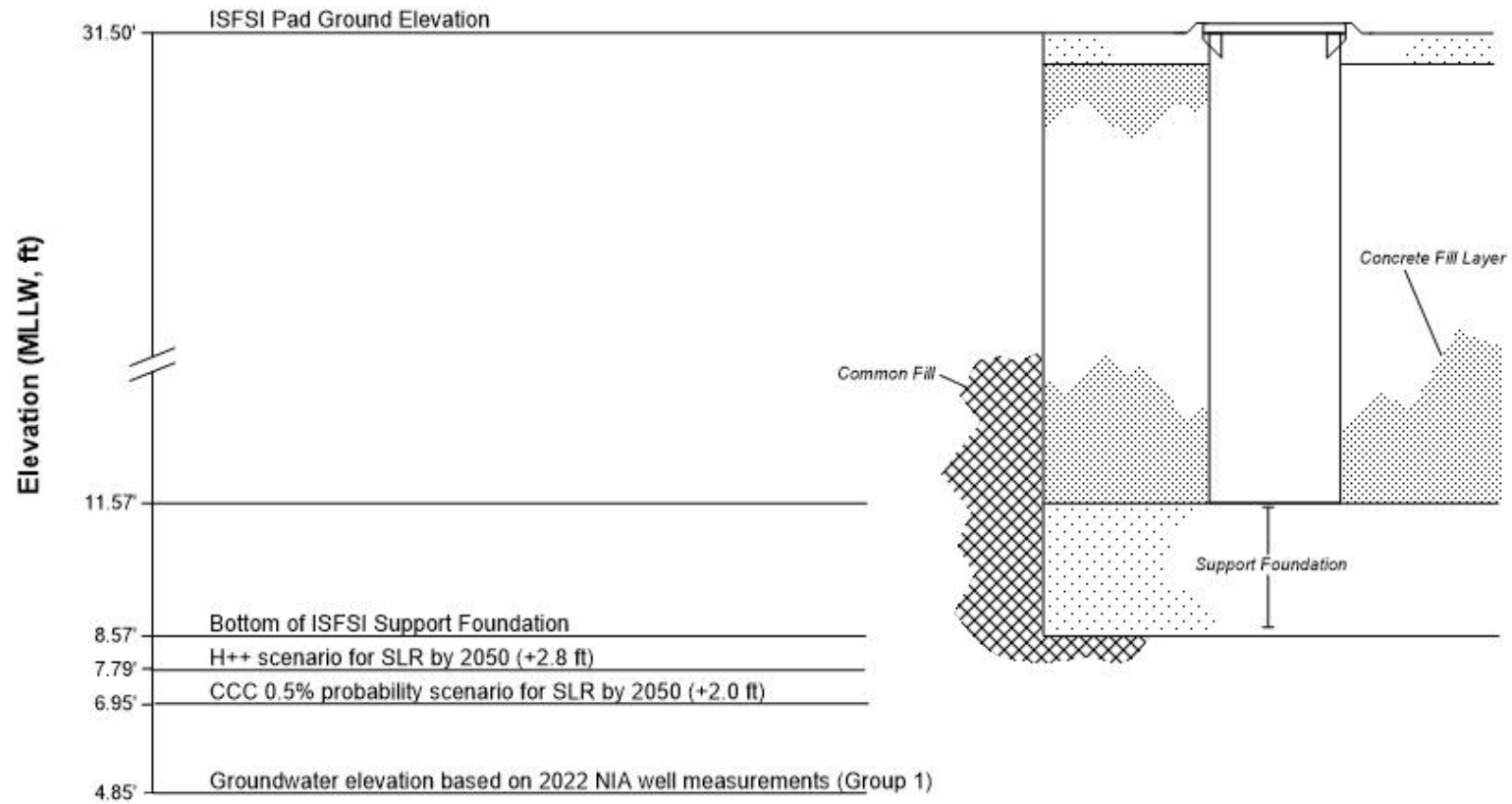


Figure 3-4. Groundwater elevations (NGVD29) in 2022 and 2050 based on the CCC and H++ SLR projections (OPC, 2018).

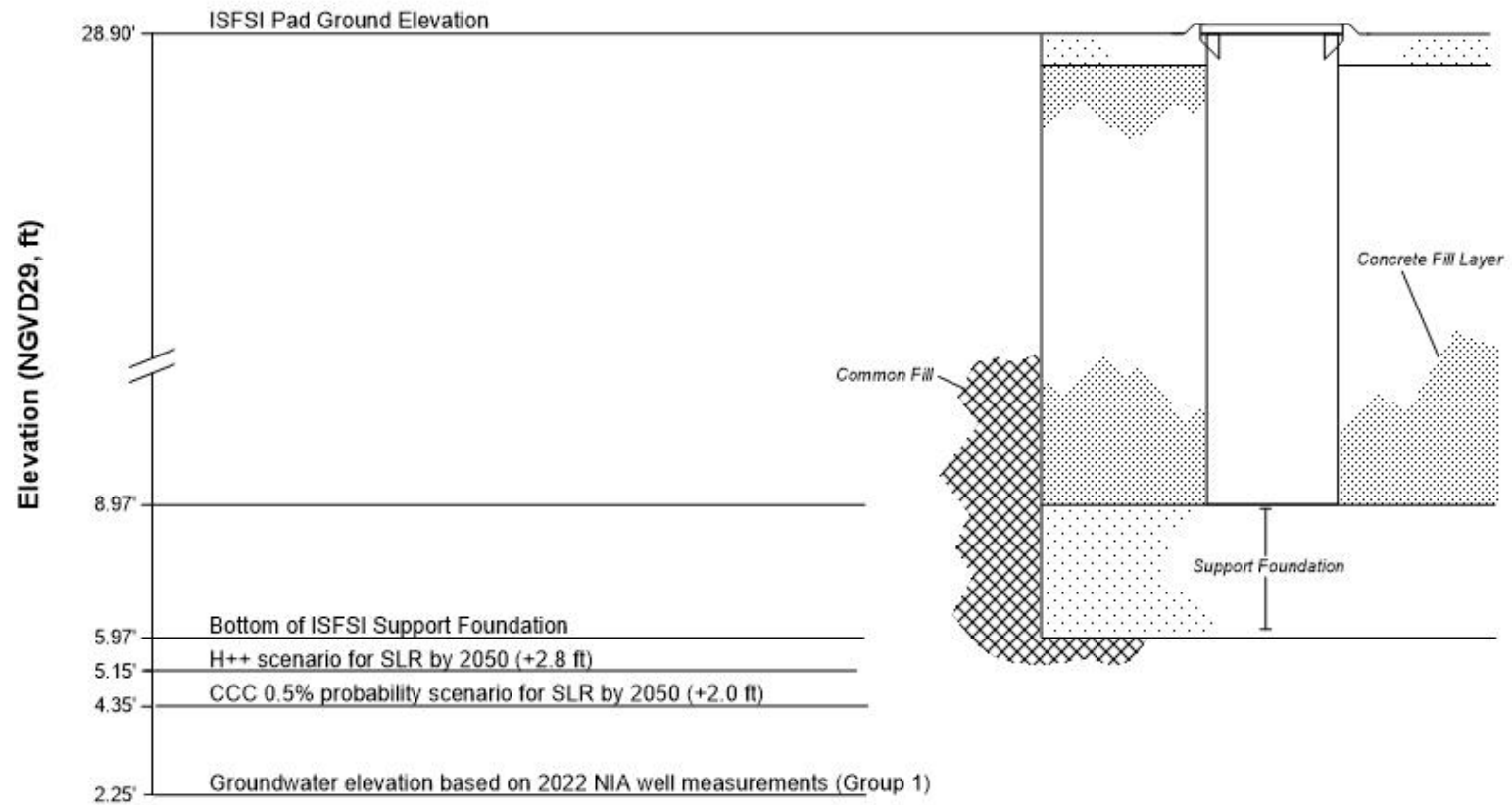


Figure 3-5. Groundwater elevations (MLLW, Epoch 1941-1959) in 2022 and 2050 based on the CCC and H++ SLR projections (OPC, 2018).

4.0 CONCLUSIONS

On average, Group 1 and Group 2 wells, located closer to the shoreline, have lower mean groundwater levels that closely match the MHW level at the ocean (approximately 2.31 ft, NGVD29). Group 3 wells are located at higher elevations and their groundwater elevations are higher than Groups 1 and 2.

Group 1 wells were selected to estimate groundwater elevations underneath the ISFSI pads. Because Group 1 wells are located closest to the ISFSI pads, their mean groundwater elevation provides a good estimate for groundwater elevations at the ISFSI. The OPC has several scenarios for how high sea levels will rise by 2050 (OPC, 2018). As sea levels rise, groundwater levels will increase in about the same value.

As shown in Figure 3-4, the highest H++ projected groundwater elevation scenario is 5.35 ft, NGVD and rests 0.82 ft below the Holtec UMAX ISFSI support foundation in 2050. The medium-high risk aversion CCC scenario has a 0.5% probability of SLR meeting or exceeding a +2 ft projection; this scenario puts groundwater elevations at SONGS 1.62 ft below the Holtec UMAX ISFSI support foundation in 2050. It should also be pointed out that the upper surface support foundation is 3 ft above the bottom surface of the ISFSI support foundation (i.e., the support foundation pad is 3 ft thick), minimizing any chance that the groundwater will contact the Cavity Enclosure Containers (CECs) in which the spent nuclear fuel is stored.

5.0 REFERENCES

- California Coastal Commission, 2015 (updated 2018). *California Coastal Commission Sea Level Rise Policy Guidance, Interpretive Guidelines for Addressing Sea Level Rise in Local Coastal Programs and Coastal Development Permits*, California Coastal Commission, San Francisco, CA, 307 pp.
- Ocean Protection Council, 2018. *State of California Sea-Level Rise Guidance, 2018 Update*, Sacramento, CA: California Natural Resources Agency, 84 pp.
<http://www.opc.ca.gov/updating-californias-sea-level-rise-guidance/>

APPENDIX A

2022 GROUNDWATER AND TIDAL DATA

Table A-1. SONGS groundwater well and ocean tide elevation data.

Well Group	Well Description	Sample Date	Quarter	Sample Time	Measured Water Depth (ft)	Ground Surface Elevation (MLLW, ft)	Groundwater Elevation (MLLW, ft)	Ground Surface Elevation (NGVD29, ft)	Groundwater Elevation (NGVD29, ft)	Ocean Tide Level (MLLW, ft)*	Ocean Tide Level (NGVD29, ft)
Group 1	NIA-1	2-Feb-22	Q1	9:32	7.29	13.79	6.5	11.19	3.9	6.89	4.29
		20-Apr-22	Q2	10:11	9.22	13.79	4.57	11.19	1.97	1.4	-1.2
		20-Jul-22	Q3	9:40	8.63	13.79	5.16	11.19	2.56	1.8	-0.8
		8-Dec-22	Q4	8:17	8.06	13.79	5.73	11.19	3.13	6.19	3.59
	NIA-2	23-Feb-22	Q1	9:36	10.76	15.4	4.64	12.8	2.04	1.35	-1.25
		19-May-22	Q2	8:55	11.33	15.4	4.07	12.8	1.47	0.27	-2.33
		1-Aug-22	Q3	9:36	10.89	15.4	4.51	12.8	1.91	2.57	-0.03
		8-Dec-22	Q4	10:12	9.45	15.4	5.95	12.8	3.35	5.12	2.52
	NIA-3	25-May-22	Q2	11:47	9.31	13.85	4.54	11.25	1.94	1.25	-1.35
	NIA-4	25-May-22	Q2	13:37	9.81	14.18	4.37	11.58	1.77	1.26	-1.34
	NIA-5	26-May-22	Q2	11:18	9.63	14.68	5.05	12.08	2.45	2.26	-0.34
	NIA-6	25-May-22	Q2	12:37	9.67	14.19	4.52	11.59	1.92	1.1	-1.5
Group 2	PA-1	3-Feb-22	Q1	7:35	24.30	28.81	4.51	26.21	1.91	4.35	1.75
		21-Apr-22	Q2	7:07	24.55	28.81	4.26	26.21	1.66	-0.15	-2.75
		21-Jul-22	Q3	14:09	24.34	28.81	4.47	26.21	1.87	4.2	1.6
		18-Oct-22	Q4	7:56	24.31	28.81	4.5	26.21	1.9	4.28	1.68
	PA-2	3-Feb-22	Q1	13:08	24.79	29.51	4.72	26.91	2.12	3.44	0.84
		21-Apr-22	Q2	8:42	26.27	29.51	3.24	26.91	0.64	-0.33	-2.93
		21-Jul-22	Q3	10:25	25.94	29.51	3.57	26.91	0.97	2.46	-0.14
		20-Oct-22	Q4	7:31	25.84	29.51	3.67	26.91	1.07	4.82	2.22
	PA-3	3-Feb-22	Q1	9:30	25.68	29.32	3.64	26.72	1.04	6	3.4
		21-Apr-22	Q2	11:40	25.71	29.32	3.61	26.72	1.01	1.51	-1.09
		21-Jul-22	Q3	8:37	25.32	29.32	4	26.72	1.4	2.61	0.01
		19-Oct-22	Q4	8:40	25.54	29.32	3.78	26.72	1.18	4.34	1.74
	PA-4	3-Feb-22	Q1	10:30	23.40	28.94	5.54	26.34	2.94	6	3.4
		21-Apr-22	Q2	13:20	25.98	28.94	2.96	26.34	0.36	2.58	-0.02
		21-Jul-22	Q3	6:55	25.07	28.94	3.87	26.34	1.27	3.07	0.47
		19-Oct-22	Q4	11:25	24.87	28.94	4.07	26.34	1.47	3.33	0.73

* = Tidal Datum Epoch (1983-2001).

Table A-1, cont. SONGS groundwater well and ocean tide elevation data.

Well Group	Well Description	Sample Date	Quarter	Sample Time	Measured Water Depth (ft)	Ground Surface Elevation (MLLW, ft)	Groundwater Elevation (MLLW, ft)	Ground Surface Elevation (NGVD29, ft)	Groundwater Elevation (NGVD29, ft)	Ocean Tide Level (MLLW, ft)*	Ocean Tide Level (NGVD29, ft)
Group 3	OCA-1	7-Feb-22	Q1	13:19	41.65	47.69	6.04	45.09	3.44	2.78	0.18
		25-Apr-22	Q2	14:42	41.95	47.69	5.74	45.09	3.14	0.77	-1.83
		25-Jul-22	Q3	7:40	41.56	47.69	6.13	45.09	3.53	3.41	0.81
		7-Dec-22	Q4	11:26	41.58	47.69	6.11	45.09	3.51	2.92	0.32
	OCA-2	7-Feb-22	Q1	10:22	110.42	116.39	5.97	113.79	3.37	2.19	-0.41
		25-Apr-22	Q2	12:16	110.56	116.39	5.83	113.79	3.23	-0.14	-2.74
		25-Jul-22	Q3	10:59	110.24	116.39	6.15	113.79	3.55	3.75	1.15
		7-Dec-22	Q4	9:28	110.34	116.39	6.05	113.79	3.45	5.47	2.87
	OCA-3	7-Feb-22	Q1	8:16	100.94	105.7	4.76	103.1	2.16	1.92	-0.68
		25-Apr-22	Q2	7:54	100.85	105.7	4.85	103.1	2.25	3.85	1.25
		25-Jul-22	Q3	14:05	100.78	105.7	4.92	103.1	2.32	3.04	0.44
		24-Oct-22	Q4	9:51	100.25	105.7	5.45	103.1	2.85	5.78	3.18

* = Tidal Datum Epoch (1983-2001).